EMPIRICAL CORRELATIONS FOR 5-SPOT WATER FLOODING PERFORMANCE WITH DIFFERENT PERMEABILITY SORTINGS

BY

USAMA YOUSUF

A Thesis Presented to the

DEANSHIP OF GRADUATE STUDIES

KING FAHD UNIVERSITY OF PETROLEUM & MINERALS

DHAHRAN, SAUDI ARABIA

In Partial Fulfillment of the
Requirements for the Degree of

MASTER OF SCIENCE

In

PETROLEUM ENGINEERING

APRIL, 2016

KING FAHD UNIVERSITY OF PETROLEUM & MINERALS

DHAHRAN- 31261, SAUDI ARABIA

DEANSHIP OF GRADUATE STUDIES

This thesis, written by **USAMA YOUSUF** under the direction of his thesis advisor and approved by his thesis committee, has been presented and accepted by the Dean of Graduate Studies, in partial fulfillment of the requirements for the degree of **MASTER OF SCIENCE IN PETROLEUM ENGINEERING.**

Dr. Sidqi A. Abu-Khamsin
(Advisor)

Dr. Abdullah S. Sultan
Department Chairman

Dr. Hasan Y. Al-Yousef
(Member)

Dr. Salam A. Zummo
Dean of Graduate Studies

Dr. Rahul N. Gajbhiye
(Member)

25/07/2016

Date

© Usama Yousuf

2016

Dedication

I dedicate my work to my loving family, my fiancée and friends who had been a constant support in all my endeavors.

ACKNOWLEDGMENTS

All praise to the Almighty for his countless blessings bestowed upon me and giving me the strength to complete this work. Without his help nothing is possible.

I would like to express my sincere appreciation and gratitude to my thesis advisor Dr. Sidqi Abu-Khamsin and my thesis committee members Dr. Hasan Al-Yousef and Dr. Rahul Gajbhiye for their continuous support throughout my research period. I especially acknowledge the support of Dr. Sidqi Abu-Khamsin and I am thankful to him for his precious time and commitment. His precious guidance and advice helped me grow confidence and ultimately making me capable of achieving and completing this research. I am also thankful to Dr. Hasan Al-Yousef without whom this research may not have been completed.

I would like to thank my family for their strong support and encouragement throughout my study period and who were a source of continuous inspiration throughout my Master's degree. Special thanks are due to the Department of Petroleum Engineering at King Fahd University of Petroleum & Minerals, including Faculty, Staff and Friends who contributed directly or indirectly to the accomplishments of this work.

I also gratefully acknowledge the help of Shams Kalam, Muzammil Hussain Rammay, Rizwan Ahmed Khan, Waqas Ahmed, Danish and Zeeshan Tariq for their help in resolving issues related to my thesis work. At the end, I am so grateful to all my colleagues at my work especially Aamir Akhtar, Syed Tahir Ali, Ahmed El-Toum, Muhammed Arsalan and Abdulwaheed who supported and encouraged me continuously in completing my master's degree.

TABLE OF CONTENTS

ACKNOWLEDGMENTS ..... **V**

TABLE OF CONTENTS ..... **VI**

LIST OF TABLES ..... **IX**

LIST OF FIGURES ..... **X**

LIST OF ABBREVIATIONS ..... **XVII**

ABSTRACT (ENGLISH) ..... **XX**

ABSTRACT (ARABIC) ..... **XXII**

CHAPTER 1 INTRODUCTION **1**

1.1 Overview **1**

1.2 Flood Patterns **1**

1.3 Mobility Ratio **2**

1.4 Permeability Variation Coefficient **5**

1.5 Wettability Indicator **5**

1.6 Recovery Factor **8**

1.7 Displacement in a Five-Spot Pattern **10**

1.8 Reservoir Simulation **11**

1.9 Thesis Organization **11**

CHAPTER 2 LITERATURE REVIEW **12**

CHAPTER 3 PROBLEM STATEMENT AND RESEARCH OBJECTIVES **26**

3.1 Research Objectives **27**

CHAPTER 4 SIMULATION AND CALCULATIONS 28

4.1 Methodology 28

4.2 Conditions and Limitations 29

4.3 Calculation of Coefficient of Permeability Variation and Permeabilities 29

4.4 Calculation of Oil to Water Density Ratio 34

4.5 Calculation of Oil-Water Relative Permeabilites 34

4.6 Calculation of Fractional Flow Curve, Oil Viscosity and Mobility Ratio 37

4.7 Reservoir Simulation Model 42

4.7.1 Eclipse® 100 Input Data 42

4.7.2 Model Description 44

4.8 Simulation Runs 45

4.9 Calculation of Movable Oil Recovery Factor 49

4.10 Simulation Model Sensitivities 50

4.10.1 Layers Random Sorting Sensitivity 50

4.10.2 Pattern Area Sensitivity 52

4.10.3 Reservoir Thickness Sensitivity 54

CHAPTER 5 SIMULATION RESULTS 55

5.1 Effect of Mobility Ratio 55

5.2 Effect of Reservoir Heterogeneity 62

5.3 Effect of Density 62

5.4 Effect of Wettability 81

5.5 Effect of Permeability Arrangement 90

CHAPTER 6 CORRELATION DEVELOPMENT 97

6.1 Statistical Technique 97

6.1.1 Artificial Neural Networks 97

6.2 Correlation Development **100**

6.2.1 Input Normalization **103**

6.2.2 Output De-Normalization **103**

6.3 Correlation Testing **110**

6.3.1 Case 1: Wettability Indicator = 0.8 ..... **110**

6.3.2 Case 2: Wettability Indicator = 1.51 ..... **116**

6.3.3 Wettability Indicator Testing **121**

6.4 Comparison with Field Data **130**

6.4.1 Case 1: Field A **130**

6.4.2 Case 2: Field B **133**

6.5 Comparison with Craig-Geffen-Morse (CGM) Method **137**

CHAPTER 7 CONCLUSIONS AND RECOMMENDATIONS **139**

7.1 Conclusions **139**

7.2 Recommendations for Future Work **140**

REFERENCES **142**

VITAE **145**

LIST OF TABLES

Table 1 Wettability Preferences 7
Table 2 Parameter ranges used in simulation 28
Table 3 Reservoir Permeability Data 31
Table 4 Data to plot permeability vs. cumulative frequency distribution 31
Table 5 Values of $k_{84.1}$ 33
Table 6 Values of k_x, k_y permeabilities used in simulation model 34
Table 7 Parameters Used in Relative Permeability Curves 35
Table 8 Data for oil viscosity and mobility ratio calculation 38
Table 9 Model properties including reservoir and fluid properties 45
Table 10 Parameter values used in simulation model 46
Table 11 Input and Output Variables for the new correlation 99
Table 12 Statistical Description of the Input and Output Data Used for Training 104
Table 13 Weights and Bias Values for RF_m Artificial Neural Network Model for Ascending Case 105
Table 14 Weights and Bias Values for RF_m Artificial Neural Network Model for Descending Case 106
Table 15 Accuracy measurement of training and testing data 107
Table 16 Correlation testing parameters 110
Table 17 Correlation testing parameters (with several values of WI) 122
Table 18 Data for Field A 131
Table 19 Data for Field B 134

LIST OF FIGURES

Figure 1 Illustration of water flood patterns (Craig, F.F. Jr. 1971) 2
Figure 2 Fluid distribution during water flood of water-wet rock (Craig, F.F. Jr. 1971) ... 6
Figure 3 Fluid distribution during water flood of oil-wet rock (Craig, F.F. Jr. 1971)..... 7
Figure 4 Single five-spot pattern with a circle showing one quadrant 10
Figure 5 Oil production: comparison between the Dykstra-Parsons method and numerical simulation for 2-layered model, i_w = 800 STB/D 26
Figure 6 Plot of permeability vs. cumulative frequency distribution 32
Figure 7 Plot of permeability vs. cumulative frequency distribution for various V 33
Figure 8 System A, Wettability Indicator = 0.5 36
Figure 9 System B, Wettability Indicator = 1.12 36
Figure 10 System C, Wettability Indicator = 3 37
Figure 11 Fractional flow curve for system B at mobility ratio 0.1 39
Figure 12 Fractional flow curve for system B at mobility ratio 0.2 39
Figure 13 Fractional flow curve for system B at mobility ratio 0.5 40
Figure 14 Fractional flow curve for system B at mobility ratio 1.0 40
Figure 15 Fractional flow curve for system B at mobility ratio 2.0 41
Figure 16 Fractional flow curve for system B at mobility ratio 4.0 41
Figure 17 Breakthrough Case for Ascending case, system B at V=0.1, M=0.1, β= 0.7... 46
Figure 18 Simulation for Ascending case, system B at f_w = 0.5, V=0.5, M=0.5, β= 0.8 . 47
Figure 19 Simulation for Ascending case, system B at f_w = 0.95, V=0.9, M=2.0, β= 0.9 47
Figure 20 Breakthrough Case for Descending case, system B at V=0.3, M=0.2, β= 0.9 . 48
Figure 21 Simulation for Descending case, system B at f_w = 0.5, V=0.5, M=0.5, β= 0.8 48
Figure 22 Simulation for Descending case, system B at f_w = 0.7, V=0.7, M=1.0, β= 1.0 49
Figure 23 Layers Random Sorting Sensitivity for System A 51
Figure 24 Layers Random Sorting Sensitivity for System B 51
Figure 25 Layers Random Sorting Sensitivity for System C 52
Figure 26 Area Sensitivity for ascending case for system B at different mobility ratio... 53
Figure 27 Area Sensitivity for descending case for system B at different mobility ratio. 53
Figure 28 Thickness Sensitivity for ascending case for system B at different mobility ratio 54
Figure 29 Thickness Sensitivity for descending case for system B at different mobility ratio 54
Figure 30 Effect of mobility ratio on oil recovery factor at water breakthrough for system A ascending case 56
Figure 31 Effect of mobility ratio on oil recovery factor beyond water breakthrough for system A ascending case 56
Figure 32 Effect of mobility ratio on oil recovery factor at water breakthrough for system B ascending case 57

Figure 33 Effect of mobility ratio on oil recovery factor beyond water breakthrough for system B ascending case 57
Figure 34 Effect of mobility ratio on oil recovery factor at water breakthrough for system C ascending case 58
Figure 35 Effect of mobility ratio on oil recovery factor beyond water breakthrough for system C ascending case 58
Figure 36 Effect of mobility ratio on oil recovery factor at water breakthrough for system A descending case 59
Figure 37 Effect of mobility ratio on oil recovery factor beyond water breakthrough for system A descending case 59
Figure 38 Effect of mobility ratio on oil recovery factor at water breakthrough for system B descending case 60
Figure 39 Effect of mobility ratio on oil recovery factor beyond water breakthrough for system B descending case 60
Figure 40 Effect of mobility ratio on oil recovery factor at water breakthrough for system C descending case 61
Figure 41 Effect of mobility ratio on oil recovery factor beyond water breakthrough for system C descending case 61
Figure 42 Effect of density ratio on oil recovery factor at water breakthrough for system A ascending case-Case 1 63
Figure 43 Effect of density ratio on oil recovery factor at water breakthrough for system A ascending case-Case 2 63
Figure 44 Effect of density ratio on oil recovery factor at water breakthrough for system A ascending case-Case 3 64
Figure 45 Effect of density ratio on oil recovery factor beyond water breakthrough for System A ascending case-Case 1 64
Figure 46 Effect of density ratio on oil recovery factor beyond water breakthrough for System A ascending case-Case 2 65
Figure 47 Effect of density ratio on oil recovery factor beyond water breakthrough for System A ascending case-Case 3 65
Figure 48 Effect of density ratio on oil recovery factor at water breakthrough for system B ascending case-Case 1 66
Figure 49 Effect of density ratio on oil recovery factor at water breakthrough for system B ascending case-Case 2 66
Figure 50 Effect of density ratio on oil recovery factor at water breakthrough for system B ascending case-Case 3 67
Figure 51 Effect of density ratio on oil recovery factor beyond water breakthrough for System B ascending case-Case 1..... 67
Figure 52 Effect of density ratio on oil recovery factor beyond water breakthrough for System B ascending case-Case 2..... 68

Figure 53 Effect of density ratio on oil recovery factor beyond water breakthrough for System B ascending case-Case 3 68
Figure 54 Effect of density ratio on oil recovery factor at water breakthrough for system C ascending case-Case 1 69
Figure 55 Effect of density ratio on oil recovery factor at water breakthrough for system C ascending case-Case 2 69
Figure 56 Effect of density ratio on oil recovery factor at water breakthrough for system C ascending case-Case 3 70
Figure 57 Effect of density ratio on oil recovery factor beyond water breakthrough for System C ascending case-Case 1 70
Figure 58 Effect of density ratio on oil recovery factor beyond water breakthrough for System C ascending case-Case 2 71
Figure 59 Effect of density ratio on oil recovery factor beyond water breakthrough for System C ascending case-Case 3 71
Figure 60 Effect of density ratio on oil recovery factor at water breakthrough for system A descending case-Case 1 72
Figure 61 Effect of density ratio on oil recovery factor at water breakthrough for system A descending case-Case 2 72
Figure 62 Effect of density ratio on oil recovery factor at water breakthrough for system A descending case-Case 3 73
Figure 63 Effect of density ratio on oil recovery factor beyond water breakthrough for System A descending case-Case 1 73
Figure 64 Effect of density ratio on oil recovery factor beyond water breakthrough for System A descending case-Case 2 74
Figure 65 Effect of density ratio on oil recovery factor beyond water breakthrough for System A descending case-Case 3 74
Figure 66 Effect of density ratio on oil recovery factor at water breakthrough for system B descending case-Case 1 75
Figure 67 Effect of density ratio on oil recovery factor at water breakthrough for system B descending case-Case 2 75
Figure 68 Effect of density ratio on oil recovery factor at water breakthrough for system B descending case-Case 3 76
Figure 69 Effect of density ratio on oil recovery factor beyond water breakthrough for System B descending case-Case 1 76
Figure 70 Effect of density ratio on oil recovery factor beyond water breakthrough for System B descending case-Case 2 77
Figure 71 Effect of density ratio on oil recovery factor beyond water breakthrough for System B descending case-Case 3 77
Figure 72 Effect of density ratio on oil recovery factor at water breakthrough for system C descending case-Case 1 78

Figure 73 Effect of density ratio on oil recovery factor at water breakthrough for system C descending case-Case 2 78
Figure 74 Effect of density ratio on oil recovery factor at water breakthrough for system C descending case-Case 3 79
Figure 75 Effect of density ratio on oil recovery factor beyond water breakthrough for System C descending case-Case 1..... 79
Figure 76 Effect of density ratio on oil recovery factor beyond water breakthrough for System C descending case-Case 2..... 80
Figure 77 Effect of density ratio on oil recovery factor beyond water breakthrough for System C descending case-Case 3..... 80
Figure 78 Effect of wettability on oil recovery factor at water breakthrough for ascending at M=0.2 82
Figure 79 Effect of wettability on oil recovery factor at water breakthrough for ascending at M=4 82
Figure 80 Effect of wettability on movable oil recovery factor at water breakthrough for ascending at M=0.2 83
Figure 81 Effect of wettability on movable oil recovery factor at water breakthrough for ascending at M=4 83
Figure 82 Effect of wettability on oil recovery factor beyond water breakthrough for ascending at M=0.2 84
Figure 83 Effect of wettability on oil recovery factor beyond water breakthrough for ascending at M=4 84
Figure 84 Effect of wettability on movable oil recovery factor beyond water breakthrough for ascending at M=0.2..... 85
Figure 85 Effect of wettability on movable oil recovery factor beyond water breakthrough for ascending at M=4..... 85
Figure 86 Effect of wettability on oil recovery factor at water breakthrough for descending at M=0.1 86
Figure 87 Effect of wettability on oil recovery factor at water breakthrough for descending at M=4 86
Figure 88 Effect of wettability on movable oil recovery factor at water breakthrough for descending at M=0.1 87
Figure 89 Effect of wettability on movable oil recovery factor at water breakthrough for descending at M=4 87
Figure 90 Effect of wettability on oil recovery factor beyond water breakthrough for descending at M=0.1 88
Figure 91 Effect of wettability on oil recovery factor beyond water breakthrough for descending at M=4 88
Figure 92 Effect of wettability on movable oil recovery factor beyond water breakthrough for descending at M=0.1..... 89

Figure 93 Effect of wettability on movable oil recovery factor beyond water breakthrough for descending at M=4 89
Figure 94 Effect of permeability arrangement on oil recovery factor beyond water breakthrough for system A at β=0.7 91
Figure 95 Effect of permeability arrangement on oil recovery factor beyond water breakthrough for system A at β=0.8 91
Figure 96 Effect of permeability arrangement on oil recovery factor beyond water breakthrough for system A at β=0.9 92
Figure 97 Effect of permeability arrangement on oil recovery factor beyond water breakthrough for system A at β=1.0 92
Figure 98 Effect of permeability arrangement on oil recovery factor beyond water breakthrough for system B at β=0.7 93
Figure 99 Effect of permeability arrangement on oil recovery factor beyond water breakthrough for system B at β=0.8 93
Figure 100 Effect of permeability arrangement on oil recovery factor beyond water breakthrough for system B at β=0.9 94
Figure 101 Effect of permeability arrangement on oil recovery factor beyond water breakthrough for system B at β=1.0 94
Figure 102 Effect of permeability arrangement on oil recovery factor beyond water breakthrough for system C at β=0.7 95
Figure 103 Effect of permeability arrangement on oil recovery factor beyond water breakthrough for system C at β=0.8 95
Figure 104 Effect of permeability arrangement on oil recovery factor beyond water breakthrough for system C at β=0.9 96
Figure 105 Effect of permeability arrangement on oil recovery factor beyond water breakthrough for system C at β=1.0 96
Figure 106 Topology of a Basic ANN network 99
Figure 107 Topology of RF_m prediction FFNN-based model 101
Figure 108 Scatter plot for ascending training data 108
Figure 109 Scatter plot for ascending testing data 108
Figure 110 Scatter plot for descending training data 109
Figure 111 Scatter plot for descending testing data 109
Figure 112 Relative permeability curves for case 1 111
Figure 113 Fractional flow curve for M=0.7 at WI=0.8 111
Figure 114 Fractional flow curve for M=1 at WI=0.8 112
Figure 115 Fractional flow curve for M=4 at WI=0.8 112
Figure 116 Comparison between simulator and ANN model at M=0.7 for Ascending case 113
Figure 117 Comparison between simulator and ANN model at M=1 for Ascending case 113

Figure 118 Comparison between simulator and ANN model at M=4 for Ascending case 114
Figure 119 Comparison between simulator and ANN model at M=0.7 for Descending case 114
Figure 120 Comparison between simulator and ANN model at M=1 for Descending case 115
Figure 121 Comparison between simulator and ANN model at M=4 for Descending case 115
Figure 122 Relative permeability curves for case 2 116
Figure 123 Fractional flow curve for M=0.7 at WI=1.51 117
Figure 124 Fractional flow curve for M=1 at WI=1.51 117
Figure 125 Fractional flow curve for M=4 at WI=1.51 118
Figure 126 Comparison between simulator and ANN model at M=0.7 for Ascending case 118
Figure 127 Comparison between simulator and ANN model at M=1 for Ascending case 119
Figure 128 Comparison between simulator and ANN model at M=4 for Ascending case 119
Figure 129 Comparison between simulator and ANN model at M=0.7 for Descending case 120
Figure 130 Comparison between simulator and ANN model at M=1 for Descending case 120
Figure 131 Comparison between simulator and ANN model at M=4 for Descending case 121
Figure 132 Relative permeability curves for WI=0.6 122
Figure 133 Relative permeability curves for WI=0.7 123
Figure 134 Relative permeability curves for WI=0.8 123
Figure 135 Relative permeability curves for WI=1 124
Figure 136 Relative permeability curves for WI=1.51 124
Figure 137 Relative permeability curves for WI=2.26 125
Figure 138 Relative permeability curves for WI=2.73 125
Figure 139 Fractional flow curves for WI=0.6 126
Figure 140 Fractional flow curves for WI=0.7 126
Figure 141 Fractional flow curves for WI=0.8 127
Figure 142 Fractional flow curves for WI=1 127
Figure 143 Fractional flow curves for WI=1.51 128
Figure 144 Fractional flow curves for WI=2.26 128
Figure 145 Fractional flow curves for WI=2.7 129
Figure 146 Scatter plot for WI testing between simulator Vs. ANN correlation for ascending 129

Figure 147 Scatter plot for WI testing between simulator Vs. ANN correlation for descending..... 130
Figure 148 Relative permeability curves for field A 132
Figure 149 Factional flow curve for field A 132
Figure 150 Comparison of water flood performance of two different wells from Field A with the developed correlation..... 133
Figure 151 Relative permeability curves for field B 135
Figure 152 Factional flow curve for field B 135
Figure 153 Comparison of water flood performance of two different wells from Field B with the developed correlation..... 136
Figure 154 Fractional flow curve for System B at M=1.062..... 137
Figure 155 Comparison of Ascending Correlation with CGM Method 138
Figure 156 Comparison of Descending Correlation with CGM Method 138

LIST OF ABBREVIATIONS

β	:	Density ratio
Φ	:	Porosity
λ_D	:	Displacing fluid mobility
λ_d	:	Displaced fluid mobility
μ_o	:	Oil viscosity, cP
μ_w	:	Water viscosity, cP
1D	:	One Dimensional
2D	:	Two Dimensional
ANN	:	Artificial Neural Networks
B_o	:	Oil formation volume factor, RB/STB
B_w	:	Water formation volume factor, RB/STB
D_x	:	Number of cells in x-direction
D_y	:	Number of cells in y-direction
D_z	:	Number of cells in z-direction
DR	:	Density ratio
E_D	:	Displacement efficiency
E_A	:	Areal sweep efficiency
E_i	:	Vertical sweep efficiency
E_V	:	Volumetric sweep efficiency
FFNN	:	Feedforward Neural Network
f_w	:	Production water cut
k_{rw}	:	Relative permeability to water
k_{ro}	:	Relative permeability to oil

$\mathbf{k_{rwe}}$	:	Endpoint relative permeability to water
$\mathbf{k_{roe}}$	:	Endpoint relative permeability to oil
$(\mathbf{k_{rw}})_{\mathbf{S_{or}}}$	:	End point relative permeability to water at residual oil saturation
$(\mathbf{k_{ro}})_{\mathbf{S_{wc}}}$	:	End point relative permeability to oil at connate water saturation
$(\mathbf{k_{rw}})_{\overline{\mathbf{S_{wf}}}}$	:	End point relative permeability to water at average water saturation behind the front
$(\mathbf{k_{ro}})_{\overline{\mathbf{S_{wf}}}}$	:	End point relative permeability to oil at average water saturation behind the front
$\mathbf{k_x}$	:	Permeability in x-direction, mD
$\mathbf{k_y}$	:	Permeability in y-direction, mD
$\mathbf{k_z}$	:	Permeability in z-direction, mD
$\mathbf{k_{50}}$	:	Mean permeability, mD
$\mathbf{k_{84.1}}$	:	Permeability at one standard deviation above mean value, mD
$\mathbf{k_z/k_x}$	:	Permeability anisotropy ratio
L	:	Lorenz coefficient
M	:	Mobility ratio
$\mathbf{M_{ep}}$	:	End point mobility ratio
$\mathbf{M_C}$	:	CGM mobility ratio
NMR	:	Nuclear Magnetic Resonance
$\mathbf{N_p}$	:	Cumulative oil produced, STB
$\mathbf{N_G}$	:	Gravity Number
$\mathbf{n_o}$	:	Corey's Oil exponent
$\mathbf{n_w}$	:	Corey's Water exponent

PV	:	Pore Volumes
q_i	:	Injection rate, STB/D
q_p	:	Production rate, STB/D
R^2	:	Regression coefficient
RF	:	Oil recovery factor
RF_m	:	Movable oil recovery factor
$\overline{S_{wf}}$	:	Average water saturation behind the flood front
$\overline{S_w}$	:	Average water saturation
S_{wi}	:	Initial water saturation
S_{wc}	:	Connate water saturation
S_{or}	:	Residual oil saturation
S_g	:	Gas saturation
S_o	:	Oil saturation
S_w	:	Water saturation
S_{woc}	:	Crossover water saturation in relative permeability curves
V	:	Dykstra-Parsons Permeability Variation Coefficient
V_p	:	Reservoir pore volume, ft^3
WI	:	Wettability Indicator
WOR	:	Water Oil Ratio

ABSTRACT (ENGLISH)

Full Name : Usama Yousuf

Thesis Title : Empirical Correlations for 5-Spot Water Flooding Performance with Different Permeability Sortings

Major Field : Petroleum Engineering

Date of Degree : April, 2016

Water flooding is still the recovery process responsible for most of the oil production by secondary recovery. Except for the residual oil saturation, water injected into the reservoir displaces almost all of the oil from the portions of the reservoir contacted or swept by water. An accurate estimation of flooding performance is essential for good reservoir management and proper decision making.

Different methods are used to predict water flooding performance in stratified reservoirs. The current prediction methods are based on one or more simplifying assumptions. Although commercial reservoirs simulators are available to simulate and predict the performance of water-flooding under various conditions with reasonable accuracy, but simulation is expensive and time consuming and not all engineers have access to commercial simulators. Therefore, there is a need for a correlation that can provide quick estimate with reasonable accuracy.

This study focused on developing an empirical correlation to estimate movable oil recovery factor for a five spot water-flooding pattern for communicating stratified reservoirs using a commercial simulator. Two correlations were developed by the artificial neural networks technique based on the results obtained by simulation runs covering a wide range of variables. One correlation is for ascending arrangement of permeability while the other one

is for descending arrangement of permeability. Both correlations can be used to estimate movable oil recovery factor as a function of mobility ratio (M), oil-water density ratio (β), permeability variation coefficient (V), producing water cut (f_w) and wettability indicator (WI). WI is a new parameter introduced in this study as a simple measure of wettability and is based only on features of the relative permeability curves. The correlation has been verified by using field data and simulated data.

The study aims to provide new and easy-to-use correlations to estimate performance of water-flooding projects in communicating stratified reservoirs. The use of these correlations will minimize the time and cost required for extensive simulation runs. Both correlations matched all simulator results with high accuracy. They also matched the results of simulation runs that were not utilized in developing the correlation and the performance of two different field projects with reasonable accuracy.

ABSTRACT (ARABIC)

ملخص الرسالة

الاسم الكامل: اسامه يوسف

عنوان الرسالة: علاقات تجريبية لأداء الغمر المائي على نمط النقاط الخمس مع تراتيب مختلفة للنفاذية

التخصص: هندسة البترول

تاريخ الدرجة العلمية: ابريل، 2016

ما زال الغمر المائي هو وسيلة الإستخلاص المسئولة عن معظم الزيت المنتج بوسائل الإستخلاص الثانوي. يزيح الماء المحقن في المكمن كل الزيت تقريبا من المناطق التي يلمسها او يكتسحها من المكمن. لذا يعتبر التقدير الصحيح لأداء الغمر ضروريا من أجل إدارة جيدة للمكمن وسلامة القرارات المتخذة.

هنالك العديد من الأساليب المختلفة للتنبؤ بأداء الغمر المائي في المكامن الطبقية. وتعتمد وسائل التنبؤ الحالية على واحد أو أكثر من الإفتراضات التبسيطية. وعلى الرغم من أن البرامج التجارية لمحاكاة المكامن متاحة وتستطيع محاكاة وتقدير أداء الغمر المائي تحت مختلف الظروف بدقة معقولة، إلا أن المحاكاة مكلفة وتستغرق وقتا طويلا وليست في متناول جميع المهندسين. لذلك، هنالك حاجة لعلاقة يمكنها توفير تقدير سريع وبدقة معقولة.

تمحورت هذه الدراسة حول تطوير علاقة رياضية تجريبية لتقدير معامل استخراج الزيت القابل للإزاحة بواسطة الغمر المائي على نمط النقاط الخمس لمكامن طبقية متواصلة باستخدام برنامج محاكاة تجاري. طورت علاقتان بواسطة طريقة الشبكات العصبية الاصطناعية وبناء على نتائج تشغيلات محاكاة غطت مدى واسعا من المتغيرات. احدى العلاقات هي لترتيب تصاعدي للنفاذية بينما الأخرى لترتيب تنازلي للنفاذية. ويمكن استخدام كلتا العلاقتين لتقدير معامل استخراج الزيت القابل للإزاحة كدالة في نسبة القابلية للحركة (M) ، ونسبة كثافة الزيت الى الماء (β) ، ومعامل تفاوت النفاذية (V)، ونسبة الماء المنتج (f_w) ومؤشر البلل (WI) . ومؤشر البلل هذا تم إستنباطه في هذه الدراسة كمقياس بسيط للتبلل ويعتمد فقط على خصائص منحنيات النفاذية النسبية. ولقد تم التحقق من صلاحية العلاقتين بمقارنتهما ببيانات محاكاة وأخرى حقلية.

وتهدف هذه الدراسة إلى تقديم علاقات جديدة وسهلة الاستخدام لتقدير أداء مشروعات الغمر المائي في مكامن طبقية متواصلة، حيث إن استخدام هذه العلاقات يخفض التكلفة والوقت اللذان تتطلبهما دراسة محاكاة مكثفة. ولقد طابقت كلتا العلاقتين جميع نتائج المحاكاة بدقة عالية. كما طابقتا نتائج محاكاة لم تستعمل في تطوير العلاقتين إضافة إلى أداء مشروعين حقليين مختلفين بدرجة معقولة من الدقة.

CHAPTER 1

INTRODUCTION

1.1 Overview

Water flooding is considered as one of the most successful oil recovery method. Water flooding has been widely applied in hydrocarbon fields either to support the reservoir pressure during depletion and/or to increase hydrocarbon production as a secondary recovery process. The technique consists of injecting water in a reservoir with the purpose of maintaining pressure and/or displacing and producing hydrocarbons. Water flood performance can be estimated by various analytical and empirical methods based upon several assumptions.

In this chapter some important factors related to water flooding are discussed briefly. The following chapters will discuss the most relevant previous works done related to thesis, research objectives and statement of problem, methodology, results, conclusions and recommendation.

1.2 Flood Patterns

Based on the reservoir continuity, especially considering continuity of the floodable pore volume, the injection scheme may be peripheral or have a specific injection pattern. As shown in Figure 1, there are several basic well patterns that are commonly used in water flooding, such as Four Spot, Five Spot, Seven Spot, Nine Spot, Direct Line Drive and Staggered Line Drive. Each pattern results in unique water flood performance. The five spot is the most commonly used pattern.

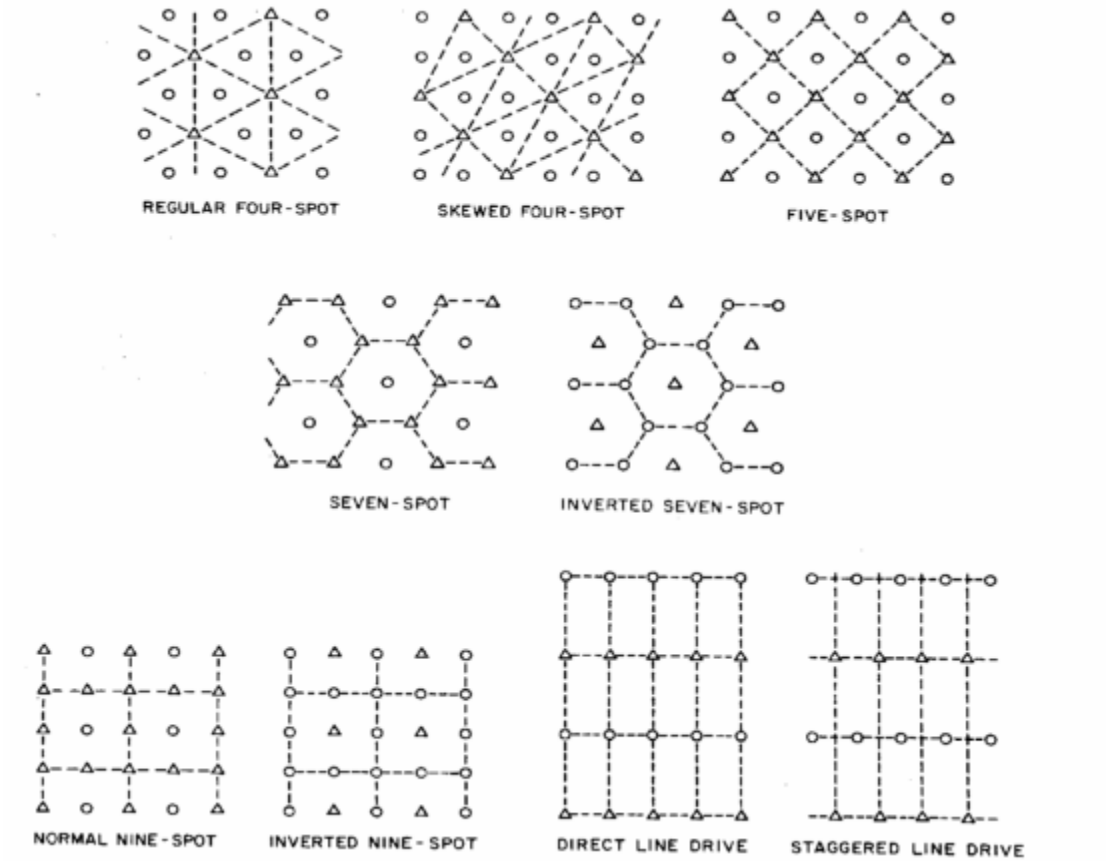

Figure 1 Illustration of water flood patterns (Craig, F.F. Jr. 1971)

1.3 Mobility Ratio

A key factor that influences the performance of a water flood and, thus, dictates the choice of flood pattern is the flood mobility ratio (*M*).

The mobility ratio (*M*) is simply the ratio of the mobility of the displacing phase (λ_D) to that of the displaced phase (λ_d)

$$M = \frac{\lambda_D}{\lambda_d} \tag{1.1}$$

Where,

M = Mobility ratio

λ_D = mobility of the displacing phase (water)

λ_d = mobility of the displaced phase (oil)

Mobility ratio is a function of viscosity and relative permeability, which in turn depends on saturation. The relative permeability to a fluid is the ratio of its effective permeability to some reference permeability, which is usually the effective permeability to oil at the connate water saturation $(k_{ro})_{Swc}$. This makes the relative permeability to oil at S_{wc} always equal to 1.0. An important aspect of mobility ratio is deciding at which saturations the mobility ratio is being evaluated. Different definitions of *M* are as follows:

(i) Mobility ratio for a water flood where piston-like flow is assumed with only water flowing behind the front and only oil flowing ahead of the front, is defined as below. The relative permeability of water and oil are obtained from the permeability/water saturation curves for a water flood

$$M_{ep} = \frac{\frac{(k_{rw})_{S_{or}}}{\mu_w}}{\frac{(k_{ro})_{S_{wc}}}{\mu_o}} \quad (1.2)$$

Where,

M_{ep} = End point mobility ratio

$(k_{rw})_{S_{or}}$ = End point relative permeability to water at residual oil saturation

$(k_{ro})_{S_{wc}}$ = End point relative permeability to oil at connate water saturation

μ_o and μ_w = Oil and water viscosities respectively

(ii) Another variation of mobility ratio is Craig's mobility ratio (M_C) given by below equation in which k_{rw} is evaluated at the average water saturation in the flooded zone at the water breakthrough instead of k_{rw} evaluated at the residual oil saturation

$$M_C = \frac{\frac{(k_{rw})_{\overline{S_{wf}}}}{\mu_w}}{\frac{(k_{ro})_{S_{wc}}}{\mu_o}} \quad (1.3)$$

Where,

M_C = Craig mobility ratio

$(k_{rw})_{\overline{S_{wf}}}$ = End point relative permeability to water at average water saturation behind the front

(iii) In this research, M has been defined by considering both k_{rw} and k_{ro} at the average water saturation behind the front $(\overline{S_{wf}})$ instead of $(k_{rw})_{S_{or}}$. In this definition, the mobility of the displacing phase incorporates the mobilities of both water and oil evaluated at$(\overline{S_{wf}})$, while the displaced phase is oil at initial conditions. This definition better represents frontal displacement in the porous media and was employed in this study which is represented in equation 1.4

$$M = \frac{\frac{(k_{rw})_{\overline{S_{wf}}}}{\mu_w} + \frac{(k_{ro})_{\overline{S_{wf}}}}{\mu_o}}{\frac{(k_{ro})_{S_{wc}}}{\mu_o}} \quad (1.4)$$

Where,

$(k_{ro})_{\overline{S_{wf}}}$ = End point relative permeability to oil at average water saturation behind the front

1.4 Permeability Variation Coefficient

Reservoirs exist with various degrees of heterogeneity due to reservoir's geological conditions. As a measure of reservoir heterogeneity, Dykstra and Parsons introduced the coefficient of permeability variation. This coefficient of permeability variation (*V*) indicates the heterogeneity of a reservoir. The complete steps to calculate *V* are given in Chapter 4. The value of *V* varies from 0 to 1 with 0 indicating a homogeneous reservoir while a value of 1 corresponds to a completely heterogeneous reservoir. It can be defined as

$$V = \frac{k_{50} - k_{84.1}}{k_{50}} \tag{1.5}$$

Where,

k_{50} = Permeability value at 50 % from permeability-log distribution graph

$k_{84.1}$ = Permeability value at 84.1% from permeability-log distribution graph

1.5 Wettability Indicator

Wettability is the tendency of one fluid to adhere to or spread on to a specific solid surface in the presence of another immiscible fluid. When two immiscible fluids come in contact with a solid surface, one of the fluids is usually attracted more to the solid than the other. This fluid is generally called the wetting phase and the other is termed as non-wetting phase. Wettability is explained quantitatively by examining the force balances between two immiscible fluids at the contact line between the two fluids and the solid. Generally, one of the fluids is water. As such, the contact angle measured through the water phase is the basis of measurement of the wetting phase. Contact angles less than 90 are called water-wet, and those approaching 180 are termed as oil-wet systems. When the contact angle is around 90, then it is called intermediate wettability. Other methods to assess or quantify wettability include Amott method, NMR (Nuclear Magnetic Resonance) etc.

Rock wettability is an important factor, which affects the flow behavior in oil reservoirs. It has a profound effect on the shape of relative permeability and capillary pressure curves and consequently on oil displacement processes in porous media. The residual oil is high in oil wet rocks when compared to water wet rocks as can be seen from Figures 2 and 3. Oil wet rocks usually cause low oil recovery compared to water wet rocks. In water wet rocks, the connate water saturation is low in unaffected portions of the reservoir and exists as a film around sand grains while the remaining pore are full of oil. In portions where both oil and water are flowing, some oil exists in continuous channels while the other oil has been isolated and trapped by the invasion of water. At floodout, only isolated and trapped oil exists in the rock resulting in high recovery. As the water is injected and enters an oil wet reservoir, it forms continuous flow channels through the largest pores. With the passage of time as the injection continues, smaller pores are also invaded and form other continuous channels and once there are sufficient channels, the water flows easily while the oil flow ceases. The residual oil saturation exists in smaller flow channels and as a film in larger, water-filled channels.

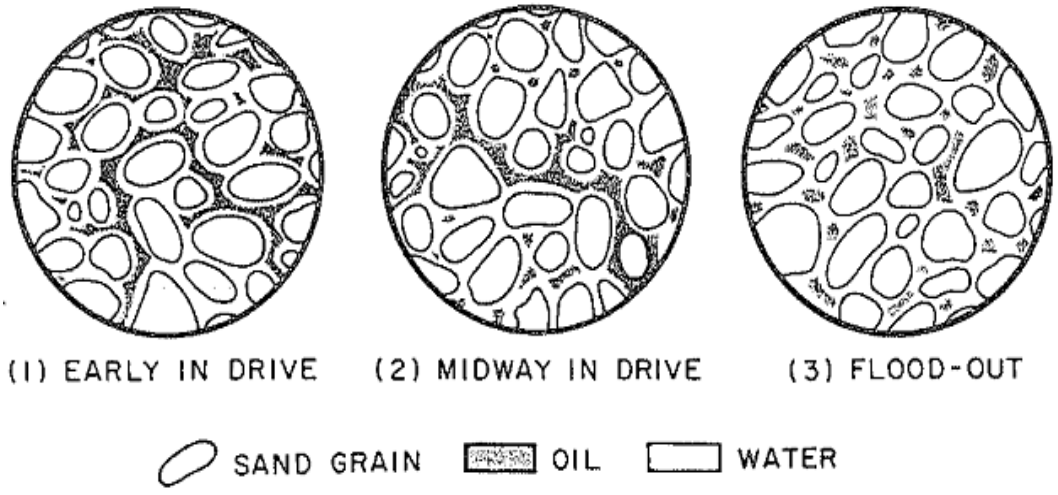

Figure 2 Fluid distribution during water flood of water-wet rock (Craig, F.F. Jr. 1971)

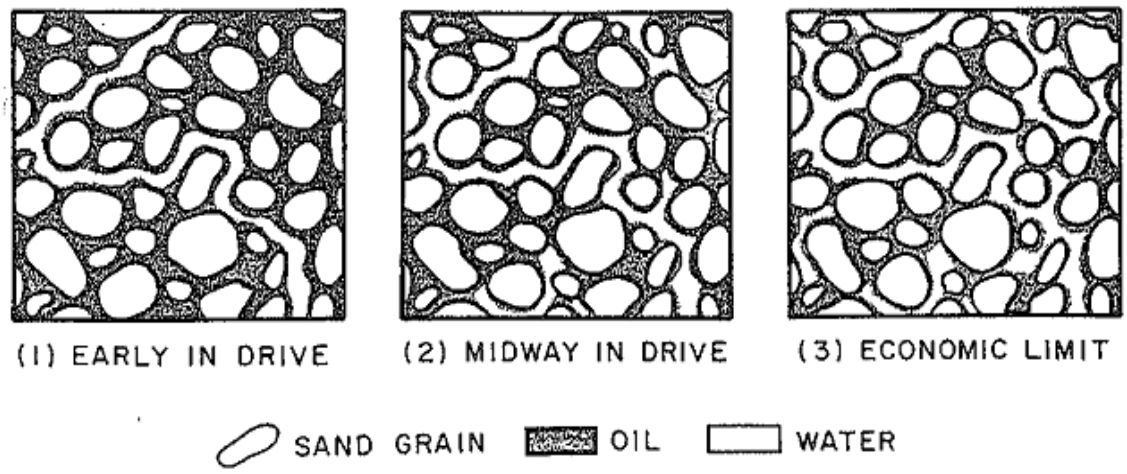

Figure 3 Fluid distribution during water flood of oil-wet rock (Craig, F.F. Jr. 1971)

Wettability, thus, affects the shape of the relative permeability curves. The relative permeability characteristics are a direct measure of the ability of a porous medium to conduct one fluid when one or more fluids are present. The differences in the flow properties that indicate the different wettability preferences can be illustrated by the following rule of thumb as shown in Table 1.

Table 1 Wettability Preferences

Characteristic	**Water-Wet**	**Oil-wet**
Connate water saturation	Usually greater than 20 to 25 % PV	Generally less than 15 % PV and frequently less than 10 %
Saturation at which oil and water relative permeabilites are equal	Greater than 50 % water saturation	Less than 50 % water saturation
Relative permeability to water at maximum water saturation (at floodout)	Generally less than 30 %	Greater than 50 % and approaching 100 %

To consider the effect of rock wettability – through the relative permeability curves - on recovery factor, a new term called the "Wettability Indicator *(WI)*" is introduced in this work. *WI* is based only on features of the relative permeability curves, which are the crossover water saturation and the relative permeability to water at residual oil saturation as shown in equation 1.6.

$$WI = \frac{S_{woc}}{(k_{rw})_{S_{or}}} \quad (1.6)$$

Where,

S_{woc} = Crossover water saturation in relative permeability curves

$(k_{rw})_{S_{or}}$ = End point relative permeability to water at residual oil saturation

The crossover water saturation is the water saturation at which the relative permeability curves of oil and water intersect each other. *WI* is less than 1 for oil-wet systems and greater than 1 for water-wet systems.

1.6 Recovery Factor

The success of any water flooding project depends on the recovery factor (*RF*). The recovery factor is the product of the displacement efficiency (E_D) and the volumetric sweep efficiency (E_V).

$$RF = E_D \times E_V \quad (1.7)$$

E_D is the fraction of oil displaced from a contacted volume of reservoir rock on a microscopic (pore) scale. It depends on the relative permeability characteristics of the rock as well as the viscosities of the displacing and displaced fluids. It can be estimated as a function of water and oil saturations

$$E_D = \frac{\overline{S_w} - S_{wc} - S_g}{1.0 - S_{wc} - S_g} \quad (1.8)$$

Where,

S_{wc} = connate (initial) water saturation in the contacted volume, fraction

S_g = gas saturation in the contacted volume, fraction

$\overline{S_w}$ = average water saturation in the contacted volume after flooding by water, fraction

E_V represents the fraction of the reservoir volume swept by the injected water at a given time. It is the product of the areal and vertical sweep efficiencies. The areal sweep efficiency (E_A) is the fraction of the area of the flood pattern swept by water and is a result of the nonlinear flow between injection and production wells. It depends on the oil and water relative permeabilities (k_{ro} and k_{rw}), areal heterogeneity, flood pattern, the mobility ratio, and the amount of injected water expressed in pore volumes of displaceable hydrocarbons. The vertical sweep efficiency (E_i) is the fraction of the vertical cross-sectional area of the reservoir between the injection and production wells that is swept by water at a given time. The vertical sweep efficiency is mainly dependent on the permeability variation in the producing zone but also depends on the mobility ratio of the displacing fluid to the displaced fluid.

Two types of recovery factors have been used in our work which can be defined as follows:

1- Recovery factor (*RF*) values that are obtained directly from simulation output are based on initial oil in place

2- Recovery factor (RF_m) that is based on movable oil saturation and is defined as

$$RF_m = \frac{N_P}{V_P\left(\frac{1- S_{wi} - S_{or}}{B_o}\right)} \tag{1.9}$$

Where,

N_P = Cumulative oil produced, STB

V_P = Reservoir pore volume, RB

B_o = Oil formation volume factor, RB/ STB

S_{wi} = Initial water saturation, dimensionless

S_{or} = Residual oil saturation, dimensionless

RF_m = Movable recovery factor, dimensionless

The reason for converting *RF* to RF_m is that the movable oil saturation represents the maximum fraction of oil that can be moved or produced ultimately, hence, the values obtained for RF_m will be more realistic for flood efficiency purposes.

1.7 Displacement in a Five-Spot Pattern

Analysis of a five-spot pattern in a reservoir can be simplified by examining the behavior of a single five-spot pattern. A regular five-spot pattern consists of a production well surrounded by four injection wells. It is assumed that the injection rates are equal to the production rates. Thus flow is symmetric around each injection well with 0.25 of the injection rate from each well confined to the pattern and results in four symmetric quadrants (Figure 4). In simulation, use of single quadrant model will result in significant saving in CPU time. We used single quadrant in our simulation model.

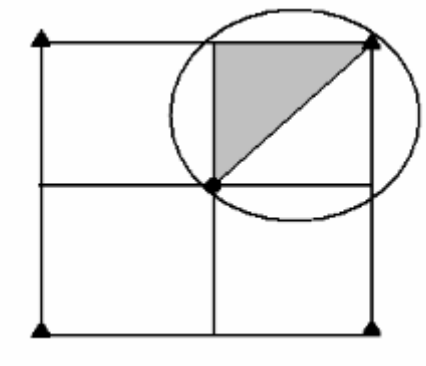

Figure 4 Single five-spot pattern with a circle showing one quadrant

1.8 Reservoir Simulation

A commercial reservoir simulator was employed in this study to generate the data. Reservoir simulation is now one of the most comprehensive and widely used water flood prediction tools. When used properly, it can be a very useful tool for water flood design, planning, and surveillance. Simulation is a powerful technique when used to develop forecasts of a complex reservoir with varying fluid properties. However, while simulation can yield results that are superior to and more detailed than other methods, it also generally requires a lot more data and time. A range of uncertainty in the input data leads to a resulting band of uncertainty in the output. A good understanding of the uncertainties, multiple realizations, and sensitivity analysis will significantly increase the value and usefulness of the simulation results.

1.9 Thesis Organization

This thesis report has been divided into seven chapters. Chapter 2 presents a literature review. Chapter 3 states the problem and the research objectives. Chapter 4 covers the details related to simulation and methodology used in various calculations. Chapter 5 reports all the simulation results and discusses them. Chapter 6 covers all the work related to developing and testing an empirical correlation while Chapter 7 provides the conclusions and recommendations for future work.

CHAPTER 2

LITERATURE REVIEW

The discovery of water flooding was accidental and dates back to the 18th century. Since its discovery, numerous works have been carried out to better understand how oil is displaced by water and the factors affecting the displacement efficiency. During the past 60 years, several attempts have been made to forecast water flood performance by modeling the sweeping process of water displacing oil through the porous medium. Different researchers came up with different models and correlations. Some correlations are available to estimate volumetric sweep efficiency while others are used to estimate areal and vertical sweep efficiencies. Therefore, during the course of this thesis, emphasis is placed in finding literature pertaining to the methods developed to estimate various efficiencies used to predict water flood performance. A review of previous research works carried out on the subject is presented and discussed briefly in the following paragraphs.

Buckley and Leverett (Buckley et. al, 1942) presented the frontal advance theory to explain the mechanism of oil displacement by water in a linear one dimensional (1D) system. In their approach, oil displacement occurred under a seemingly diffuse flow condition, which signified the uniform fluid saturations distribution with respect to thickness, in a linear displacement path. The authors presented a 1D flow equation – the frontal advance equation - that described this immiscible displacement. The equation also described the velocity of the oil displacing constant water saturation plane in a 1D linear system.

Stiles (Stiles, 1949) developed a method for predicting the performance of water flood operations that basically involves accounting for permeability (*k*) variations i.e. vertical distribution of flow capacity (*kh*). The most important assumption made was that within the reservoir of various permeabilities, injected water sweeps first the zones of higher permeability and that first breakthrough occurs in these layers. The different flood-front positions in liquid-filled linear layers having different permeabilities is different with each layer being insulated from the others. Stiles assumed that the rate of water injected into each layer depends only upon the *kh* of that layer. This is equivalent to assuming a mobility ratio (*M*) of unity. Also it was assumed that fluid flow was linear and the distance of penetration of the flood front was proportional to its permeability-thickness product.

The Stiles method assumed a piston-like oil displacement, which meant that there was only water production after the occurrence of water breakthrough in any layer. In his work, Stiles rearranged the layers according to their permeabilities in descending manner.

A correlation was presented by Dykstra and Parsons (Dykstra et. al, 1950) between water flooding recovery and both mobility ratio and permeability distribution. This correlation was based on calculations applied to a layered linear model with no crossflow.

This first work on vertical stratification with inclusion of mobility ratios other than unity was presented in their work. They had developed an approach for handling stratified reservoirs, which allowed for calculating water flood performance in multi-layered systems. But their method was based on piston-like assumption.

More than 200 flood tests were conducted on more than 40 California core samples in which initial fluid saturations, mobility ratios, producing WOR's, and fractional oil recoveries were measured. The permeability distribution was measured by the coefficient of permeability variation (*V*).

The correlations presented by Dykstra and Parsons relate oil recovery at producing WOR's of 1, 5, 25, and 100 as a fraction of the initial oil in place to the permeability variation, mobility ratio and the connate-water and flood-water saturations. The values obtained assumed a linear flood since they were based upon linear flow tests.

The Dykstra-Parsons method considered the effect of vertical variations of horizontal permeabilities for the water flood performance calculation and permeabilities were arranged in descending order. Following is a full list of assumptions for Dykstra-Parsons approach.

1. Linear flow
2. Incompressible flow
3. Piston-like displacement
4. Each layer is homogenous
5. No crossflow between layers
6. Pressure drop for all layers is the same
7. Constant water injection rate
8. Velocity of the front is proportional to absolute permeability and end point mobility ratio of the layer

H.J. Welge (Welge, 1952) presented a simplified method to the frontal advance equation. This method dealt with attaining the average water saturation behind the water front. This was achieved by integrating the entire distribution of water saturation from the injection point to the water front.

A.B Dyes et al. (A.B Dyes et. al, 1953) studied the effect of the fluid mobilities on the sweep out pattern due to the injection of water or gas after breakthrough of the injected fluid. Mobility ratios for miscible phases in the range of 0.1 to 17 were studied for several pattern floods (five-spot, staggered-line drive and direct-line drive).

The experimental data required for those studies were obtained by the use of the x-ray shadowgraph technique using miscible oil phases of different viscosities in porous plate models of a reservoir element.

For floods in which no saturation gradient is present in either the swept or un-swept region, the mobility ratio of the system could be characterized by the ratio of the sum of the mobility of each phase flowing in the un-swept region ahead of the front to the sum of the mobility of each phase flowing in the swept region behind the front.

The information obtained represented the conditions of the model in which the mobility ahead of the front and that behind the front was constant, the thickness and absolute permeability were uniform, no flow of the displaced phase occurred behind the front and only one mobile phase was present in the un-swept region.

High ultimate sweep out pattern efficiencies were obtained (85-100 per cent) for most mobility ratios encountered in field operations; and the economic aspects of the rate of oil recovery and the total amount of fluid to be injected caused the higher mobility ratio floods to be much more favorable.

Craig et al. (Craig et. al, 1954) developed a correlation for areal sweep efficiency at and after breakthrough by conducting a series of water and gas injection pattern floods in the laboratory to study the oil recovery performance of these systems. The model floods were scaled to reproduce

field performance under gas and water five-spot injection for a homogeneous medium. A method was developed for applying the concept of mobility ratio to dispersed gas drives and water flooding in a five-spot well pattern. The areal sweep efficiency of dispersed gas drives lied in the range of 50 to 100 percent, greatly higher than previously expected.

In the same study a method was brought forward for predicting the water-oil performance in water flooded uniform sands for five spot well patterns. The method was proved experimentally for the condition of no initial free gas and for gas saturation values normally encountered in fields following depletion operations. Production performance for pattern gas injection was also predictable by this method.

The mobility ratio was calculated with the assumption that the relative permeability to water at residual oil saturation was the same throughout in the invaded zone.

Results obtained in this manner were not coherent with published correlations; and this was true in particular for the lower range of the calculated mobility ratios. The constant decrease in the mobility of injected fluid in immiscible fluid flooding was also taken into consideration in this study. Many methods were tested to attain a singular representative water permeability value for the overall water conductivity in the invaded zone. The method that demonstrated good fitting involved the use of relative water permeability at the mean water saturation behind the stabilized region.

Carl E. Johnson Jr., (Johnson, 1956) presented Dykstra-Parsons' correlation between permeability variation *(V)*, water oil saturation (S_w), mobility ratio *(M)* and recovery on a single graph for producing water/oil ratios (*WOR*) of 1, 5, 25 and 100. A linear flood recovery can be estimated from the graphs based on the values *V*, *M*, S_w and *WOR*.

E. T. Guerrero and R. C. Earlougher, (Guerrero et. al, 1961) used an empirical method to predict water flood reserves and performance and compared the results with four analytical methods: Stiles, modified Stiles, Dykstra-Parsons, and Prats et al. The results were compared on two water floods where the water-flood recovery and performance were known. The principal assumption involved in the method was that the performance of a water flood can be predicted based upon the known performance of a similar flood or the average known performance of many water floods. Another consideration was that it must be possible to attain and maintain a predetermined water-injection rate throughout the flood life. The empirical method was found to give as good or better results than most of the analytical approaches. For the two floods studied, the Prats et al. and empirical methods developed in this paper resulted in the best fit with actual performance.

Martin Felsenthal et al. (Felsenthal et. al, 1962) developed a method that allowed a more realistic evaluation of water flood oil recovery from depleted stratified reservoirs than was possible by the other prediction methods at that time. This method modified the Dykstra-Parsons' equation to allow for liquid resaturation of the free gas space in each individual layer. The method is especially useful for evaluating the optimum formation pressure at which to start a flood in order to produce the greatest total yield of primary and secondary oil. Other modifications allowed for layer-to-layer variations of porosity and initial and final saturations, but the effects of these latter modifications were not believed to be large enough to justify their use in water flood predictions.

J. E, Warren and J. J. Cosgrove (Warren et. al, 1964) proposed a model based on modification of Dietz's theory. The model approximated the effect of crossflow in predicting how a stratified reservoir would behave while undergoing a water flooding operation. The effect of variable porosity on the recovery was also considered. For the cases studied, an assumption was made that the hydrocarbon pore volume and the permeability could be characterized by a normal and a log-

normal distribution, respectively. A simple graphical technique was developed to foretell the performance of a stratified system and the results obtained by this method were compared with the ones obtained by the Dykstra-Parsons method. It was concluded that: (1) in a stratified system the crossflow effect could be significant, mainly at extremely favorable or unfavorable mobility ratios and (2) under normal conditions, however, the porosity variation effects could be neglected.

Using a finite difference method C S. Goddln et al. (Goddln et. al, 1966) computed water-flood performance of a stratified system that was water wet and experienced crossflows. The effects of 5 dimensionless factors on the oil displacement efficiency, crossflow rates and water saturation contours were assessed without gravity forces. Crossflow as a result of viscous and capillary forces was shown to impart a substantial effect on the oil recovery in a field scale model of a dual layered, water wet sandstone reservoir system. Maximum crossflow was encountered in the locality of the front advancing in the more permeable layer. Under favorable conditions (mobility ratio <1), the computed oil recovery along with the effect of crossflow always lied between the values predicted for a layered reservoir without crossflow and that for a uniform reservoir.

W.J McGuire (McGuire, 1968) developed a simple mathematical model capable of predicting flooding efficiency in a stratified reservoir and tested the results of the model against visual observations in fluid flow models. In the design of the mathematical model, the original assumptions of Dykstra and Parsons were made with two exceptions. Firstly, the difference in the two fluids was one of viscosity only, and the effects of relative permeability difference were not considered. Secondly, crossflow between strata was allowed.

The developed mathematical model was capable of predicting breakthrough efficiency in a stratified system with a degree of accuracy comparable to laboratory investigations. It was found that the degree of inter-strata flow induced by viscosity differences in displacing and displaced

fluids at mobility ratios greater than unity was significant and the ratio of strata widths was an important variable, particularly when large mobility ratios were concerned.

F. F. Craig, Jr. (Craig, 1970) studied the effect of the number of layers on performance prediction of a five spot fluid injection scheme. A log normal permeability distribution was assumed for each layer with the coefficients of variation lying between 0 and 0.8. The variation in the number of layers ranged from a single producing layer to 100 layers. The effect of mobility ratio on the performance was extensively studied over the range from 0.05 to 5.0. Its effect on fluid injectivity and on volumetric sweep at breakthrough was also studied.

It was concluded that for a multilayered reservoir, the injected fluid distribution amid the greatest and the smallest permeable layers was affected by the mobility ratio. Also, in a 5-spot pattern, the main influence of mobility ratio on breakthrough was between the mobility ratio of 0.1 and 10, with the greatest effect encountered near the value of 1. At particular M and k values, the volumetric sweep efficiency gets reduced with respect to increasing number of layers at the time of breakthrough.

Mobarak (Mobarak, 1975) predicted and compared *WOR*-recovery performance for three different systems using standard Dykstra-Parsons method, the modified Dykstra-Parsons and the numerical model for different layered systems. Results show good agreement between the performances predicted by the modified Dykstra-Parsons method and the numerical model. The standard Dykstra-Parsons method showed low oil recoveries over the whole range of *WOR*.

Mohammed E. Osman and Djebbar Tiab (Osman et. al, 1981) modified Dykstra-Parsons technique to forecast the water flooding performance in multi-layered composite reservoirs. The modification considered the variations in reservoir properties and dimensions both vertically and horizontally. Two important cases, constant rate of injection and constant injection pressure, were considered. It was found that the mobility ratio is the controlling factor of the water flooding performance in multi-layered composite linear reservoirs. The following conclusions were made:

1. For a particular mobility ratio the coverage, water-oil ratio, cumulative water injection and cumulative oil production are not functions of injection rate or the pressure drop. It is because oil displacement is assumed to be piston like. However, the rate of oil production increases with increasing injection rate and/or pressure drop.
2. For a specific stratified composite reservoir, the breakthrough order of its layers is dependent upon the mobility ratio. As the mobility ratio rises, the water breaks through earlier.
3. For unit mobility ratio, the pressure drop is constant for a constant rate of injection during the water flood life. However, for a mobility ratio different from 1, the pressure drop, and consequently the injection pressure, varies during the water flood life.

Noaman EI-Khatib (EI-Khatib, 1985) developed a mathematical technique for the performance of water-flooded, linear, stratified systems for both the cases of communicating layers with total crossflow and for layers without communication and zero crossflow. The model assumed no particular permeability distribution and accounts for the variation in other rock properties such as porosity and fluid saturations. Piston-like displacement was assumed where ahead of the displacement front only producible oil flowed and behind the front only residual oil is left. The model predicts the water cut, the total injected volume, the fractional oil recovery and the change

in injection rate or the change in the total pressure drop at the instance of water breakthrough in the sequential layers.

It was observed that reservoir systems experiencing crossflow between layers got improved oil recovery when the mobility ratio was favorable (M<1) and reduced oil recovery when it was unfavorable (*M>1*). A change in fluid saturation and porosity with respect to permeability showed increased values of oil recovery compared to uniform saturation and porosity case for both favorable and unfavorable mobility ratios. This effect was almost independent of mobility ratio for non-communicating systems and increased as the mobility ratio decreased for communicating system.

D. Tiab and M.E, Osman (Tiab et. al, 1986) modified the Dykstra-Parsons' method to predict water flooding performance of a multilayered composite reservoir. The modification was extended to the case of constant injection pressure. They proposed a model in which layers were supposed to be consisting of numerous blocks with different transmissibility (kh/μ) and storage (Φch). In their study, it was found out that it is not necessarily true that the displacing fluid sweeps faster through the higher permeability zones causing most of the oil in the less permeable layers to be produced over an extended period of time at high *WOR*. Instead, this varied from layer to layer and block to block. The water flooding performance in a layered composite reservoir depends mainly on the mobility ratio; the higher the mobility ratio, the earlier would the reservoir breakthrough.

K.K. Pande et al. (K.K. Pande et. al, 1987) studied the application of one-dimensional, frontal advance theory on the displacement processes that occur in heterogeneous porous media. They examined the assumptions required for the application of a generalized frontal advance equation in a heterogeneous porous medium. Based on these assumptions the material balance equations were derived and the theory was established by its application to the Dykstra-Parsons' flow model

in non-communicating layers. The results showed that the frontal advance theory could be applicable to flow in the said media for processes which showed linear characteristics.

It was concluded that the 2D Dykstra-Parsons' flow model in a layered system could be developed utilizing the 1D frontal advance theory with the heterogeneity effects represented in the fractional flow expression. For a linear system with unit mobility ratio an exact agreement was obtained between the 1D and 2D representations. The agreement was qualitative only for the non-unit mobility ratio case.

Pseudo-relative permeability functions can be determined that could exactly replicate the calculated oil recovery for a non-communicating layered system as computed from the Dykstra-Parsons' model. These pseudo-relative permeability functions hinge on the mobility ratio and the permeability variation.

A.O. DeSouza and W.E. Brigham (DeSouza et. al, 1995) extended Dykstra-Parsons' work by applying a more precise theoretical approach to calculate the water oil-ratio. For the sake of greater accuracy, 200 layers were considered rather than 50. Because of these differences the resulting curves were slightly modified. Using empirical simplifications with considerable success, a single curve was obtained for the entire set of 130 curves that would include the parameters: coverage, permeability variation, mobility ratio, and water-oil-ratio. This curve can be used in an equation to calculate coverage over a broad range of parameters. The permeability variation can range from 0.3 to 0.8, the mobility ratio can range from 0.1 to 10, and the water-oil ratio from 1 to 100. In this correlation, low *WOR's* of 1.0 showed greater errors in predicting coverage (up to 8% in error), but higher values of *WOR* produced errors of less than 2% over the entire range of the correlation's validity.

W. M. Cobb and F. J. Marek (Cobb at. al, 1997) presented a technique for computing volumetric sweep efficiency using only oil production data. The method is based upon volumetric material balance and standard water flooding principles and is only valid after free gas fillup. The technique for estimating volumetric sweep efficiency is applicable in those reservoirs in which the water flood is initiated when reservoir pressure is either above or below the initial bubble point pressure. The computed volumetric sweep can be coupled with routine production decline curve analysis to estimate ultimate volumetric sweep under existing injection and production practices. The technique can be used to provide insight to the oil recovery potential under alternate injection schemes. Application of the procedure is independent of water flooding pattern scheme. Parameters that greatly influence the results of the analysis are pre-water flood oil saturation, pore volume that could be effectively flooded, and connate and average water saturations of the reservoir's swept regions.

Noaman EI-Khatib (EI-Khatib, 1997) developed an analytical solution for water flooding performance of layered reservoirs with complete crossflow between layers. The permeability distribution was kept log normal and the permeability variation was characterized by the Dykstra-Parsons coefficient. The performance was expressed in terms of vertical coverage as a function of the producing *WOR*. An expression was derived for time in dimensionless domain in terms of pore volumes of injected water at a particular *WOR*. Expressions were also derived for fractional flow curves and pseudo-relative permeability functions. Pseudo-relative permeability functions are dependent on saturation and heterogeneity. The performance calculations were compared to the Warren and Cosgrove method using their data. The performance results calculated using the developed correlation chart were in agreement to the results obtained by Warren and Cosgrove method.

Noaman EI-Khatib (EI-Khatib, 2003) developed an analytical method for performance study of stratified reservoirs undergoing water flooding where the effects of gravity between neighboring layers were also accounted for. The layers were ordered as per data from core samples or well logs or as random sampling from a specific distribution. Differential equations were derived and solved for the rate of advance of the displacement fronts in a few successive layers of descending permeability.

The effects of gravity number (N_G) defined as the ratio of gravity forces to viscous forces, M and V on the water flooding performance were investigated and the pseudo-relative permeability expressions were also derived.

The results showed that crossflows due to gravitational effect caused delayed water breakthrough in highly permeable zones, boost oil recovery and reduce the water cut. For regions with unfavorable mobility ratios and for reservoirs that are highly heterogeneous ($V=1$), the effect of gravitational crossflow is more prominent on the performance. The influence of gravitational crossflow is directly related to the gravity number up until a value of one; after that the effect on performance becomes small.

Noaman EI-Khatib (EI-Khatib, 2012) modified Dykstra-Parsons equations to incorporate reservoir inclination. A mathematical model was developed that consisted of a dimensionless gravity number that incorporated both the fluid density difference (between displaced and displacing fluids) and the dip angle. The model is useful in estimating the water cut, the injectivity ratio, the fractional oil recovery and the injected pore volumes at the moment of water breakthrough in the successive producing layers. The effects of the gravity number, M and V on the performance were also investigated.

It was observed that for a positive gravity number (up dip water injection), the performance was enhanced in respect of delayed breakthrough of water, decreased water cut and increased fractional oil recovery as compared with horizontal layers. This was true for both favorable and unfavorable mobility ratios; however, it was more prominent in the case of unfavorable mobility ratio and very heterogeneous reservoirs. For the case of a negative gravity number (downdip water injection) the opposite behavior was observed.

The results were also compared with the performance of inclined communicating reservoirs having complete crossflow. The effect of communication between layers on the fractional recovery of oil was found to cause enhancement for the favorable and unit mobility ratio cases. For unfavorable mobility ratio the recovery was reduced.

CHAPTER 3

PROBLEM STATEMENT AND RESEARCH OBJECTIVES

As observed in the literature review, numerous works have been done which are either empirical or analytical. Some correlations are available to estimate areal sweep efficiency while others are used to estimate vertical sweep efficiency and are based upon several assumptions that many times are either ignored or violated. There is no standard method to estimate the recovery factor for water flooding projects. Most of the previous work is related to the line drive pattern and not much work was done on the five spot pattern, which is the most common pattern.

Most of the correlations developed are based on piston-like displacement, which results in inaccurate estimation. For example, the oil production rate predicted by Dykstra-Parsons method was compared against that from numerical simulation (GeoQuest Eclipse 100). The reservoir model is 2-layered, 1200 ft. long, 400 ft. wide, and each layer is 35 ft. thick. The total water injection rate is 800 STB/D. The results are shown in Figure 5 below [24]

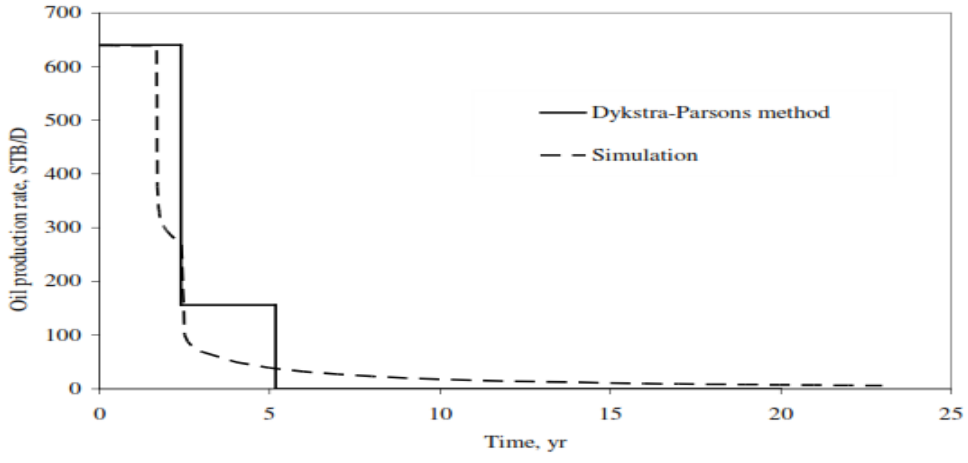

Figure 5 Oil production: comparison between the Dykstra-Parsons method and numerical simulation for 2-layered model, i_w = 800 STB/D

Two main observations can be made based on the above Figure. First, the water breakthrough time based on simulation is significantly earlier compared to that from Dykstra-Parsons method. Second, cumulative oil produced at the moment of breakthrough in layer 1, is more for the Dykstra-Parsons method compared to simulation. This is because Dykstra-Parsons model assumes that at breakthrough, all moveable oil has been swept from layer 1, whereas in the simulation model at breakthrough, there is still moveable oil behind the front.

Reservoir simulation is one of the most powerful technique used in the oil and gas industry by engineers to forecast and visualize reservoir performance efficiently. Considering the fact that extensive simulation is a costly and time-consuming practice, and not all petroleum engineers have access to the simulators, an empirical correlation that provides a quick and reasonably accurate estimate of the recovery factor based on movable oil saturation without the need to perform a simulation study will be a beneficial tool to the industry.

3.1 Research Objectives

The goal of this research is to develop an empirical correlation that estimates the recovery factor based on movable oil saturation for five-spot pattern flooding in communicating stratified reservoirs without assuming piston-like displacement. The correlation will be based on numerical simulation results. The correlation will consider the reservoir's permeability variation (V), production watercut (f_w), the flood's mobility ratio (M), rock wettability and oil-water density ratio (β). The correlation will allow the estimation of movable recoverable oil for any combination of these parameters in communicating stratified reservoirs. The correlation is to be validated using field data.

CHAPTER 4

SIMULATION AND CALCULATIONS

Simulation data is required to obtain the desired correlations. After extracting the required data from simulation results, a suitable statistical technique can be used to generate the correlation. This chapter presents the major work done in obtaining the correlation and can be divided into the following major parts:

1. Methodology
2. Development of simulation model
3. Data extraction

4.1 Methodology

To develop the new empirical correlation, water-flood performance was obtained by numerical simulation employing ECLIPSE commercial simulator. The simulated data was generated for both ascending and descending order of permeability with a constant value of anisotropy ratio (k_z / k_x) equal to 0.1, thus allowing crossflow between the layers. Five parameters are varied in the ranges shown in Table 2. Once the simulated data was obtained, artificial neural network technique was employed to generate the correlation.

Table 2 Parameter ranges used in simulation

Parameter	Range
Mobility Ratio	0.1-4
Coefficient of Permeability Variation	0.1-0.9
Oil to Water Density Ratio	0.7-1
Rock Wettability	Strong oil-wet to strong water-wet
Production Watercut (fraction)	0 -0.95

4.2 Conditions and Limitations

Some of the main assumptions for developing the simulation model were as follows:

1. Incompressible displacement
2. Except for absolute permeability, the rock and fluid properties are the same for all the layers
3. Multilayered reservoir with layers of equal thickness
4. Absolute permeability data of the layers conform to a log-normal probability distribution
5. Relative permeability curves are same for all layers and estimated using Corey-type equations
6. Cross-flow between layers (k_z/k_x = 0.1)
7. No gas present initially, S_{gi} = 0, i.e. liquid filled
8. Capillary pressure is negligible
9. Porosity is same for all layers
10. Confined ¼ of five spot pattern
11. Constant injection and production volumetric rates, $q_i = q_p$

4.3 Calculation of Coefficient of Permeability Variation and Permeabilities

In order to obtain a value of permeability for each layer corresponding to each coefficient of permeability variation (V), it is assumed that the reservoir has a log normal permeability distribution. The permeability of each layer for V values of 0.1, 0.3, 0.5, 0.7 and 0.9 has been calculated. Before describing the method of assigning permeability values to the layers, the

procedure outlined by Dykstra-Parsons [8] to calculate *V* for a reservoir is presented below for better understanding:

1. Obtain permeability values for samples representing equal intervals.

2. Arrange the permeability data in decreasing order.

3. Determine for each value the percent of values with greater permeability and express each number as cumulative percentage, or ―percent greater than.

4. Plot the data on log-probability graph, with permeability on the log scale and percent on the probability scale.

5. Estimate the best fit for a straight line and determine permeability values at 84.1% and at 50% probabilities.

6. Determine the Dykstra-Persons coefficient using the expression:

$$V = \frac{k_{50} - k_{84.1}}{k_{50}} \tag{4.1}$$

A set of permeability values is assumed for 10 layers as shown in Table 3. Following the Dykstra-Parsons procedure, a value of k_{50} is determined to be 58 mD as illustrated by Table 4 and Figure 6.

Table 3 Reservoir Permeability Data

Thickness, h (ft)	Permeability (mD)
1	2
2	40
2	45
2	120
2	80
2	145
2	110
2	74
2	48
1	5

Table 4 Data to plot permeability vs. cumulative frequency distribution

Permeability k_x,k_y (mD)	Thickness (h), ft	h with greater 'k'	Cumulative frequency distribution (% of h with greater k)
145	2	0	0
120	2	2	11.11
110	2	4	22.22
80	2	6	33.33
74	2	8	44.44
48	2	10	55.56
45	2	12	66.67
40	2	14	77.78
5	1	16	88.89
2	1	17	94.44
	Total = 18’		

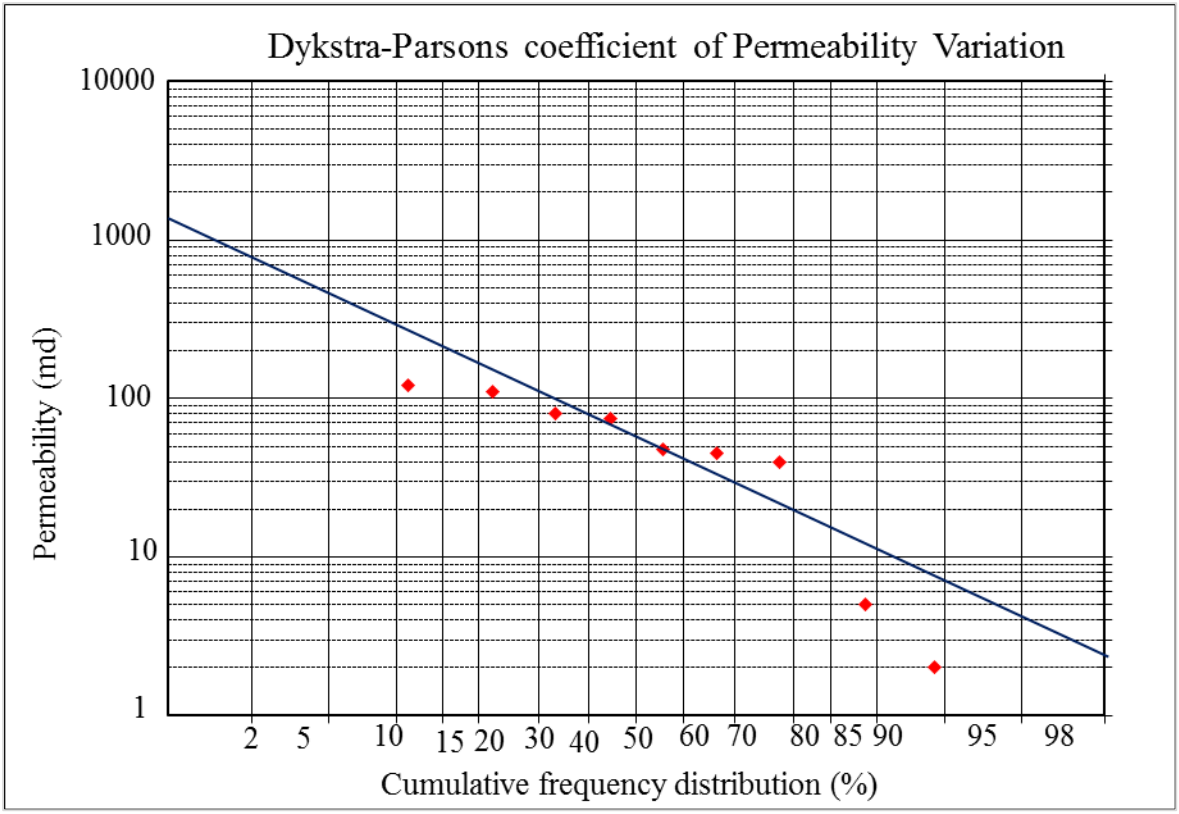

Figure 6 Plot of permeability vs. cumulative frequency distribution

Since the value of k_{50} will be same for each set of permeabilities, for every selected value of V, equation 4.1 has been used to calculate the value of $k_{84.1}$ for each case. These values are listed in Table 5. Using the values of k_{50} and $k_{84.1}$, a straight line has been drawn for each case of V as shown in Figure 7 from which the values of permeabilities ($k_x = k_y$) have been obtained at midpoint intervals of the frequency distribution. These permeability values for each V are shown in Table 6 and have been used in the simulation model. To obtain permeability values in vertical direction (k_z), we multiplied k_x by a factor of 0.1.

Table 5 Values of $k_{84.1}$

V	$k_{84.1}$ (mD)
0.1	52.2
0.3	40.6
0.5	29
0.7	17.4
0.9	5.8

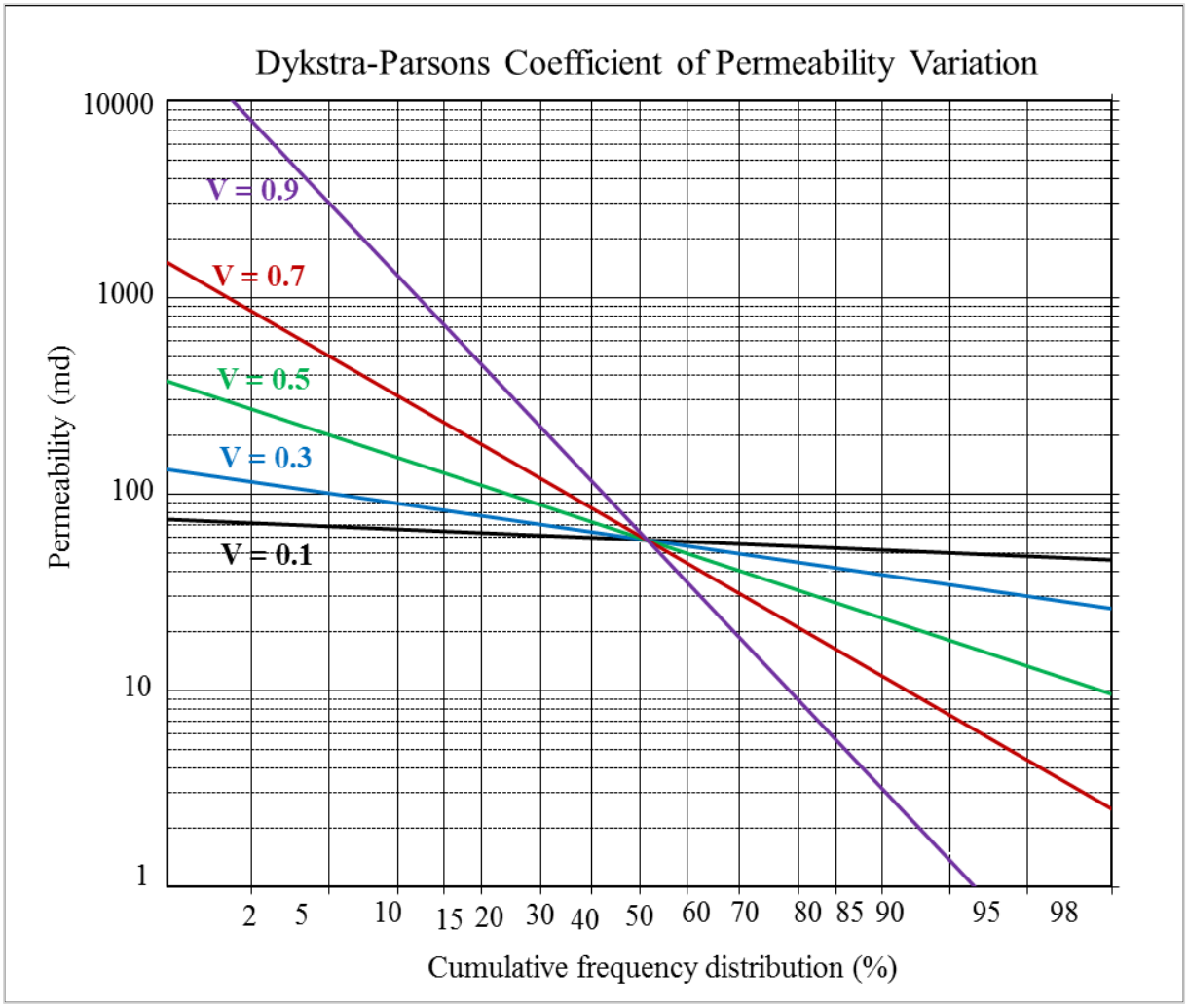

Figure 7 Plot of permeability vs. cumulative frequency distribution for various V

Table 6 Values of k_x, k_y permeabilities used in simulation model

Layer	**Midpoint of frequency distribution (%)**	**Permeability k_x, k_y (mD)**				
		V = 0.1	**V = 0.3**	**V = 0.5**	**V = 0.7**	**V = 0.9**
1	5	69	102	202	510	3200
2	15	65	85	140	250	750
3	25	62	72	100	160	310
4	35	61	67	80	100	170
5	45	60	61	65	75	90
6	55	60	58	57	53	50
7	65	58	52	45	38	25
8	75	58	48	36	26	14
9	85	55	43	28	16	5
10	95	51	36	18	7.5	1.5

4.4 Calculation of Oil to Water Density Ratio

API gravities of crude oil usually fall in the range of 10° to 47° [27]. Considering these gravity ranges, the oil density was assumed to be in the range of 43 lb/ft^3 to 63 lb/ft^3 and water density is taken as 63 lb/ft^3. With those fluid density values, the oil/water density ratio (β) was assigned values of 0.7, 0.8, 0.9 and 1 in the simulation model.

4.5 Calculation of Oil-Water Relative Permeabilites

Three different relative permeability systems have been used considering a wide range of wettability indicator. For relative permeability calculations, Corey-type relative permeability curves have been used.

For oil

$$k_{ro} = k_{roe}\left[\frac{(1-S_w-S_{or})}{(1-S_{wc}-S_{or})}\right]^{n_o} \quad (4.2)$$

Where n_o is Corey exponent of oil and k_{roe} is endpoint oil relative permeability at S_{wc}

For water

$$k_{rw} = k_{rwe}\left[\frac{(S_w-S_{wc})}{(1-S_{wc}-S_{or})}\right]^{n_w} \quad (4.3)$$

Where n_w is Corey exponent of water and k_{rwe} is endpoint water relative permeability at S_{or}

The parameters listed in Table 7 were used for each reservoir system. Note that the three systems represent a strongly oil-wet reservoir, a neutral wettability reservoir and a strongly water-wet reservoir.

Table 7 Parameters Used in Relative Permeability Curves

	S_{wi}	**S_{or}**	**k_{rwe}**	**k_{roe}**	**n_o**	**n_w**	**S_{woc}**	**WI**	**Wettability**
System A	0.1	0.4	0.74	1	2	2	0.37	0.5	Oil wet
System B	0.22	0.2	0.5	1	2	2	0.56	1.12	Neutral
System C	0.4	0.25	0.215	1	2	2.5	0.645	3	Water wet

Using Corey equation 4.2 and 4.3, the relative permeability curves were obtained as shown in Figure 8, 9 and 10.

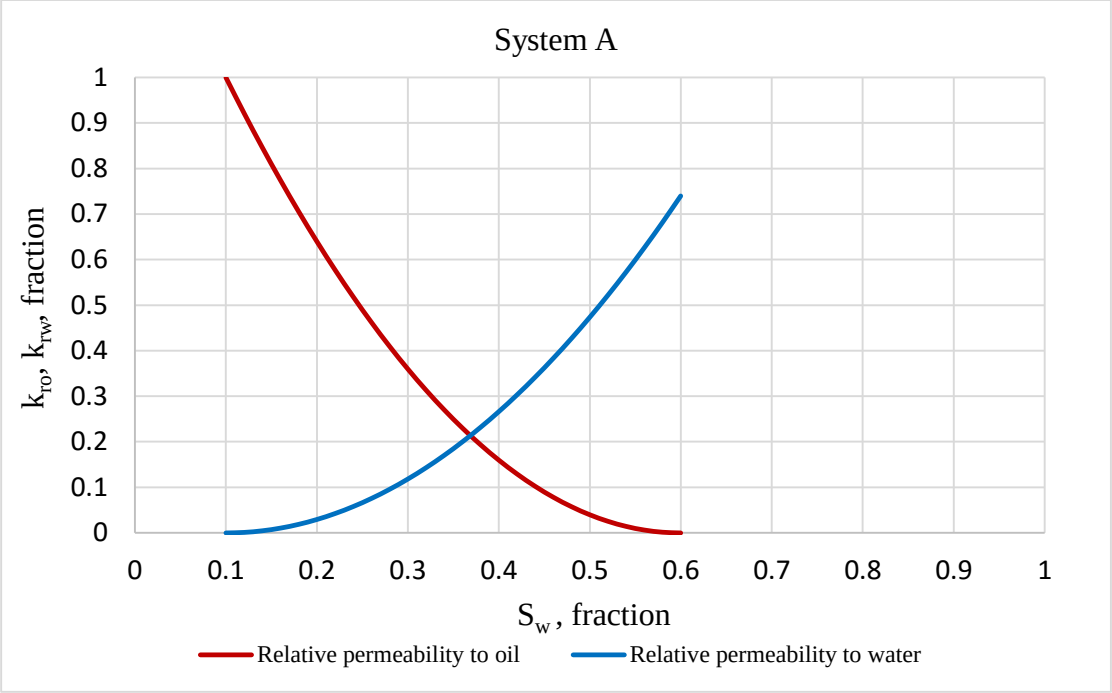

Figure 8 System A, Wettability Indicator = 0.5

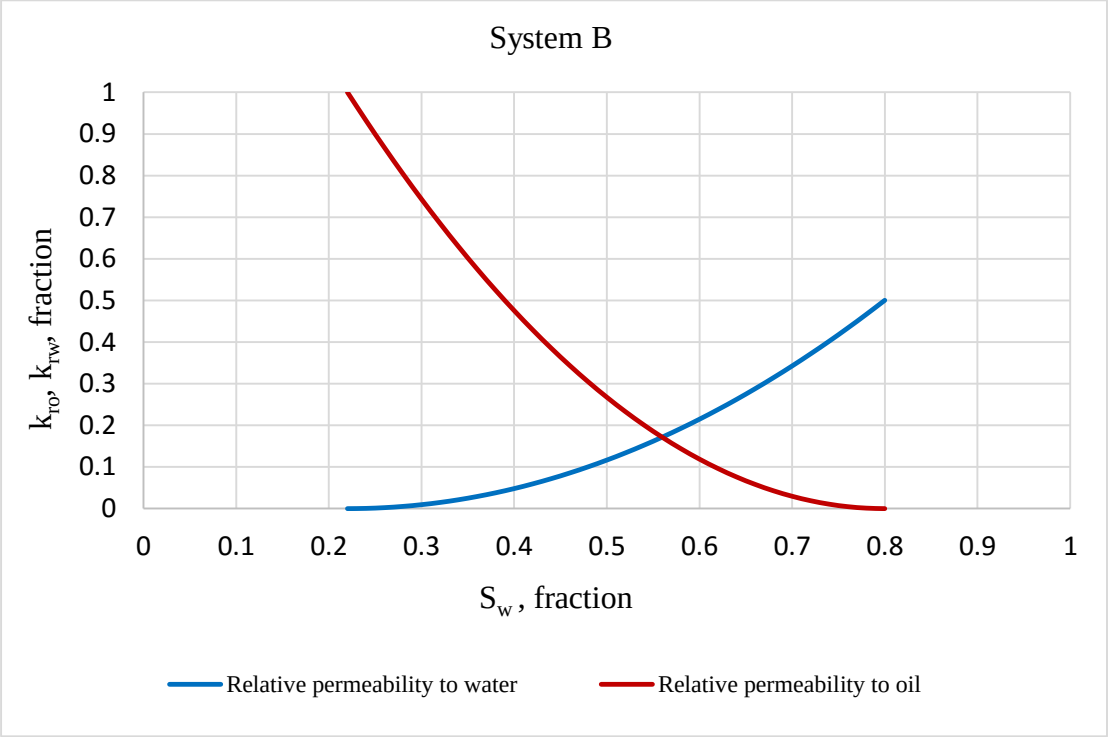

Figure 9 System B, Wettability Indicator = 1.12

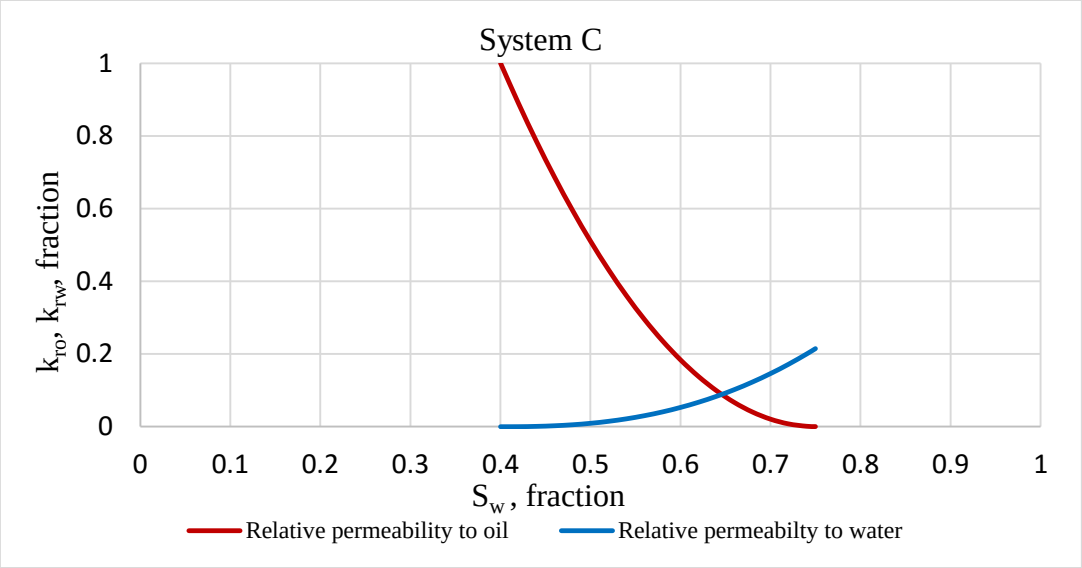

Figure 10 System C, Wettability Indicator = 3

4.6 Calculation of Fractional Flow Curve, Oil Viscosity and Mobility Ratio

In a water flood in which no saturation gradient exists behind the water flood front, there is no ambiguity about the value of water relative permeability to be used.

For frontal displacement, however, the mobility ratio depends on the fluid viscosities through the fractional-flow curve. Therefore, to arrive at a given value of mobility ratio, the following procedure was employed:

1. An oil viscosity is assumed. The fractional flow curve is constructed (Equation 4.4) using the relative permeability curves of the studied system (system B in this illustration) and a water viscosity of 1 cP. For mobility ratio of 4, a water viscosity of 0.25 cP was used.

$$f_w = \frac{1}{1+\left(\frac{k_{ro}}{\mu_o}\right)\left(\frac{\mu_w}{k_{rw}}\right)} \tag{4.4}$$

2. Next, the average water saturation behind the front ($\overline{S_{wf}}$) is estimated by drawing a tangent to the fractional-flow curve.

3. The values of k_{ro} and k_{rw} are then read from the relative permeability curve at this $\overline{S_{wf}}$.
4. Along with the assumed value of μ_o, the values of k_{ro} and k_{rw} obtained in step 3 are then plugged in Equation 1.4 to obtain the mobility ratio. If the mobility ratio value is not the desired one, the oil viscosity is modified and steps 2 – 4 are repeated until convergence.

This study tested the following values of mobility ratio: 0.1, 0.2, 0.5, 1, 2 and 4. The corresponding values of M, $\overline{S_{wf}}$, $(k_{rw})_{\overline{S_{wf}}}$, $(k_{ro})_{\overline{S_{wf}}}$, μ_w, and μ_o are listed in Table 8 for the three systems. The fractional flow curves for each mobility ratio for system B are shown in Figures 11 to 16.

Table 8 Data for oil viscosity and mobility ratio calculation

M	$\mathbf{\overline{S_{wf}}}$	$\mathbf{(k_{rw})_{\overline{S_{wf}}}}$	$\mathbf{(k_{ro})_{\overline{S_{wf}}}}$	**μ_w (cp)**	**μ_o (cp)**
System A					
0.1	0.5876	0.7037	0.0006	1	0.141
0.2	0.5753	0.6688	0.0024	1	0.295
0.5	0.5393	0.5712	0.0147	1	0.85
1	0.4815	0.4308	0.0562	1	2.2
2	0.3752	0.2242	0.2021	1	8.02
4	0.1858	0.0218	0.6862	0.25	38
System B					
0.1	0.782	0.4694	0.001	1	0.22
0.2	0.77	0.4496	0.0027	1	0.45
0.5	0.73	0.3866	0.0146	1	1.25
1	0.665	0.2943	0.0542	1	3.20
2	0.54	0.1522	0.201	1	11.84
4	0.3458	0.6863	0.0147	0.25	56.3
System C					
0.1	0.7414	0.2021	0.0006	1	0.49
0.2	0.7331	0.19	0.0023	1	1.04
0.5	0.7095	0.1582	0.0134	1	3.08
1	0.6739	0.1165	0.0473	1	8.18
2	0.6112	0.0608	0.1572	1	30.3
4	0.5058	0.0108	0.4868	0.25	81.3

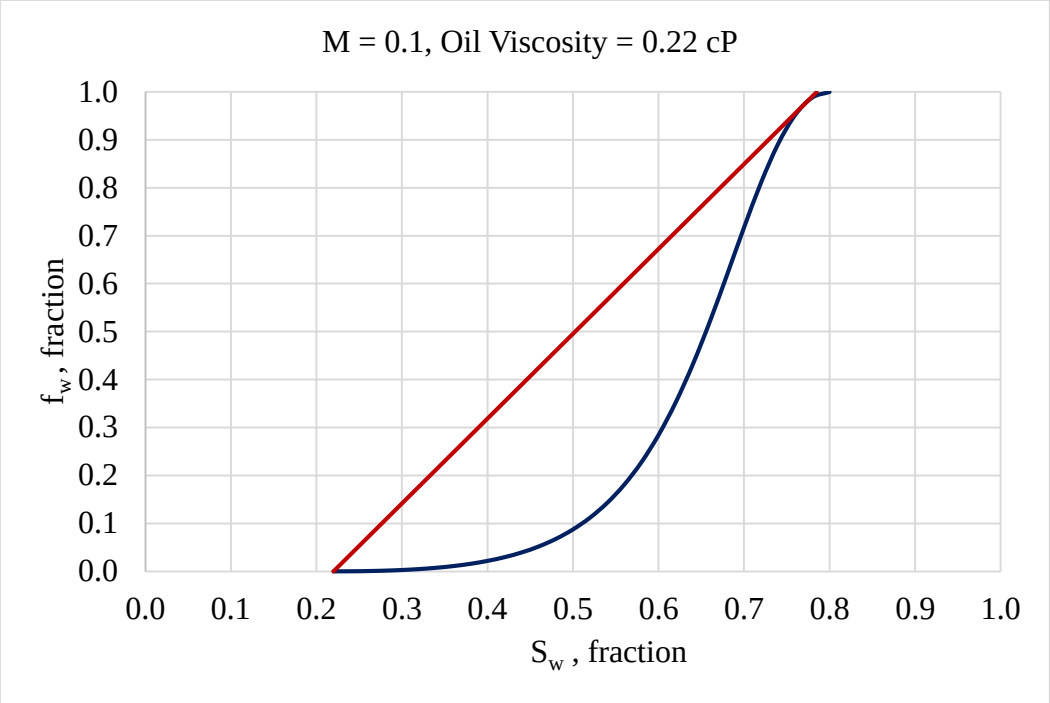

Figure 11 Fractional flow curve for system B at mobility ratio 0.1

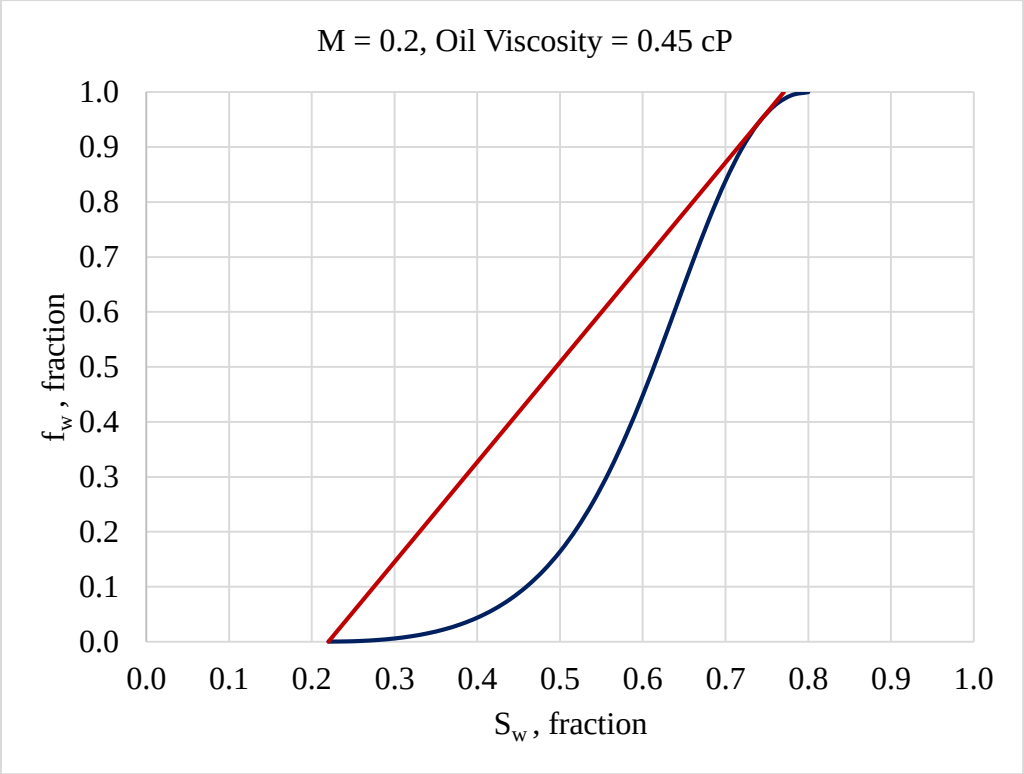

Figure 12 Fractional flow curve for system B at mobility ratio 0.2

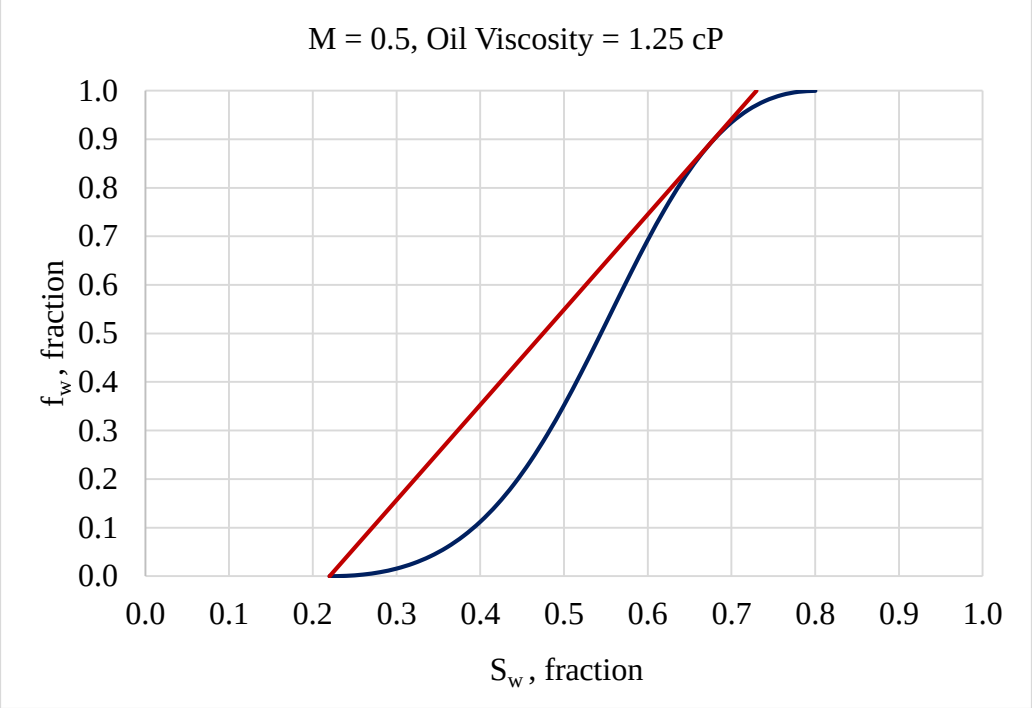

Figure 13 Fractional flow curve for system B at mobility ratio 0.5

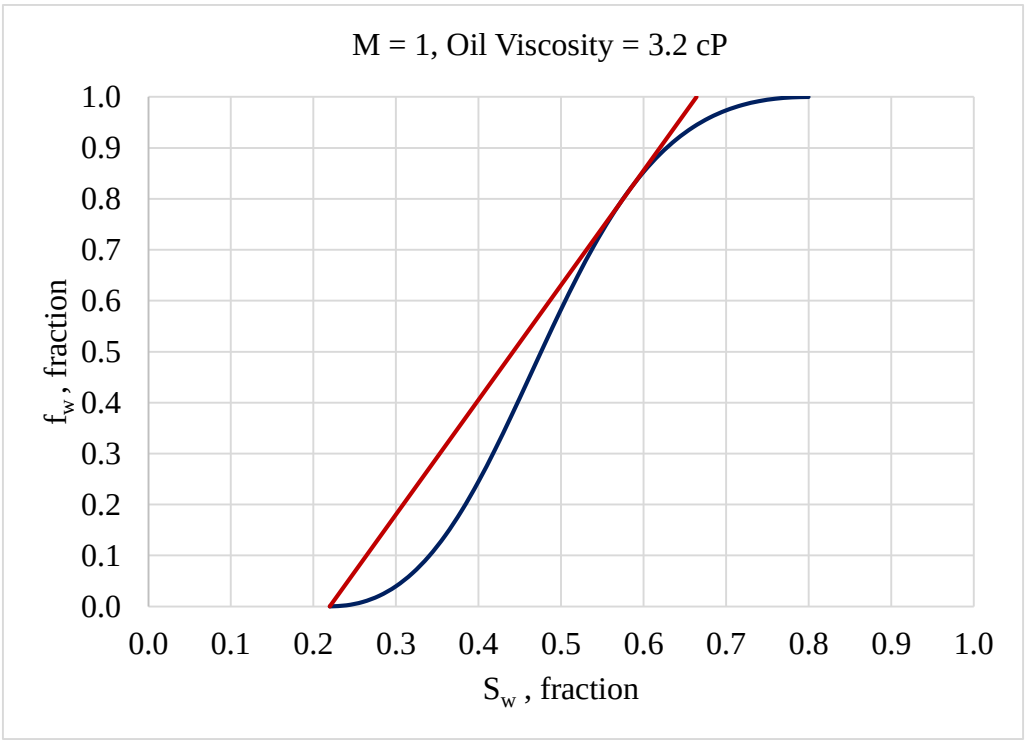

Figure 14 Fractional flow curve for system B at mobility ratio 1.0

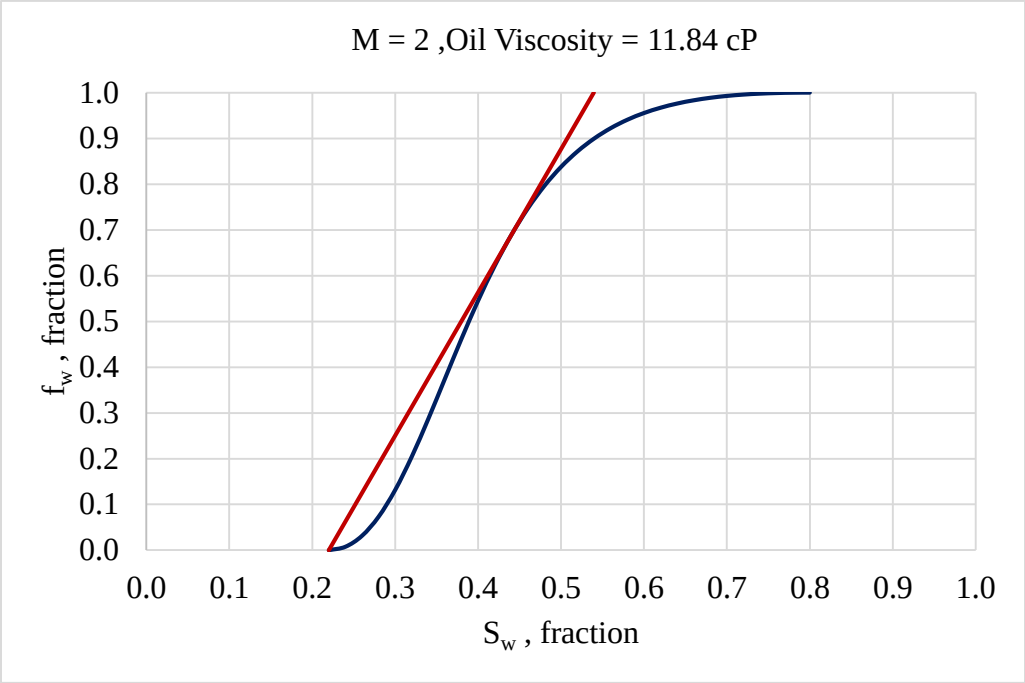

Figure 15 Fractional flow curve for system B at mobility ratio 2.0

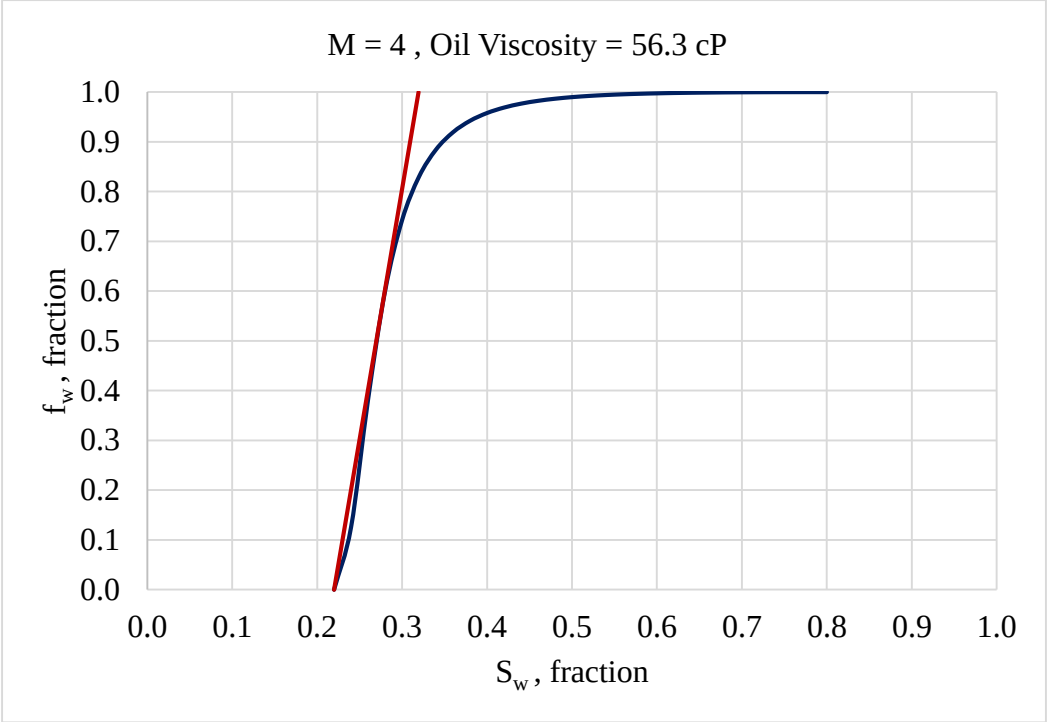

Figure 16 Fractional flow curve for system B at mobility ratio 4.0

4.7 Reservoir Simulation Model

To simulate the performance of a five spot pattern at breakthrough and after breakthrough, ECLIPSE 100 has been used with a three dimensional grid distribution. A simple two phase simulation model for heterogeneous reservoirs was built separately for ascending and descending case of permeability arrangement. The simulation runs were conducted to obtain recovery factor (*RF*) at different water cuts for different combinations of coefficient of permeability variation (*V*), mobility ratio (*M*), wettability indicator (*WI*) and oil to water density ratio (β). The details of the simulation model are given is subsequent sections.

4.7.1 Eclipse® 100 Input Data

ECLIPSE 100 is a fully-implicit, three phase, three dimensional, general purpose black oil simulator with gas condensate option [25].

The ECLIPSE 100 data file consists of eight main sections out of which five are mandatory and three are optional. The brief function of each section is defined below

RUNSPEC (required)	Used for title, problem dimensions, switches, phases present, components etc
GRID (required)	Used for specification of geometry of computational grid (location of grid block corners), and of rock properties (porosity, absolute permeability, etc.) in each grid block
EDIT (optional)	Modifications to calculated pore volumes, grid block center depths and transmissibilities

PROPS (required)	Tables of properties of reservoir rock and fluids as functions of fluid pressures, saturations and compositions (density, viscosity, relative permeability, capillary pressure, etc.). Contains the equation of state description in compositional runs
REGIONS (optional)	Splits computational grid into regions for calculation of: • PVT properties (Fluid densities and viscosities) •Saturation properties (Relative permeabilities and capillary pressures) • Initial conditions (Equilibrium pressures and saturations) • Fluids in place (Fluid in place and inter-region flows) • EOS regions (For compositional runs)
SOLUTION (required)	Specification of initial conditions in reservoir -may be: • Calculated using specified fluid contact depths to give potential equilibrium • Read from a restart file set up by an earlier run • Specified by the user for every grid block
SUMMARY (optional)	Specification of data to be written to the Summary file after each time step. Necessary if certain types of graphical output (for example water-cut as a function of time) are to be generated after the run has finished. If this section is omitted no Summary files are created.

SCHEDULE (required)	Specifies the operations to be simulated (production and injection controls and constraints) and the times at which output reports are required. Vertical flow performance curves and simulator tuning parameters may also be specified in the SCHEDULE section

4.7.2 Model Description

Our simulation model is a 3-D, two-phase (oil and water) model. The grid dimensions are 80 cells in x-direction, 80 cells in y-direction and 10 cells in z-direction. The total number of cells are 64,000. The reservoir has 10 layers of equal thickness with different permeabilities in both ascending and descending order. The length of each cell is 30 ft in the *x* and *y* directions and 25 ft in the *z* direction. It is ¼ of a 5-spot pattern unit with one producer and one injector completed in all layers. Production and injection rates are constant at 7,500 STB/D. The production control method is by reservoir voidage, and the water flood strategy is pressure maintenance. Crossflow is allowed by assigning an anisotropy ratio (k_z/k_x) of 0.1. The solution method is fully implicit based on finite difference method.

The above number of cells is the optimum that was selected after doing a sensitivity test for a different number of cells and time taken to run the simulation for a different configuration of number of cells. This sensitivity was done to minimize the numerical dispersion in simulation model. The main reservoir and fluid properties used in the model are given in Table 9.

In order to avoid convergence error with large mobility ratios, the water viscosity was reduced to 0.25 cP for mobility ratio of 4.

Table 9 Model properties including reservoir and fluid properties

Property	Value / Description
Grid dimensions, number (x,y,z)	80,80,10
Total number of cells	64,000
Grid size (D_x, D_y, D_z,) feet	30, 30, 25
Layers	10
Number of wells (*injector/producer*)	1/1
Producer completions	80,80, 1-10 (all layers)
Injector completions	1, 1, 1-10 (all layers)
Production rate, STB/D	7500
Injection rate, STB/D	7500
Production control methods	Prod Reservoir voidage (RESV)
Water flood strategy	Pressure maintenance
Relative permeability curves	Variable – Corey's functions
Solution method	Implicit
Simulation technique	Finite difference
Porosity, fraction	0.15
Phases(oil and water)	2
Water viscosity, cP	0.25 and 1
Oil viscosity, cP	Variable
Water density , lb /ft^3	63
Oil density , lb /ft^3	Variable
Anisotropic ratio (k_z/k_x)	0.1
Permeability variation coefficient, V	Variable
Payzone thickness, ft	250
Reservoir area (1/4 of pattern), ft^2	2400 x 2400 (132 acres)
Reservoir Depth, ft	8000
Average Reservoir pressure, psi (constant)	4500
Water Oil contact, ft	8500
Oil formation volume factor, RB/STB	1.285
Water formation volume factor, RB/STB	1.02
Wetting medium	Variable
Pattern	5-spot

4.8 Simulation Runs

A total of 7920 simulation data points were obtained, equally divided between ascending and descending permeability arrangements, each ending at a production water cut of 95% for various combinations of parameters. The values of each parameter are shown in Table 10.

Examples of the simulator output for system B for various cases such as at breakthrough and after breakthrough for both ascending and descending arrangement of permeability with favorable and unfavorable mobility ratio are shown in Figures 17 to 22.

Table 10 Parameter values used in simulation model

Parameter	Range
Mobility Ratio	0.1, 0.2, 0.5, 1, 2, 4
Coefficient of Permeability Variation	0.1, 0.3, 0.5, 0.7, 0.9
Oil to Water Density Ratio	0.7, 0.8, 0.9, 1.0
Wettability Indicator	0.5, 1.12, 3

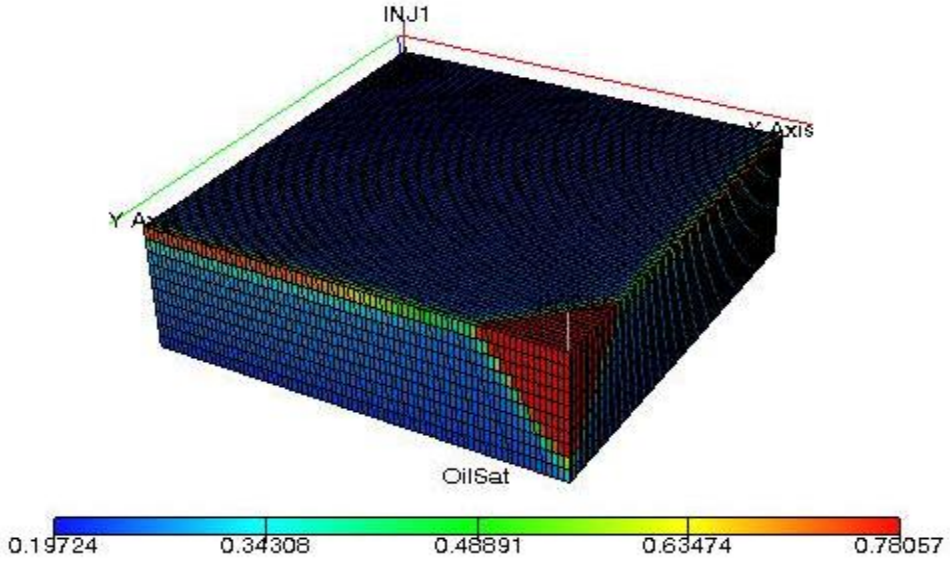

Figure 17 Breakthrough Case for Ascending case, system B at V=0.1, M=0.1, β= 0.7

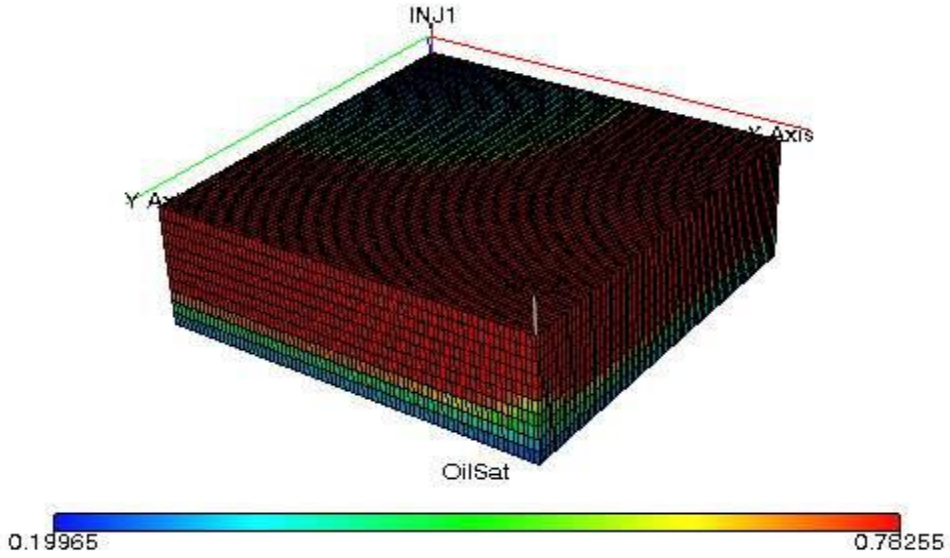

Figure 18 Simulation for Ascending case, system B at f_w = 0.5, V=0.5, M=0.5, β= 0.8

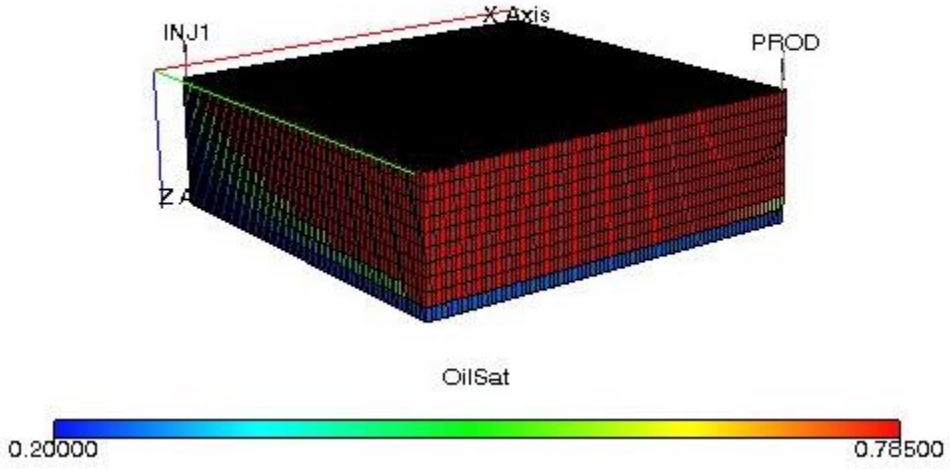

Figure 19 Simulation for Ascending case, system B at f_w = 0.95, V=0.9, M=2.0, β= 0.9

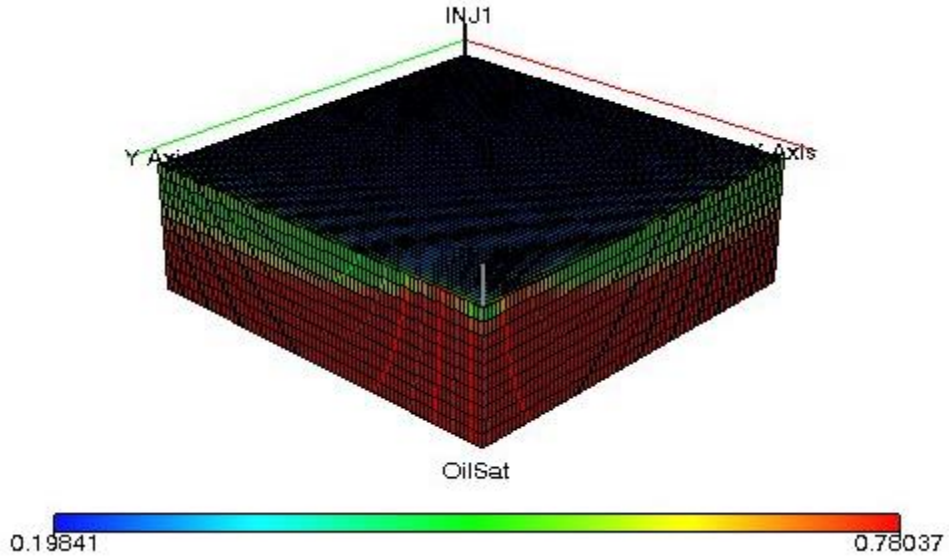

Figure 20 Breakthrough Case for Descending case, system B at V=0.3, M=0.2, β= 0.9

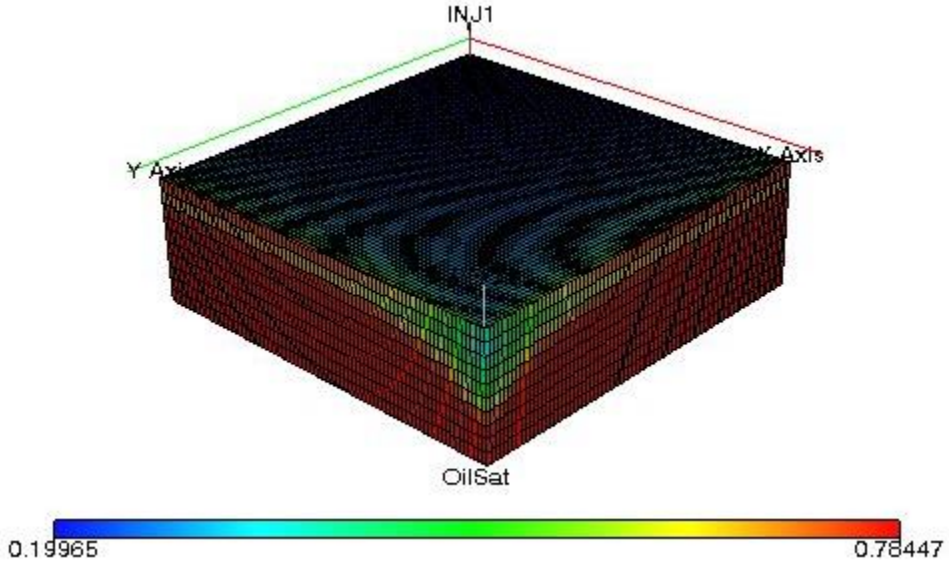

Figure 21 Simulation for Descending case, system B at f_w = 0.5, V=0.5, M=0.5, β= 0.8

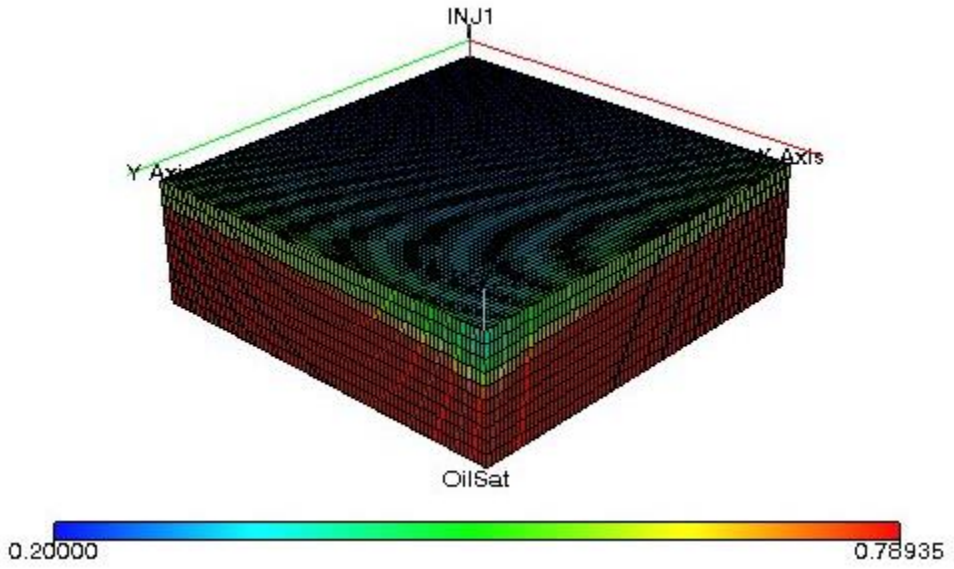

Figure 22 Simulation for Descending case, system B at f_w = 0.7, V=0.7, M=1.0, β= 1.0

4.9 Calculation of Movable Oil Recovery Factor

As mentioned in Chapter 1, the recovery factor (*RF*) reported by the simulator is based on the initial oil in place. However, it is more relevant to consider the movable oil recovery factor (RF_m) that is based on movable oil in place, which is the maximum volume of oil that can be moved or produced ultimately. *RF* is related to RF_m by the following equation:

$$RF_m = RF\left(\frac{1- S_{wi}}{1-S_{wi} - S_{or}}\right) \quad (4.5)$$

Where,

S_{wi} = Initial water saturation, dimensionless

S_{or} = Residual oil saturation, dimensionless

RF = Recovery factor, dimensionless

4.10 Simulation Model Sensitivities

The simulation model was verified by conducting three different sensitivity tests, which showed the model to be independent of these parameters. These sensitivities are:

1. Layers random sorting effect
2. Pattern area effect
3. Reservoir thickness effect

4.10.1 Layers Random Sorting Sensitivity

To minimize the number of simulation runs, two permeability arrangements were studied; these were ascending order and descending order. In real situations, however, the layers are usually randomly sorted. Two random permeability arrangements were generated and tested for each of the three systems. It can be seen from Figures 23 to 25 that random sorting results are almost the same as descending arrangement and far from the ascending arrangement. This shows that the descending arrangement can be used for representation of most reservoirs.

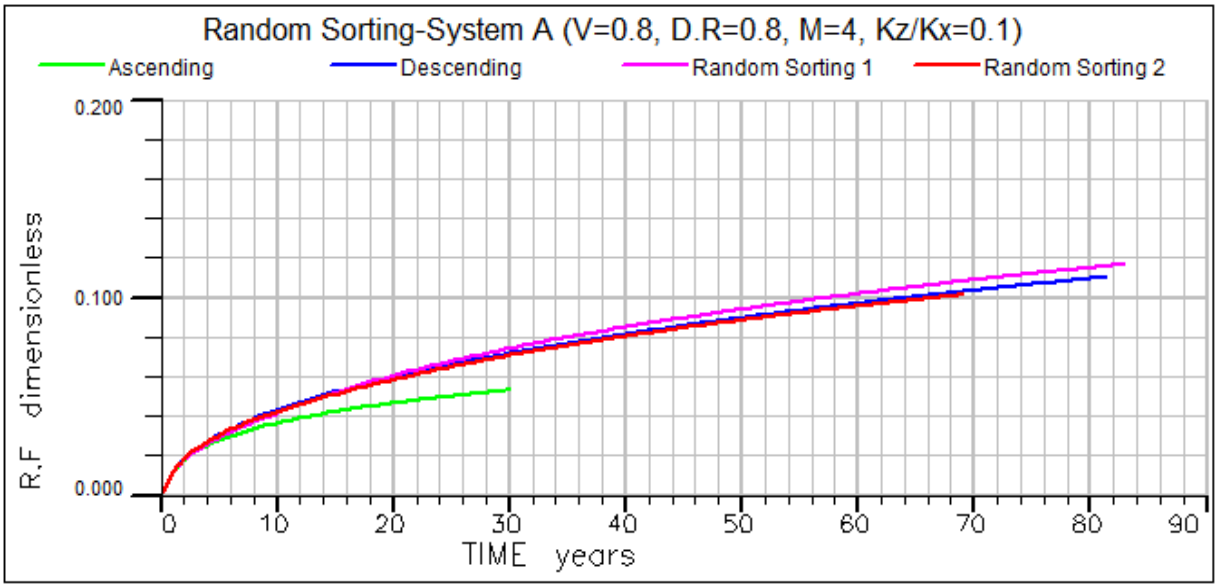

Figure 23 Layers Random Sorting Sensitivity for System A

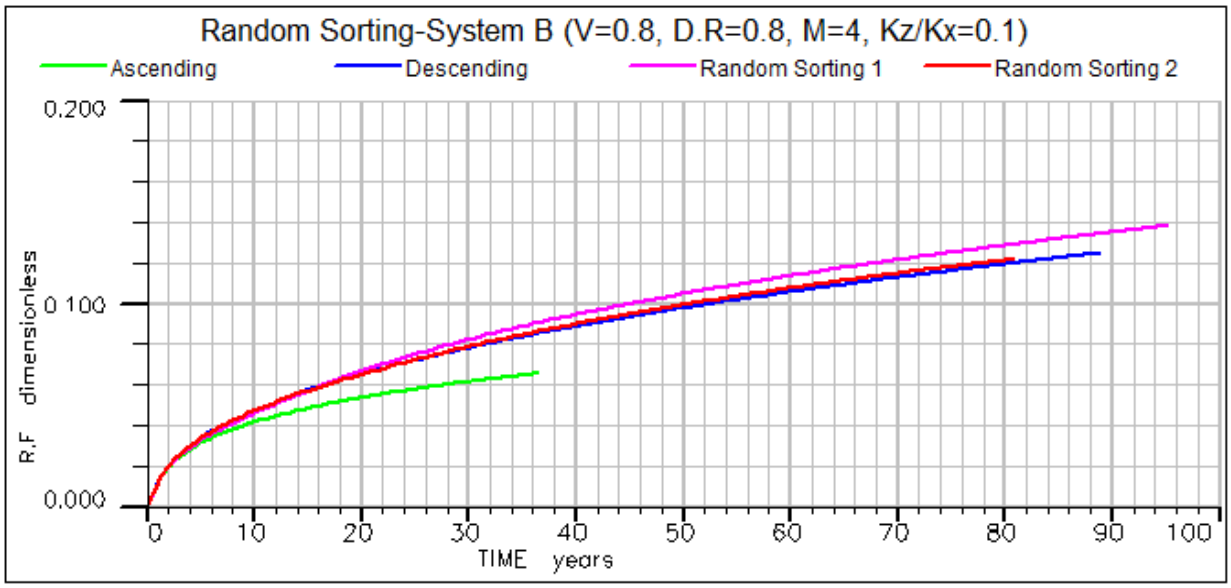

Figure 24 Layers Random Sorting Sensitivity for System B

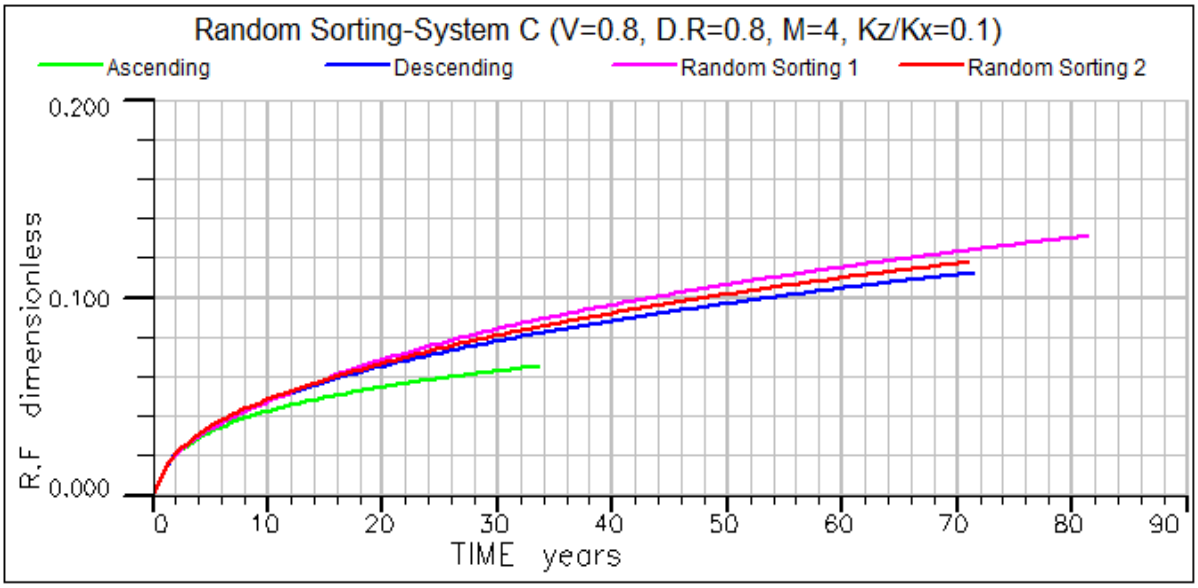

Figure 25 Layers Random Sorting Sensitivity for System C

4.10.2 Pattern Area Sensitivity

In order to verify the effect of pattern area on the recovery factor, two cases were run with different pattern areas for system B at three mobility ratios. This sensitivity is done for both ascending and descending arrangement of permeability. It can be seen from Figure 26 and Figure 27 that the oil recovery factor is independent of the pattern size.

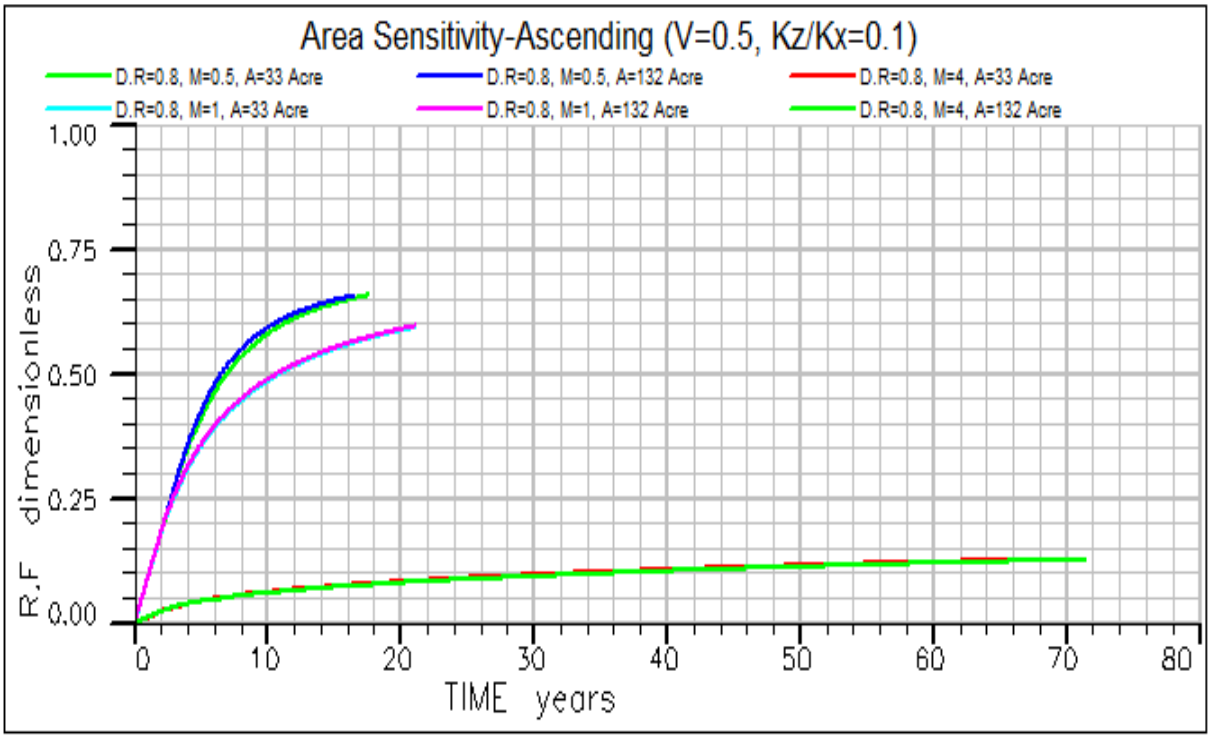

Figure 26 Area Sensitivity for ascending case for system B at different mobility ratio

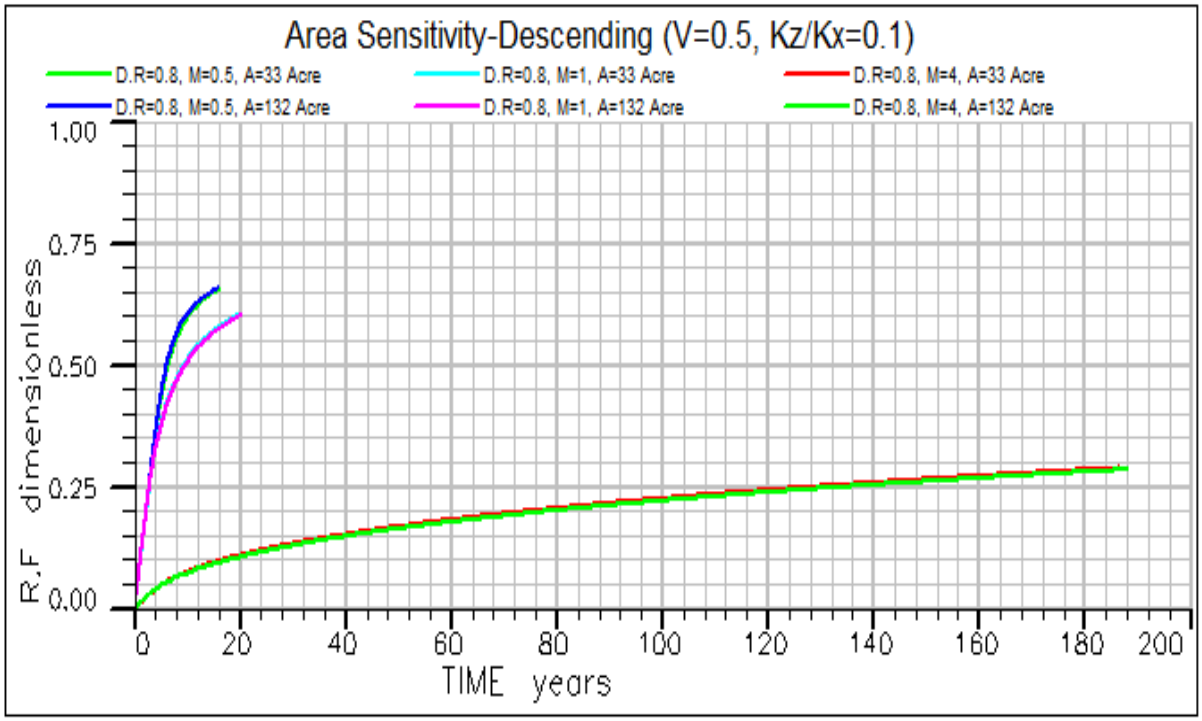

Figure 27 Area Sensitivity for descending case for system B at different mobility ratio

4.10.3 Reservoir Thickness Sensitivity

In order to verify the effect of reservoir thickness on oil recovery, two tests were run with different reservoir thicknesses for system B at two mobility ratios. This sensitivity is also done for both ascending and descending arrangement of permeability. It can be seen from Figure 28 and Figure 29 that oil recovery factor is independent of reservoir thickness.

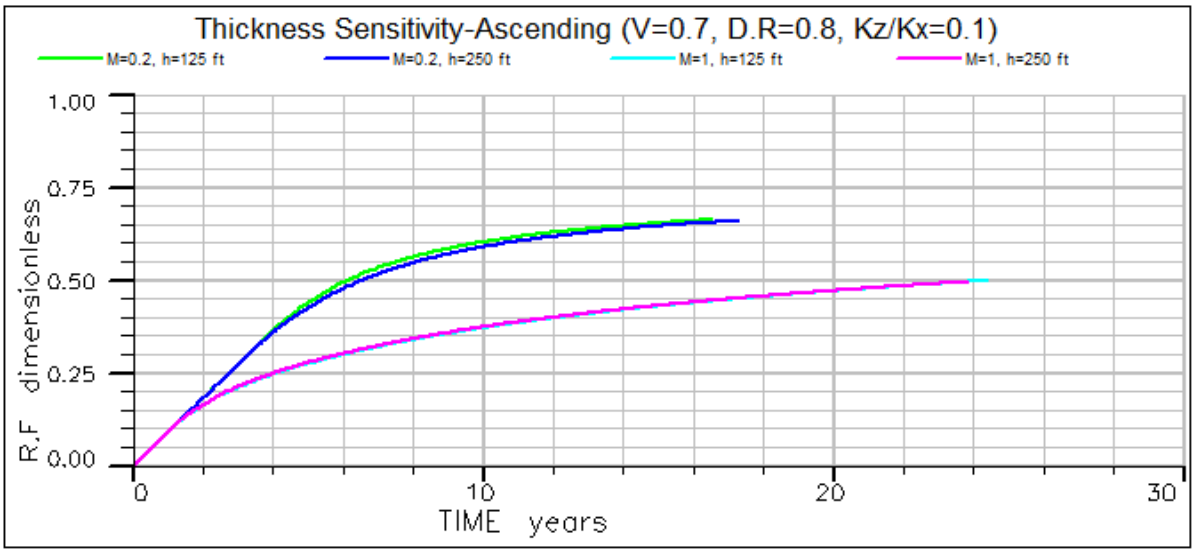

Figure 28 Thickness Sensitivity for ascending case for system B at different mobility ratio

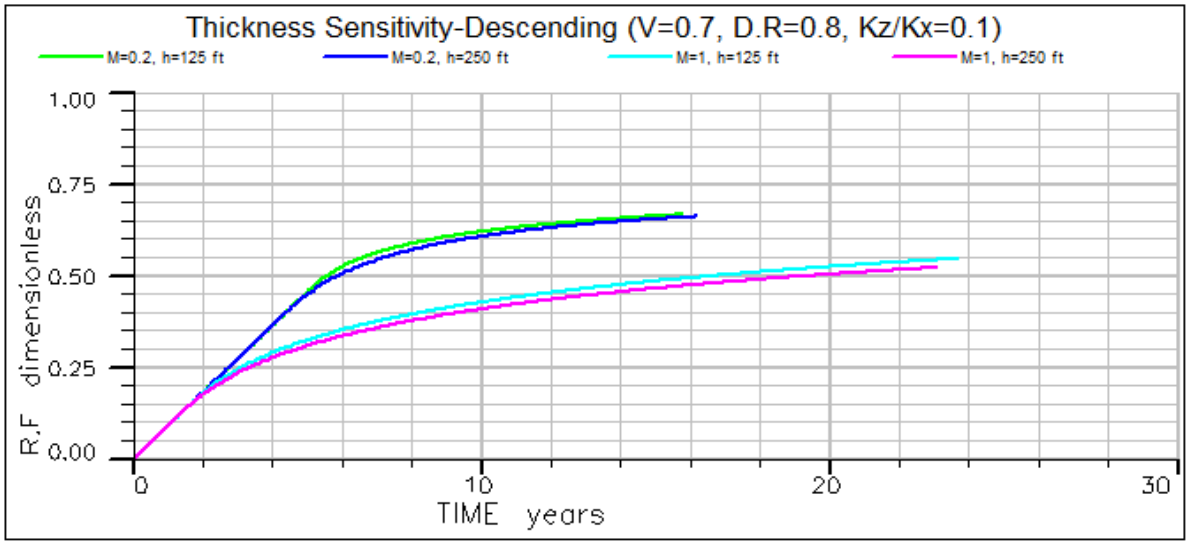

Figure 29 Thickness Sensitivity for descending case for system B at different mobility ratio

CHAPTER 5

SIMULATION RESULTS

Simulation runs were obtained using ECLIPSE 100 simulator for all possible combinations of all parameters. This chapter presents simulation results with the effect of each parameter on oil recovery factor.

5.1 Effect of Mobility Ratio

The simulation runs were done in order to cover a wide range of mobility ratio from 0.1 to 4. The effect of mobility ratio at and beyond breakthrough for ascending arrangement is shown in Figures 30 to 35 for all three systems while Figures 36 to 41 show for descending arrangement. As expected, oil reservoirs with favorable mobility ratio ($M<1$) yield higher oil recovery (RF) as compared to unfavorable mobility ratio ($M>1$) in all systems and in both arrangements.

Unfavorable mobility ratios (M >1) values mean that water will move faster than oil, therefore, water bypassing oil due to the higher mobility of the displacing phase will occur and result in early water breakthrough in producing wells. When the mobility ratio is much larger than one, oil recovery at the same volume of water injected will decrease, because water will flow through the porous medium faster than oil which results in low oil recovery. For favorable mobility ratios ($M<1$), oil will be more mobile than water resulting in higher oil recovery.

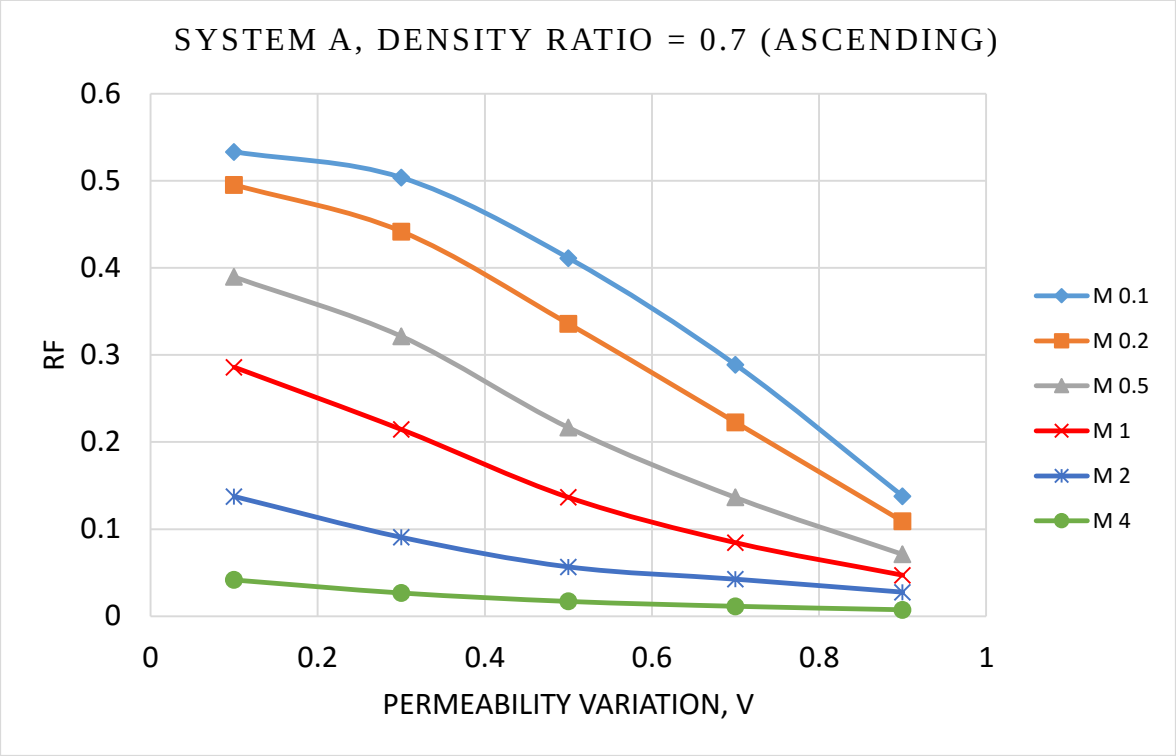

Figure 30 Effect of mobility ratio on oil recovery factor at water breakthrough for system A ascending case

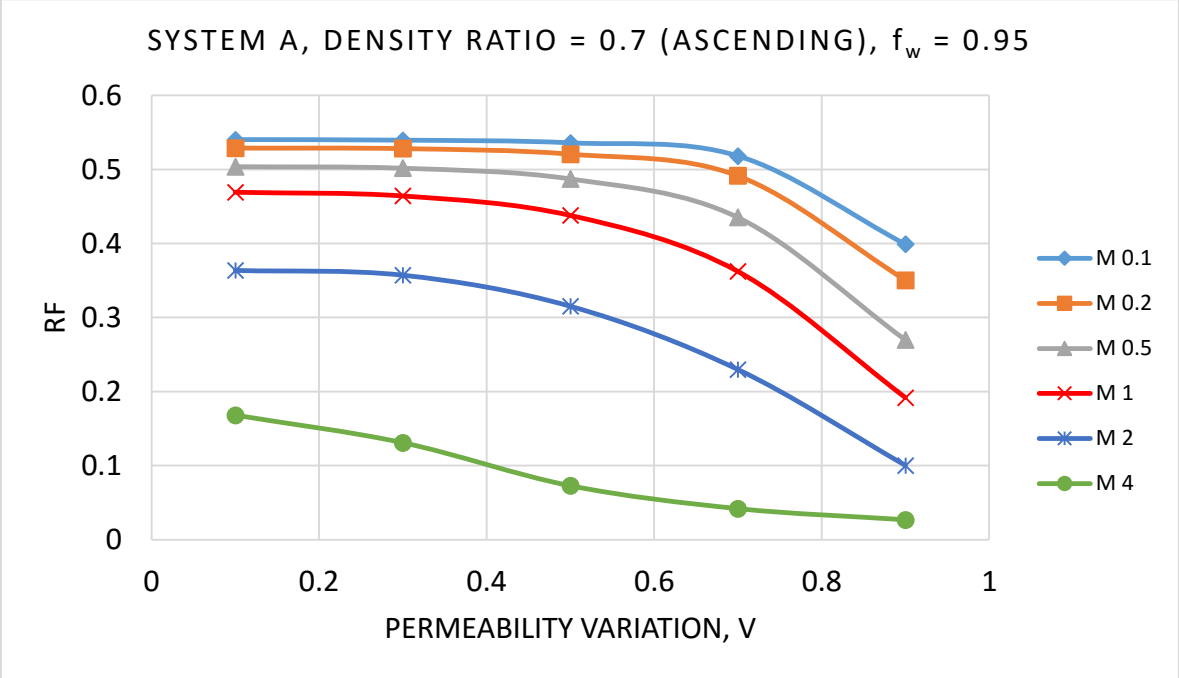

Figure 31 Effect of mobility ratio on oil recovery factor beyond water breakthrough for system A ascending case

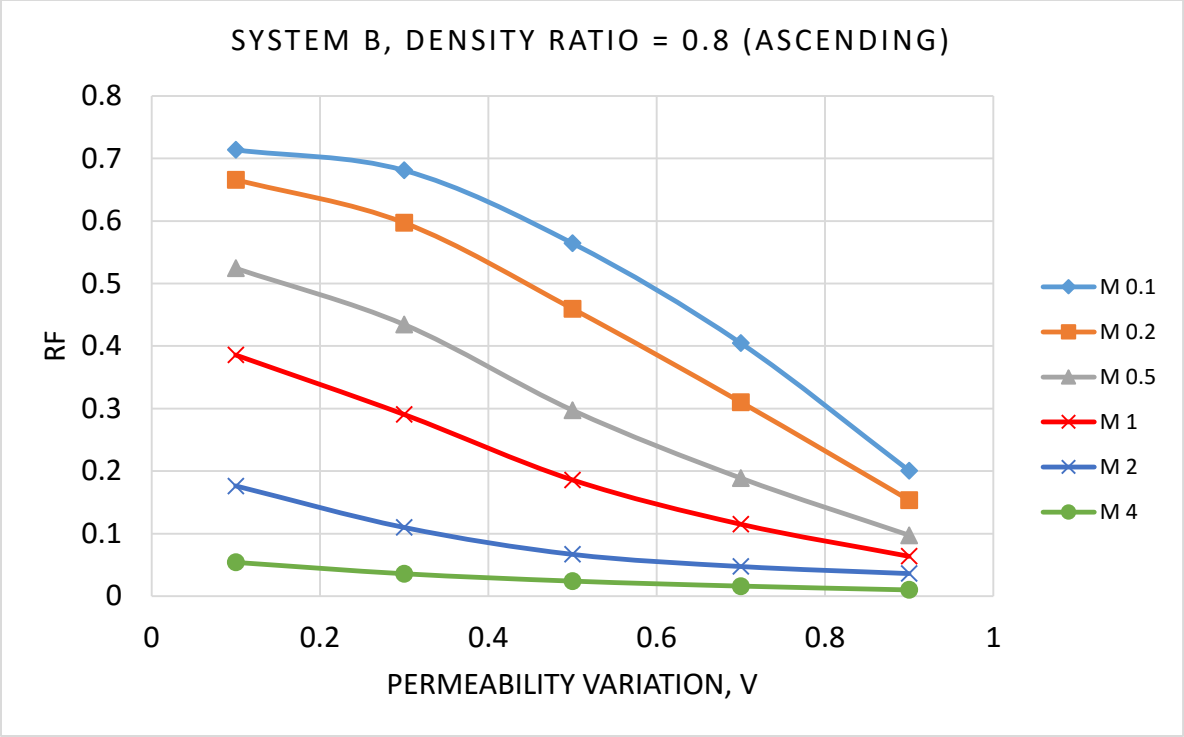

Figure 32 Effect of mobility ratio on oil recovery factor at water breakthrough for system B ascending case

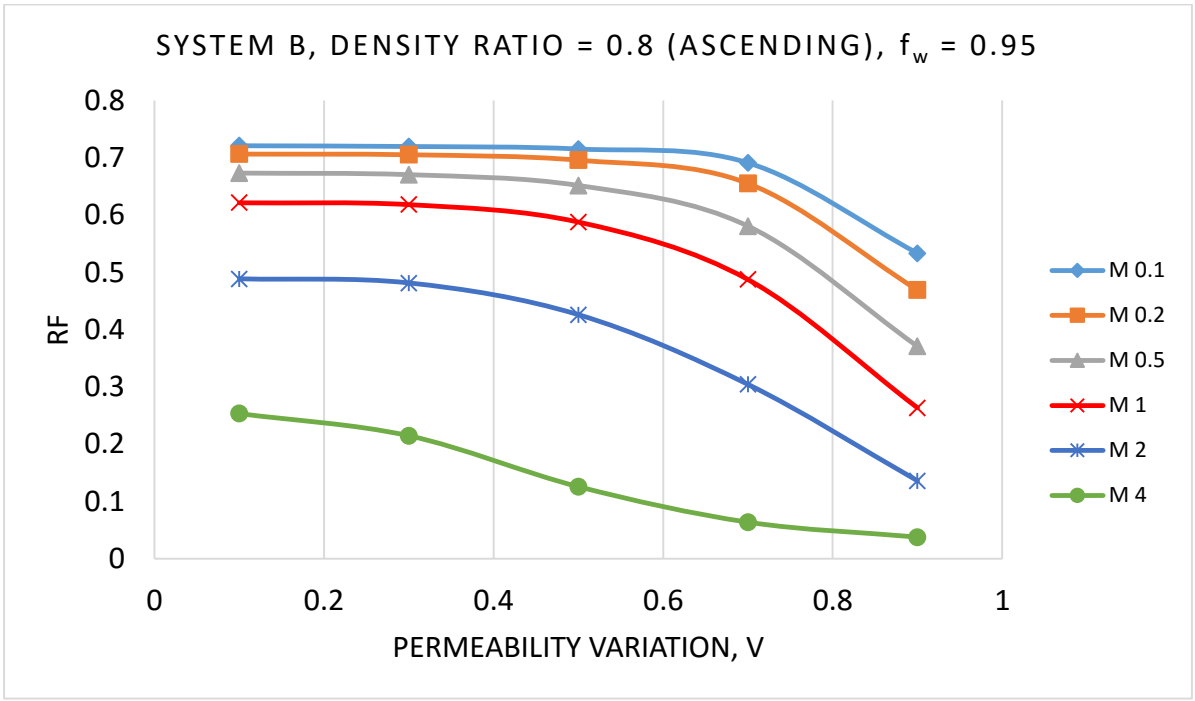

Figure 33 Effect of mobility ratio on oil recovery factor beyond water breakthrough for system B ascending case

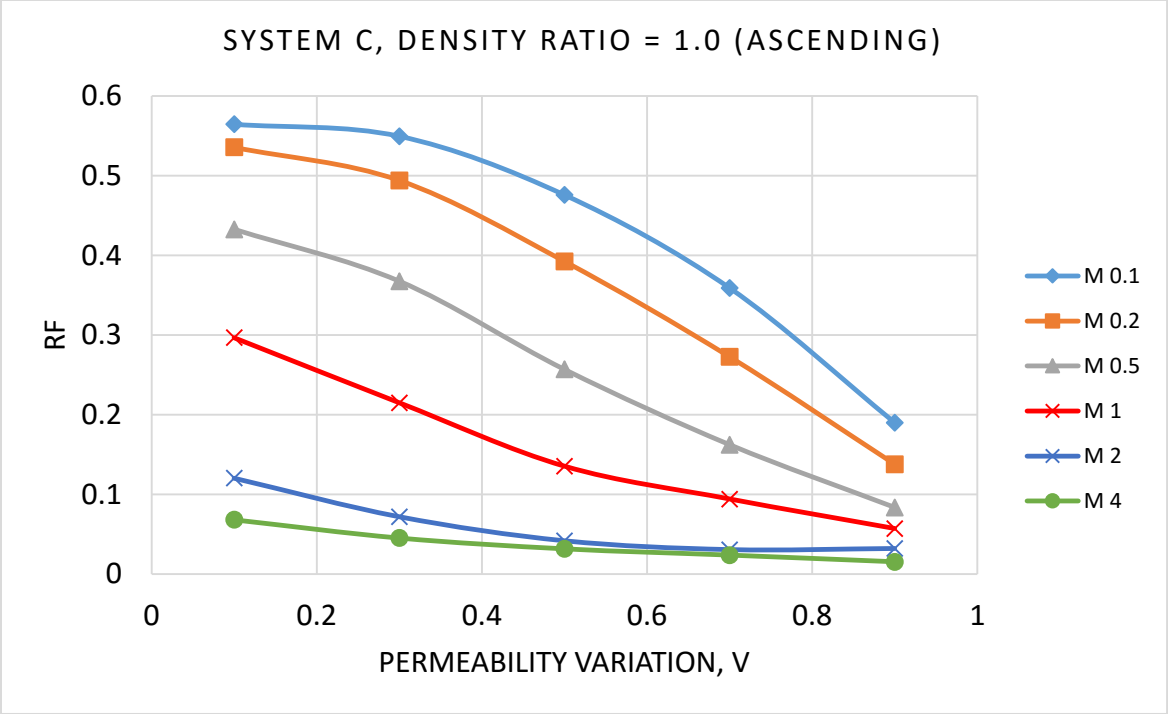

Figure 34 Effect of mobility ratio on oil recovery factor at water breakthrough for system C ascending case

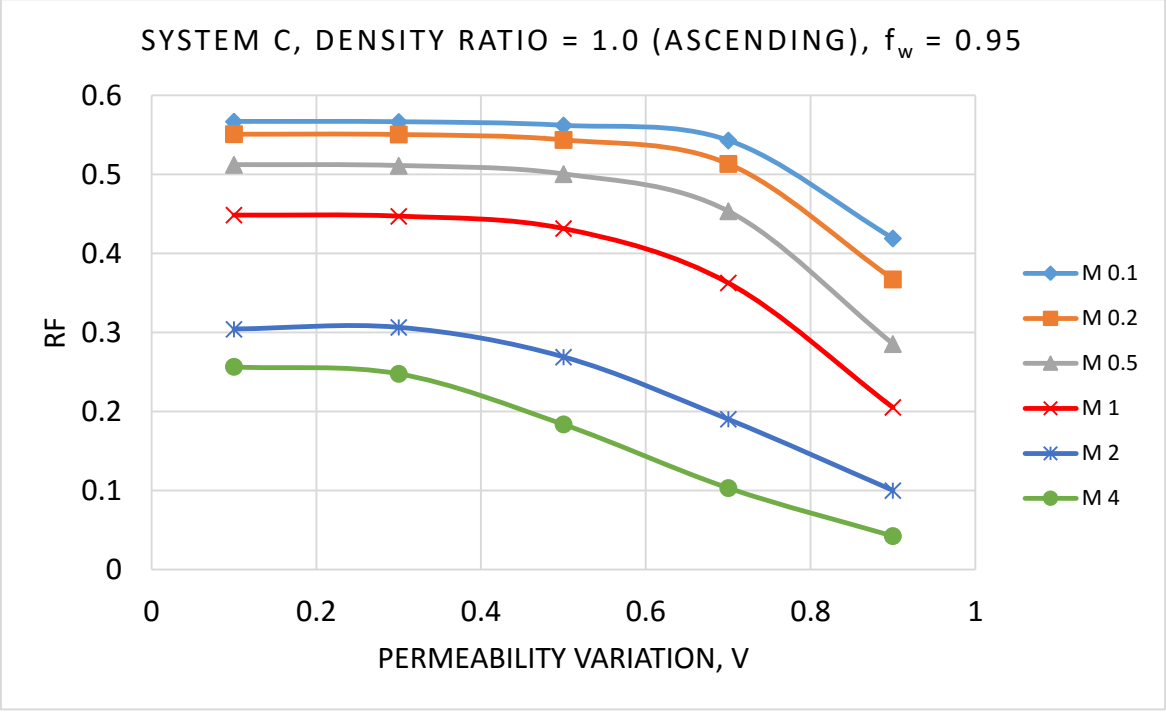

Figure 35 Effect of mobility ratio on oil recovery factor beyond water breakthrough for system C ascending case

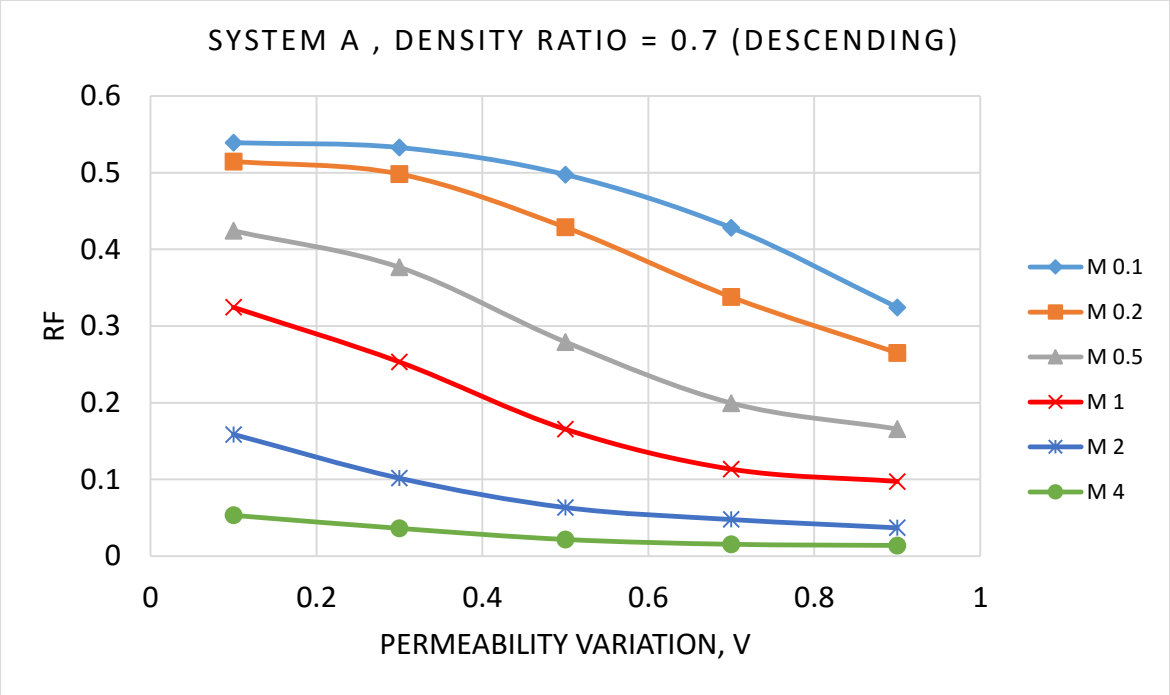

Figure 36 Effect of mobility ratio on oil recovery factor at water breakthrough for system A descending case

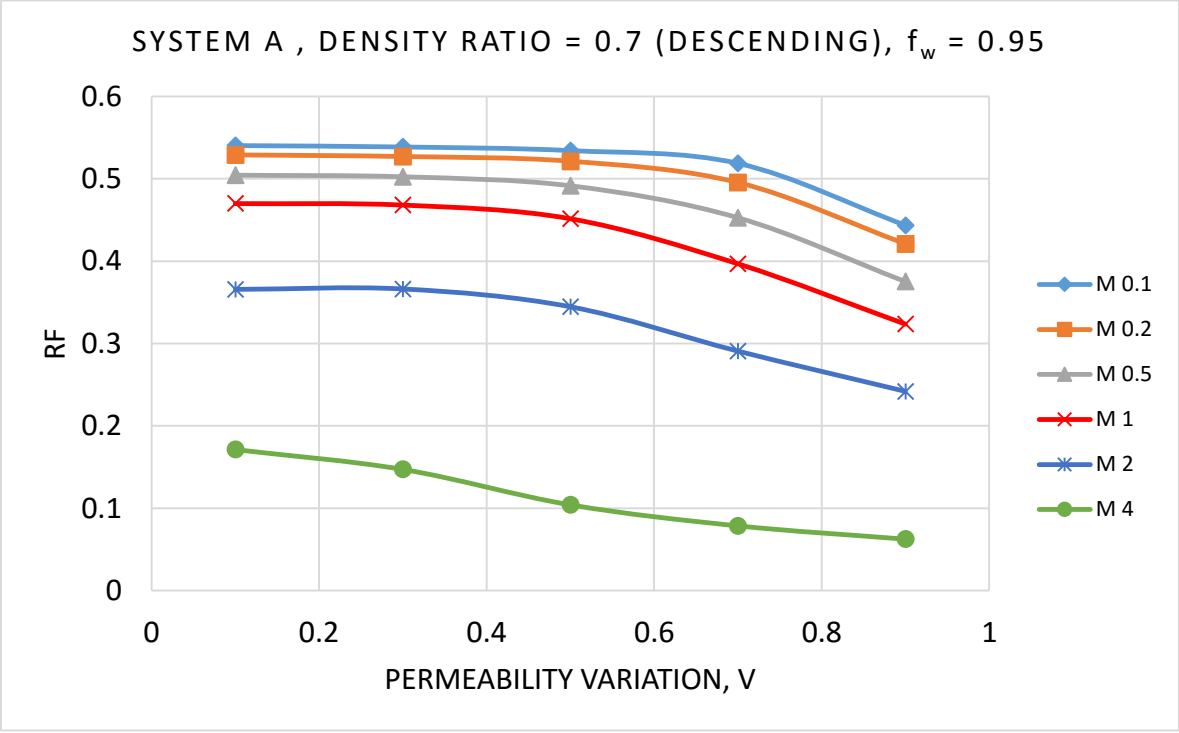

Figure 37 Effect of mobility ratio on oil recovery factor beyond water breakthrough for system A descending case

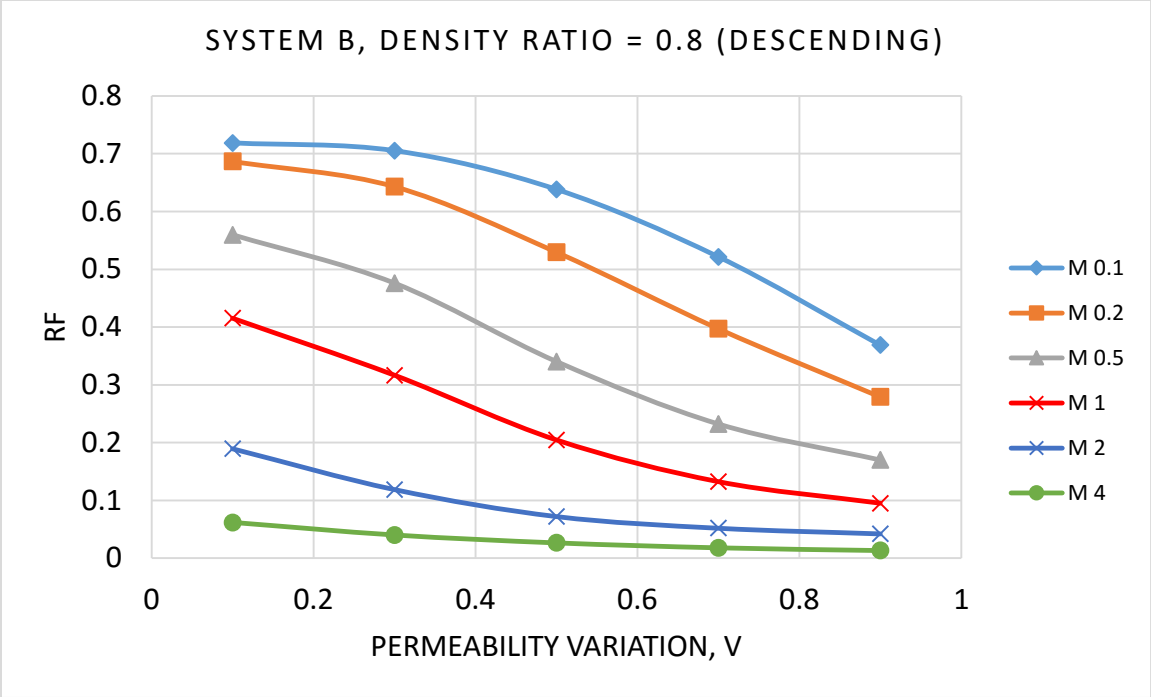

Figure 38 Effect of mobility ratio on oil recovery factor at water breakthrough for system B descending case

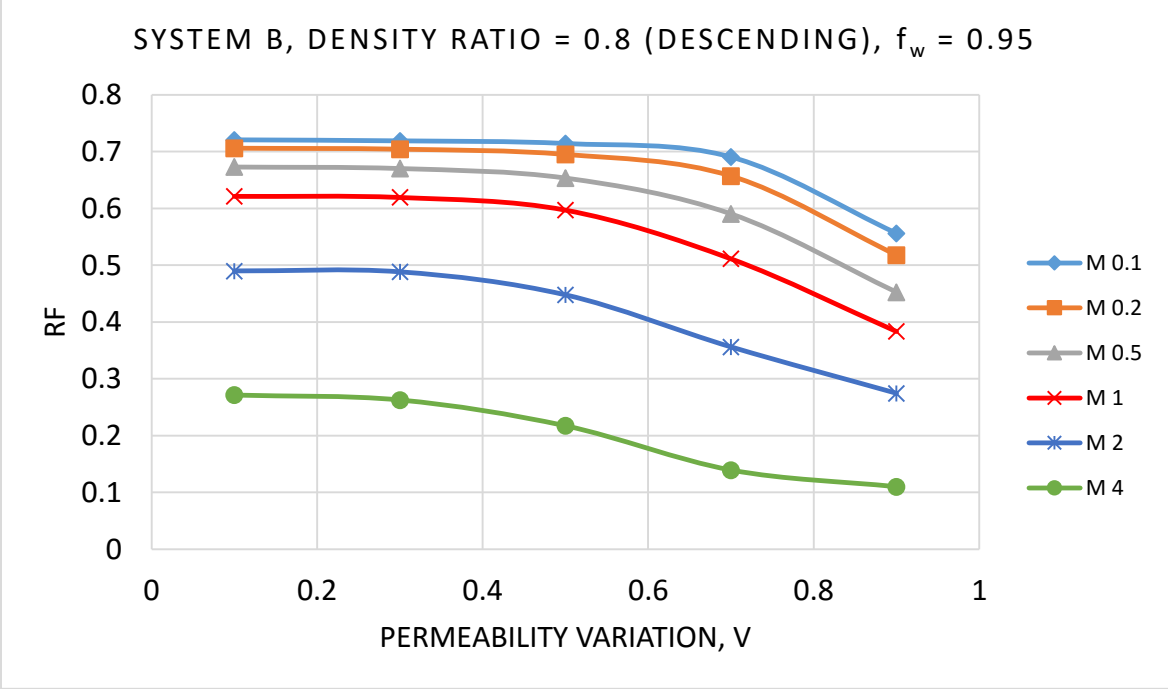

Figure 39 Effect of mobility ratio on oil recovery factor beyond water breakthrough for system B descending case

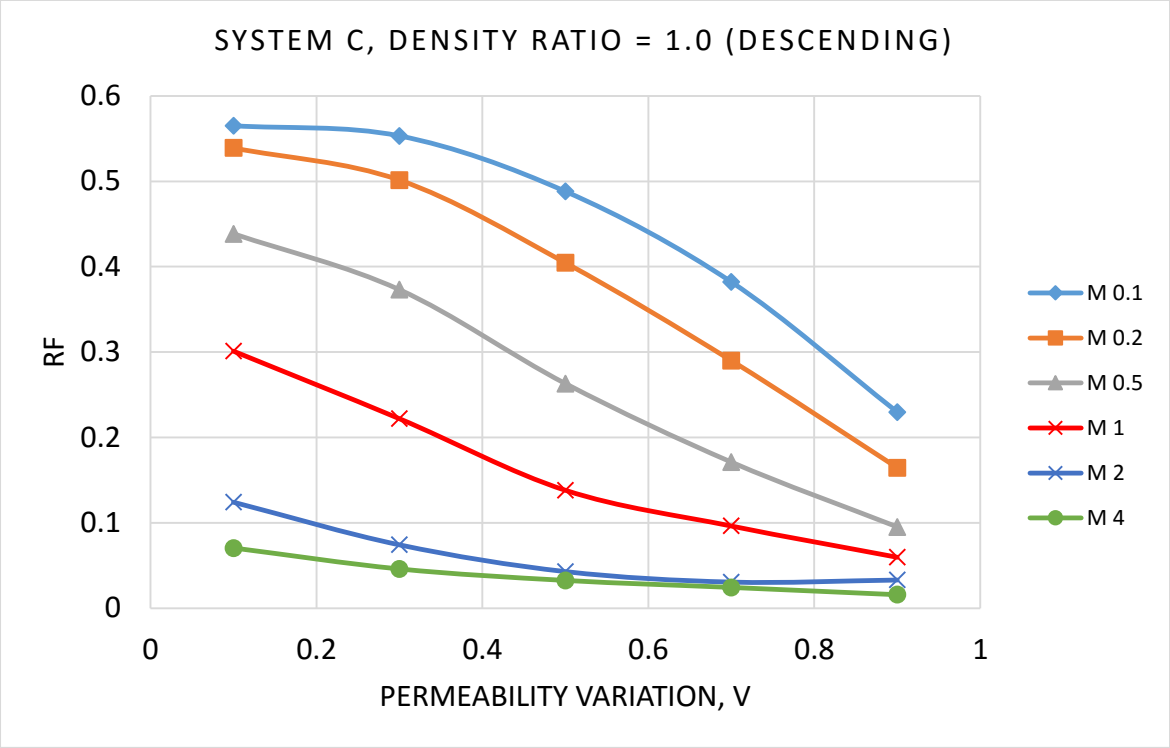

Figure 40 Effect of mobility ratio on oil recovery factor at water breakthrough for system C descending case

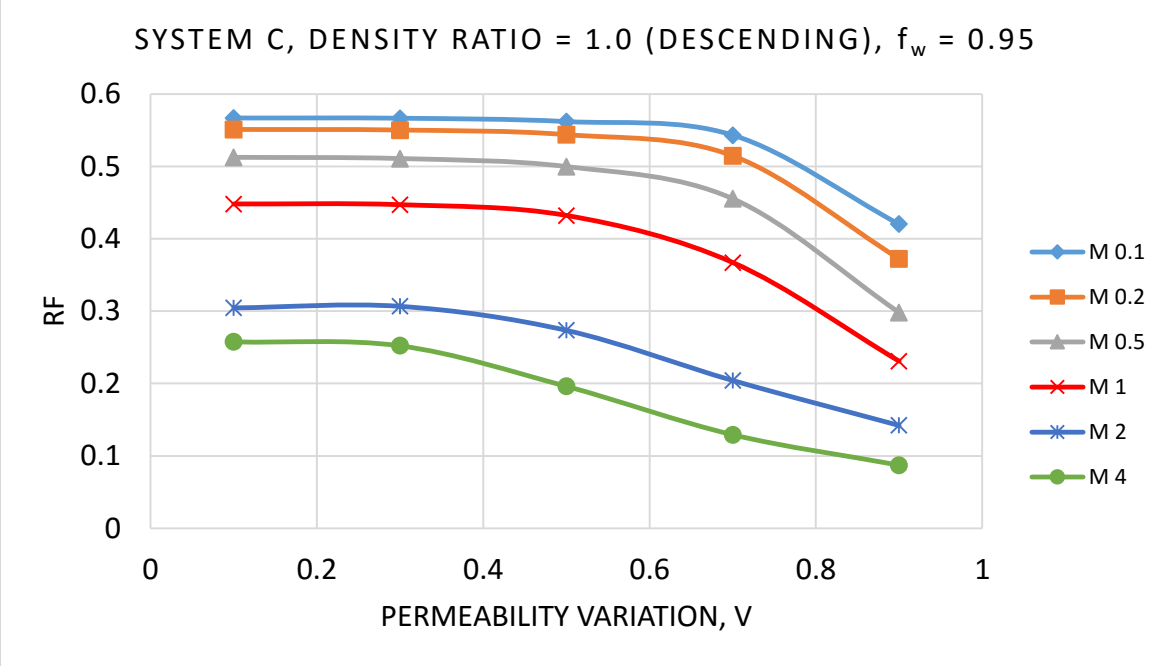

Figure 41 Effect of mobility ratio on oil recovery factor beyond water breakthrough for system C descending case

5.2 Effect of Reservoir Heterogeneity

A reservoir can be heterogeneous by having both areal and vertical variations. A reservoir may be non-uniform in all properties such as permeability, porosity, pore size distribution, wettability, connate water saturation and crude properties. In this research, permeability has been taken into consideration as it is the most important factor of heterogeneity. Oil recovery factor depends on the coefficient of permeability variation. The effect of permeability variation is shown in Figures 30 to 41 for all three systems and for both ascending and descending permeability arrangement. A similar trend is obtained in all cases which shows that as the reservoirs gets more heterogeneous, less oil will be recovered.

5.3 Effect of Density

The effect of density ratio for all three systems and for both ascending and descending arrangements at different mobility ratios is shown in Figures 42 to 77. It can be seen that the effect of density on recovery factor is less significant compared to the effect of mobility ratio and permeability variation. Due to higher density of injected water, it would move preferentially to the bottom of the formation. By allowing crossflow between the layers, the water in high permeability layer tends to cross into the underlying oil zone in a low permeability layer due to density difference. The downward flow of water and upward flow of oil due to density difference will delay water breakthrough in high permeability layers, thus increasing the oil recovery. The recovery factor is higher in case of low density difference (high density ratio) between water and oil for ascending arrangement while descending arrangement shows low recovery factor at low density difference (high density ratio).

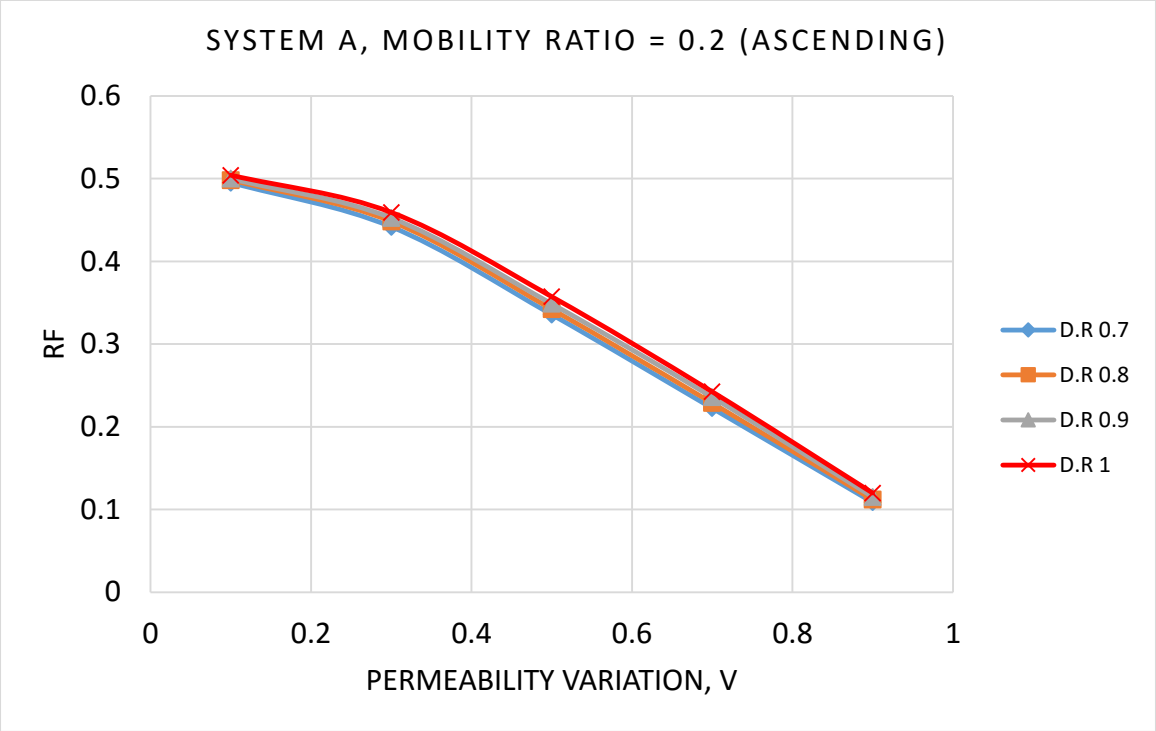

Figure 42 Effect of density ratio on oil recovery factor at water breakthrough for system A ascending case-Case 1

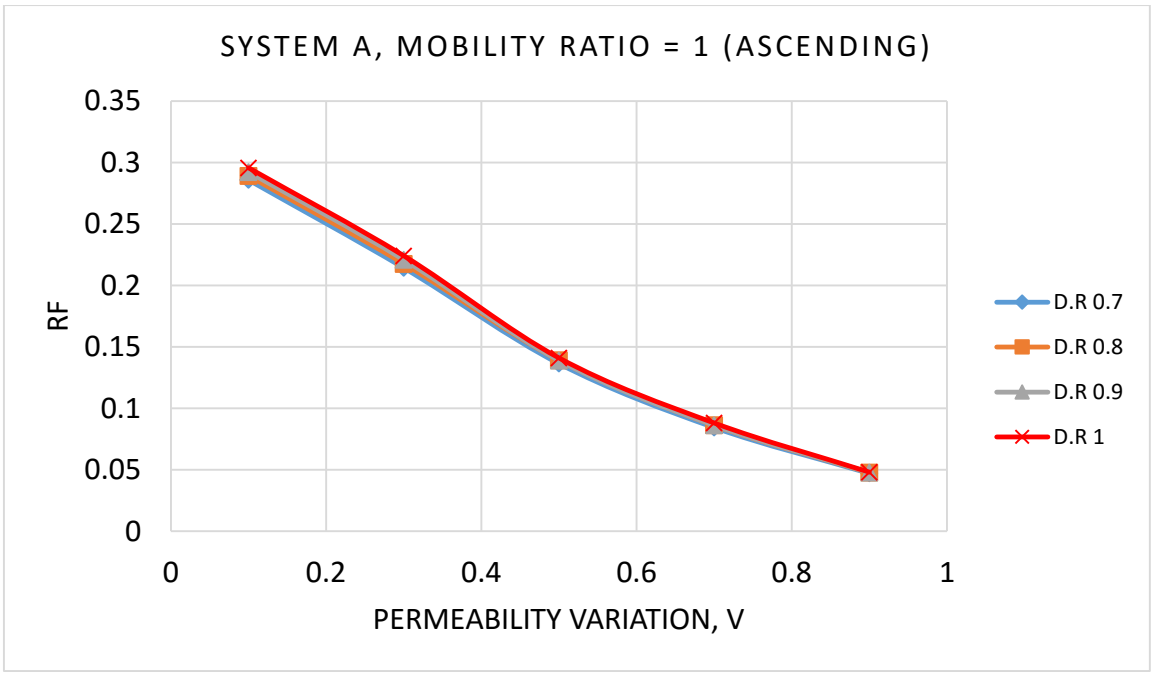

Figure 43 Effect of density ratio on oil recovery factor at water breakthrough for system A ascending case-Case 2

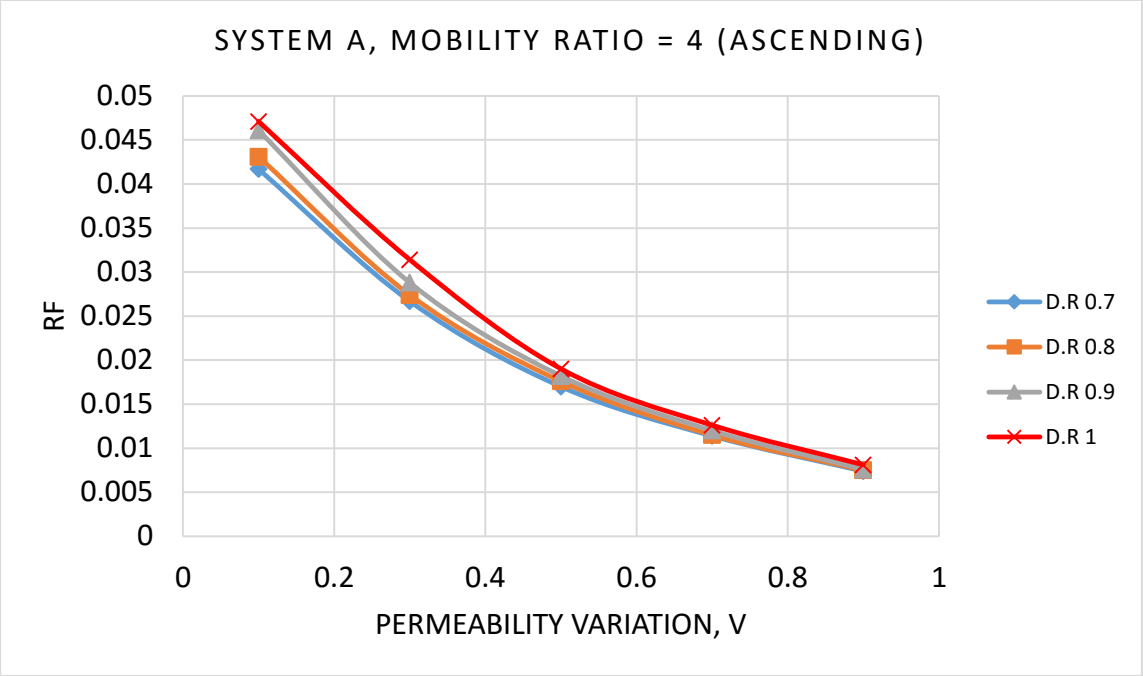

Figure 44 Effect of density ratio on oil recovery factor at water breakthrough for system A ascending case-Case 3

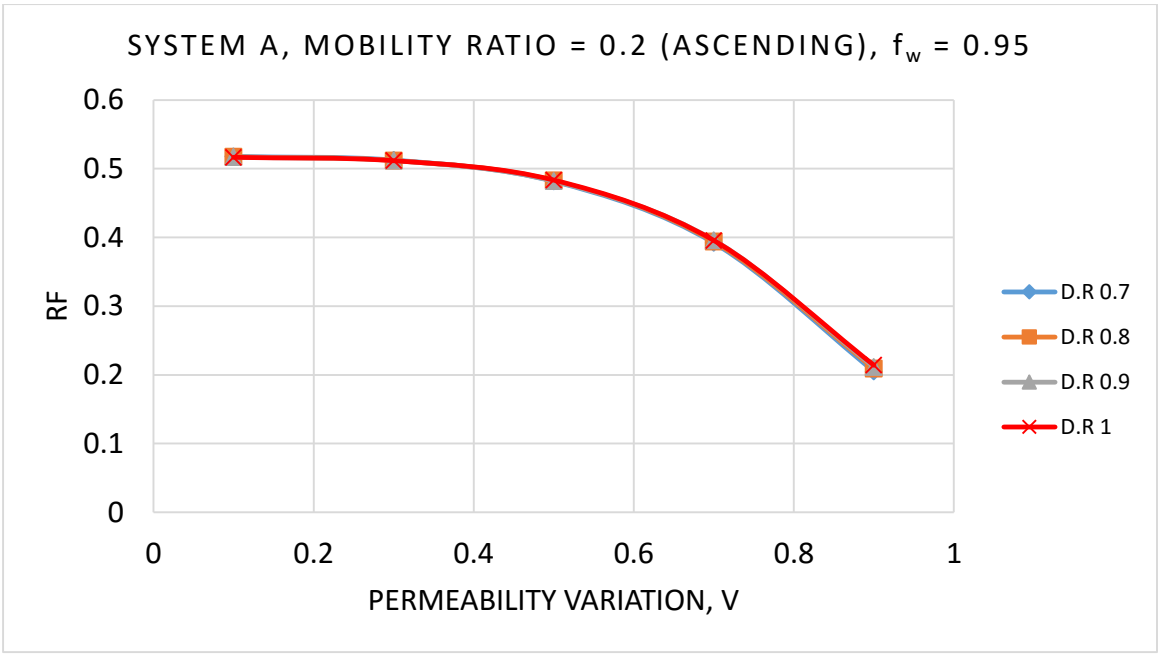

Figure 45 Effect of density ratio on oil recovery factor beyond water breakthrough for System A ascending case-Case 1

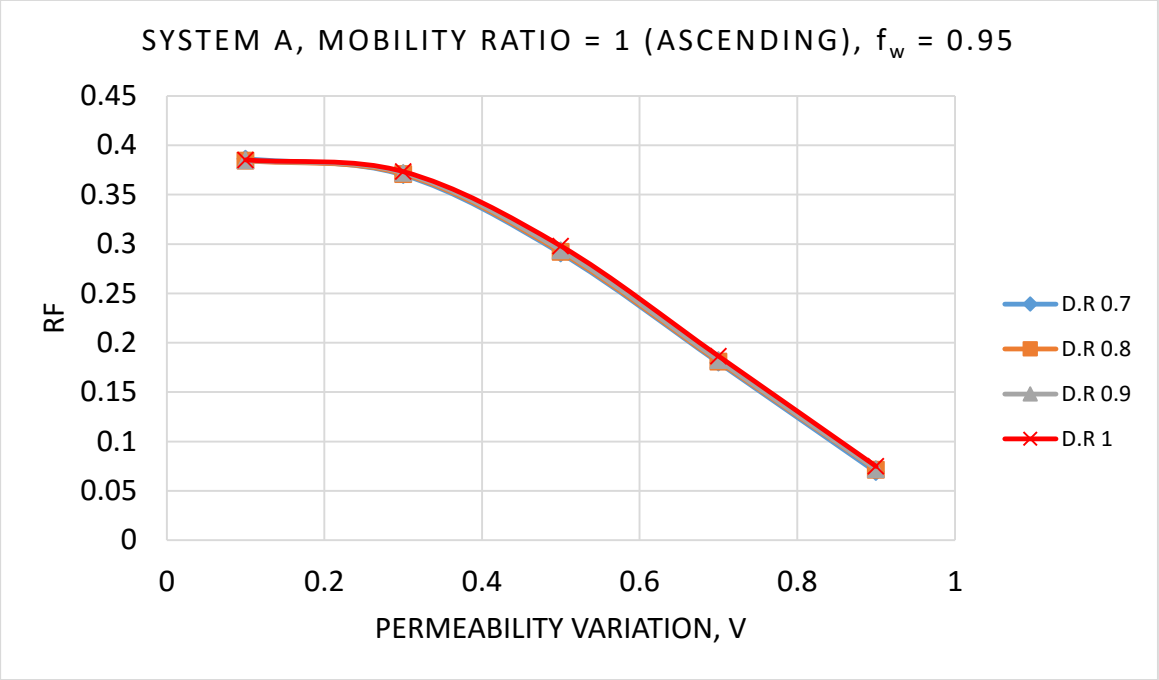

Figure 46 Effect of density ratio on oil recovery factor beyond water breakthrough for System A ascending case-Case 2

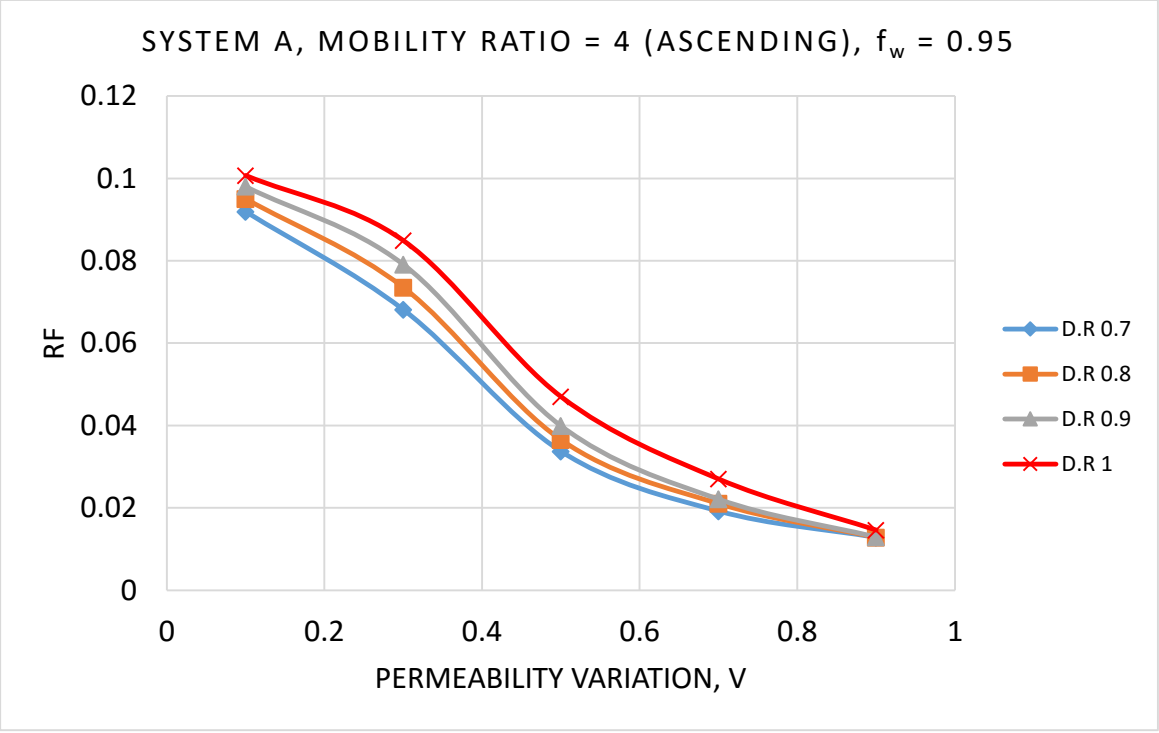

Figure 47 Effect of density ratio on oil recovery factor beyond water breakthrough for System A ascending case-Case 3

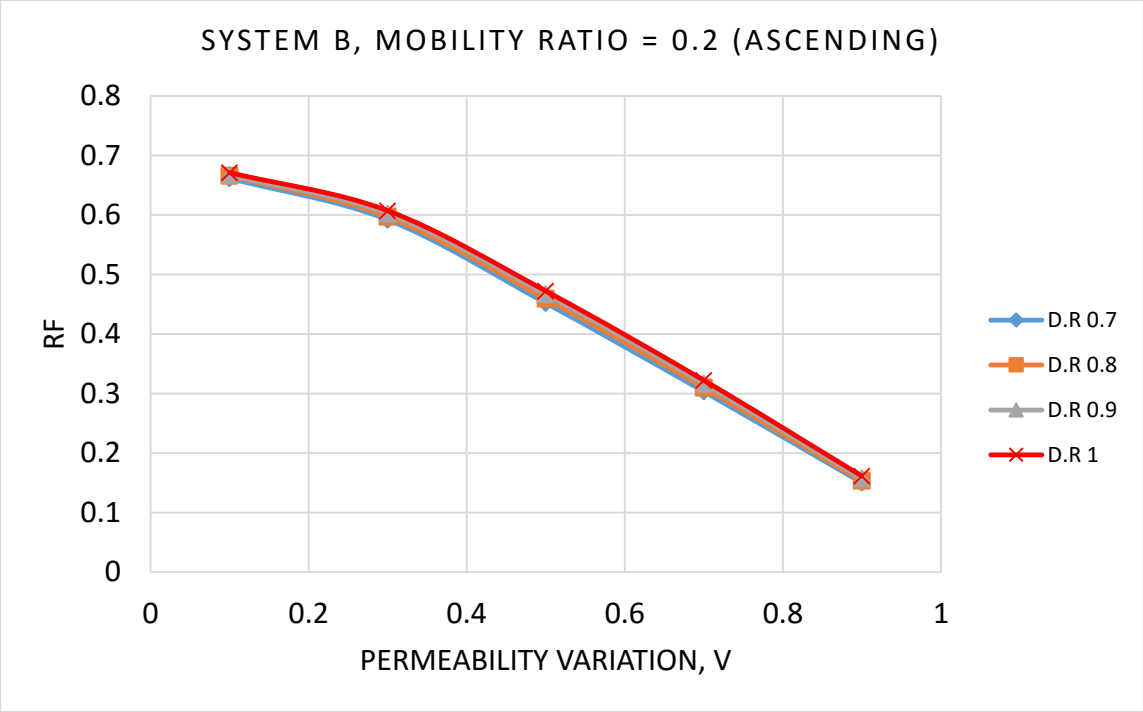

Figure 48 Effect of density ratio on oil recovery factor at water breakthrough for system B ascending case-Case 1

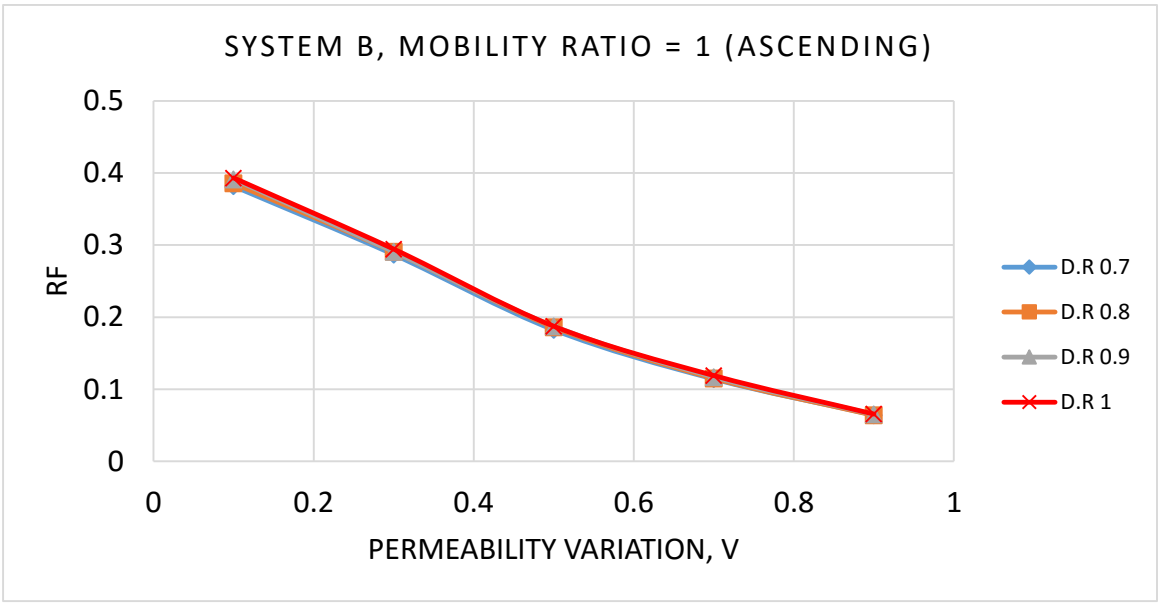

Figure 49 Effect of density ratio on oil recovery factor at water breakthrough for system B ascending case-Case 2

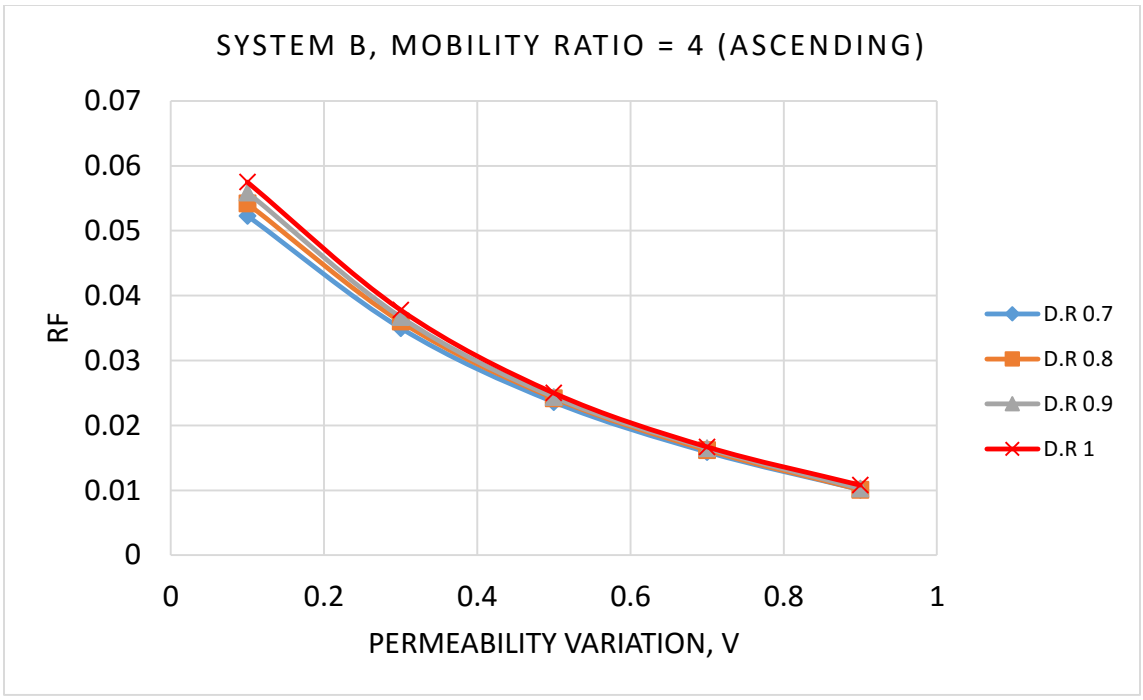

Figure 50 Effect of density ratio on oil recovery factor at water breakthrough for system B ascending case-Case 3

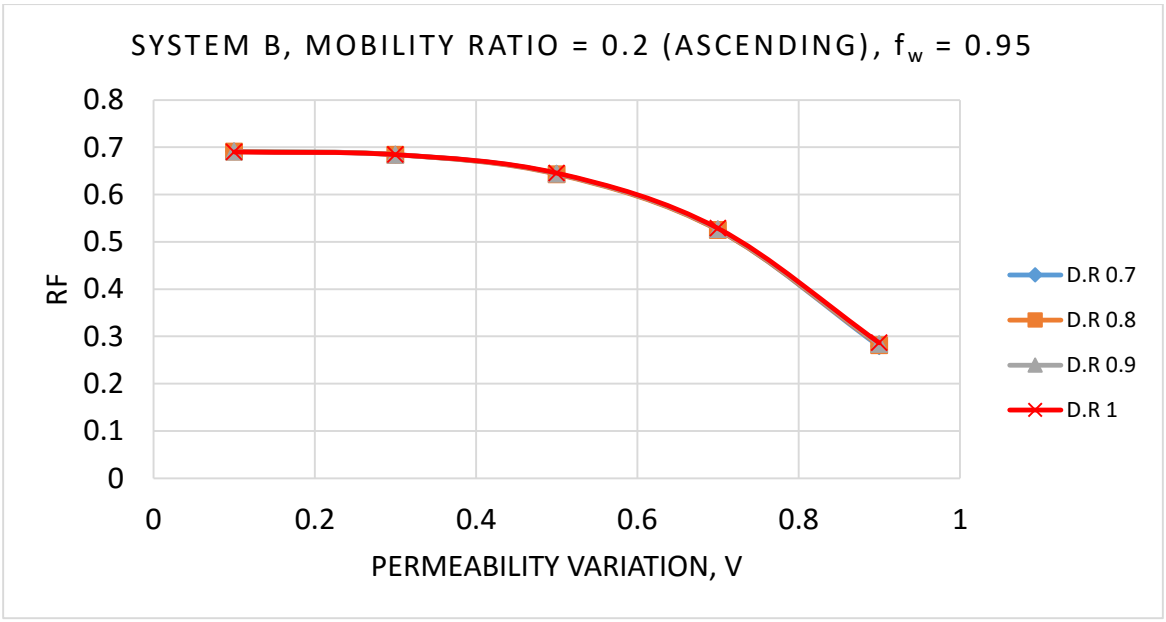

Figure 51 Effect of density ratio on oil recovery factor beyond water breakthrough for System B ascending case-Case 1

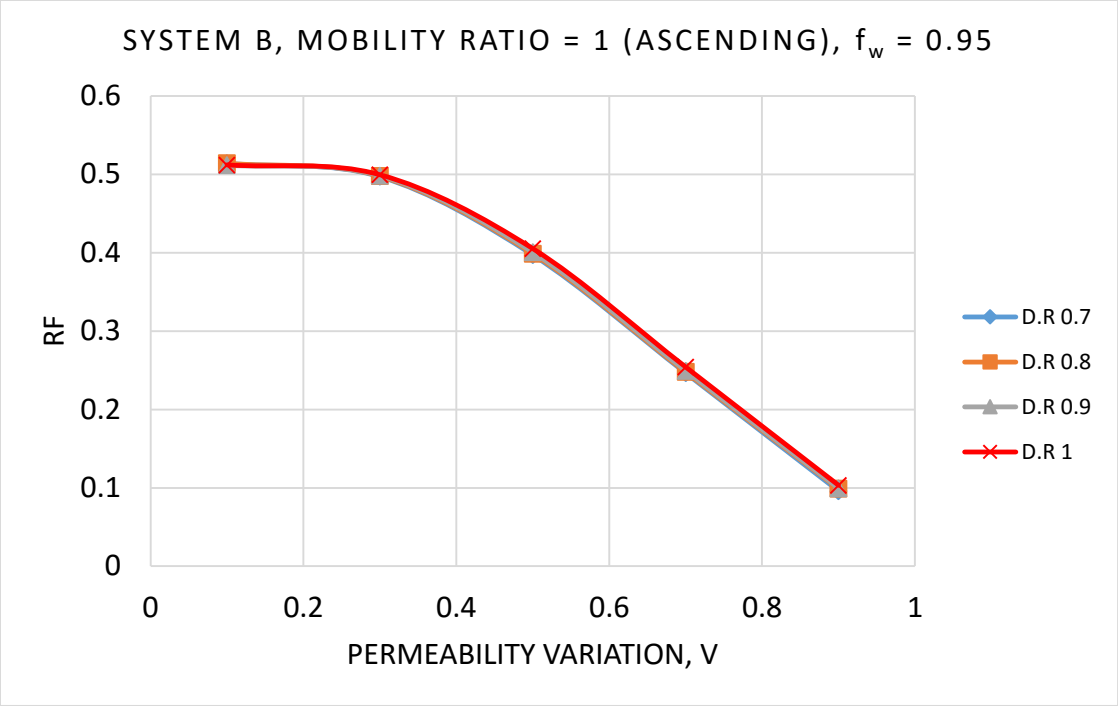

Figure 52 Effect of density ratio on oil recovery factor beyond water breakthrough for System B ascending case-Case 2

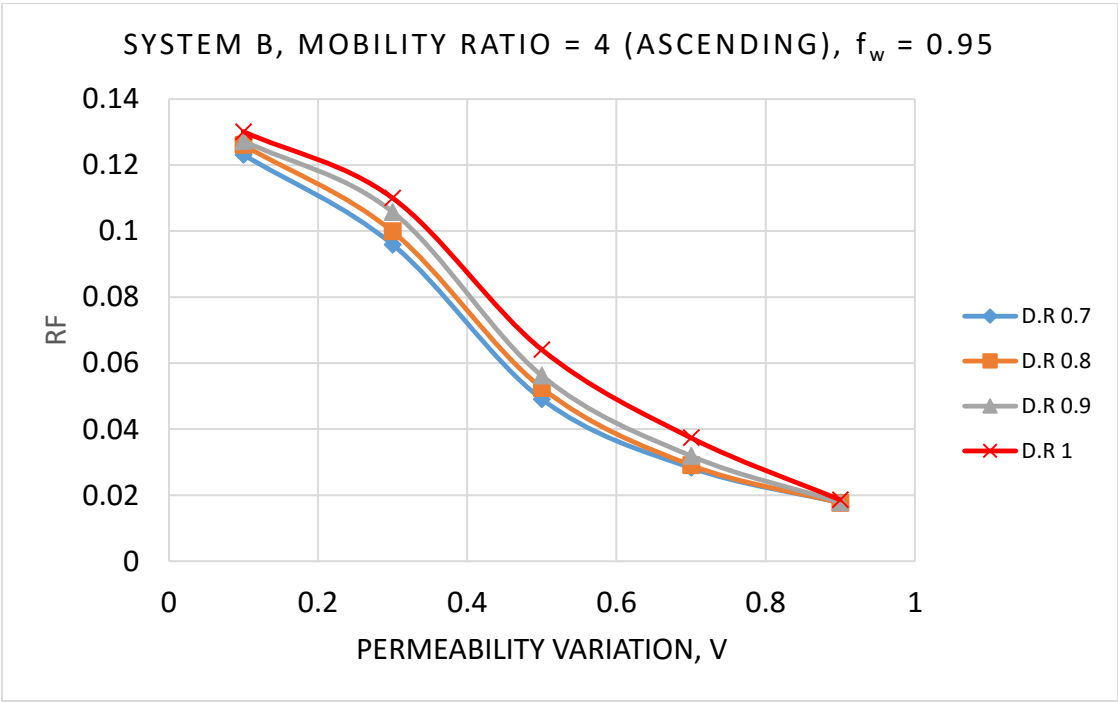

Figure 53 Effect of density ratio on oil recovery factor beyond water breakthrough for System B ascending case-Case 3

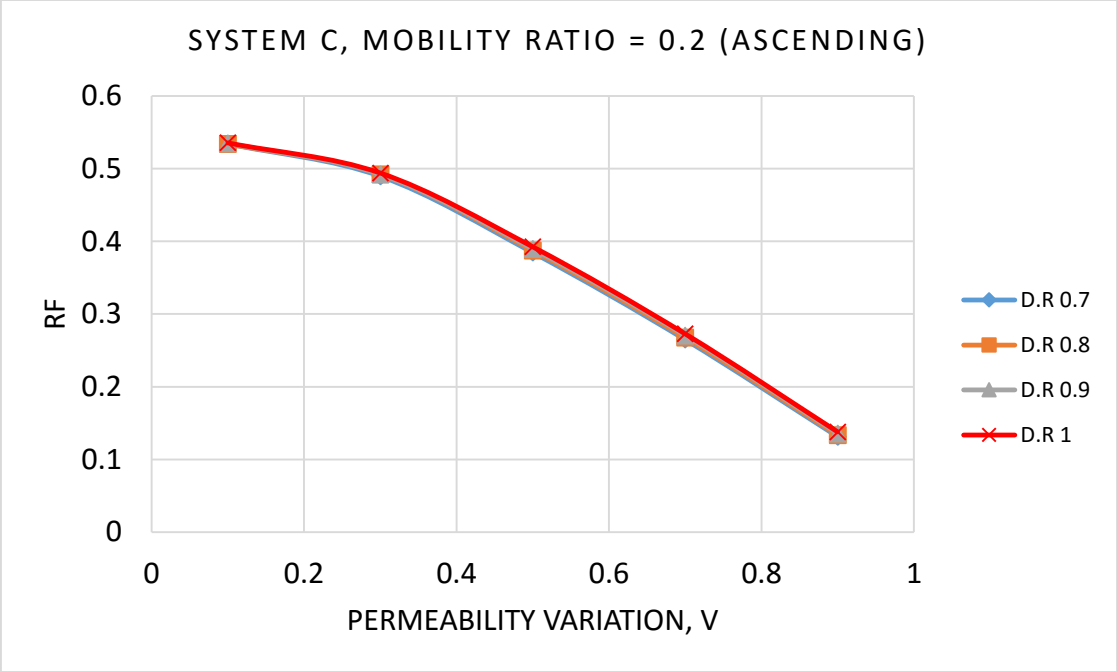

Figure 54 Effect of density ratio on oil recovery factor at water breakthrough for system C ascending case-Case 1

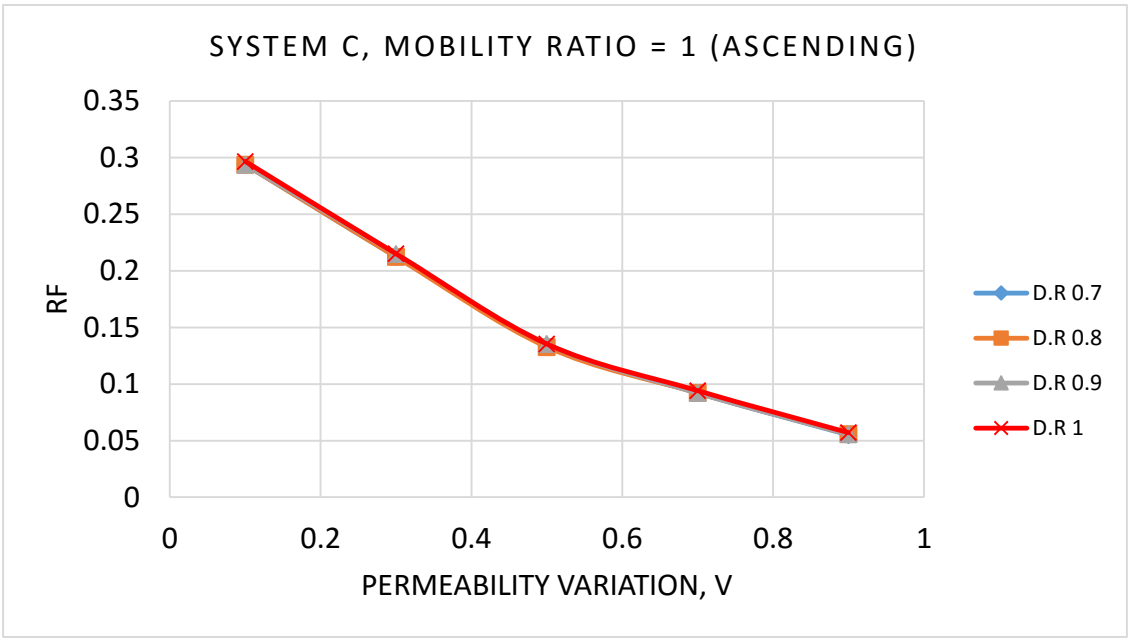

Figure 55 Effect of density ratio on oil recovery factor at water breakthrough for system C ascending case-Case 2

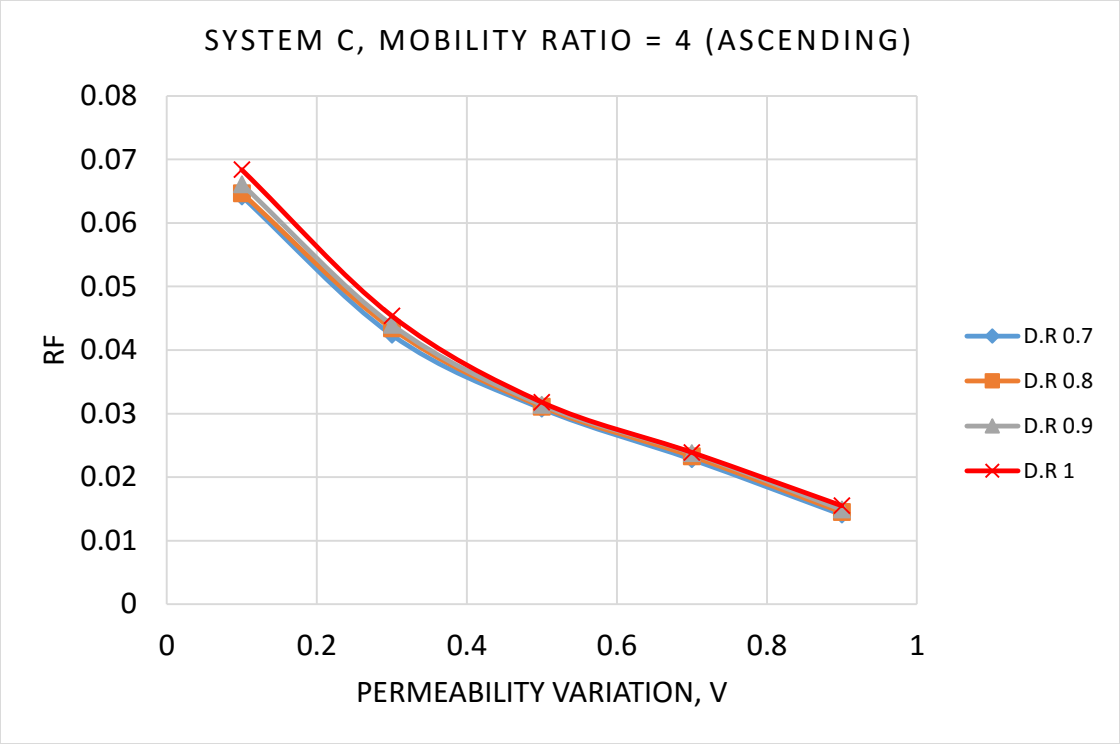

Figure 56 Effect of density ratio on oil recovery factor at water breakthrough for system C ascending case-Case 3

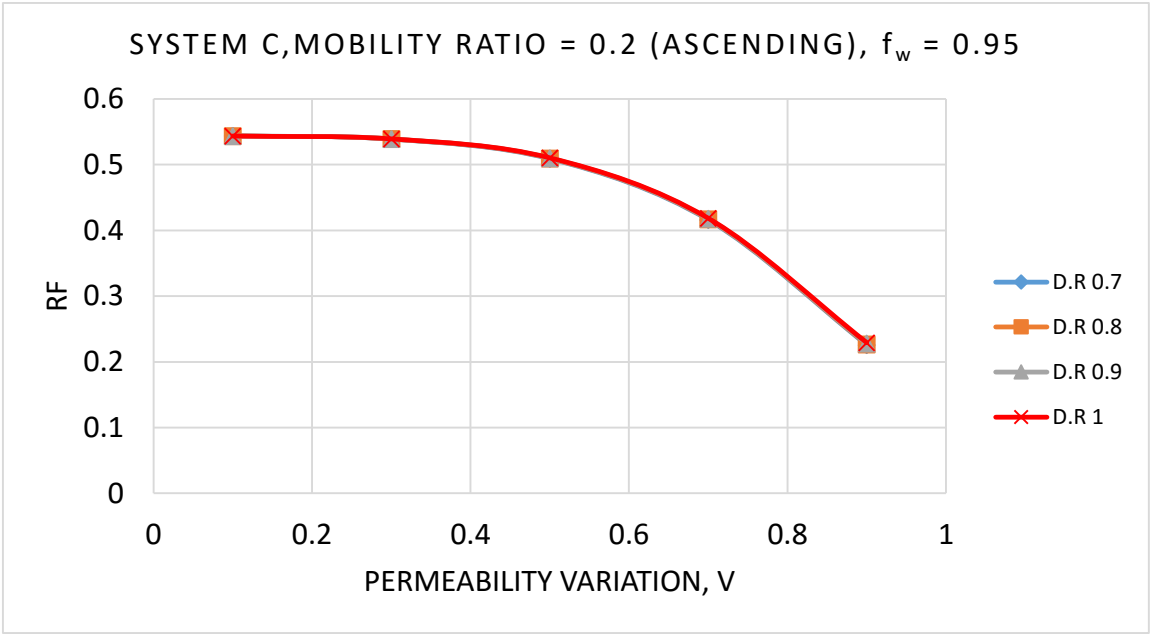

Figure 57 Effect of density ratio on oil recovery factor beyond water breakthrough for System C ascending case-Case 1

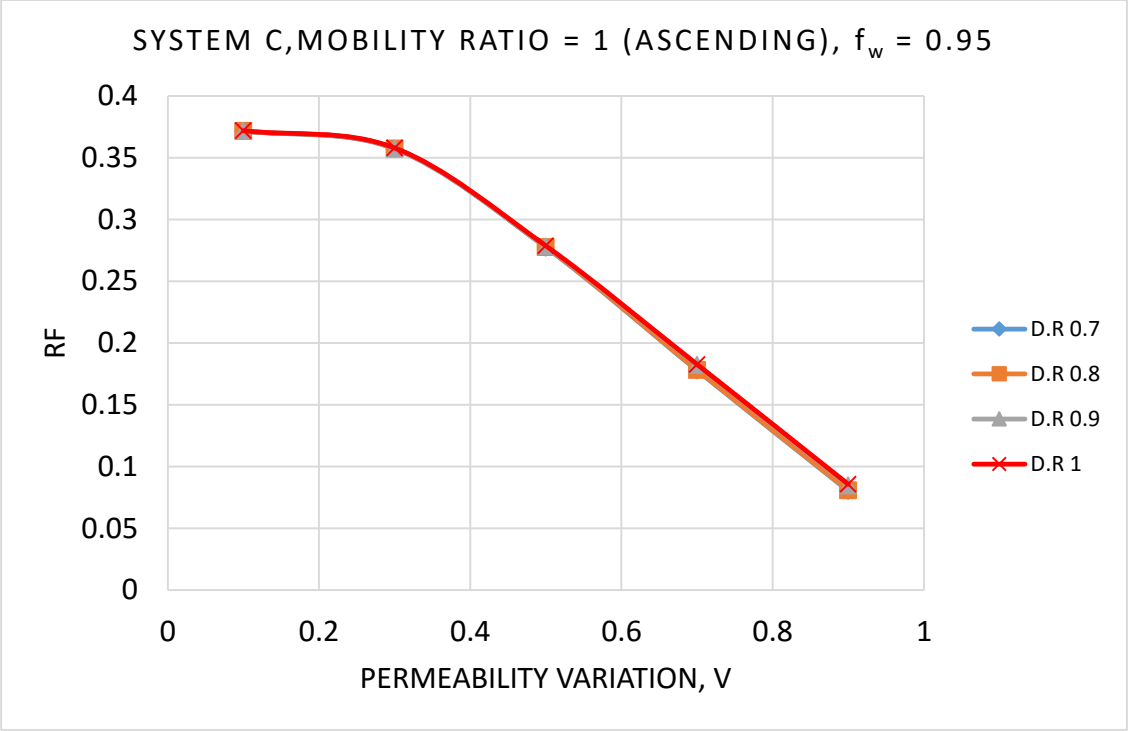

Figure 58 Effect of density ratio on oil recovery factor beyond water breakthrough for System C ascending case-Case 2

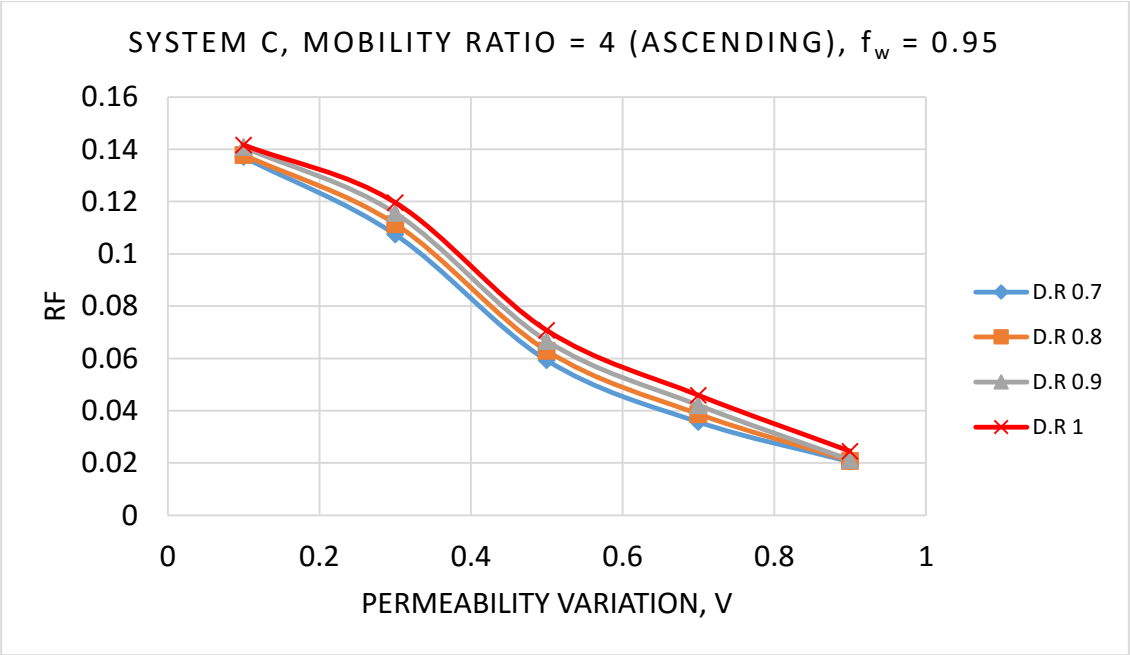

Figure 59 Effect of density ratio on oil recovery factor beyond water breakthrough for System C ascending case-Case 3

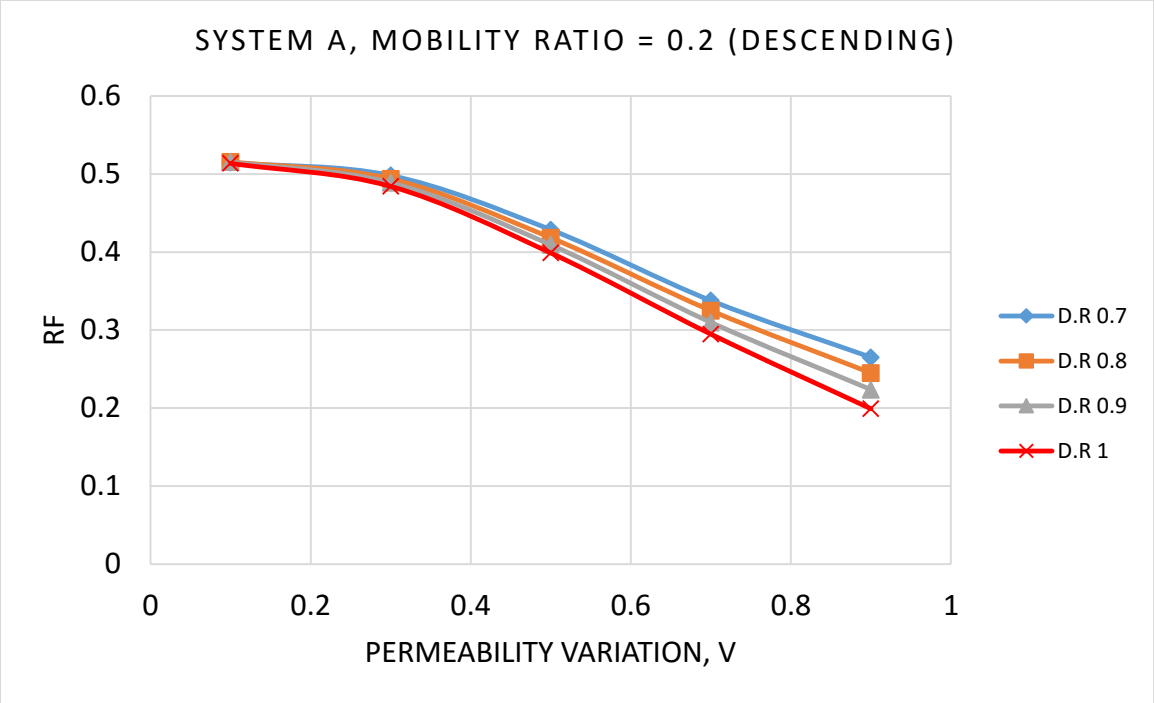

Figure 60 Effect of density ratio on oil recovery factor at water breakthrough for system A descending case-Case 1

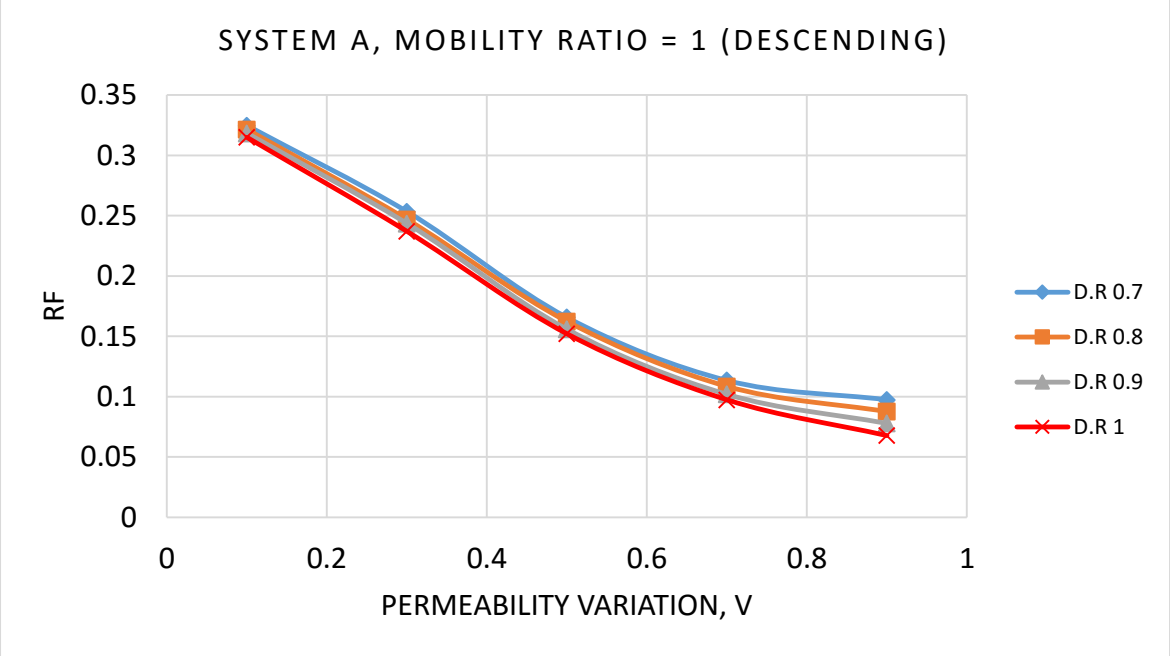

Figure 61 Effect of density ratio on oil recovery factor at water breakthrough for system A descending case-Case 2

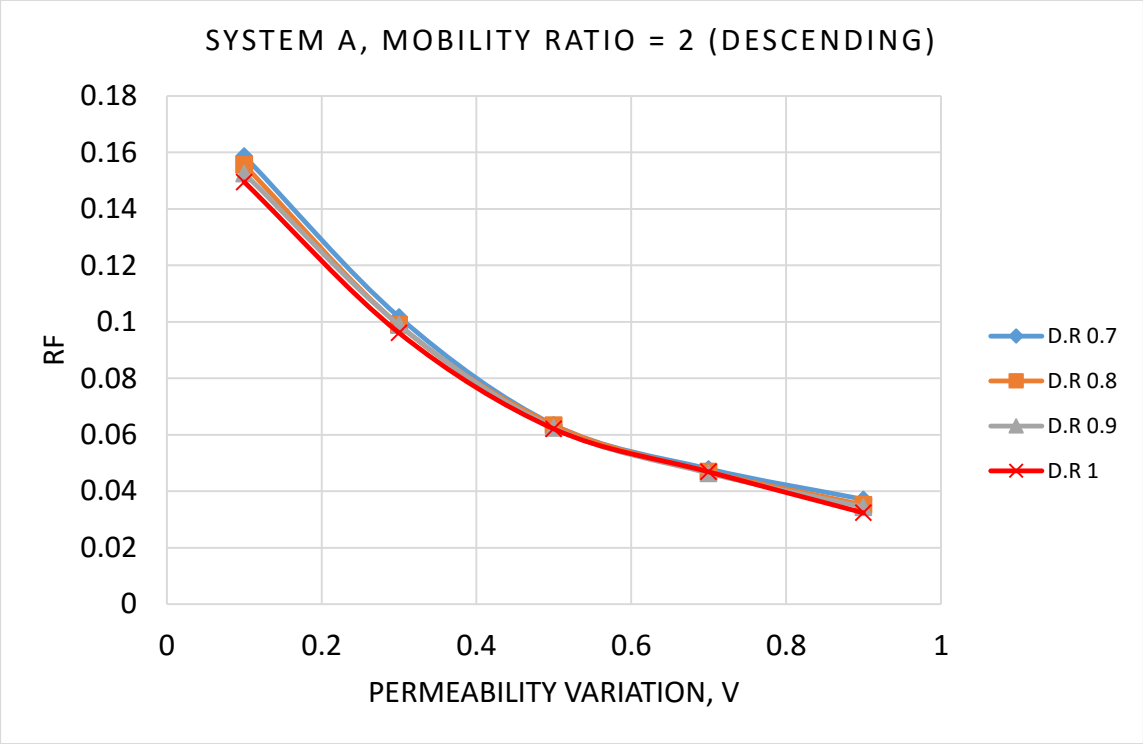

Figure 62 Effect of density ratio on oil recovery factor at water breakthrough for system A descending case-Case 3

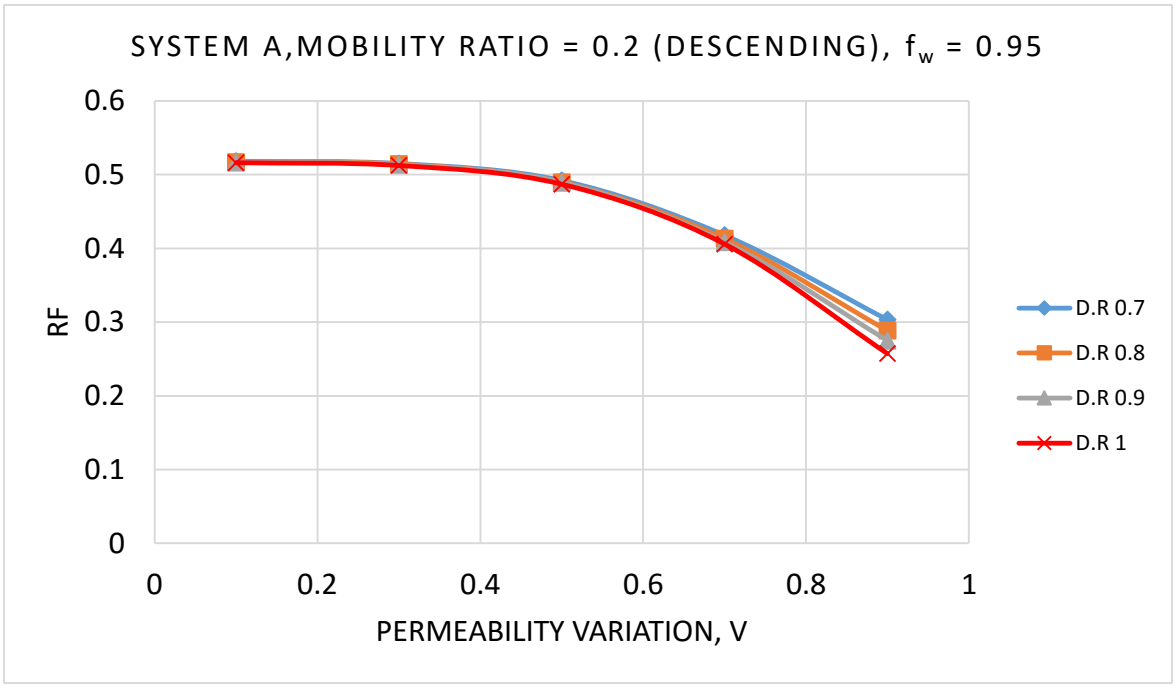

Figure 63 Effect of density ratio on oil recovery factor beyond water breakthrough for System A descending case-Case 1

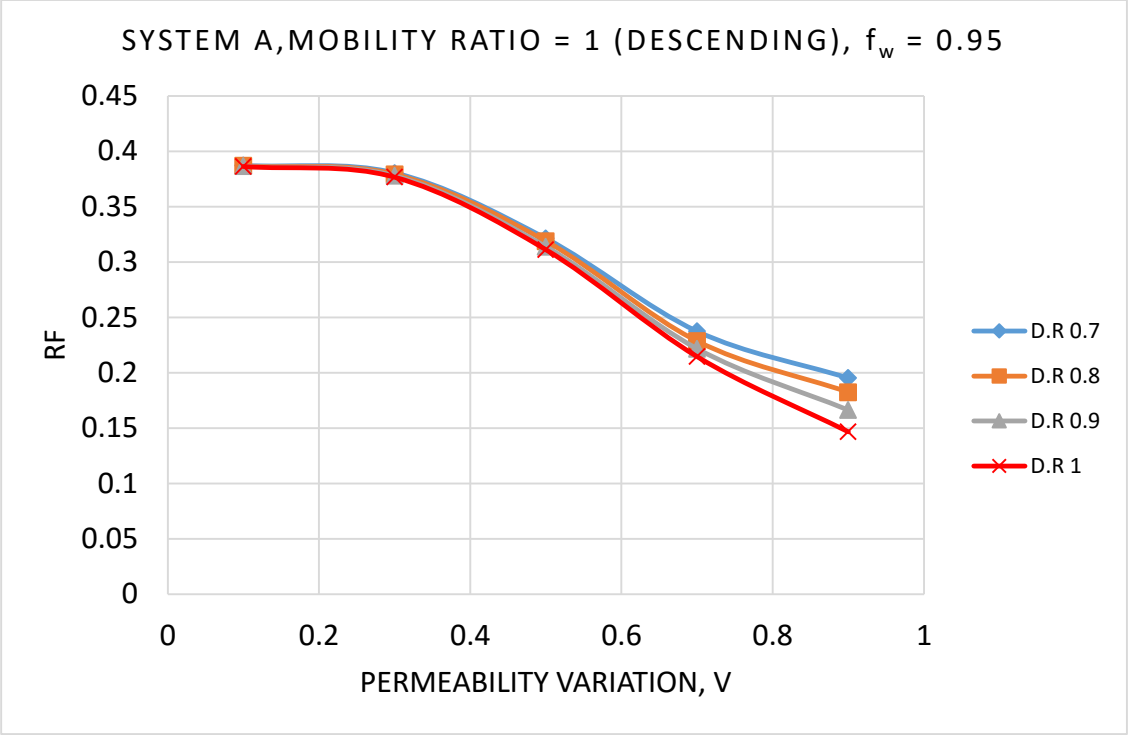

Figure 64 Effect of density ratio on oil recovery factor beyond water breakthrough for System A descending case-Case 2

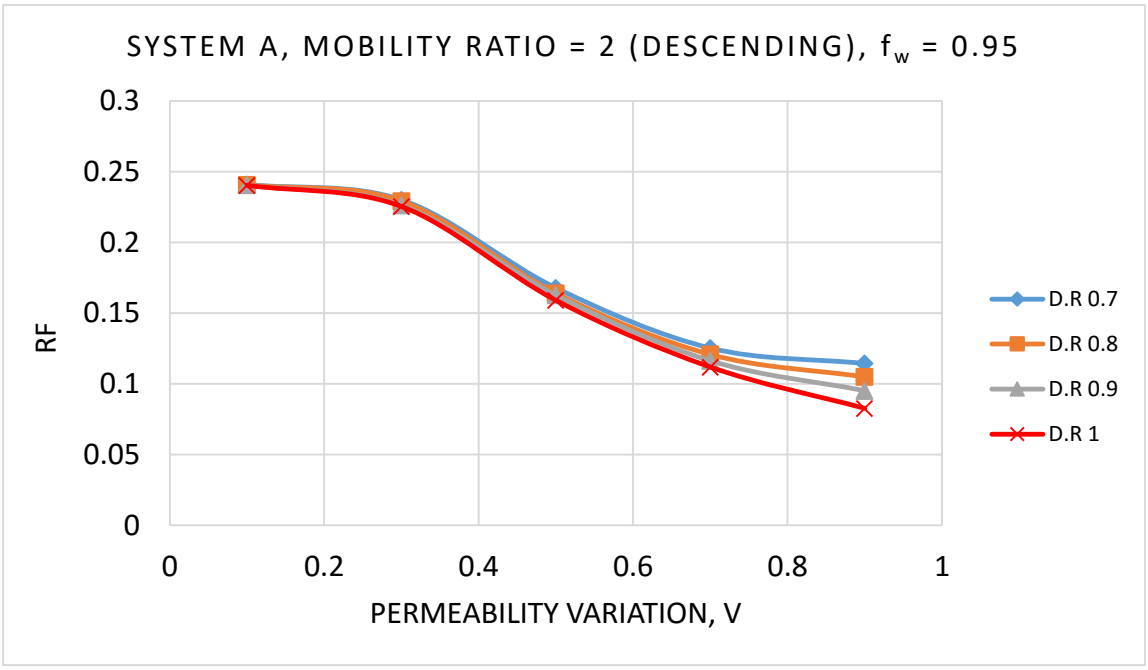

Figure 65 Effect of density ratio on oil recovery factor beyond water breakthrough for System A descending case-Case 3

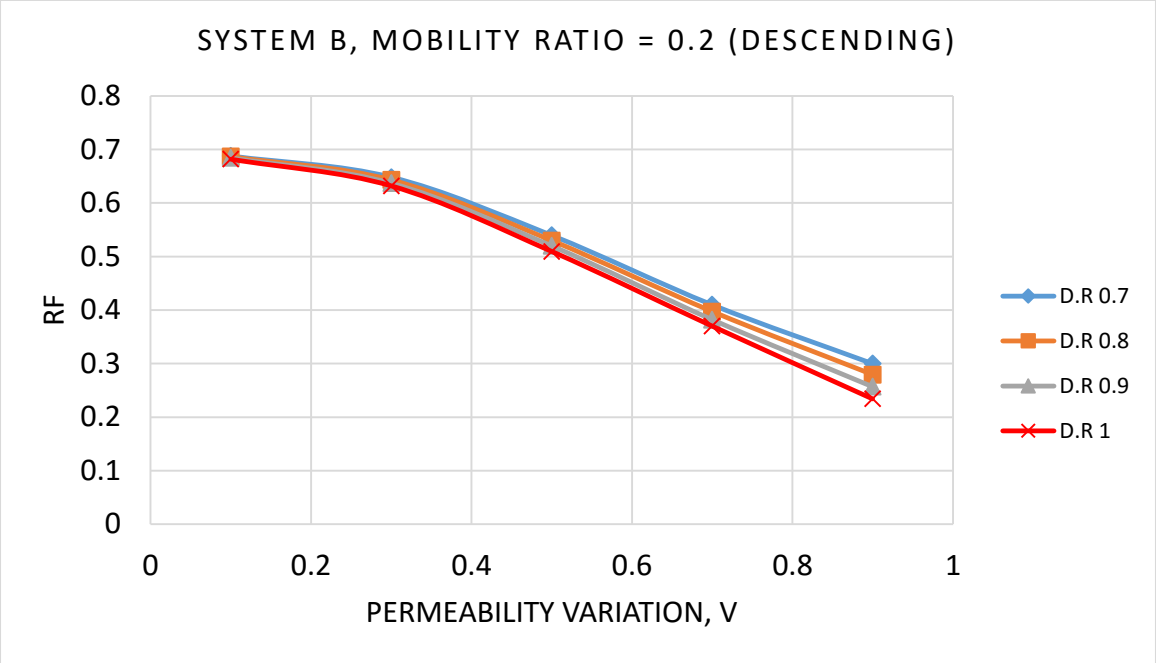

Figure 66 Effect of density ratio on oil recovery factor at water breakthrough for system B descending case-Case 1

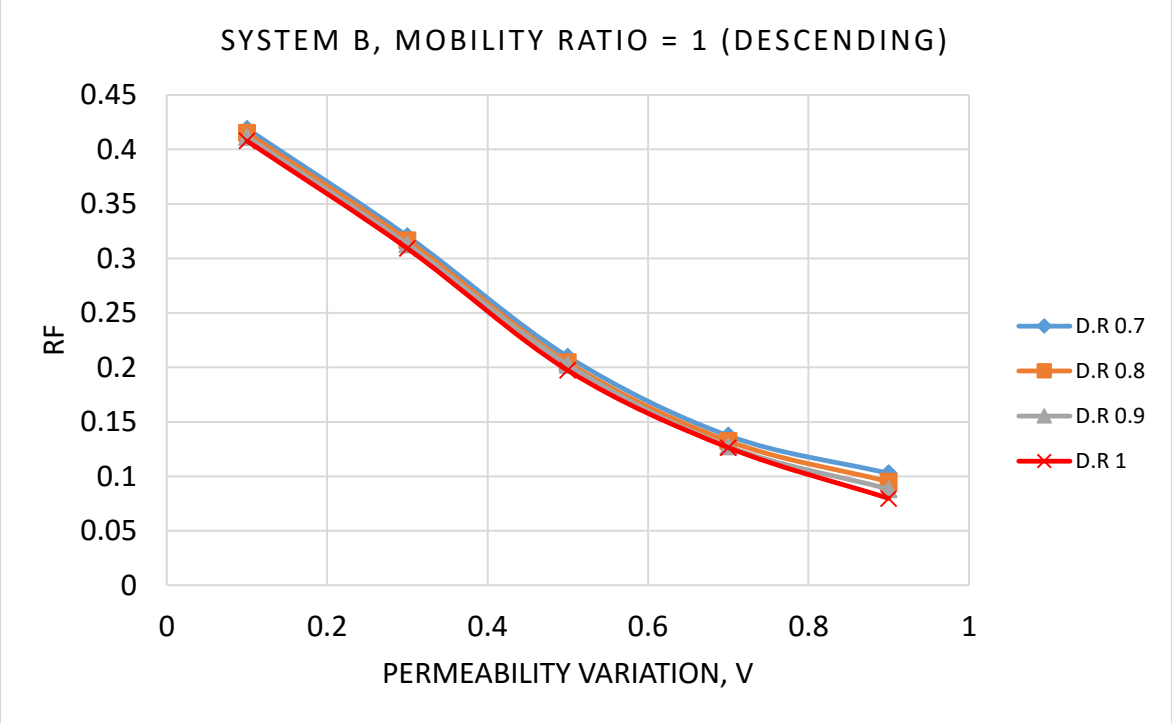

Figure 67 Effect of density ratio on oil recovery factor at water breakthrough for system B descending case-Case 2

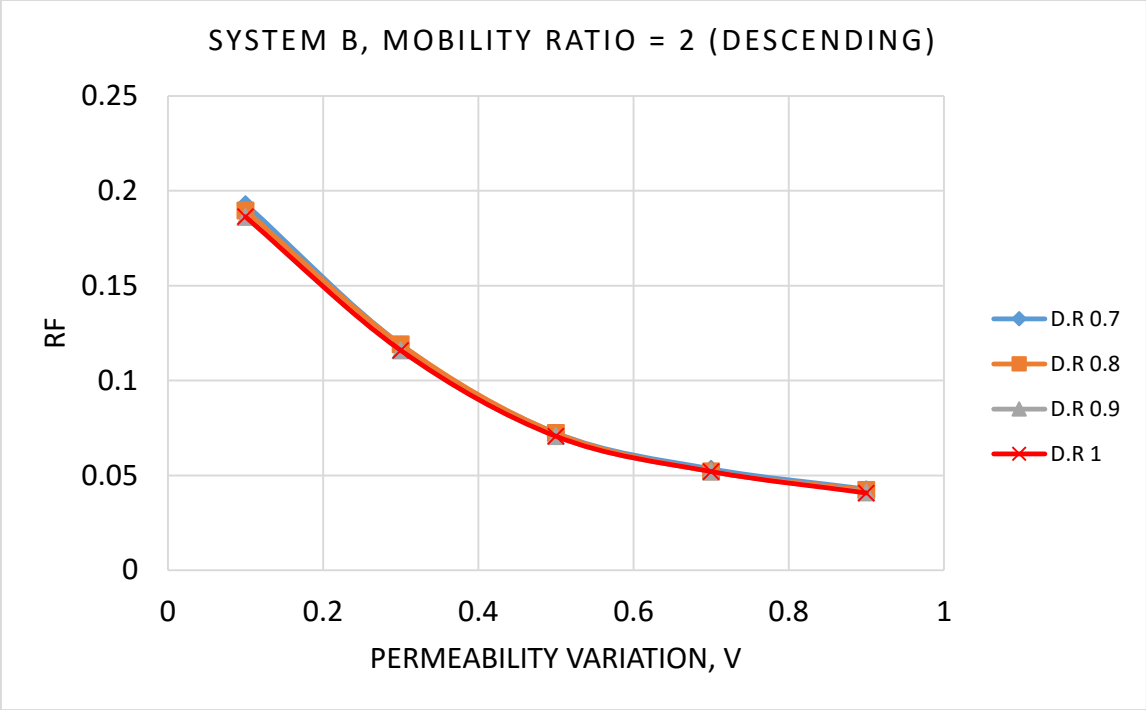

Figure 68 Effect of density ratio on oil recovery factor at water breakthrough for system B descending case-Case 3

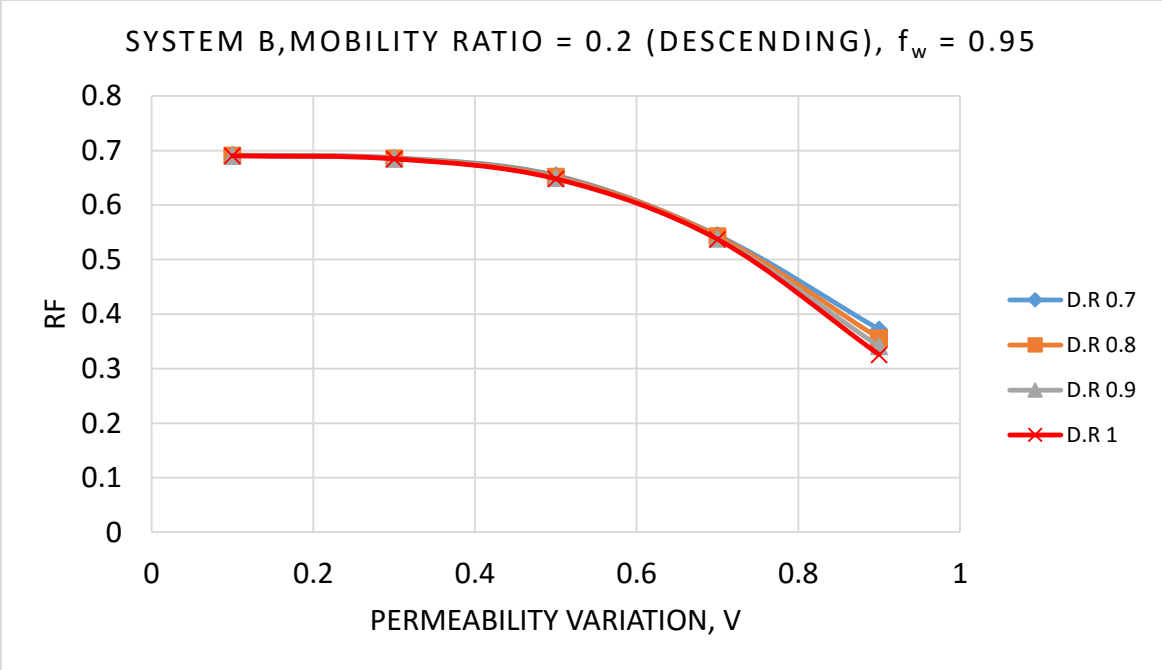

Figure 69 Effect of density ratio on oil recovery factor beyond water breakthrough for System B descending case-Case 1

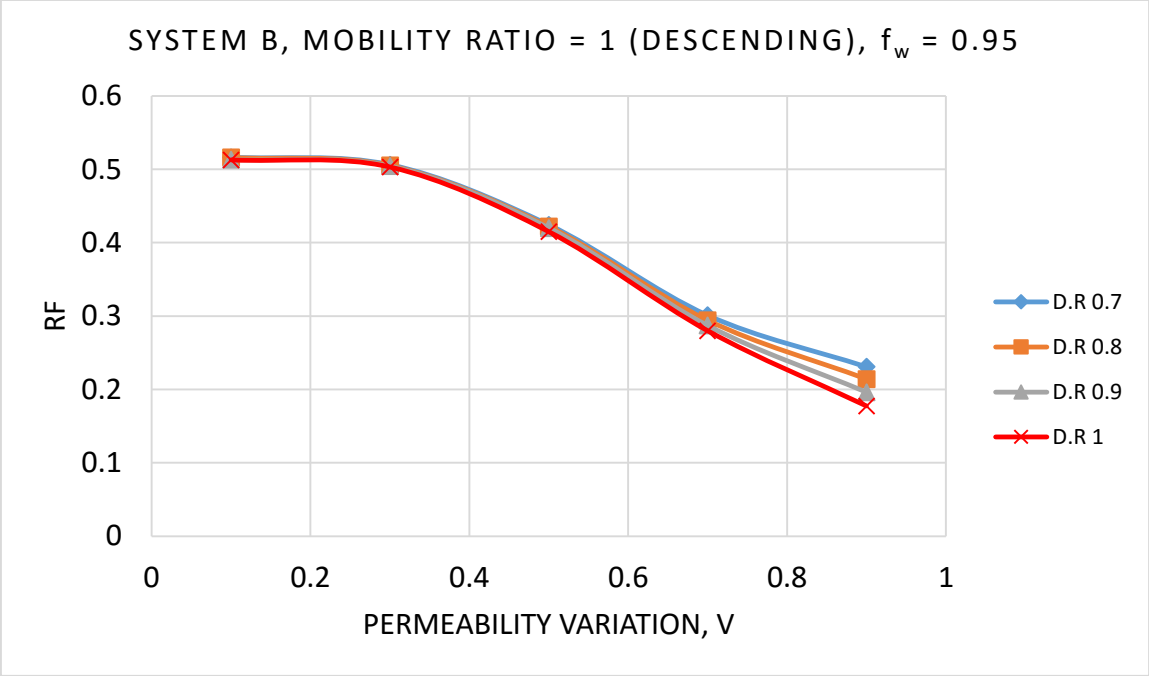

Figure 70 Effect of density ratio on oil recovery factor beyond water breakthrough for System B descending case-Case 2

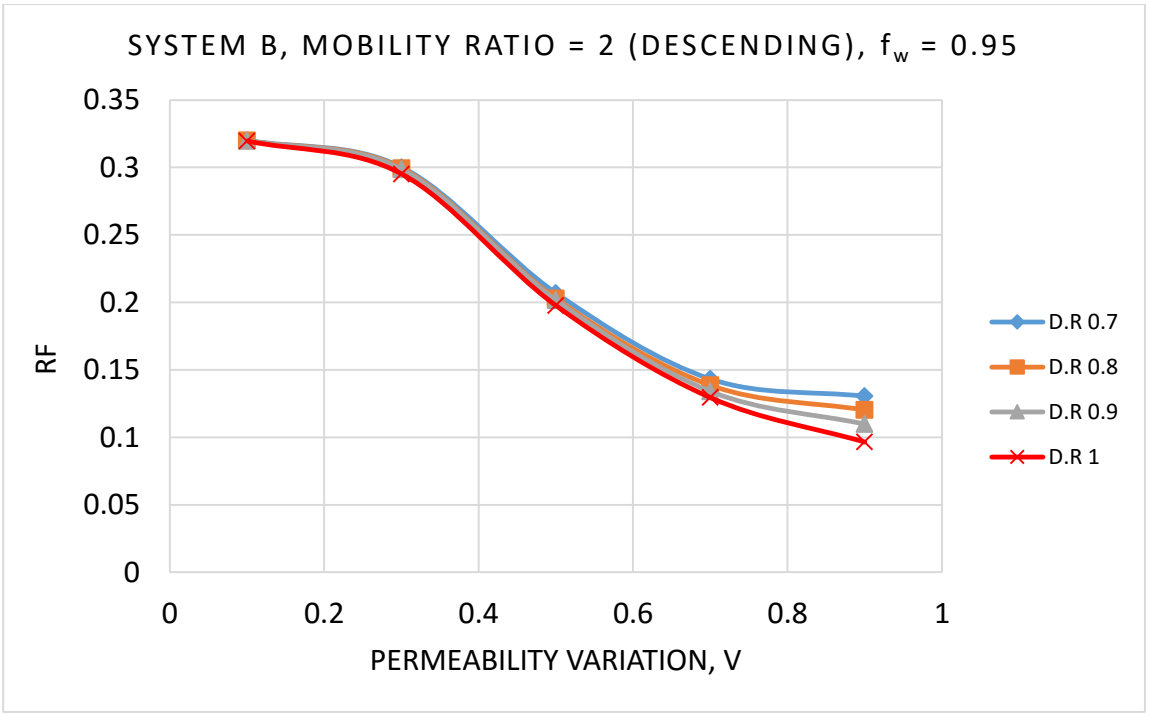

Figure 71 Effect of density ratio on oil recovery factor beyond water breakthrough for System B descending case-Case 3

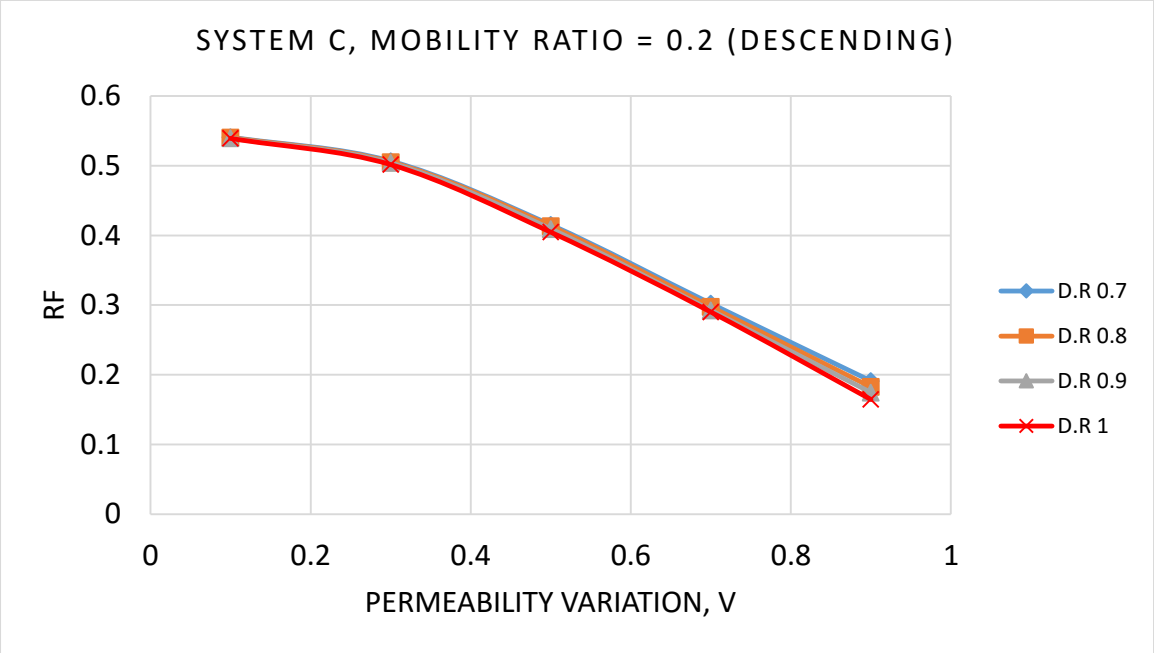

Figure 72 Effect of density ratio on oil recovery factor at water breakthrough for system C descending case-Case 1

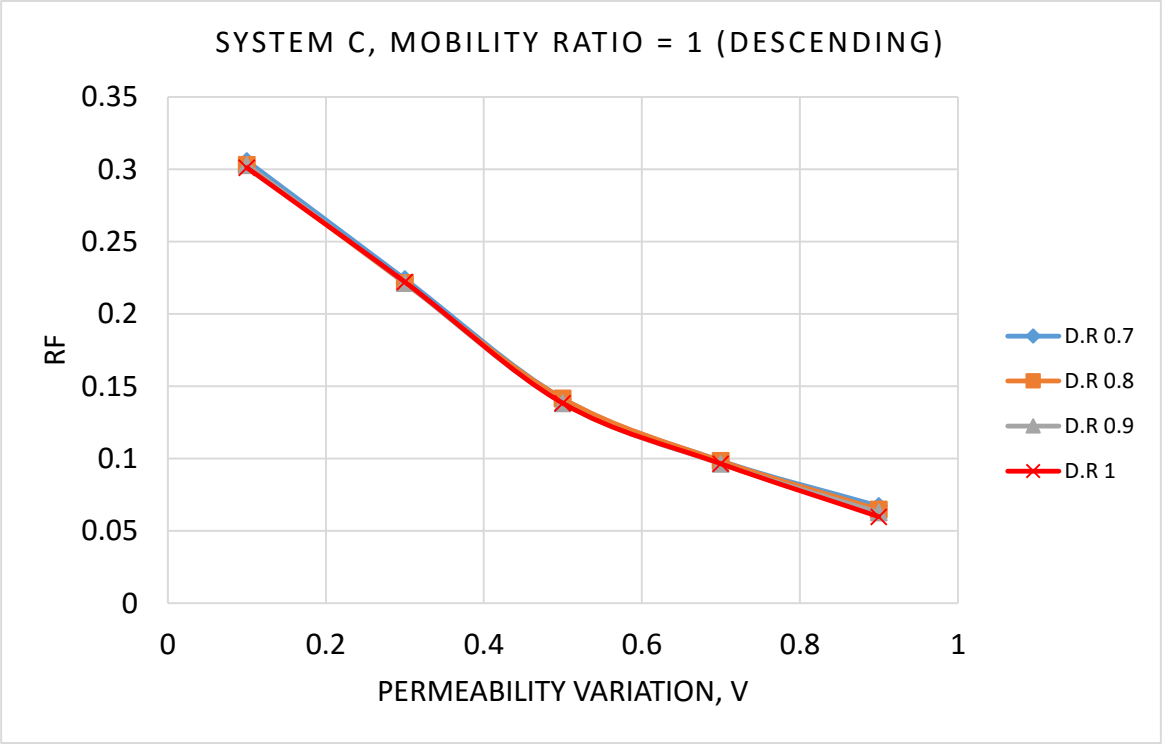

Figure 73 Effect of density ratio on oil recovery factor at water breakthrough for system C descending case-Case 2

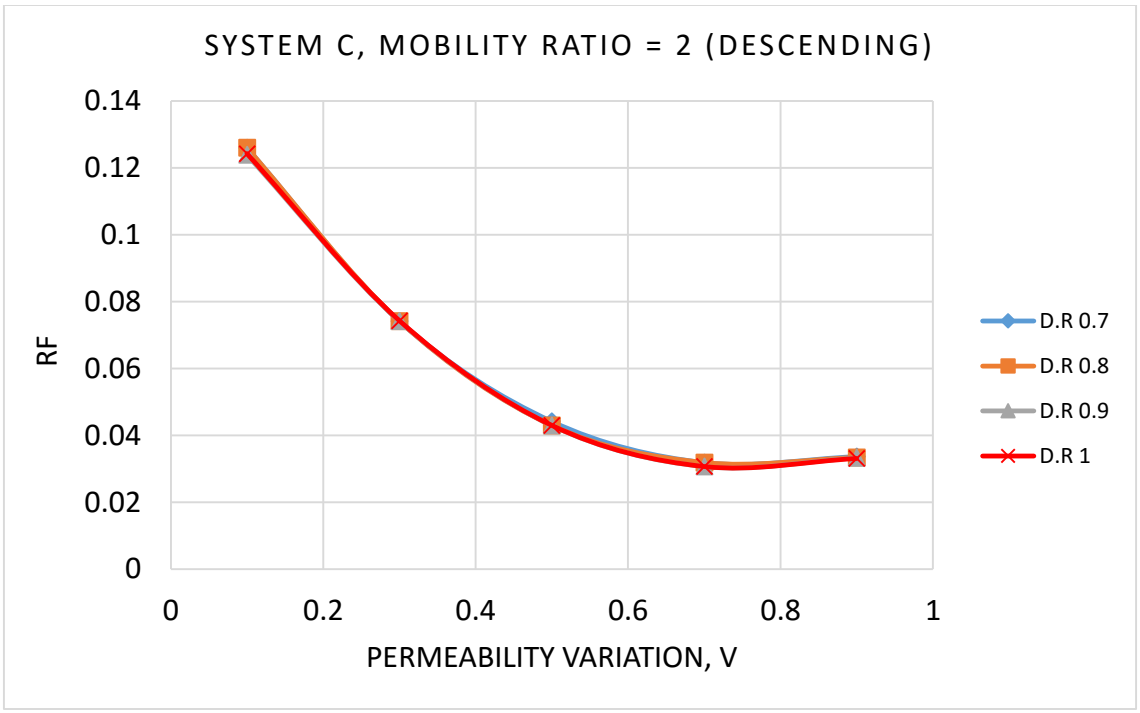

Figure 74 Effect of density ratio on oil recovery factor at water breakthrough for system C descending case-Case 3

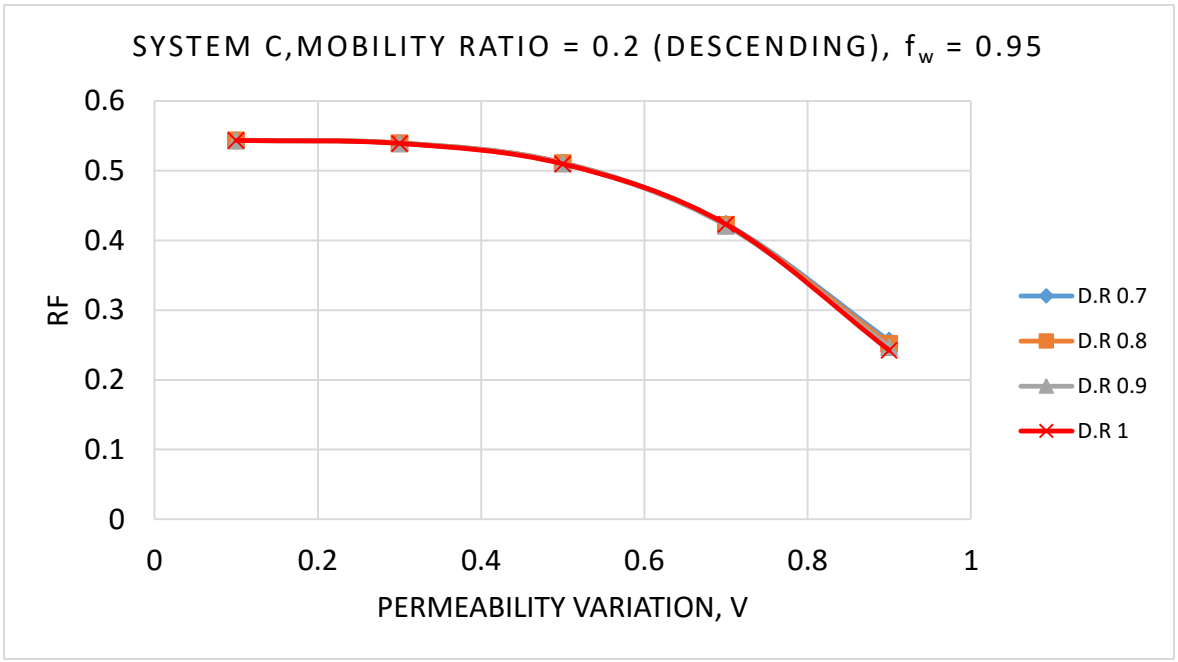

Figure 75 Effect of density ratio on oil recovery factor beyond water breakthrough for System C descending case-Case 1

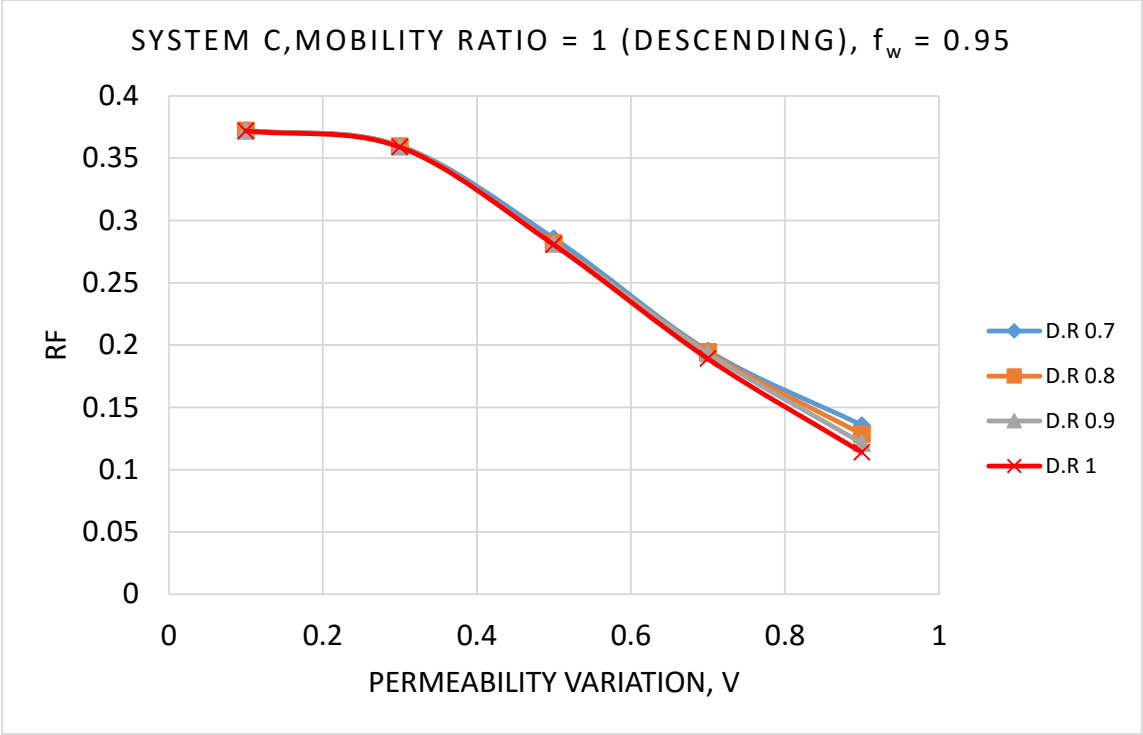

Figure 76 Effect of density ratio on oil recovery factor beyond water breakthrough for System C descending case-Case 2

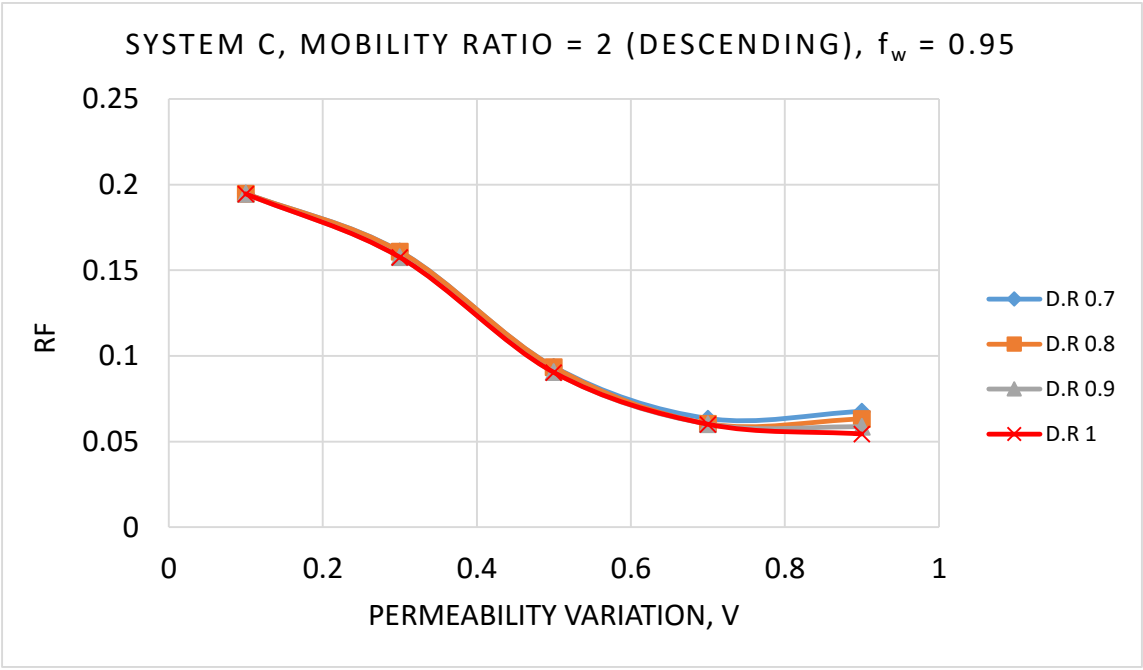

Figure 77 Effect of density ratio on oil recovery factor beyond water breakthrough for System C descending case-Case 3

5.4 Effect of Wettability

As mentioned in Chapter 1, the "Wettability Indicator" is a new parameter introduced to account for the effect of wettability. To examine the effect of wettability on recovery factor (*RF*) and movable oil recovery factor (RF_m), three reservoir systems with different wettability indicators were tested.

The effect of wettability on oil recovery at and beyond breakthrough for favorable and unfavorable mobility ratios is shown in Figures 78 to 93 for both ascending and descending cases. In both cases of permeability arrangement and at low mobility ratio, it appears that the best recovery is obtained with the neutral-wettability (system B) while the lowest recovery is obtained with the oil wet (system A). The water wet (system C) shows recovery between the other two. At high mobility ratio, the highest recovery is from the water wet (system C) while the lowest recovery is from the oil wet (system A). The neutral-wettability (system B) shows intermediate recovery. The reason for low recovery in the oil-wet rock is due to the fact that the water will flow more easily than the oil during water flooding resulting in poor recovery while in a water-wet rock the oil will flow more easily than water resulting in better oil recovery.

Another observation is that the recovery factor (*RF*) is dependent on wettability in all cases while the movable oil recovery factor (RF_m) is independent of wettability at low mobility ratios but at high mobility ratios, the effect of wettability on RF_m can be seen. These effects are shown in Figures 78 to 93.

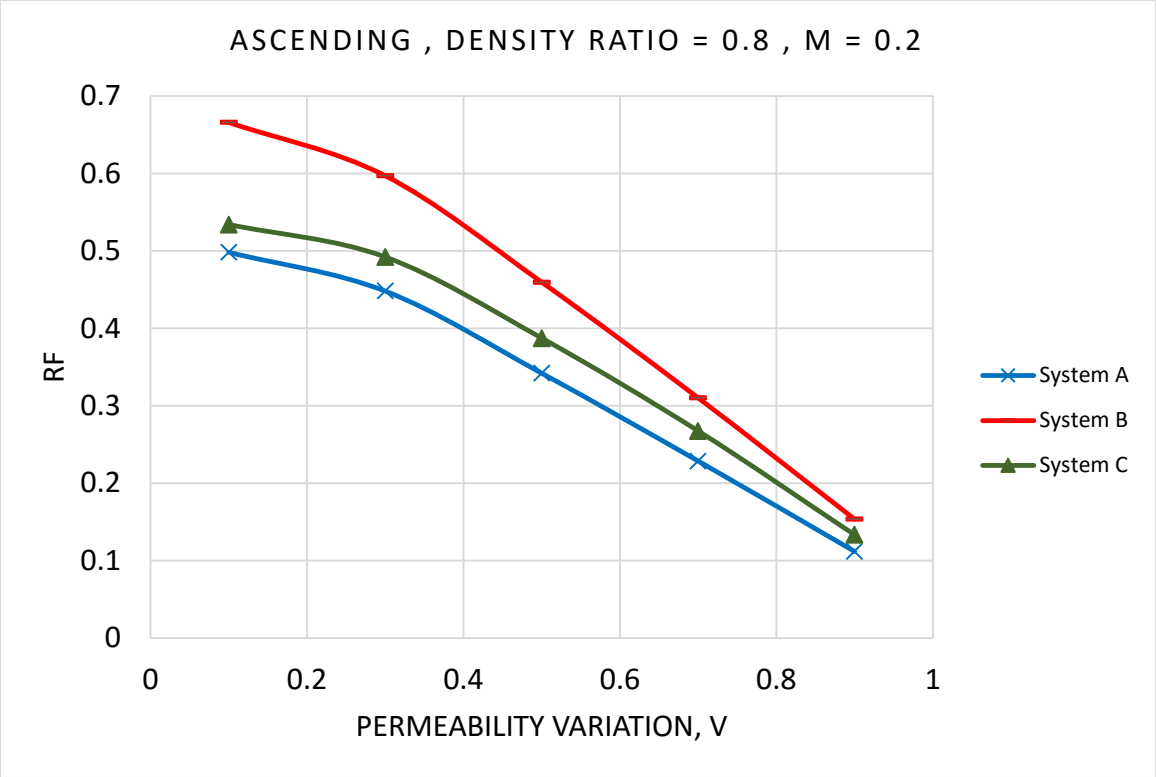

Figure 78 Effect of wettability on oil recovery factor at water breakthrough for ascending at M=0.2

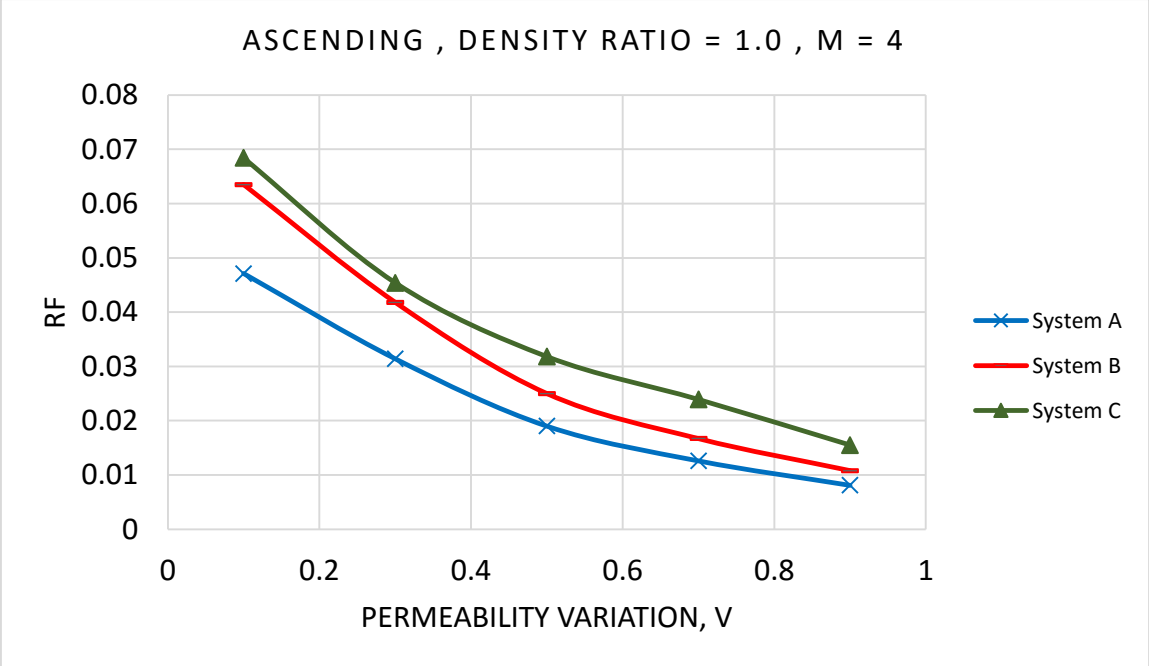

Figure 79 Effect of wettability on oil recovery factor at water breakthrough for ascending at M=4

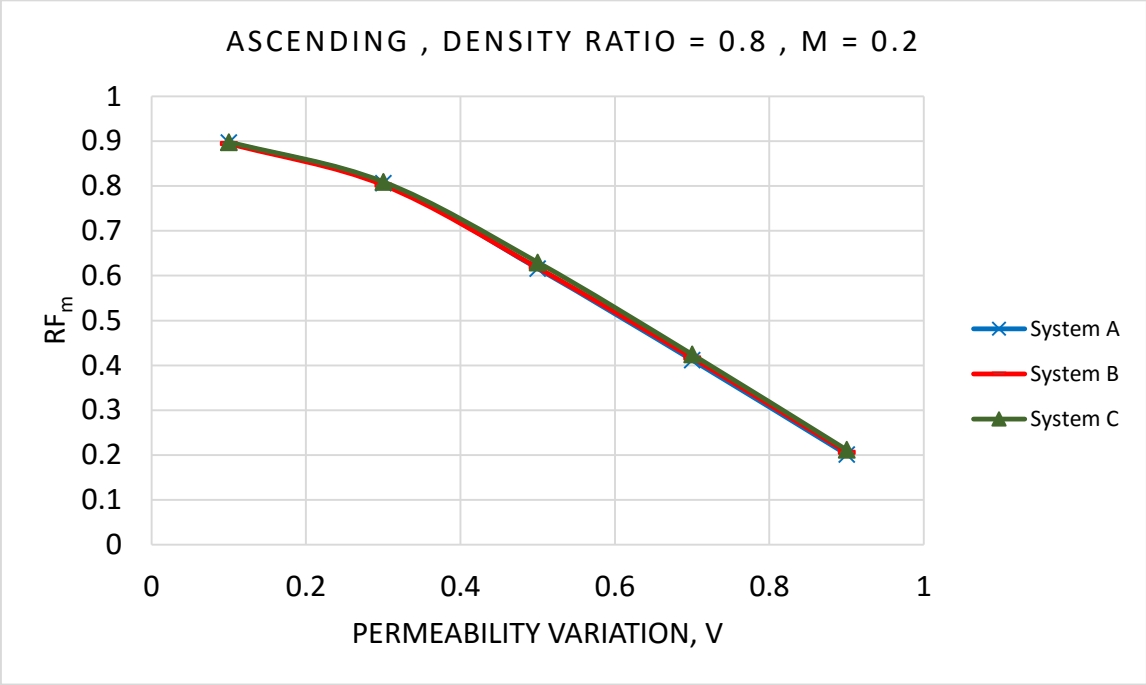

Figure 80 Effect of wettability on movable oil recovery factor at water breakthrough for ascending at M=0.2

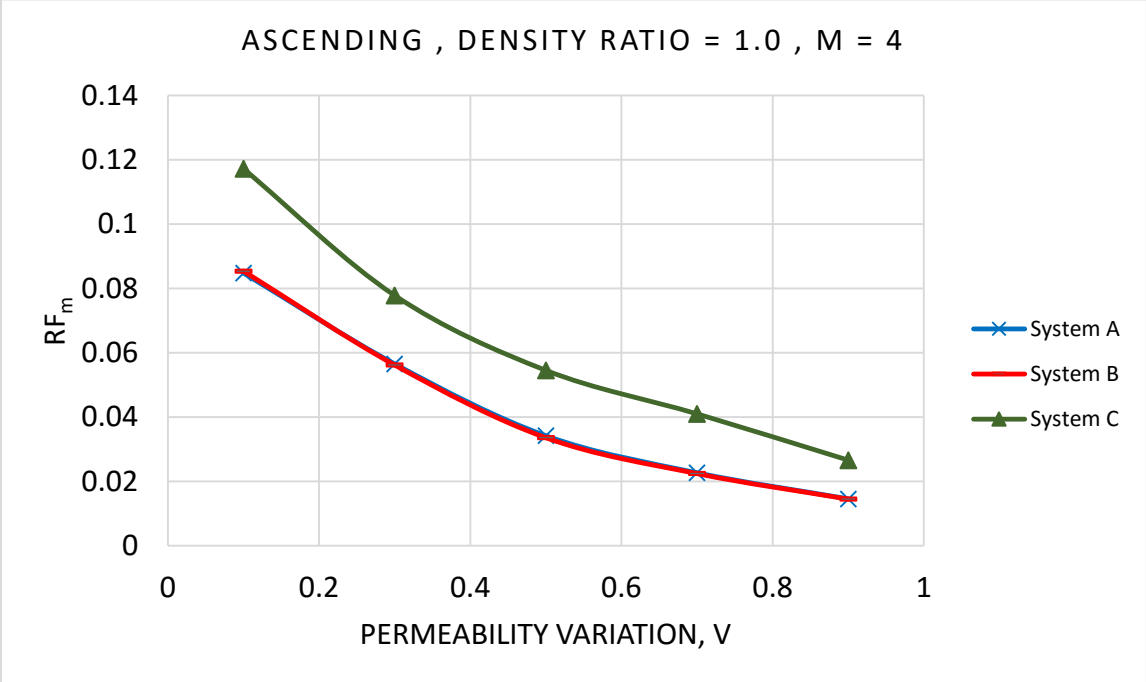

Figure 81 Effect of wettability on movable oil recovery factor at water breakthrough for ascending at M=4

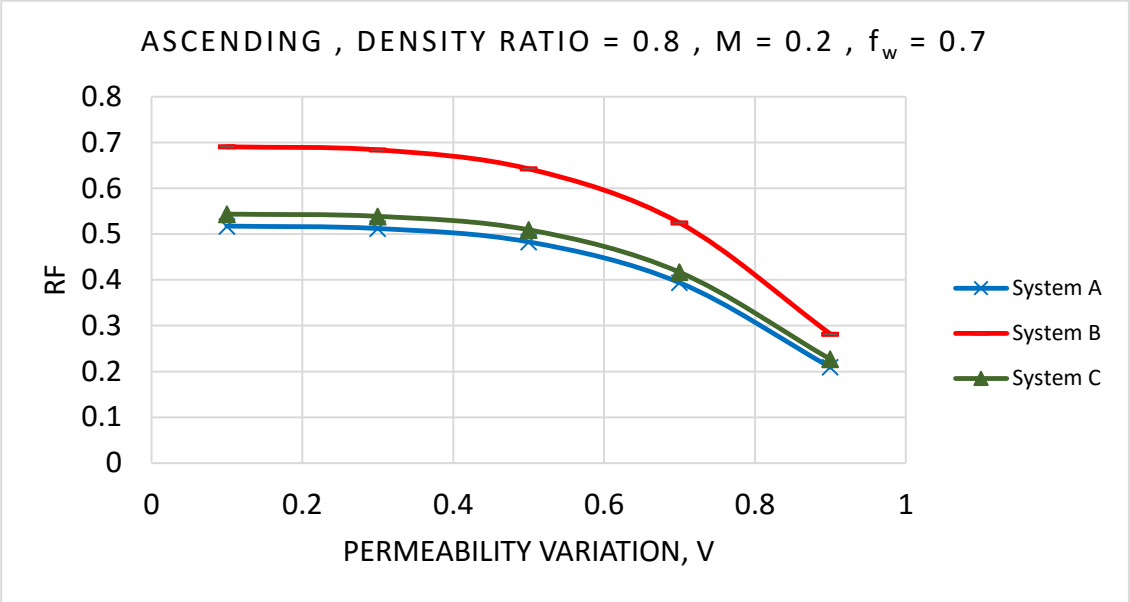

Figure 82 Effect of wettability on oil recovery factor beyond water breakthrough for ascending at M=0.2

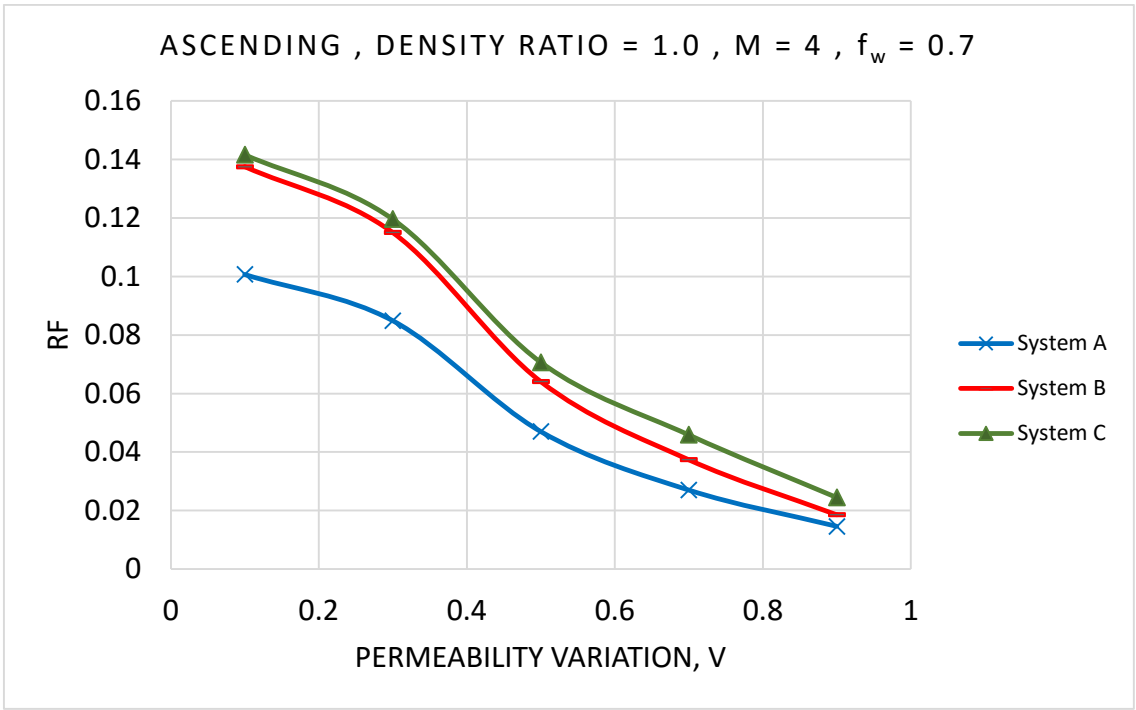

Figure 83 Effect of wettability on oil recovery factor beyond water breakthrough for ascending at M=4

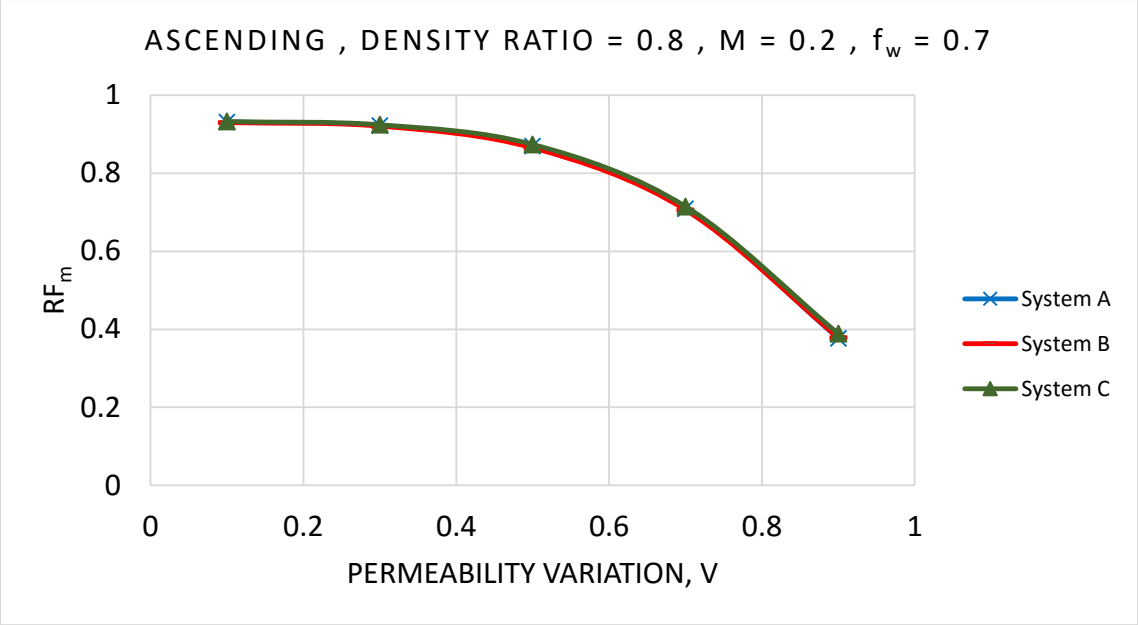

Figure 84 Effect of wettability on movable oil recovery factor beyond water breakthrough for ascending at M=0.2

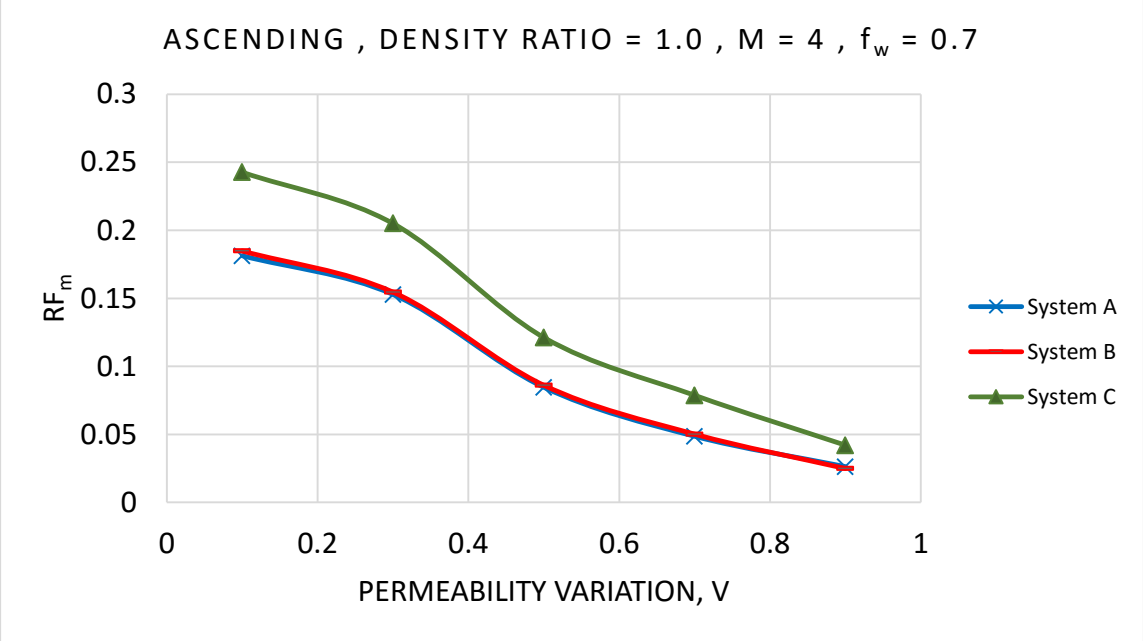

Figure 85 Effect of wettability on movable oil recovery factor beyond water breakthrough for ascending at M=4

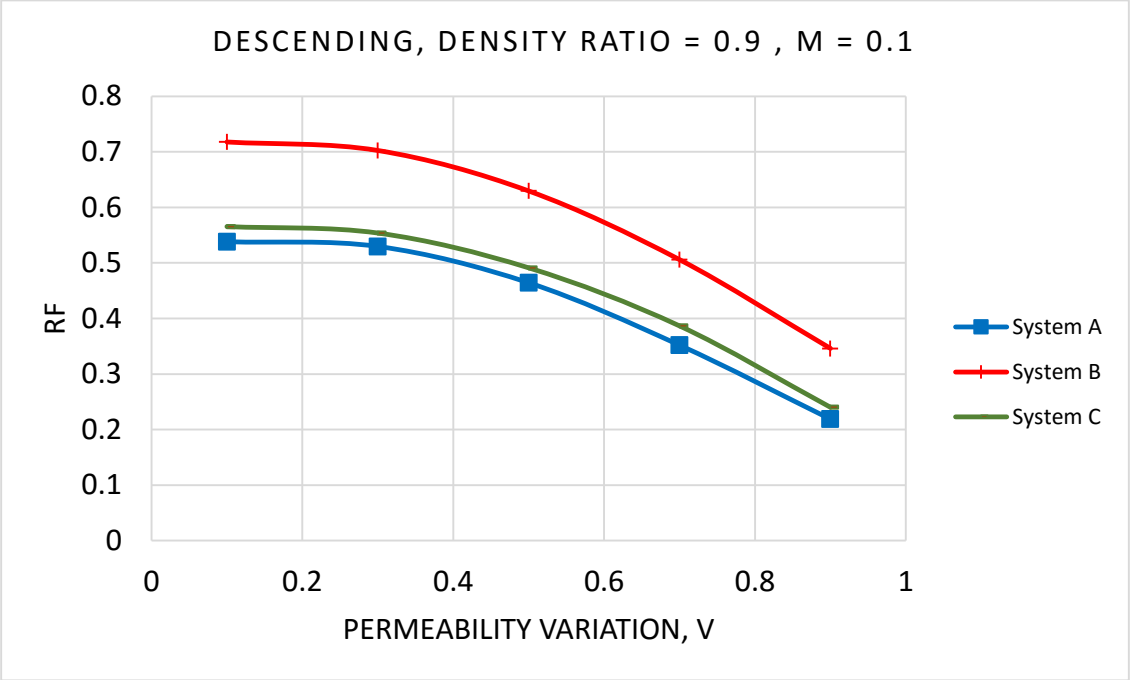

Figure 86 Effect of wettability on oil recovery factor at water breakthrough for descending at M=0.1

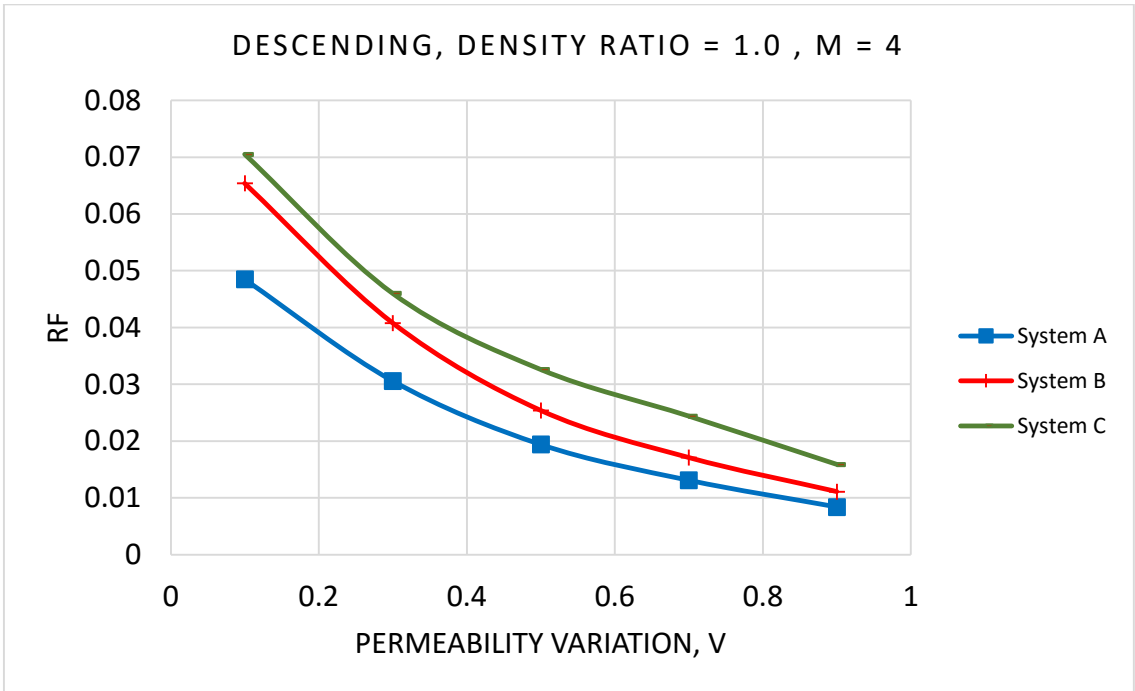

Figure 87 Effect of wettability on oil recovery factor at water breakthrough for descending at M=4

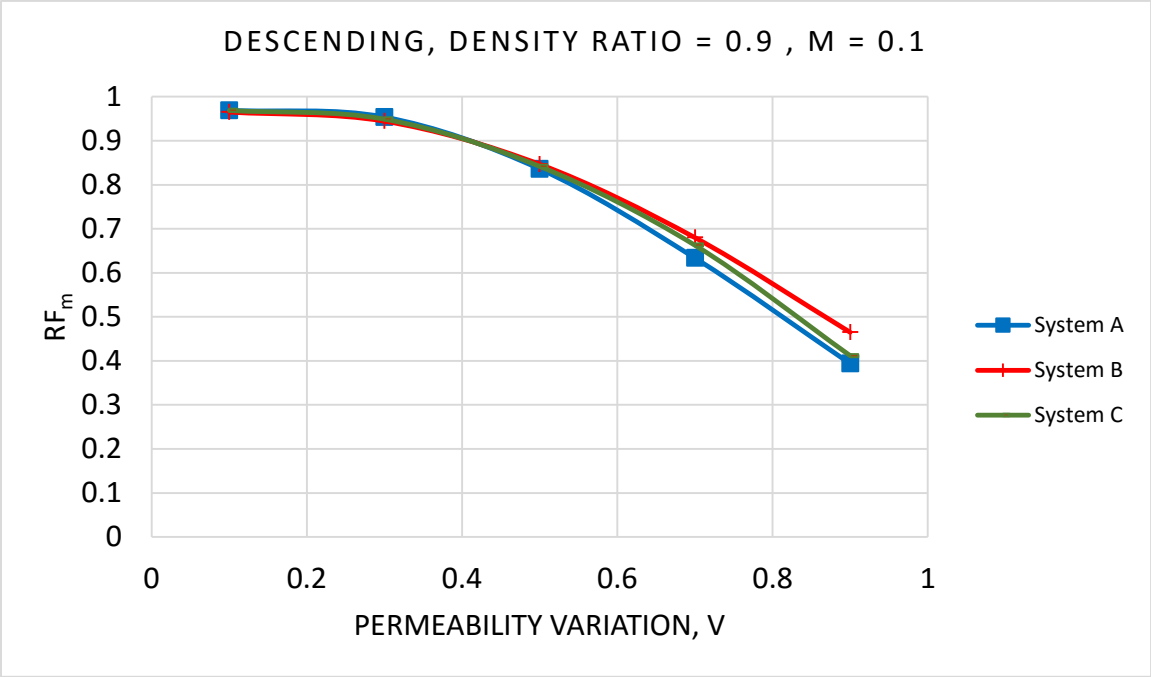

Figure 88 Effect of wettability on movable oil recovery factor at water breakthrough for descending at M=0.1

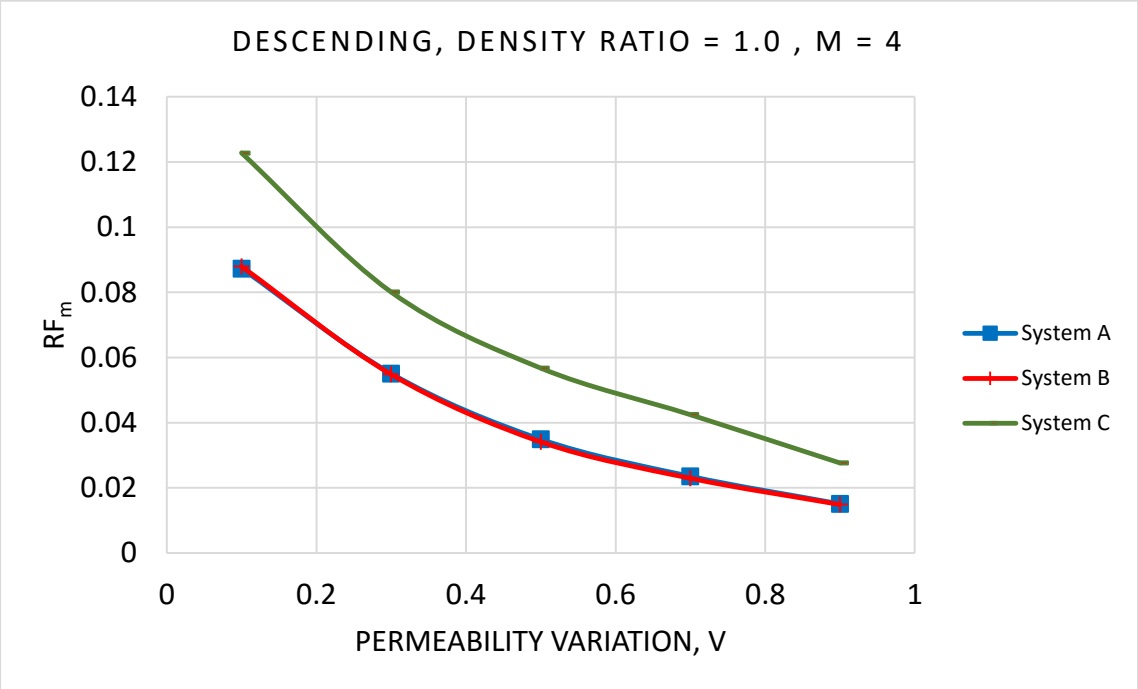

Figure 89 Effect of wettability on movable oil recovery factor at water breakthrough for descending at M=4

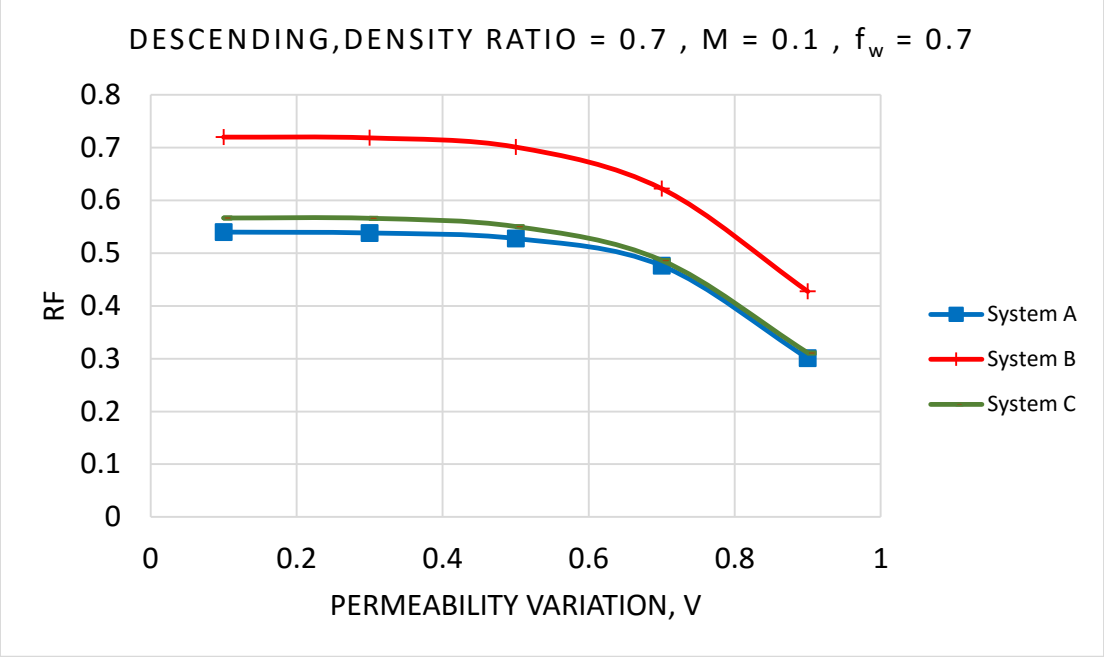

Figure 90 Effect of wettability on oil recovery factor beyond water breakthrough for descending at M=0.1

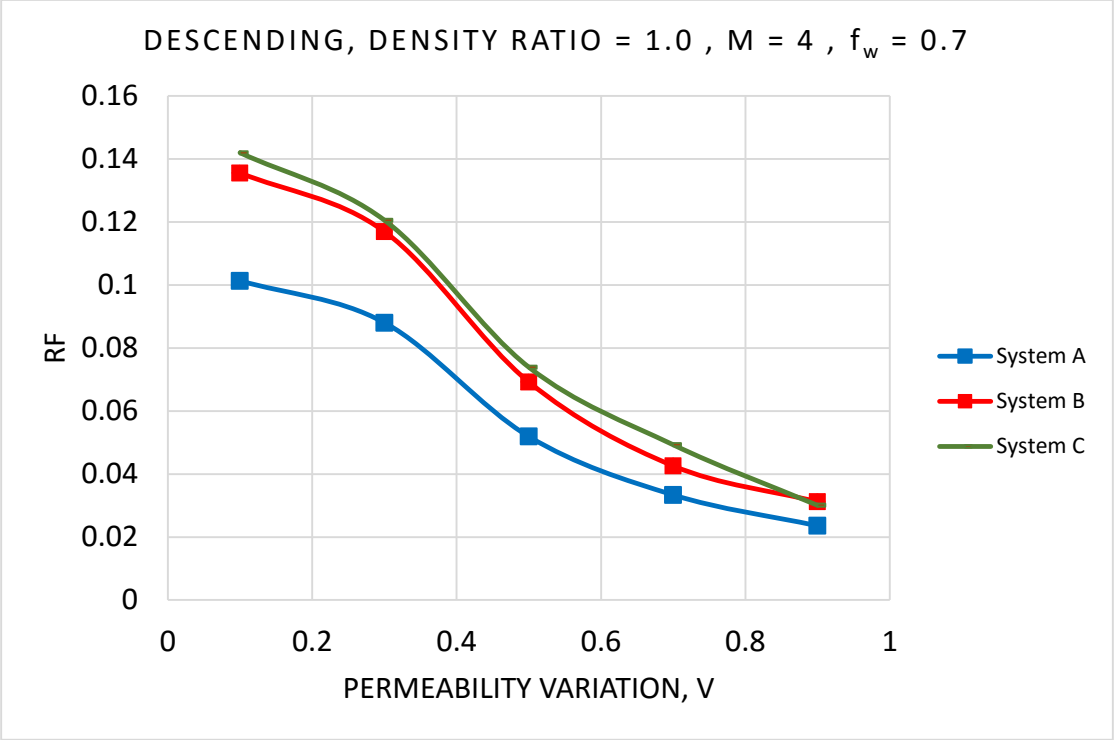

Figure 91 Effect of wettability on oil recovery factor beyond water breakthrough for descending at M=4

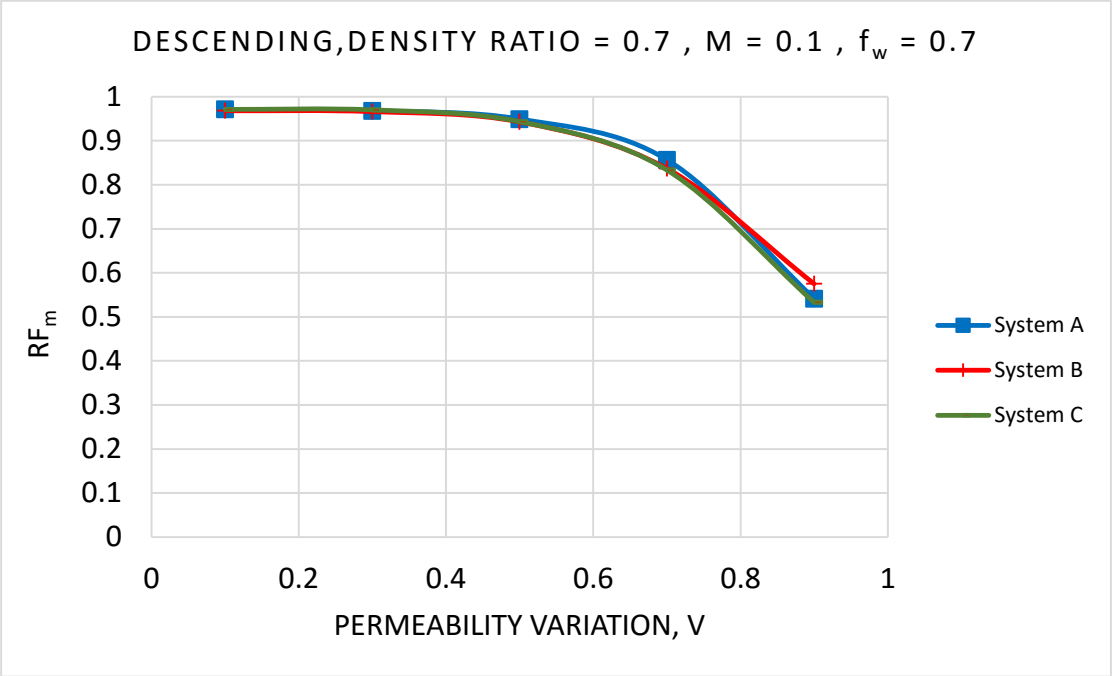

Figure 92 Effect of wettability on movable oil recovery factor beyond water breakthrough for descending at M=0.1

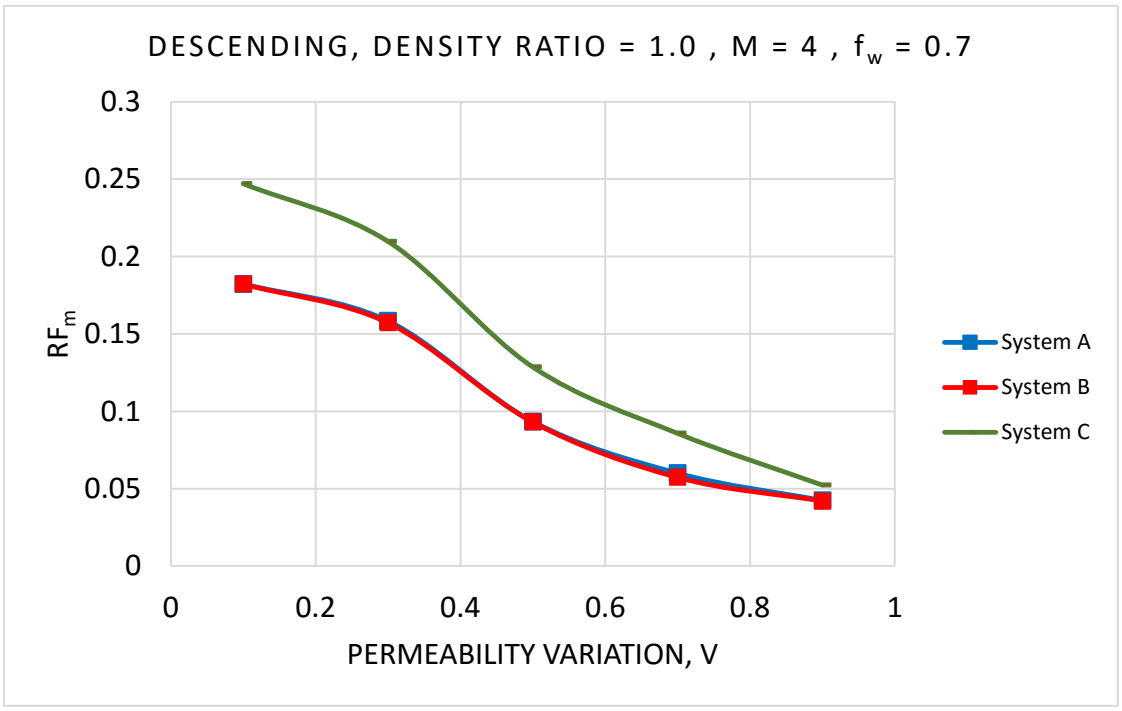

Figure 93 Effect of wettability on movable oil recovery factor beyond water breakthrough for descending at M=4

5.5 Effect of Permeability Arrangement

As mentioned earlier in Chapter 4, all runs have been executed by considering both ascending and descending permeability arrangement of the reservoir and a sensitivity for random sorting has also been tested. The gravitational crossflow caused by the density difference depends on the actual location of different layers in the reservoir. A comparison between ascending and descending arrangement beyond water breakthrough was done for all three systems as shown in Figures 94 to 105. The comparison is performed by keeping all the parameters same while changing the permeability arrangement only. It can be concluded from these Figures that in all three systems, the recovery is higher for descending arrangement compared with ascending arrangement. In all cases, as the reservoir gets more heterogeneous and at low density ratios and high mobility ratio, the difference in recovery factors for the two arrangements become more pronounced. For vertically communicating stratified reservoirs, oil recovery can be affected to a greater degree due to layer arrangement than by gravitational crossflow due to density difference.

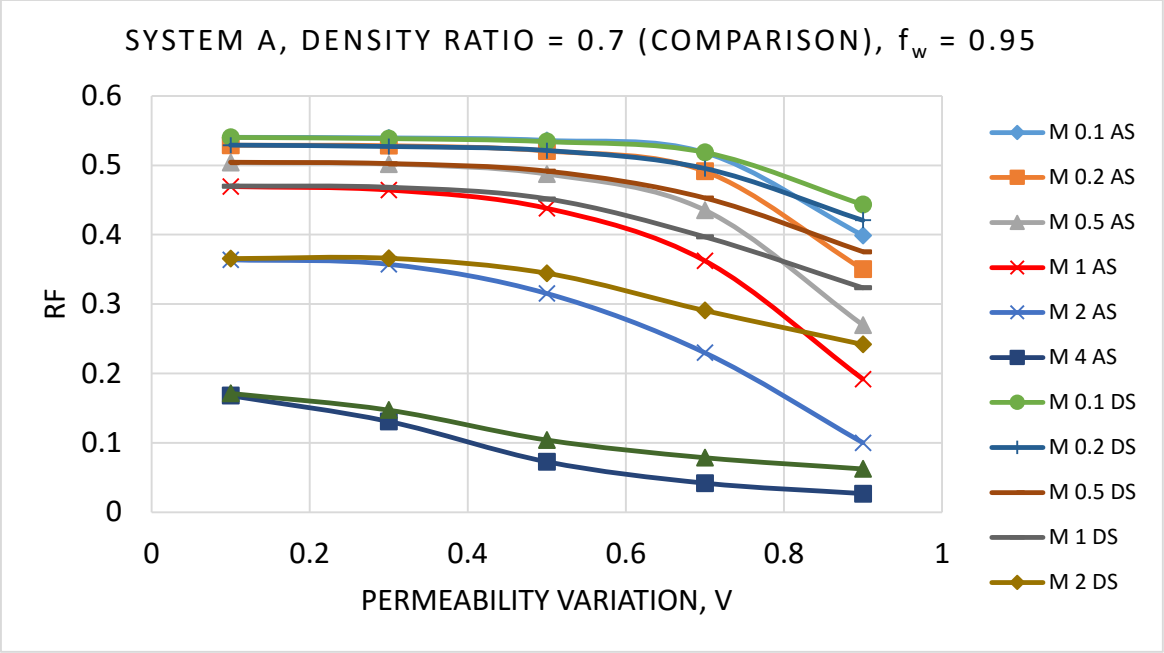

Figure 94 Effect of permeability arrangement on oil recovery factor beyond water breakthrough for system A at β=0.7

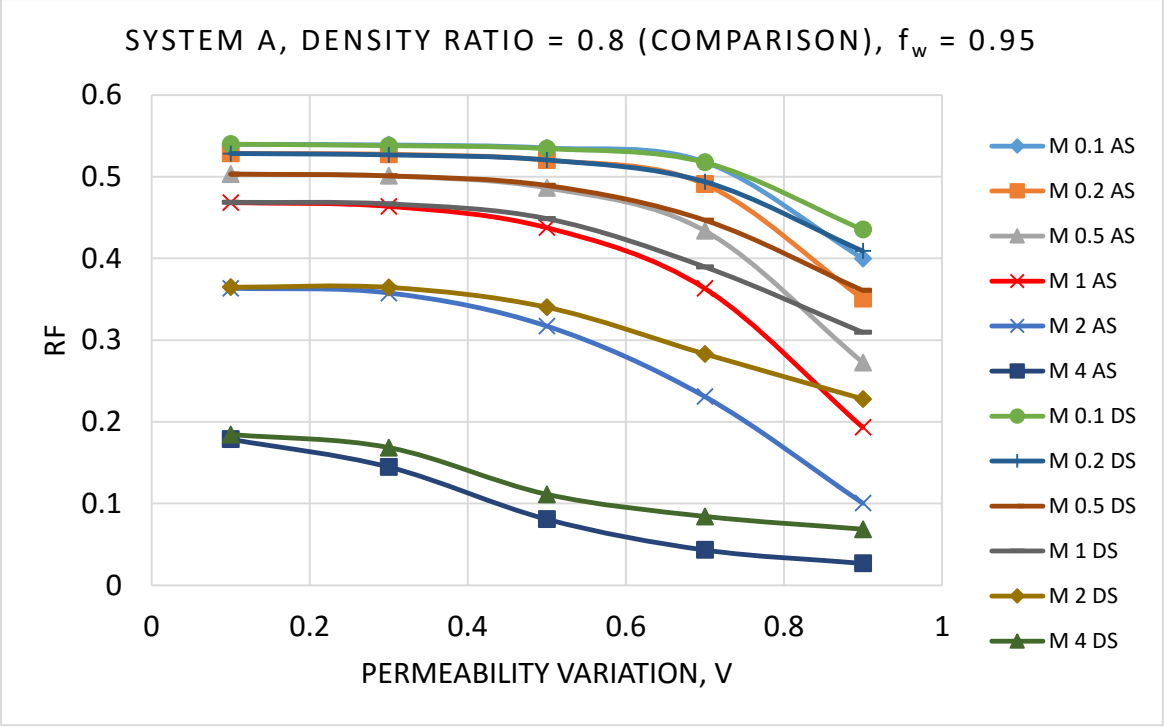

Figure 95 Effect of permeability arrangement on oil recovery factor beyond water breakthrough for system A at β=0.8

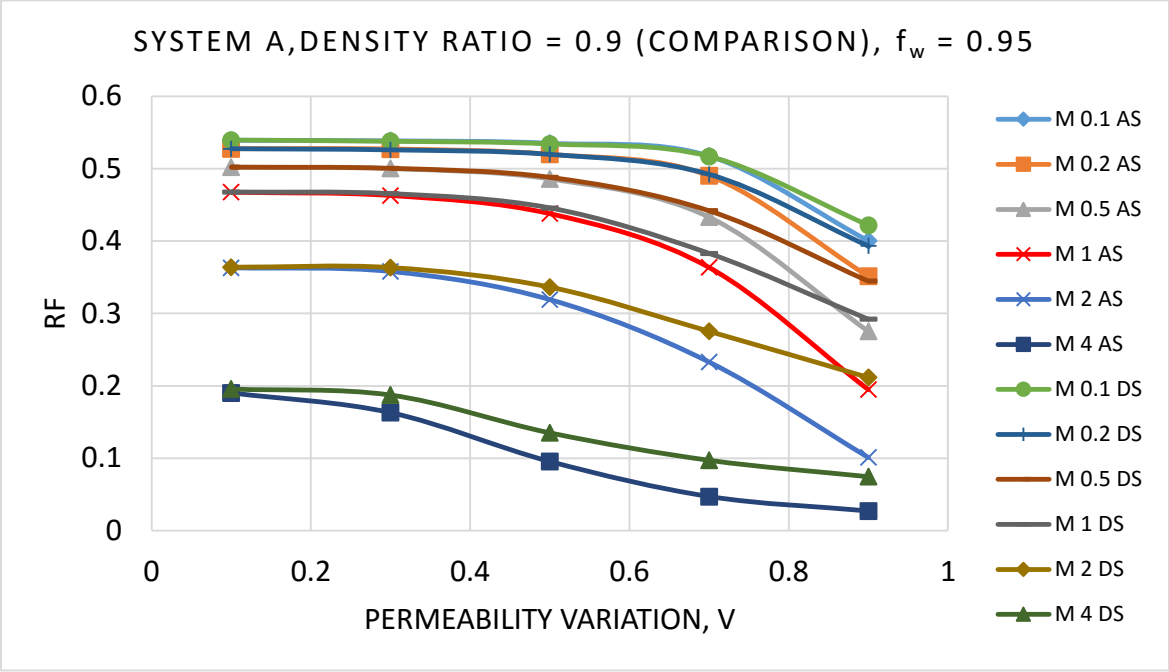

Figure 96 Effect of permeability arrangement on oil recovery factor beyond water breakthrough for system A at β=0.9

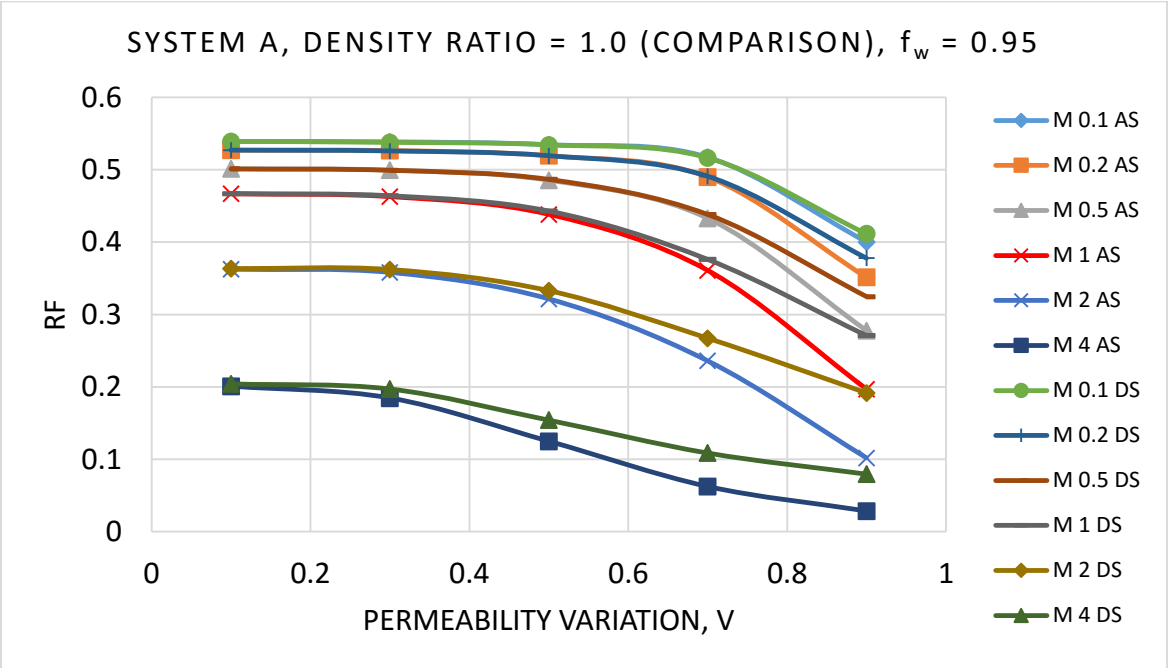

Figure 97 Effect of permeability arrangement on oil recovery factor beyond water breakthrough for system A at β=1.0

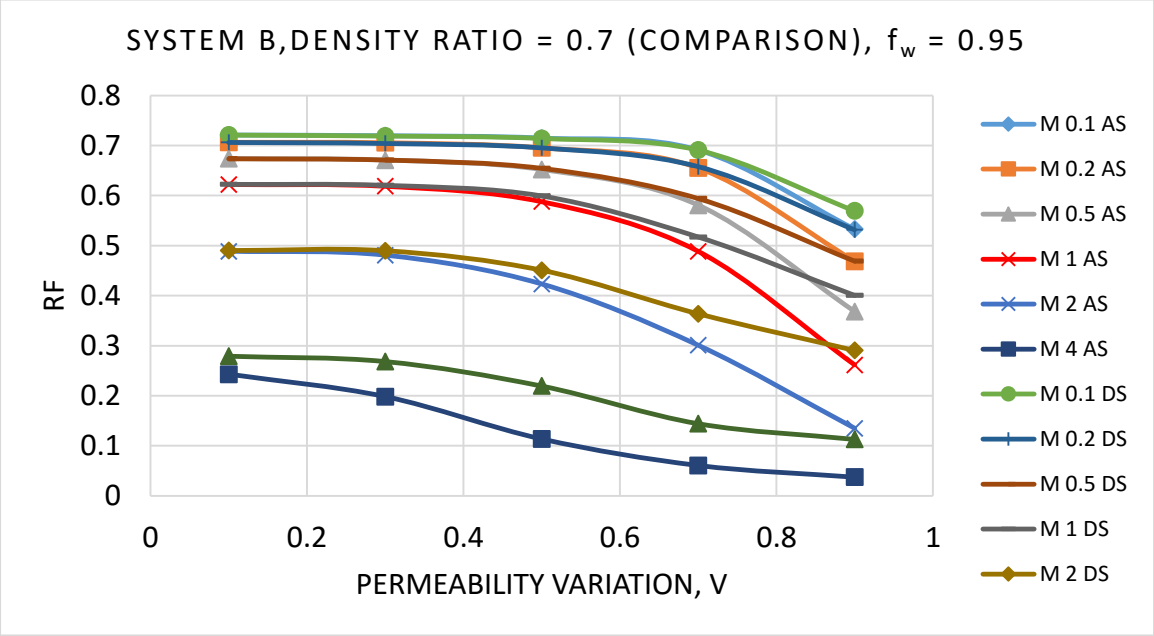

Figure 98 Effect of permeability arrangement on oil recovery factor beyond water breakthrough for system B at β=0.7

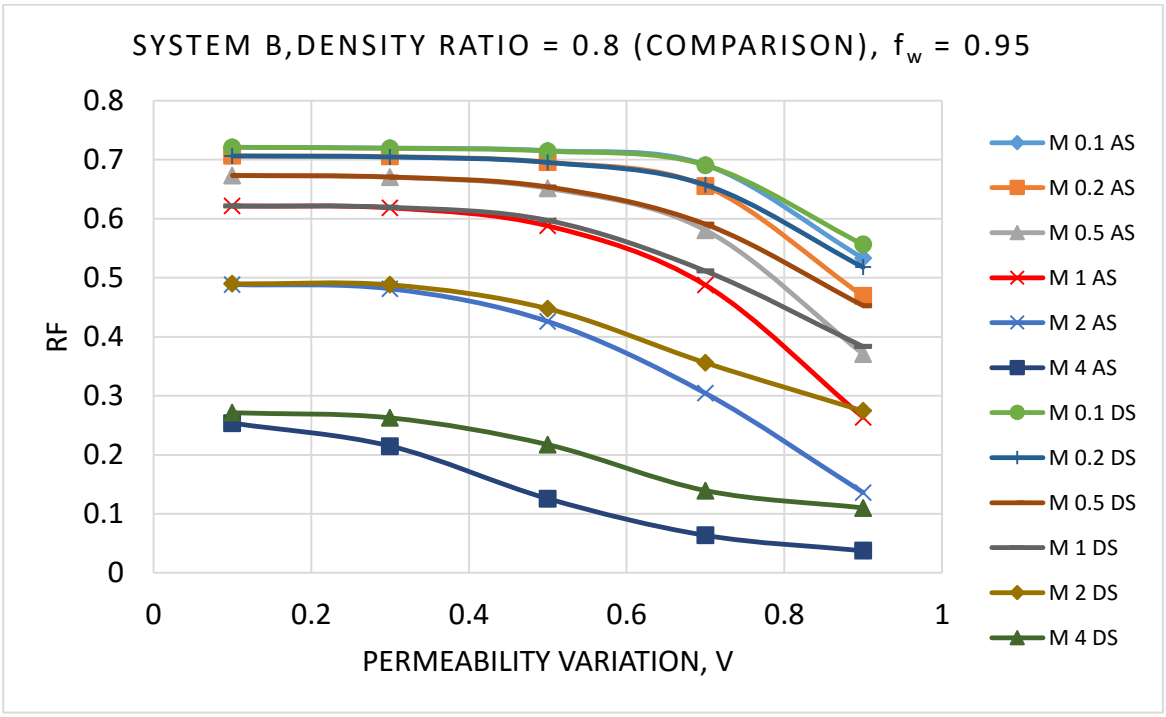

Figure 99 Effect of permeability arrangement on oil recovery factor beyond water breakthrough for system B at β=0.8

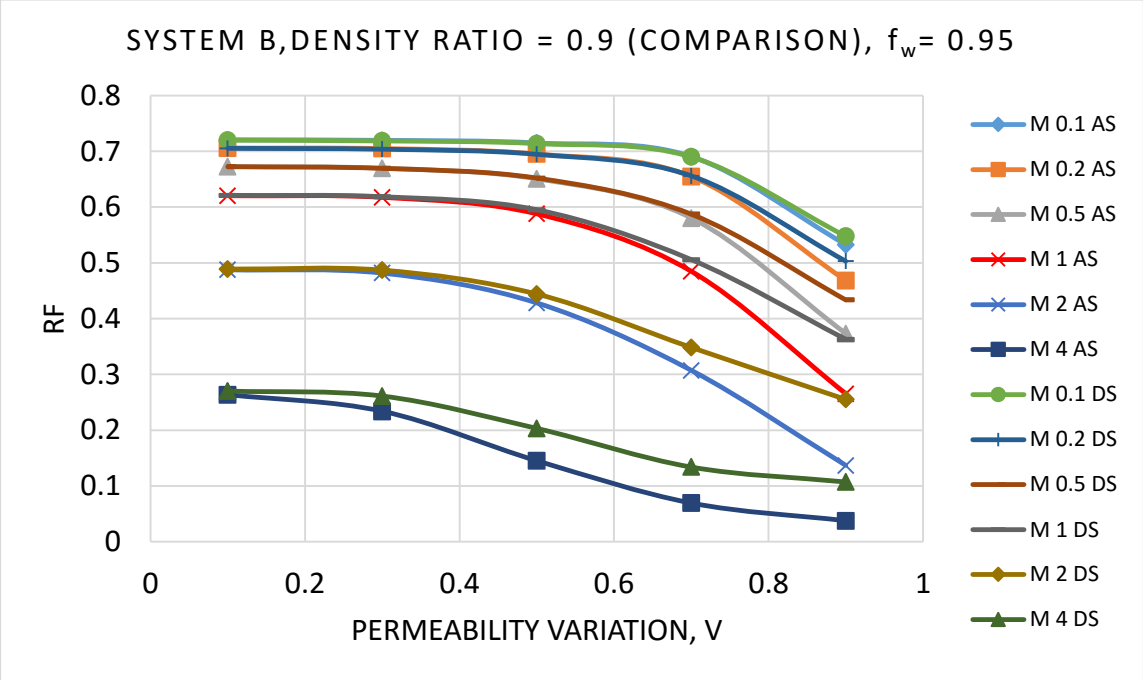

Figure 100 Effect of permeability arrangement on oil recovery factor beyond water breakthrough for system B at β=0.9

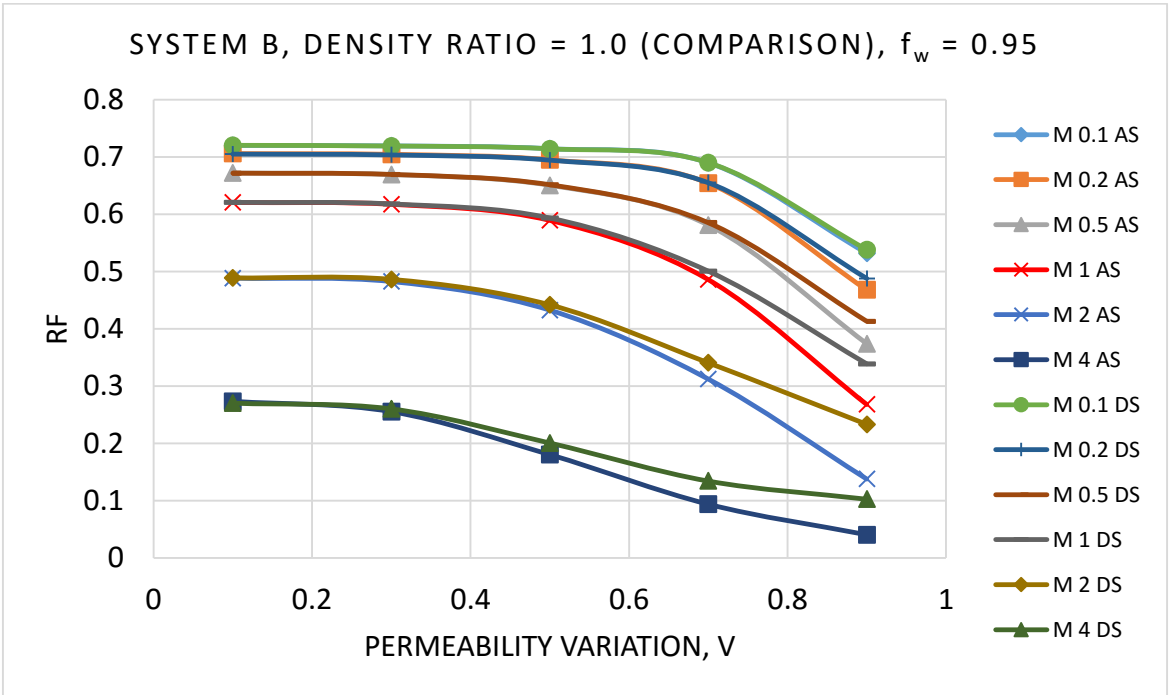

Figure 101 Effect of permeability arrangement on oil recovery factor beyond water breakthrough for system B at β=1.0

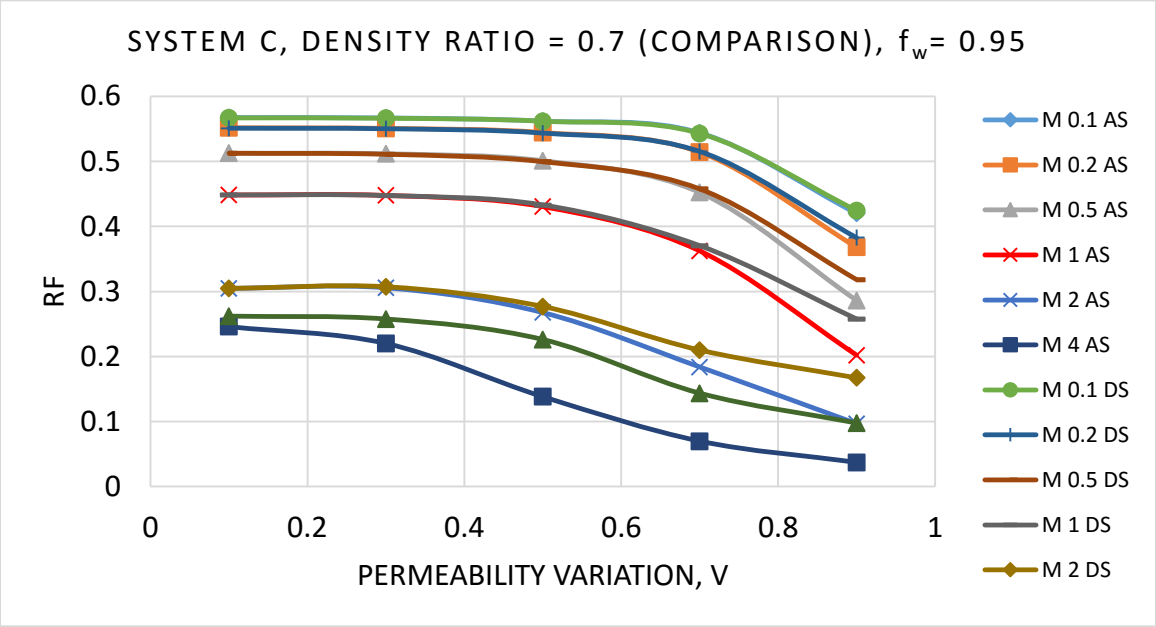

Figure 102 Effect of permeability arrangement on oil recovery factor beyond water breakthrough for system C at β=0.7

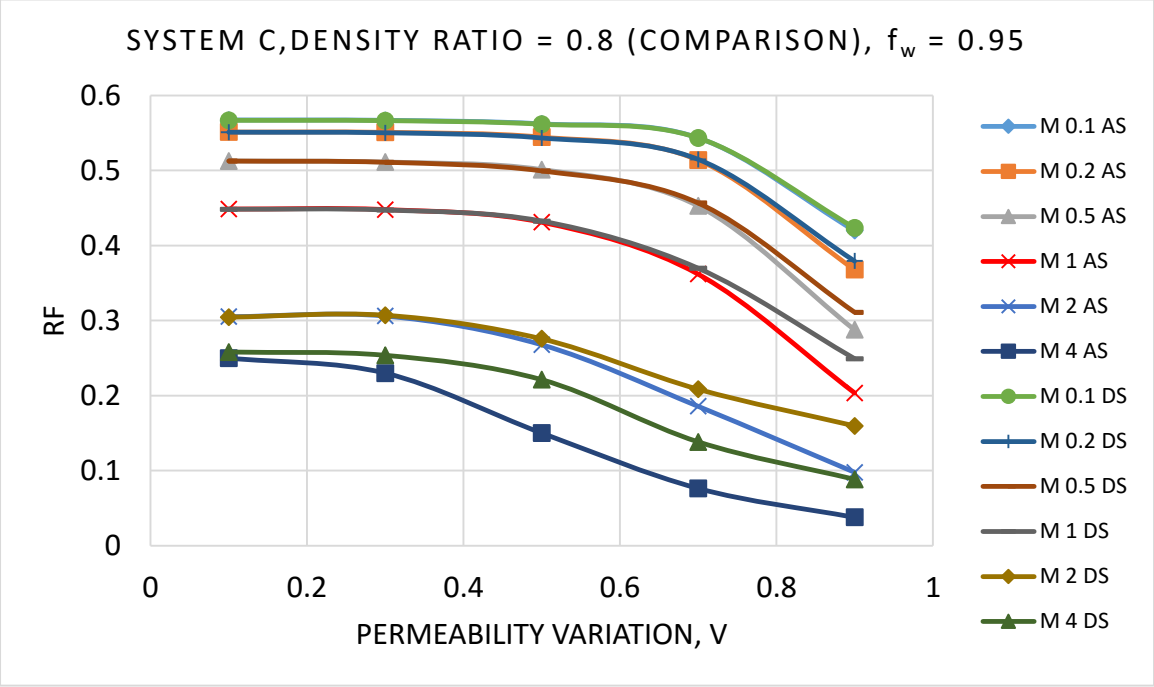

Figure 103 Effect of permeability arrangement on oil recovery factor beyond water breakthrough for system C at β=0.8

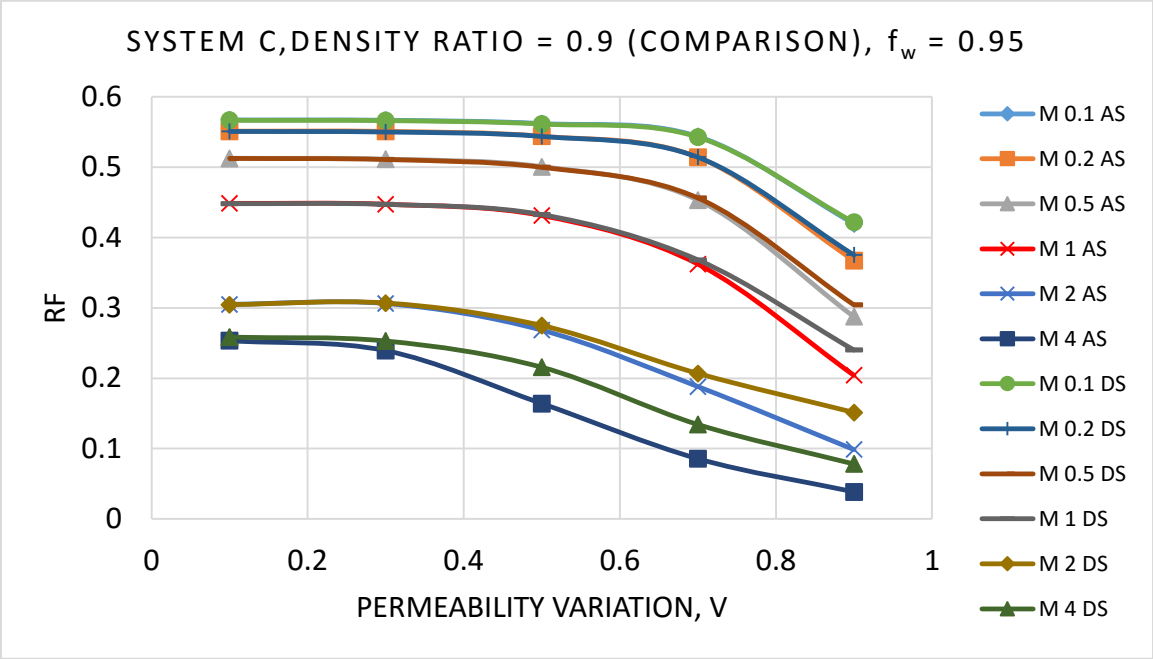

Figure 104 Effect of permeability arrangement on oil recovery factor beyond water breakthrough for system C at β=0.9

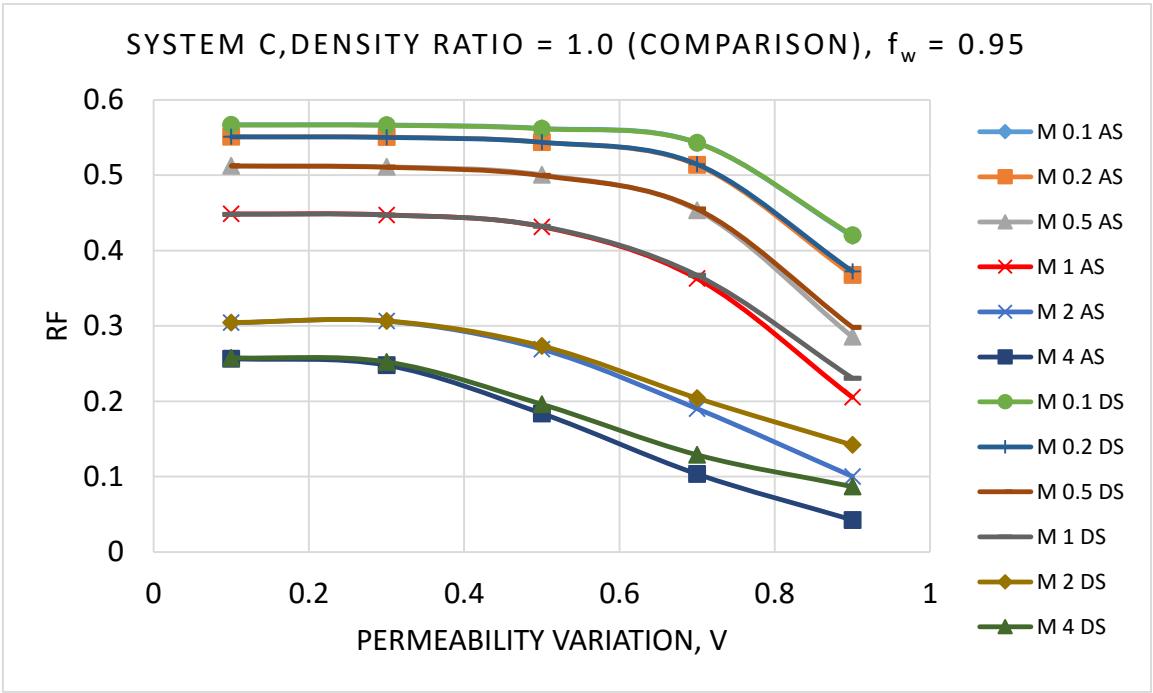

Figure 105 Effect of permeability arrangement on oil recovery factor beyond water breakthrough for system C at β=1.0

CHAPTER 6

CORRELATION DEVELOPMENT

This chapter presents the empirical correlation that was developed based on the simulation results. It also presents the testing of the correlation and a comparison of its predictions with actual field data. The last section of this chapter discusses the testing of the wettability indicator.

6.1 Statistical Technique

A correlation refers to any mathematical relationship where one or more outputs depend on one or more inputs. Different statistical techniques are available to derive a correlation, where a suitable statistical technique varies from case to case. Petroleum engineers have over the years applied new techniques from different fields of science to solve petroleum engineering problems. There are several statistical tools available to make a correlation such as regression technique, artificial neural networks, fuzzy logic, functional networks and support network machines etc. In this study, the Artificial Neural Networks (ANNs) technique was applied on simulated data to build the mathematical model and obtain a correlation.

6.1.1 Artificial Neural Networks

The ability of a neural network to approximate any complex functional relationship makes the selection of a suitable estimation for particular application unnecessary. ANNs are inherently parallel and have the capability to learn non-linear relationships, which may exist between a set of inputs and outputs. The design of a supervised neural network may be pursued in different ways.

A neural network consists of a large number of simple processing elements called neurons or nodes. Each neuron is connected to other neurons by means of directed communication links, each with an associated weight. The weights represent information being used by the network to solve a problem. Each neuron has an internal state, called its activation or activity level, which is a function of the inputs it has received. Typically, a neuron sends its activation as a signal to several other neurons. Upon exposure to training examples (patterns) the neurons in an ANN compute the activation values and transmit these values to each other in a manner that depends on the learning algorithm being used.

A typical ANN model is based on a series of three layers (input, hidden and output). Input data is given to the input layer which feed them to the hidden layer where they are processed and then fed to the output layer. Each layer comprises of a set of neurons. The neuron processes each data record based on an activation function. We used tan-sigmoid as an activation function in this case. The topology of a basic ANN network is shown in Figure 106. A mathematical model based on ANN was developed in this study, which resulted in a strong correlation.

Two correlations were obtained in this work. One correlation is applicable for ascending arrangement of permeability in layers while the other correlation is applicable to descending arrangement. These correlations estimate the movable oil recovery factor as a function of mobility ratio (M), permeability variation coefficient (V), production water cut (f_w), wettability indicator (WI) and oil to water density ratio (β). Input and output variables for the developed correlation are listed in Table 11.

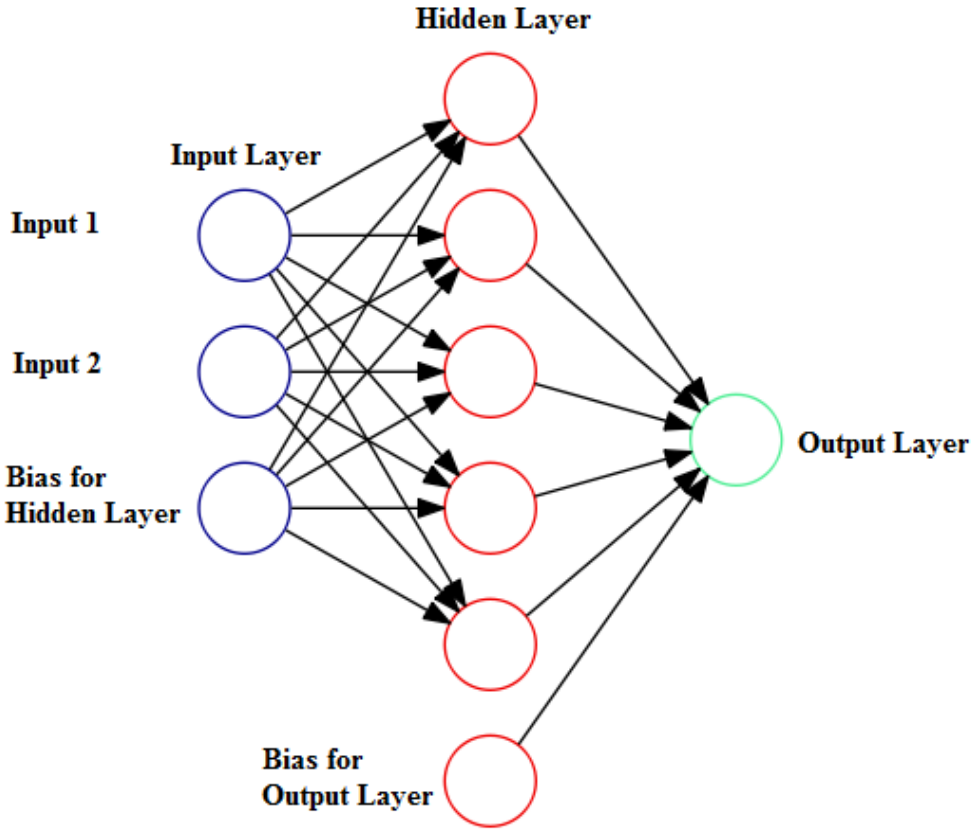

Figure 106 Topology of a Basic ANN network

Table 11 Input and Output Variables for the new correlation

Output Variable	Input Variable
RF_m	V
	M
	β
	f_w
	WI

6.2 Correlation Development

The neural network based model adopted in this study was a feedforward neural network (FFNN). A total number of 3960 data points were obtained at different water cuts for each ascending and descending case out of which 2772 (70 %) data points were used as input to the FFNN for training purposes while the remaining 1188 (30 %) data points were used to test the model.

For both correlations, the RF_m ANN model consists of five input neurons (input parameters), which are linked to V, M,β, f_w, WI, one hidden layer and one output neuron (output parameter). The output neuron was related to movable oil recovery factor. There were 10 neurons in the hidden layer, which were obtained after the sensitivity runs of a number of neurons. Tan-sigmoid and Linear Transfer functions were used in hidden and output layers, respectively. Levenberg-Marquardt back-propagation algorithm was utilized for training of the Neural Network. In order to avoid the local minimum, 2000 multiple realizations with different weights and biases initialization of training were conducted and minimum error realization was selected as the best case. The optimum weights and bias values were obtained for movable oil recovery factor after proper training and are shown in Table 13 and Table 14 for ascending and descending cases, respectively. The network of proposed correlation is shown in Figure 107 and described mathematically in equations 6.1, 6.2a and 6.2b.

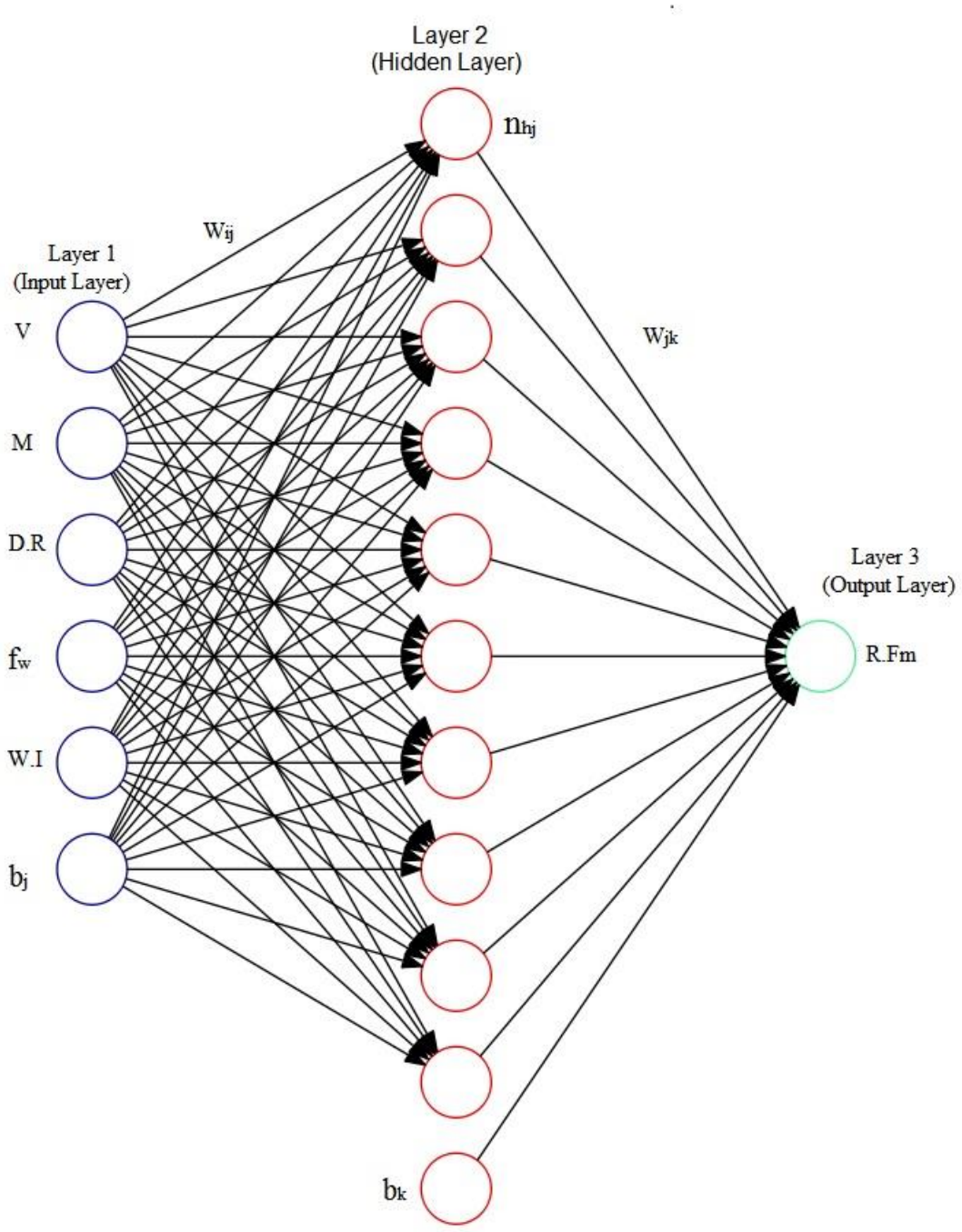

Figure 107 Topology of RF_m prediction FFNN-based model

$$\left(RF_m\right)_N = \sum_{j=1}^{N_h} w_{jk} n_{hj} + b_k \qquad 6.1$$

$$n_{hj} = f\left(\sum_{i=1}^{Ni} w_{ij} x_i + b_j\right) \qquad 6.2a$$

Or

$$n_{hj} = f\left(w_{1j} V_N + w_{2j} M_N + w_{3j} \beta_N + w_{4j} f_{w_N} + w_{5j} WI_N + b_j\right) \qquad 6.2b$$

$$f(x) = \tanh(x) = \frac{2}{1+e^{-2x}} - 1 \qquad 6.3$$

Where,

j = Number of hidden layer neurons

i = Number of input layer neurons

x_i = Input Parameters (Normalized)

b_j = Bias for hidden layer

b_k = Bias for Output layer

W_{ij} = Weights between Input and Hidden Layer

W_{jk} = weights between Hidden and Output Layer

f = Transfer function

N = Subscript 'N' shows normalized parameter

N_h = Total number of neurons in hidden layer

N_i = Total number of inputs

n_{hj} = jth neuron in hidden layer

$(RF_m)_N$= Normalized output of the output layer

Input parameters were normalized for ANN model and then the output was de-normalized, which is described in the following section.

6.2.1 Input Normalization

The normalization of input parameters was done by the following function:

$$\text{Inputs} = \frac{(y_{max} - y_{min})(x - x_{min})}{(x_{max} - x_{min})} + y_{min} \quad 6.4$$

y_{min} and y_{max} are -1 and +1, respectively, in the above equation, while values of x_{max} and x_{min} are given in Table 12. Normalization equation of each input parameter are as follows:

$$V_N = 2.5(V - 0.1) - 1 \quad 6.5a$$

$$M_N = \frac{20}{39}(M - 0.1) - 1 \quad 6.5b$$

$$\beta_N = \frac{20}{3}(\beta - 0.7) - 1 \quad 6.5c$$

$$fw_N = \frac{40}{19} fw - 1 \quad 6.5d$$

$$WI_N = 0.8(WI - 0.5) - 1 \quad 6.5e$$

6.2.2 Output De-Normalization

The output de-normalization was done by the following function:

$$\text{Output} = \frac{(y_{max} - y_{min})(x - x_{min})}{x_{max} - x_{min}} + y_{min} \quad 6.6$$

For de-normalization, x_{min} and x_{max} are -1 and +1, respectively, in the above equation, while values of y_{max} and y_{min} are given in Table 12. De-Normalization equation of the output is given below:

$$RF_m = a\left(RF_{m_N} + 1\right) + y_{min} \quad 6.7$$

Where

$a = 0.47945$, $y_{min} = 0.0133$ for ascending case

$a = 0.41085$, $y_{min} = 0.0151$ for descending case

The above equation gives the result for the newly developed ANN based correlations.

Table 12 Statistical Description of the Input and Output Data Used for Training

Parameters	**Minimum Value**	**Maximum Value**
Output Parameter		
RF_m for Ascending cases	0.0133	0.9722
RF_m for Descending cases	0.0151	0.9727
Input Parameter		
V	0.1	0.9
M	0.1	4
DR	0.7	1
f_w (Ascending)	0	0.956
f_w (Descending)	0	0.954
WI	0.5	3

Table 13 Weights and Bias Values for RF_m Artificial Neural Network Model for Ascending Case

Weights between Input Layer and Hidden Layers (w_{ij})					
Hidden Layer Neurons(j)	**Input Layer Neurons (i)**				
	1	**2**	**3**	**4**	**5**
1	-0.5501	0.9512	0.0029	0.0315	0.0582
2	-0.6110	-1.0103	0.0209	3.6875	0.1044
3	-0.1659	4.2110	-0.0085	0.0757	0.0930
4	-0.5853	-0.9326	0.0195	3.6648	0.0981
5	-1.1490	-1.1094	0.0197	0.7299	-0.0099
6	0.3648	0.6202	-0.0018	-0.2321	0.0194
7	-0.6372	-1.6737	0.0007	0.4281	0.0714
8	-0.4737	-0.1835	0.0049	0.2715	-0.0259
9	1.4527	2.1412	-0.0618	-1.5607	-3.5967
10	-0.4219	-0.3795	0.0034	0.2516	-0.0242

Bias Values for Hidden Layer Neurons (b_j)		**Weights between Hidden Layer and Output Layers (w_{jk})**	
Hidden Layer Neurons(j)	**Bias (b_j)**	**Hidden Layer Neurons (j)**	**Output One Neuron**
1	3.3740	1	27.7866
2	-4.3060	2	-7.7791
3	6.4432	3	-16.0577
4	-4.2021	4	7.8456
5	-0.3910	5	1.0069
6	0.4312	6	-19.5903
7	-0.3204	7	-1.2700
8	-0.4202	8	15.4409
9	4.4572	9	0.1360
10	-0.4188	10	-33.8079

Bias Values for Output Layer Neuron (b_k)	
Output Layer Neuron	**Bias Value (b_k)**
1	-11.7602

Table 14 Weights and Bias Values for RF_m Artificial Neural Network Model for Descending Case

Weights between Input Layer and Hidden Layers (w_{ij})					
Hidden Layer Neurons(j)	**Input Layer Neurons (i)**				
	1	**2**	**3**	**4**	**5**
1	-0.0612	-1.3013	0.0083	0.5048	-0.0141
2	-0.6000	-0.5412	0.0371	0.7529	-0.0060
3	0.7546	0.6138	-0.0227	-0.7669	0.0213
4	0.4831	0.5205	-0.0487	-0.7954	0.0063
5	1.2137	2.6222	0.0484	-0.2276	0.0788
6	0.0903	0.8767	0.0104	-0.6461	0.1362
7	0.1866	0.2228	-0.0810	1.3489	-0.0963
8	-0.6046	-6.5762	-0.0337	-0.1232	-0.0503
9	-1.5189	-0.3313	-0.2433	1.0304	4.7794
10	-0.9644	5.0400	-0.1598	0.9791	3.5994

Bias Values for Hidden Layer Neurons (b_j)		**Weights between Hidden Layer and Output Layers (w_{jk})**	
Hidden Layer Neurons(j)	**Bias (b_j)**	**Hidden Layer Neurons (j)**	**Output One Neuron**
1	-3.1633	1	-6.0037
2	-0.7879	2	13.2714
3	1.0430	3	6.7715
4	0.5784	4	6.5285
5	1.6365	5	-0.4081
6	0.6616	6	-0.8449
7	-3.4418	7	11.4660
8	-6.2032	8	0.3564
9	-4.6628	9	-0.1051
10	-8.6589	10	0.1531

Bias Values for Output Layer Neuron (b_k)	
Output Layer Neuron	**Bias Value (b_k)**
1	6.1062

Mean Absolute Percentage Error (MAPE) and coefficient of determination (R^2) are statistical tools to determine the accuracy of data. MAPE is defined mathematically in equation 6.8.

$$\text{MAPE} = \frac{100}{n}\sum_{i=1}^{n}\left|\frac{\text{Actual}_i - \text{Predicted}_i}{\text{Actual}_i}\right| \quad 6.8$$

Scatter plots were made between simulated and ANN model results for seen (training) and unseen (testing) data as shown in Figures 108 to 111. All scatter plots show R^2 above 99%, which indicates that the developed empirical model is a strong positive correlation. Mean absolute percentage error for training and testing for both correlations is shown in Table 15. Further correlation testing and comparison with the field data is presented in the next section.

Table 15 Accuracy measurement of training and testing data

Data Type	**MAPE, %**	**R^2**
Ascending Data		
Training (Seen)	4.36	0.9984
Testing (Unseen)	4.47	0.9973
Descending Data		
Training (Seen)	4.69	0.9973
Testing (Unseen)	4.5	0.9962

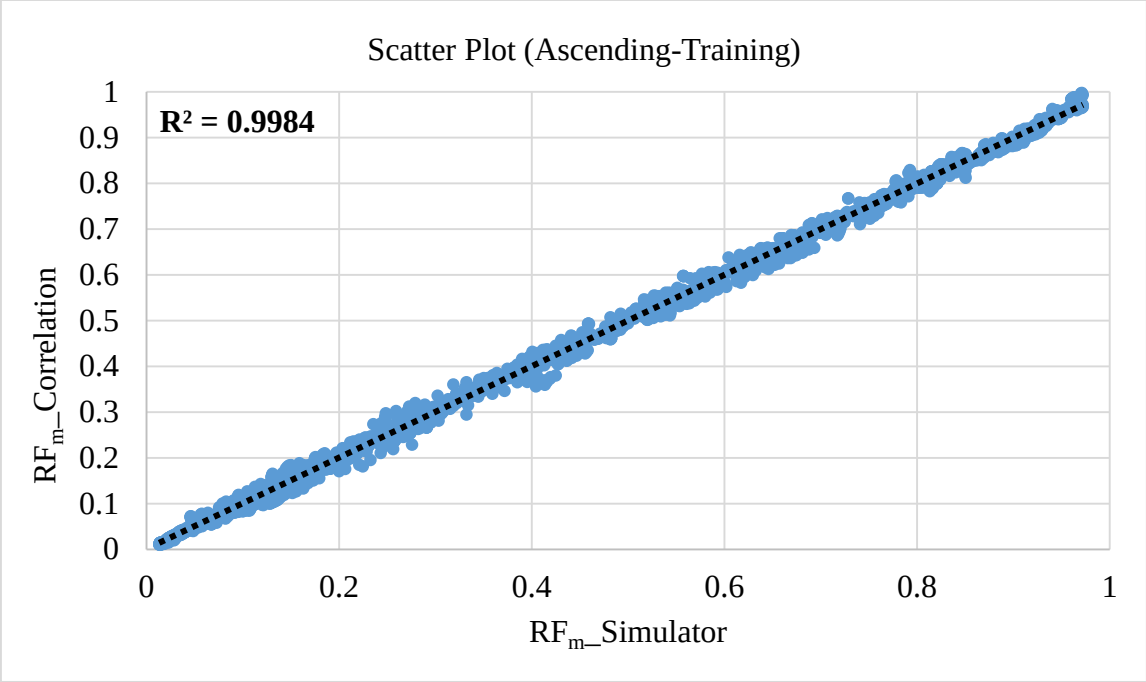

Figure 108 Scatter plot for ascending training data

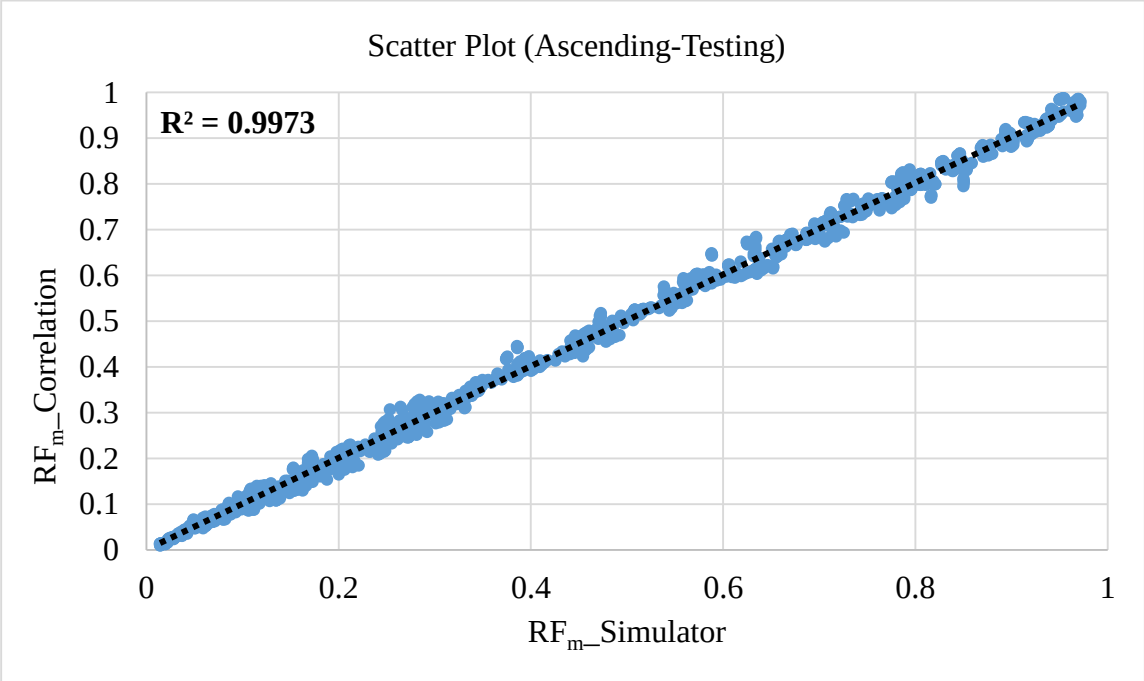

Figure 109 Scatter plot for ascending testing data

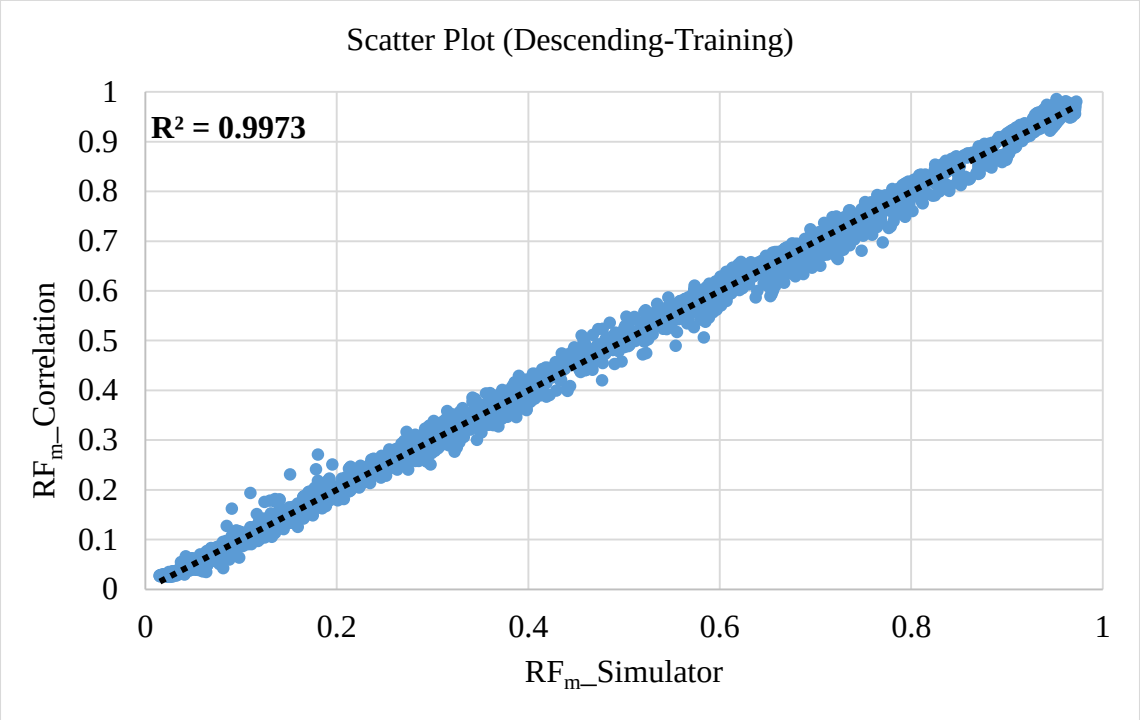

Figure 110 Scatter plot for descending training data

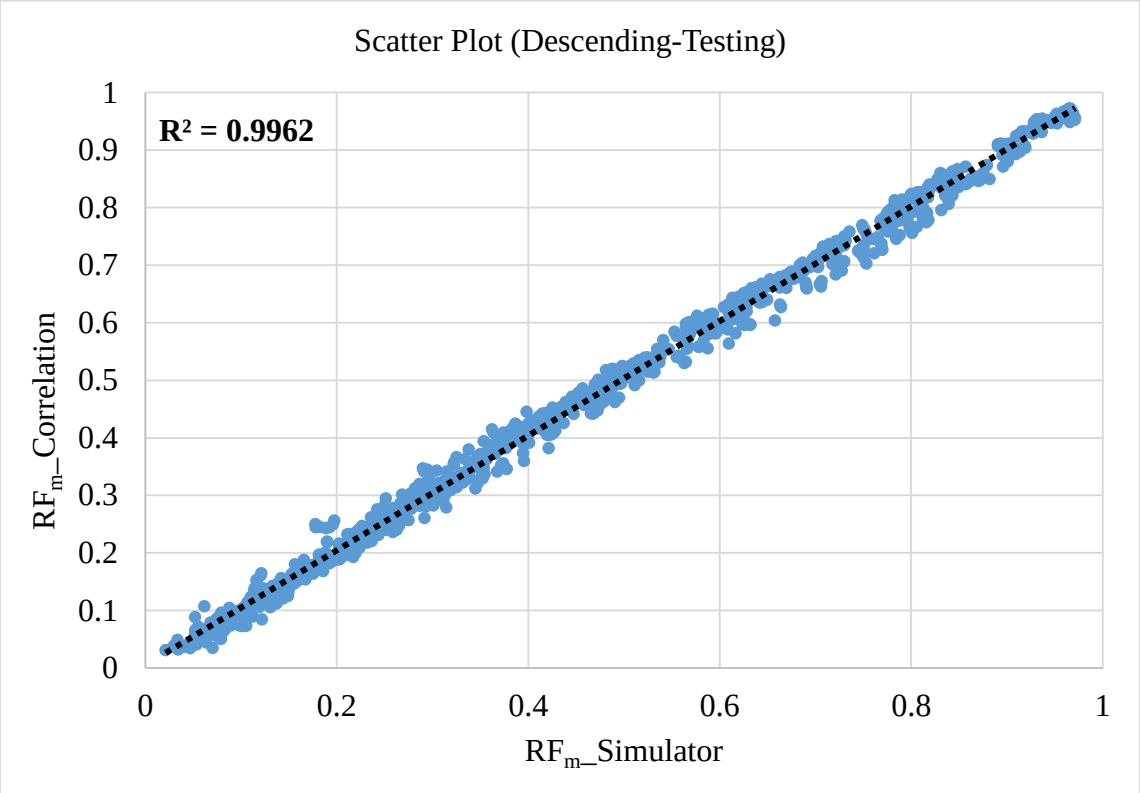

Figure 111 Scatter plot for descending testing data

6.3 Correlation Testing

The developed correlations for both ascending and descending were tested at different mobility ratios for two new wettability systems. The data points for these wettability systems had not been considered while developing the correlations. Table 16 lists the parameters used in testing both correlations.

Table 16 Correlation testing parameters

	V	**M**	**β**	**WI**
Case 1	0.6	0.7	0.85	0.8
		1		
		4		
Case 2	0.5	0.7	0.85	1.51
		1		
		4		

6.3.1 Case 1: Wettability Indicator = 0.8

Figure 112 shows the relative permeability curves of the system with WI of 0.8 and Figures 113 to 115 show the fractional flow curves at the mobility ratios used for testing. The simulation results were compared with the ANN model predictions at different mobility ratios. As shown in Figures 116 to 121, the match between ANN model and simulation results is excellent.

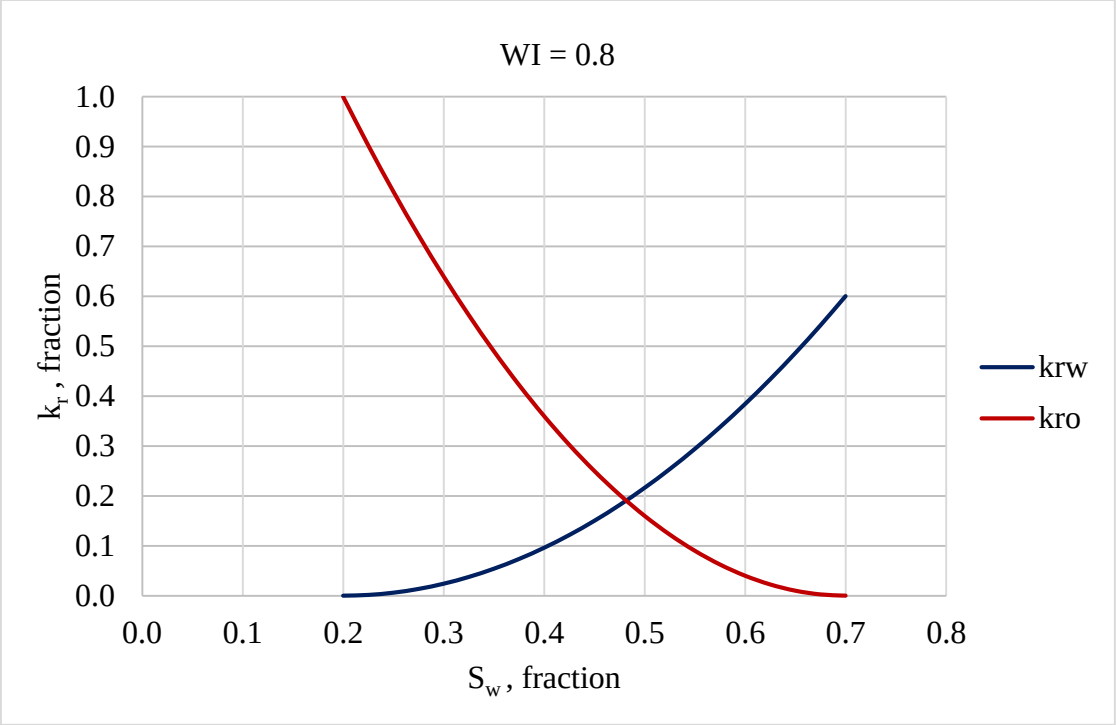

Figure 112 Relative permeability curves for case 1

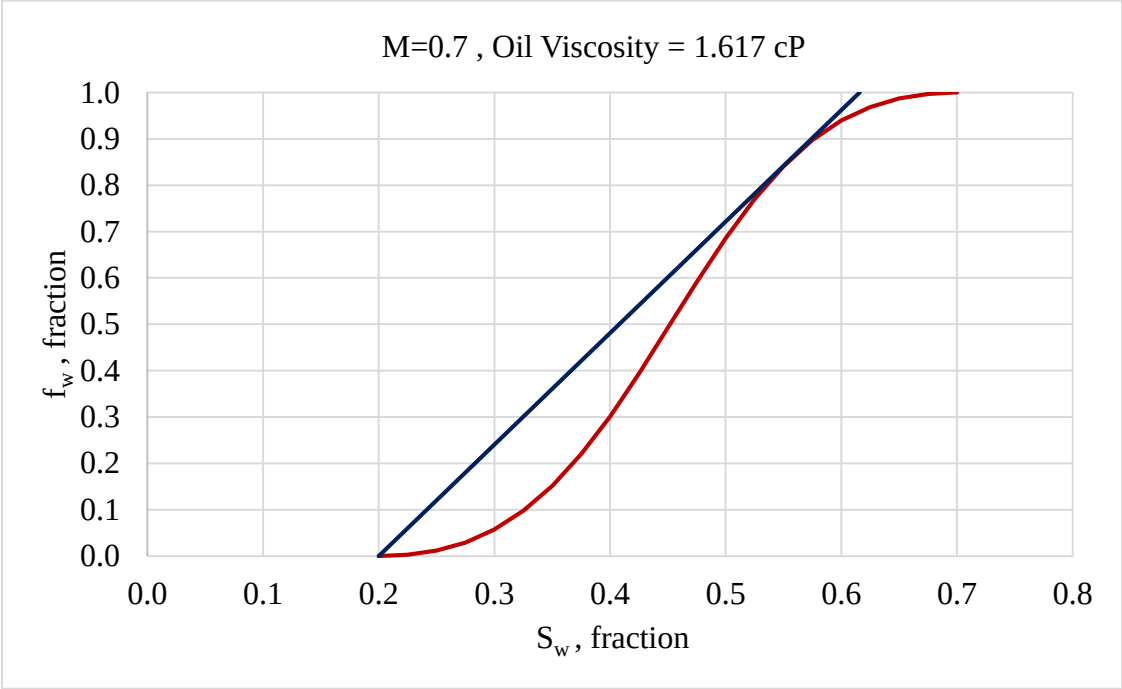

Figure 113 Fractional flow curve for M=0.7 at WI=0.8

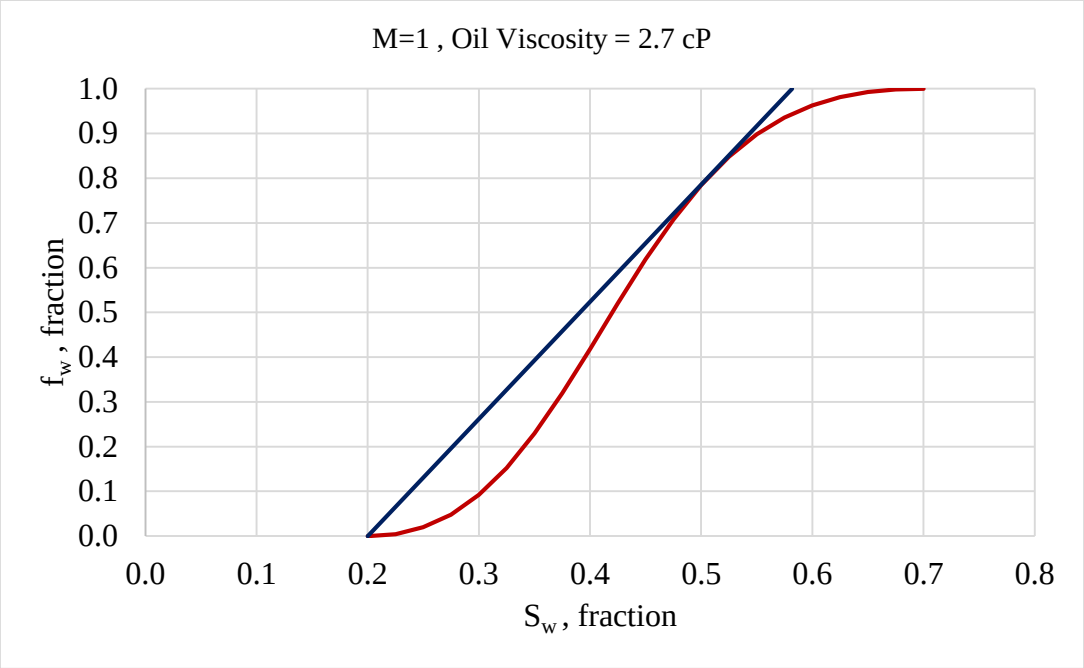

Figure 114 Fractional flow curve for M=1 at WI=0.8

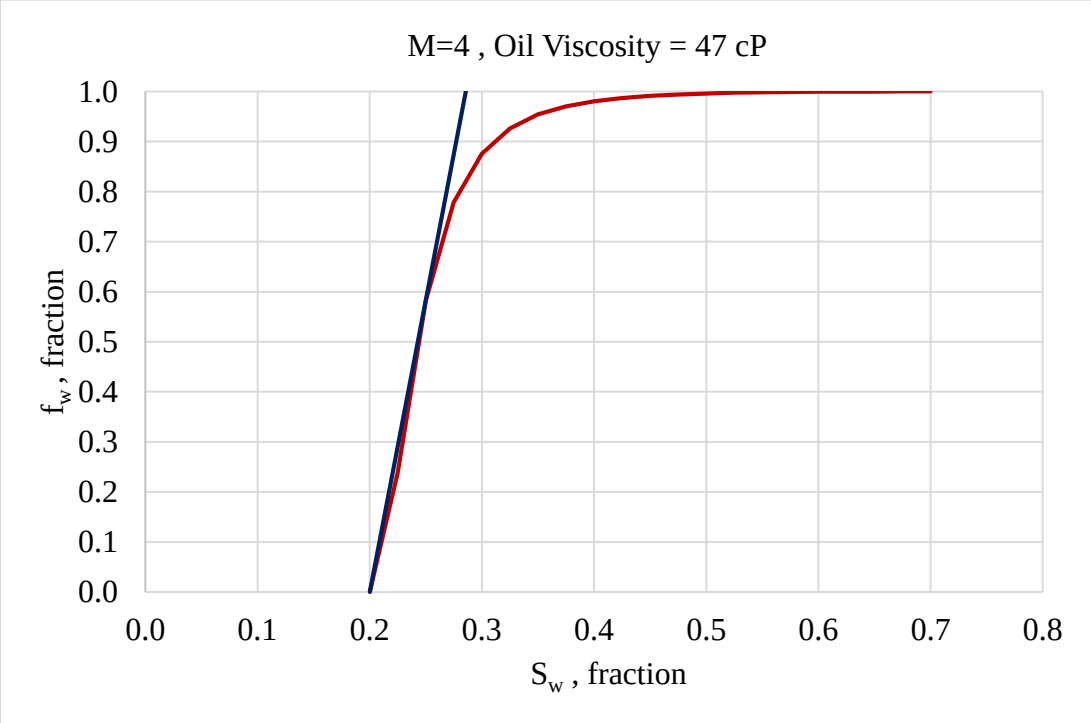

Figure 115 Fractional flow curve for M=4 at WI=0.8

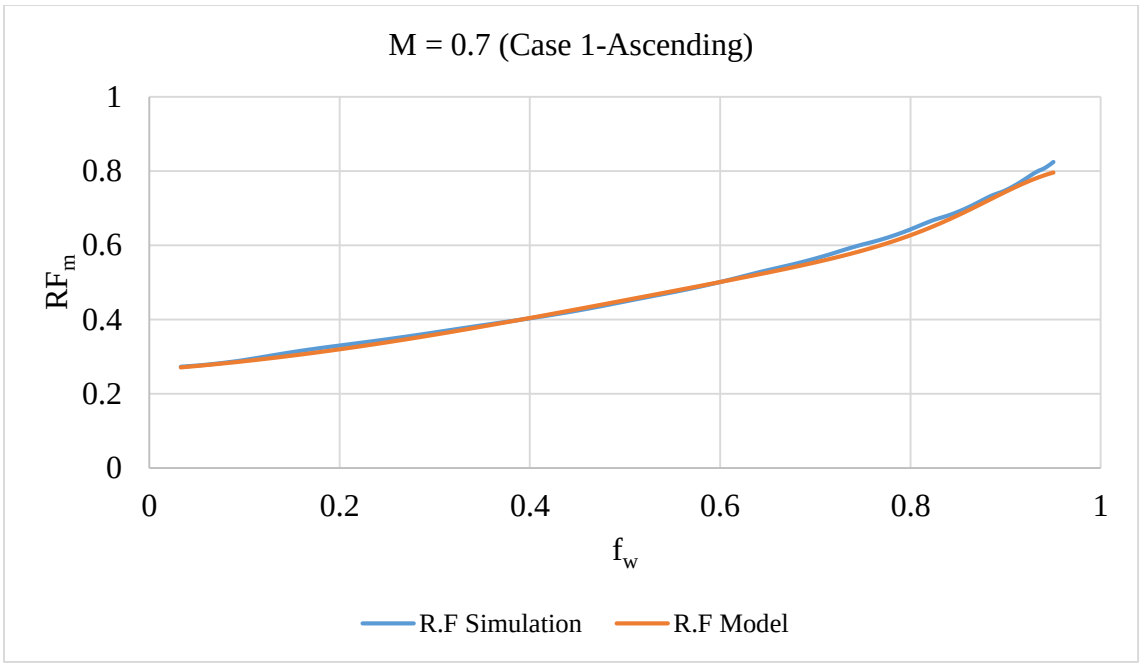

Figure 116 Comparison between simulator and ANN model at M=0.7 for Ascending case

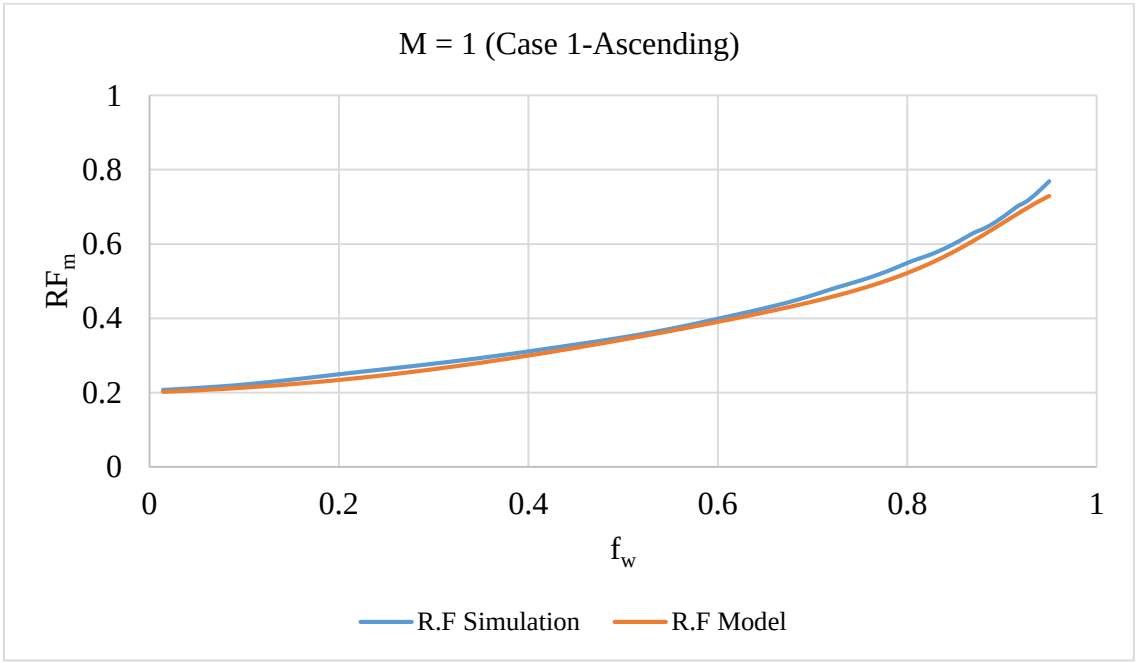

Figure 117 Comparison between simulator and ANN model at M=1 for Ascending case

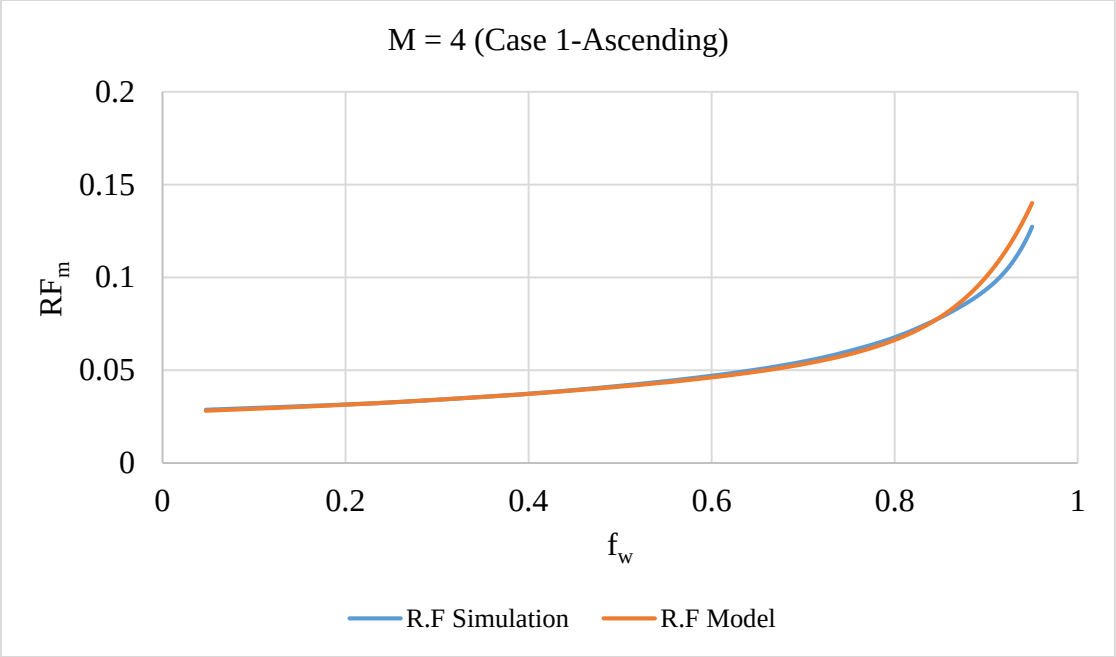

Figure 118 Comparison between simulator and ANN model at M=4 for Ascending case

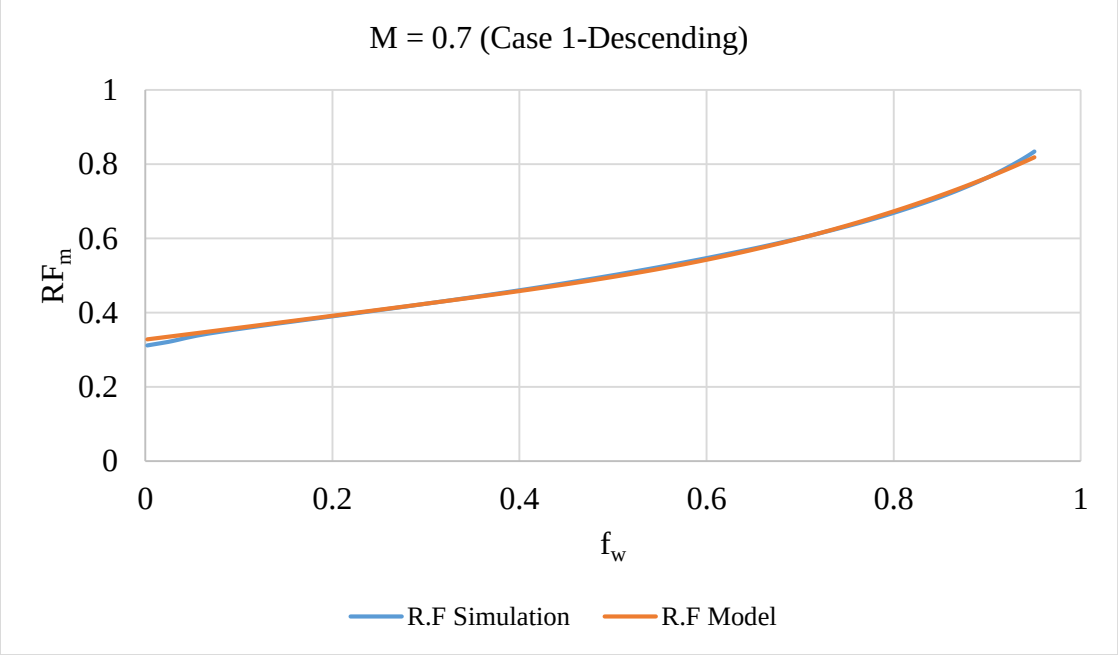

Figure 119 Comparison between simulator and ANN model at M=0.7 for Descending case

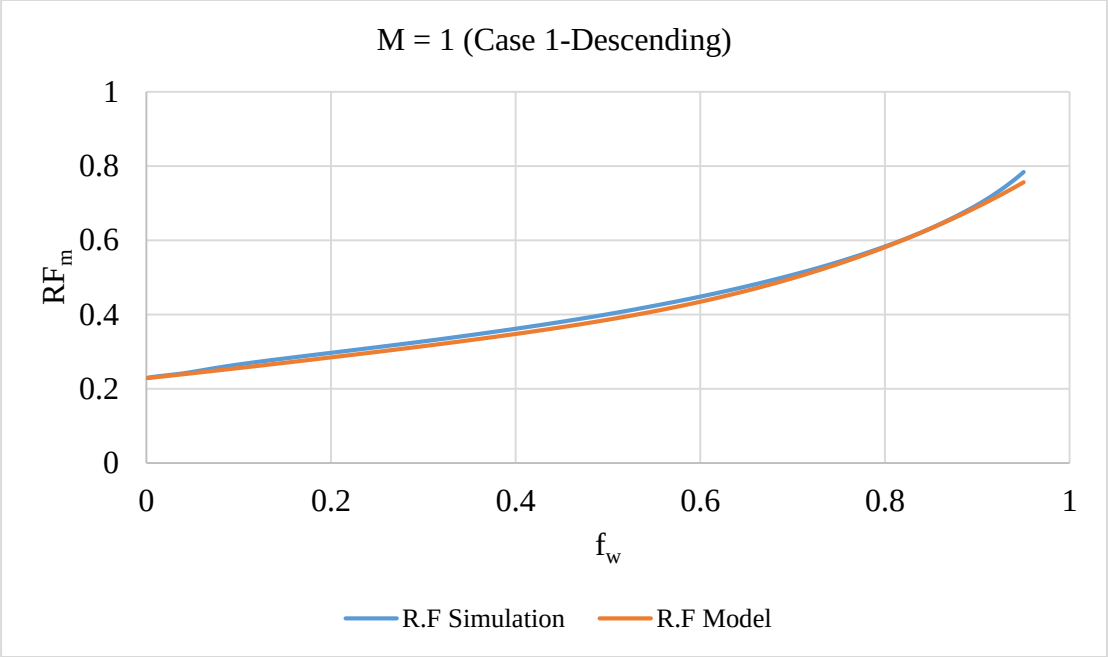

Figure 120 Comparison between simulator and ANN model at M=1 for Descending case

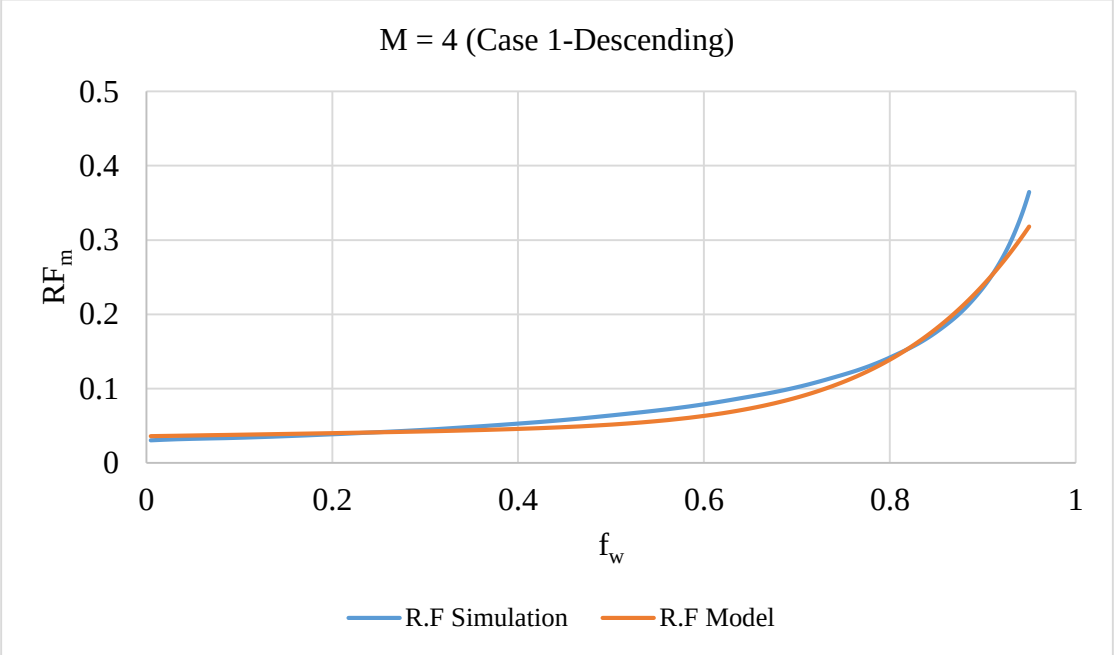

Figure 121 Comparison between simulator and ANN model at M=4 for Descending case

6.3.2 Case 2: Wettability Indicator = 1.51

Figure 122 shows the relative permeability curves of the system with WI of 1.51 and Figures 123 to 125 show the fractional flow curves at the mobility ratios used for testing. The simulation results were compared with the ANN model predictions at different mobility ratios. As shown in Figures 126 to 131, the match between ANN model and simulation results is excellent.

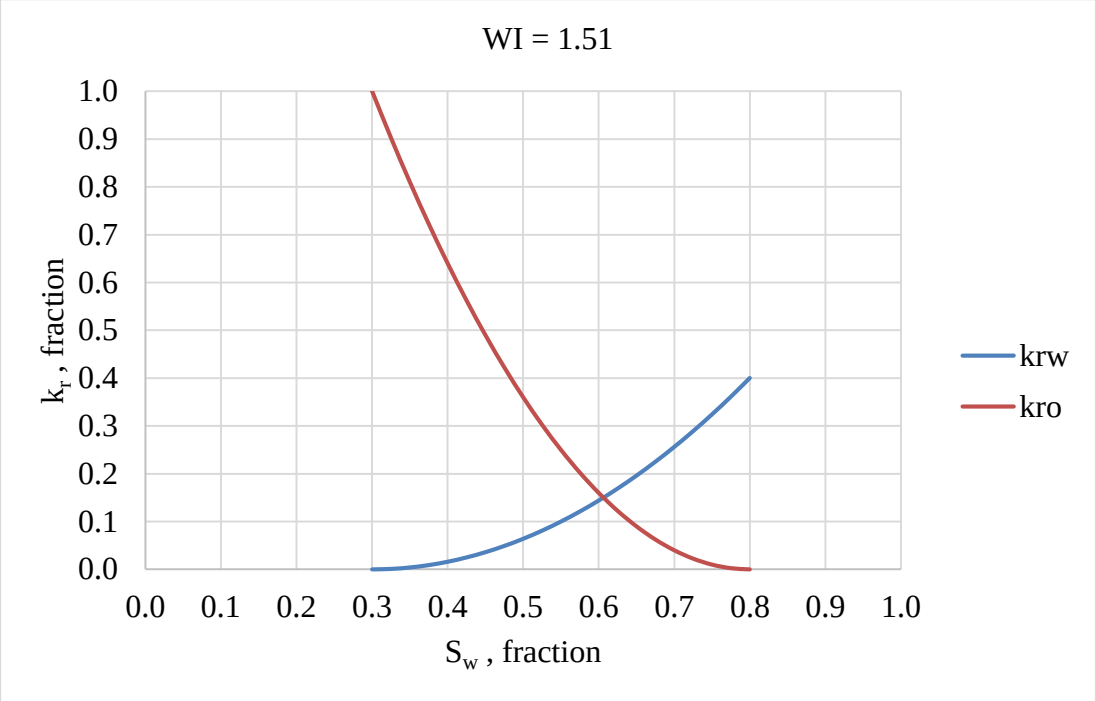

Figure 122 Relative permeability curves for case 2

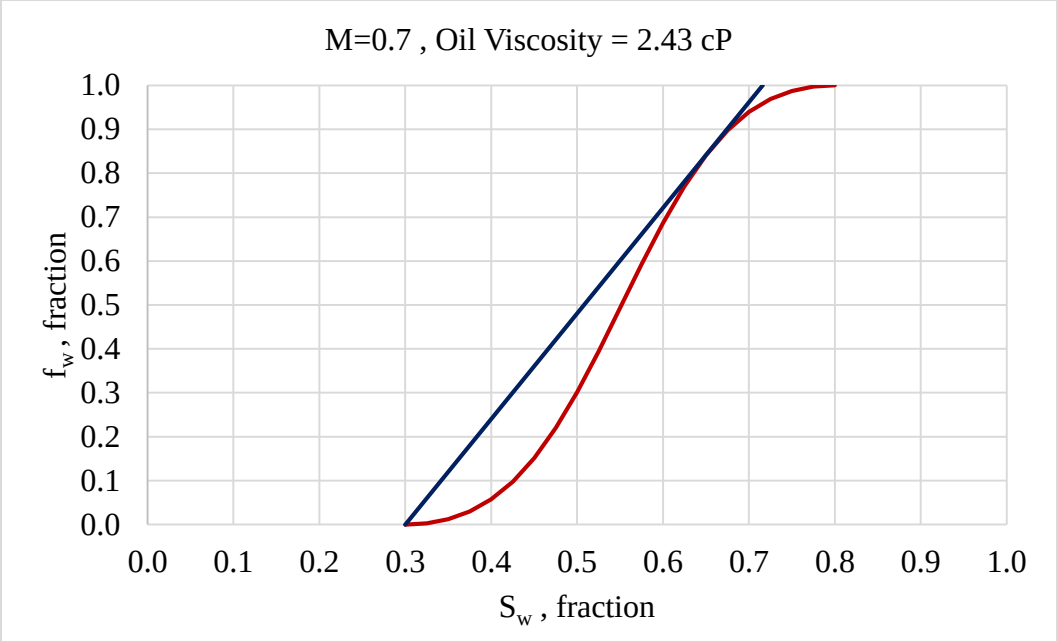

Figure 123 Fractional flow curve for M=0.7 at WI=1.51

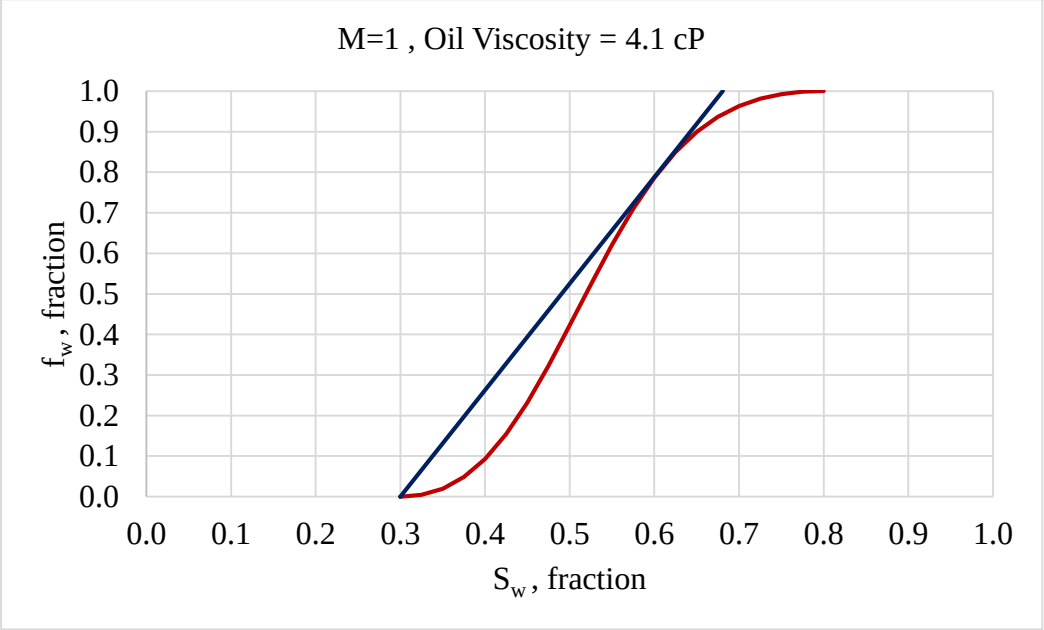

Figure 124 Fractional flow curve for M=1 at WI=1.51

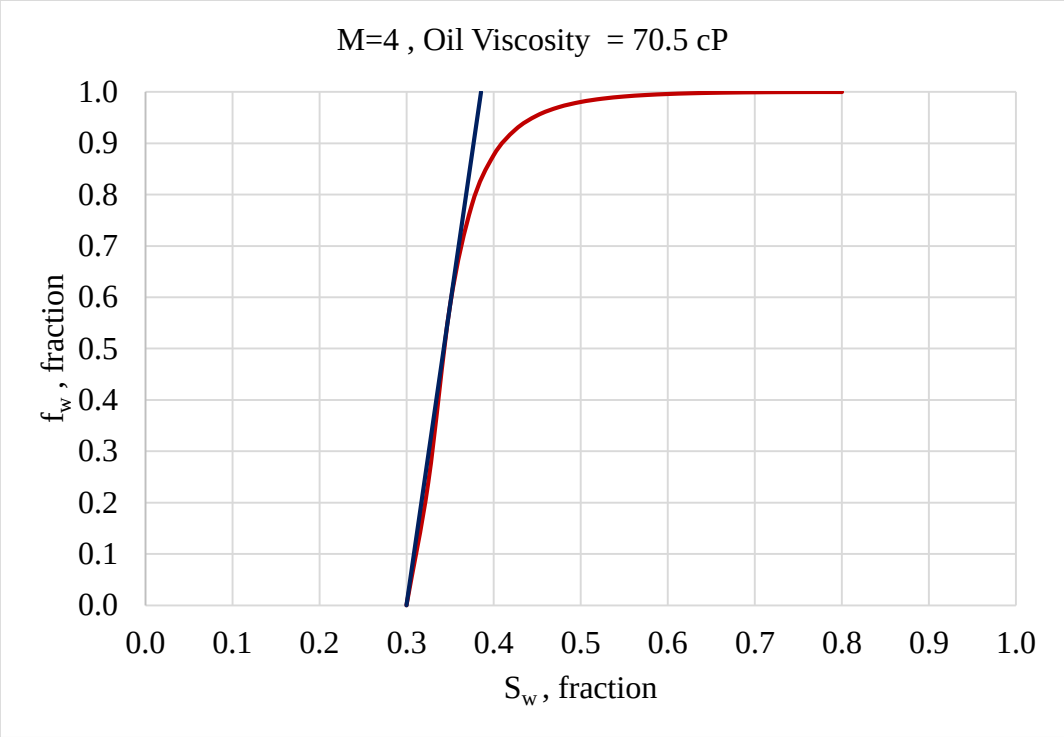

Figure 125 Fractional flow curve for M=4 at WI=1.51

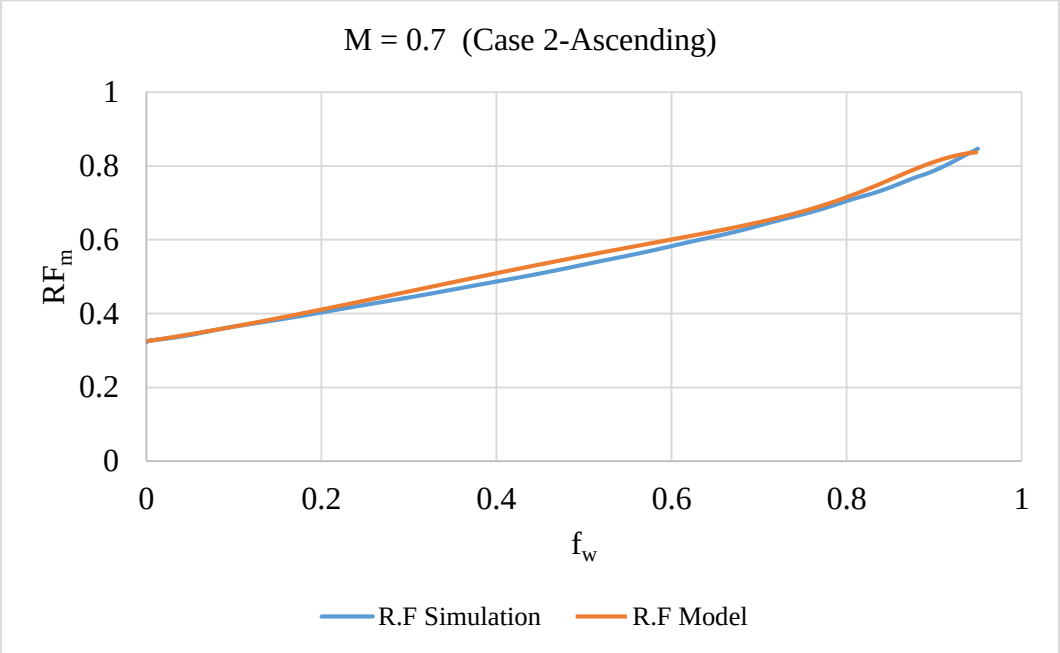

Figure 126 Comparison between simulator and ANN model at M=0.7 for Ascending case

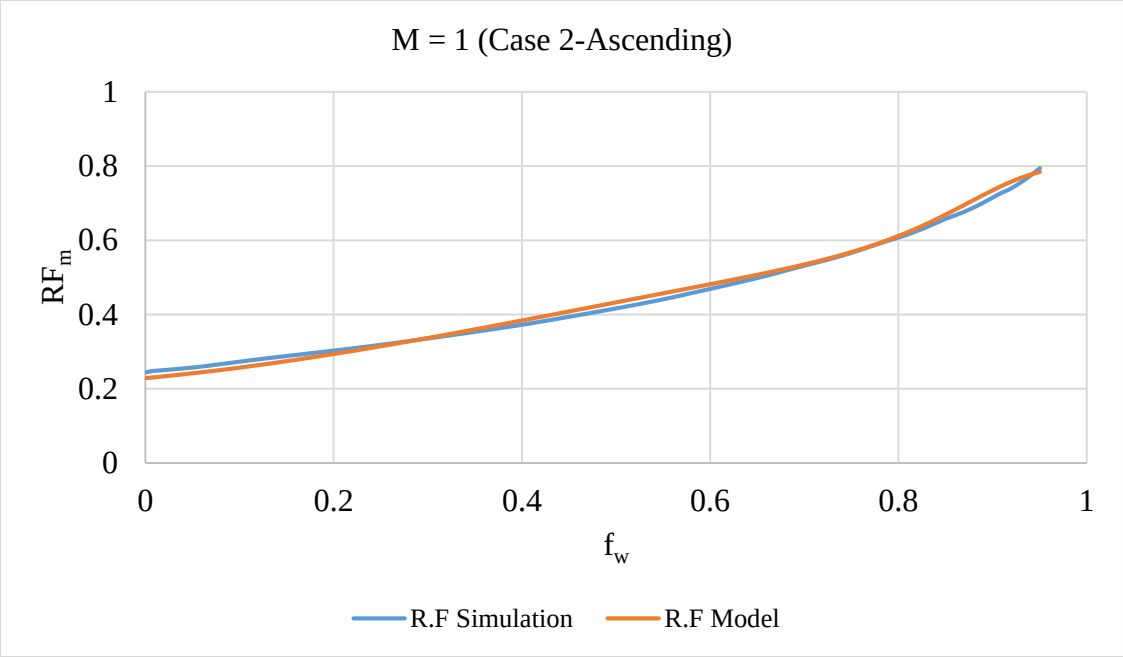

Figure 127 Comparison between simulator and ANN model at M=1 for Ascending case

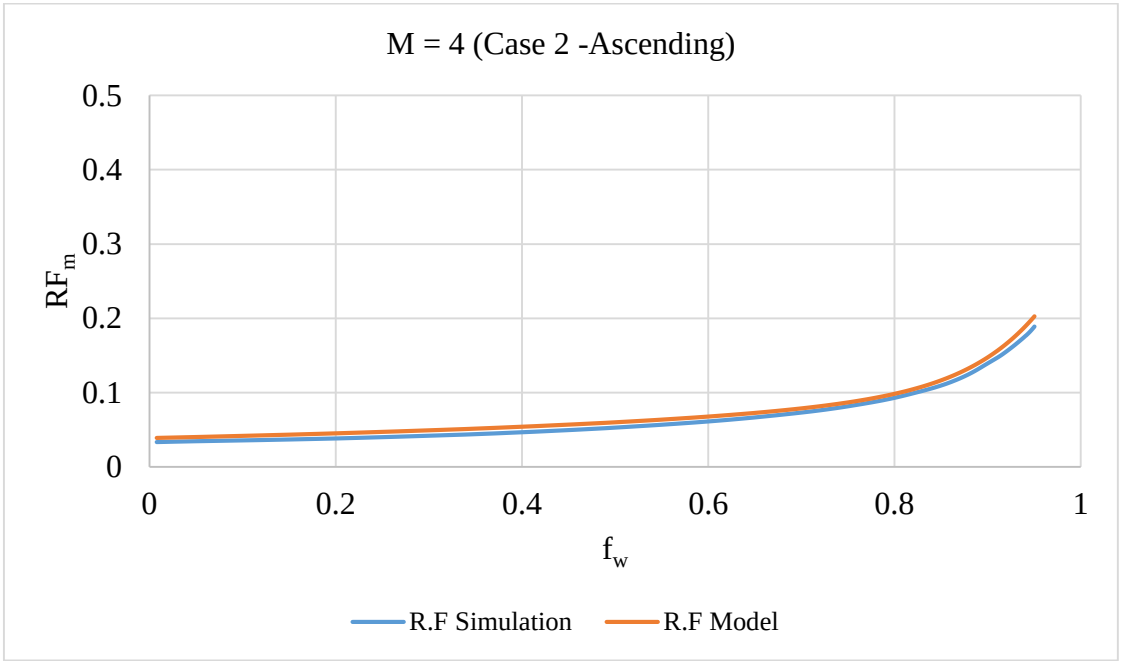

Figure 128 Comparison between simulator and ANN model at M=4 for Ascending case

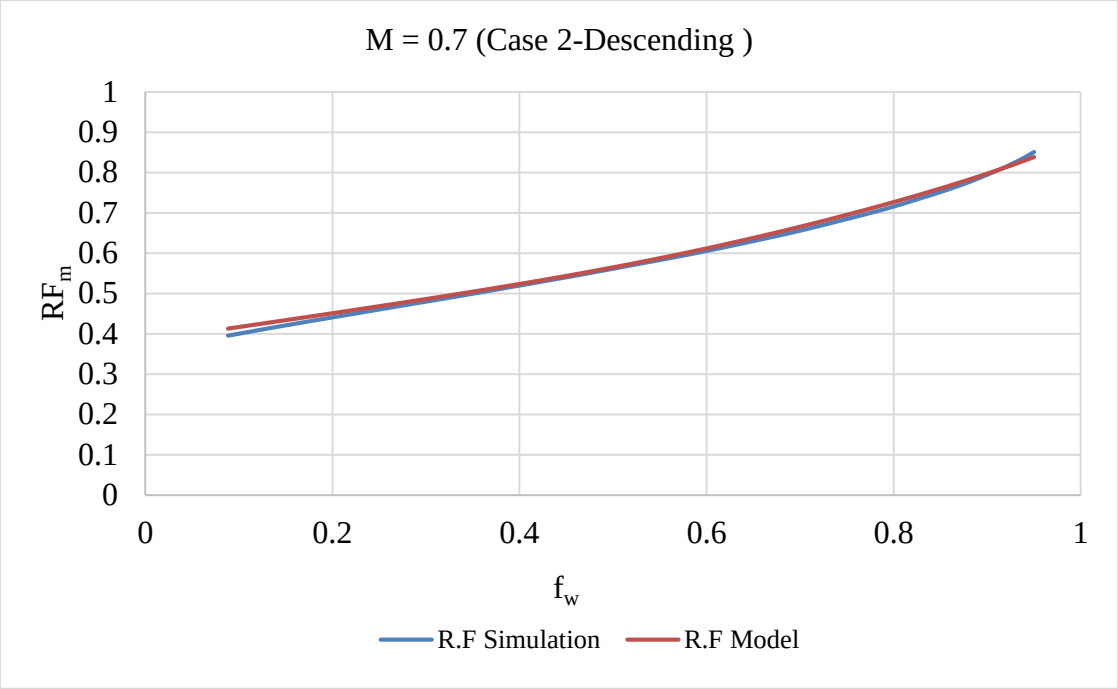

Figure 129 Comparison between simulator and ANN model at M=0.7 for Descending case

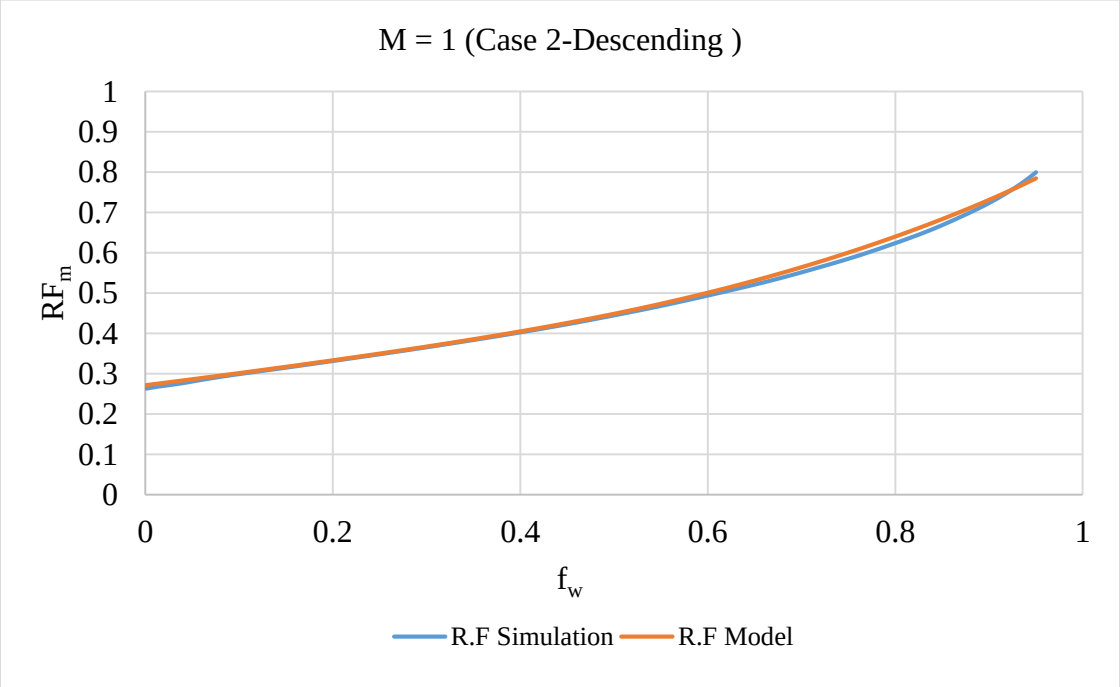

Figure 130 Comparison between simulator and ANN model at M=1 for Descending case

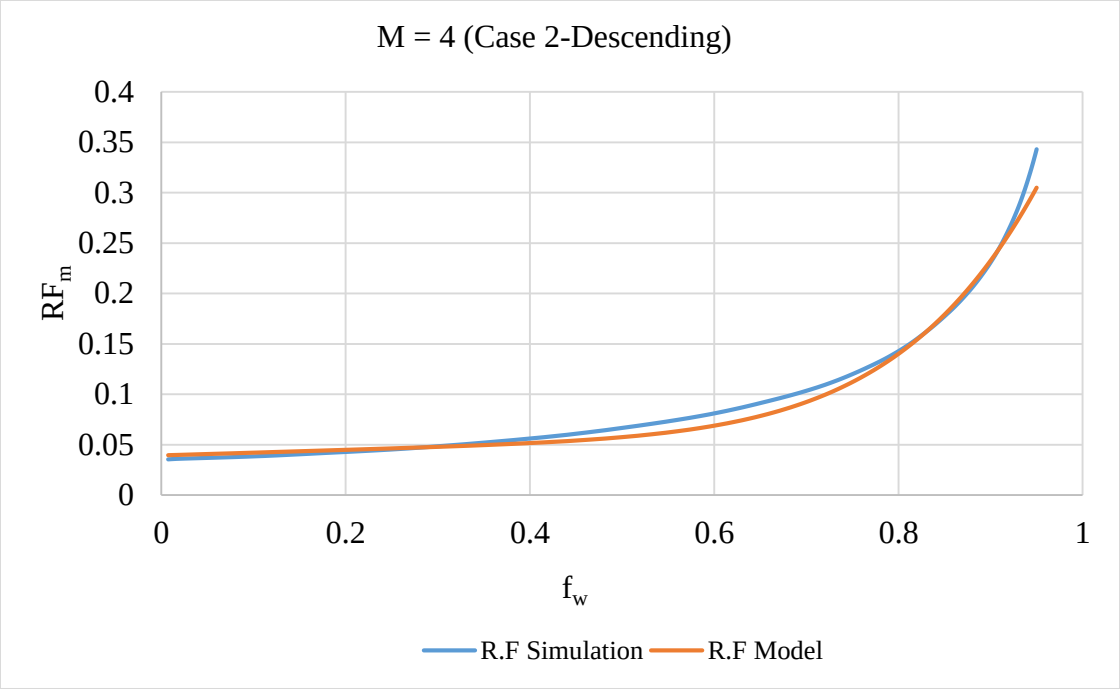

Figure 131 Comparison between simulator and ANN model at M=4 for Descending case

6.3.3 Wettability Indicator Testing

Both correlations were further tested for seven different cases involving five new wettability systems. These test were done at random values of *V*, *M*, β and f_w as detailed in Table 17. Figures 132 to 138 show relative permeability curves for each system and fractional flow curves for those cases are shown in Figures 139 to 145. Scatter plots between simulator vs. the developed ANN correlations are shown in Figure 146 and 147 for ascending and descending cases, respectively, which shows that both correlations are excellent (R^2 > 99%).

Table 17 Correlation testing parameters (with several values of WI)

Cases	V	M	β	WI
1	0.1	2	0.7	0.6
2	0.3	0.2	0.8	0.7
3	0.3	1	0.8	0.8
4	0.5	4	0.9	1
5	0.5	4	0.9	1.51
6	0.7	0.5	1	2.26
7	0.9	1	1	2.73

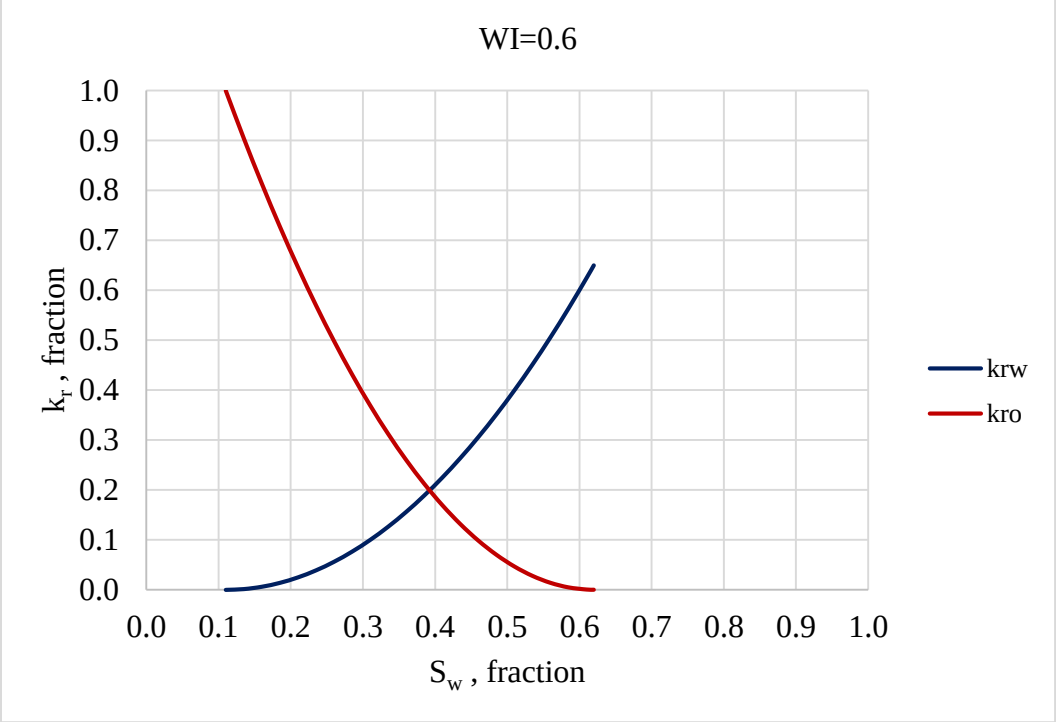

Figure 132 Relative permeability curves for WI=0.6

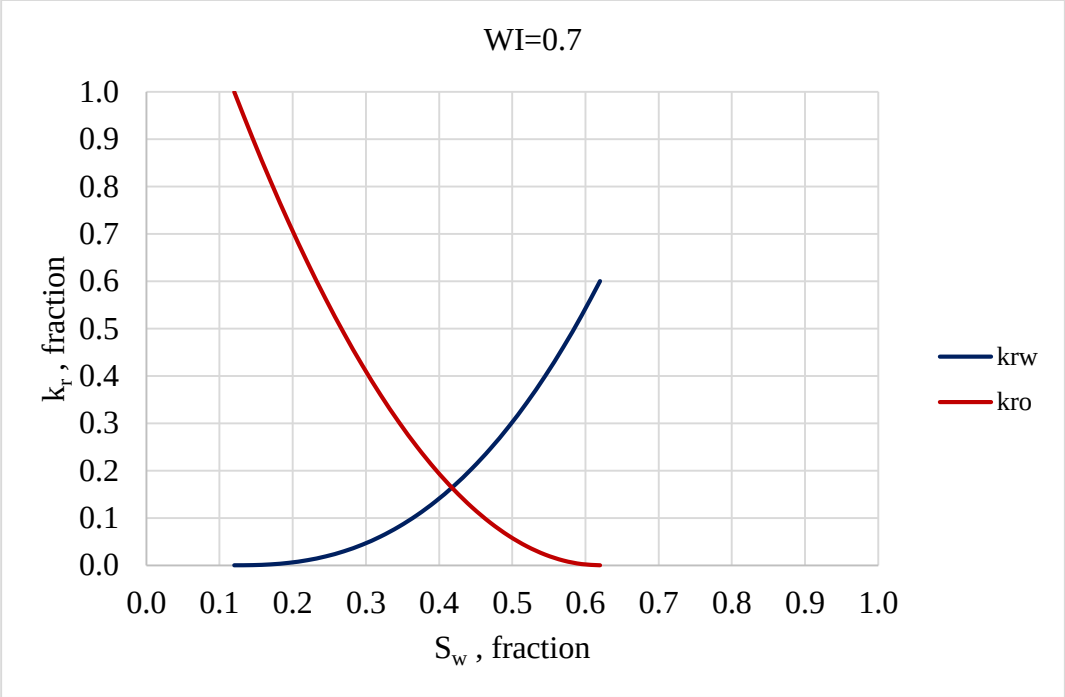

Figure 133 Relative permeability curves for WI=0.7

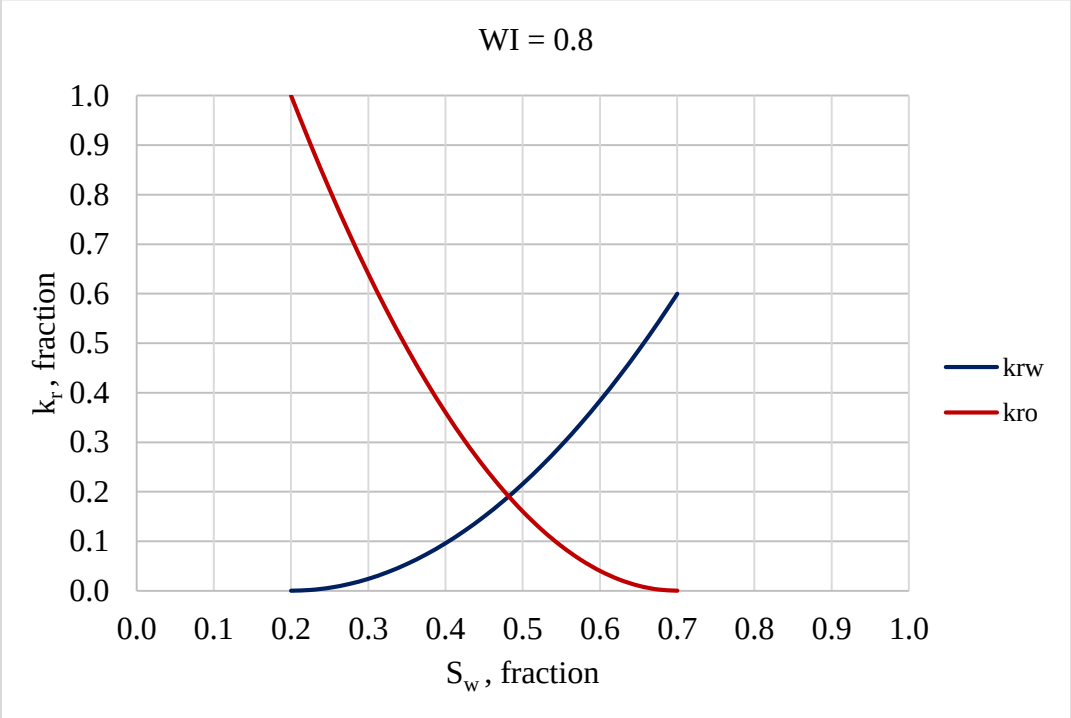

Figure 134 Relative permeability curves for WI=0.8

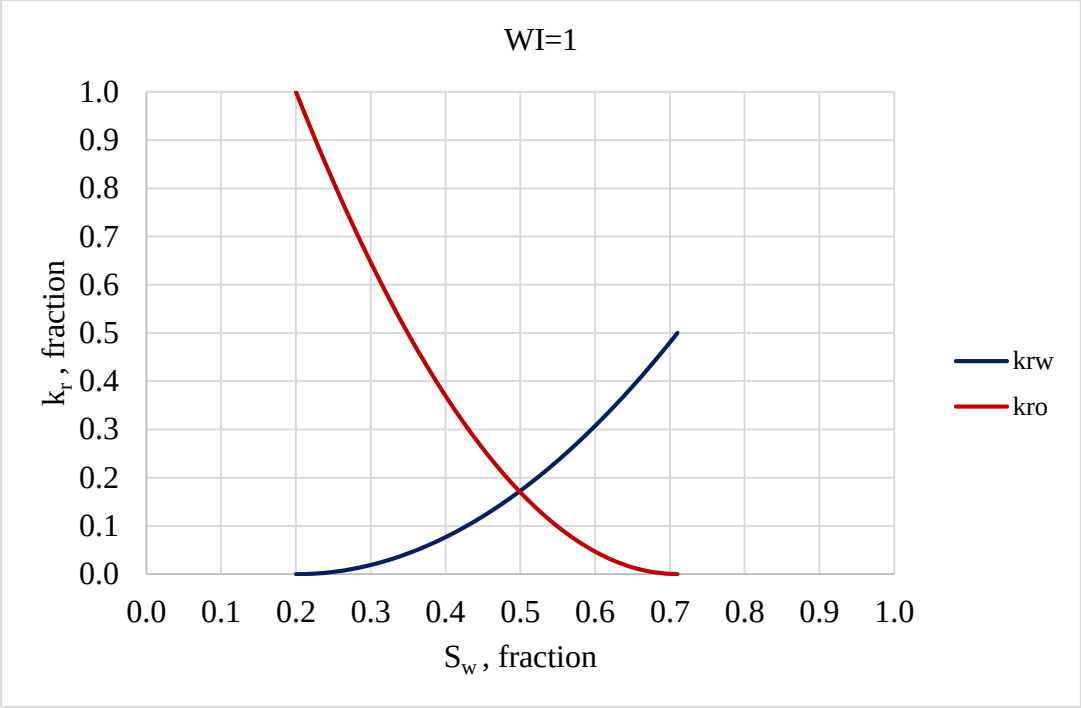

Figure 135 Relative permeability curves for WI=1

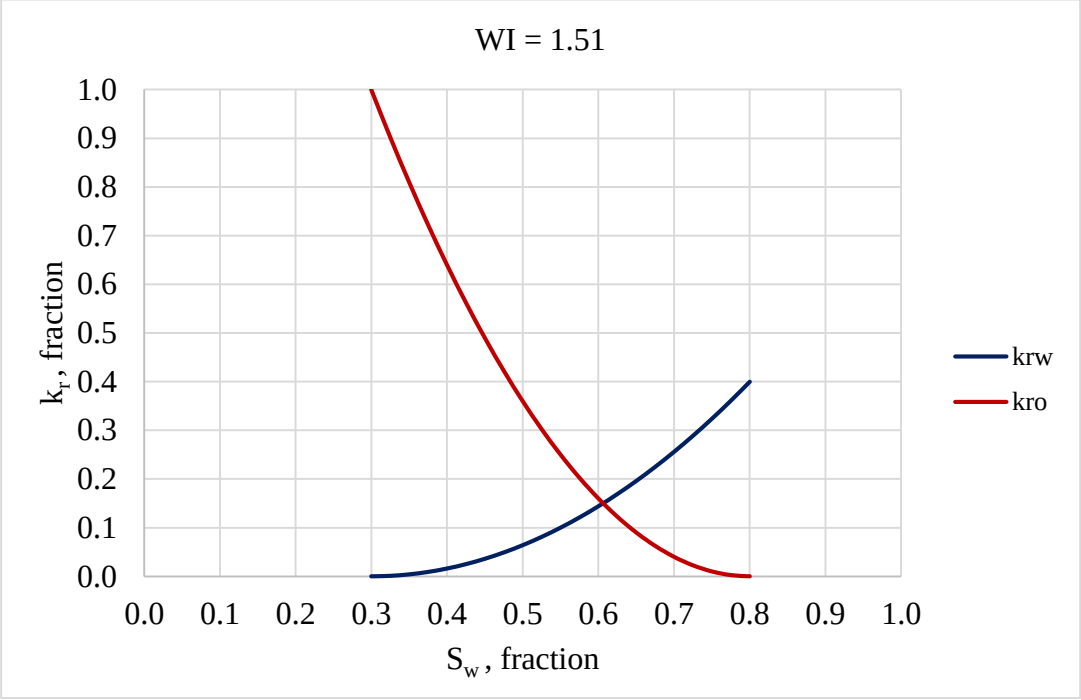

Figure 136 Relative permeability curves for WI=1.51

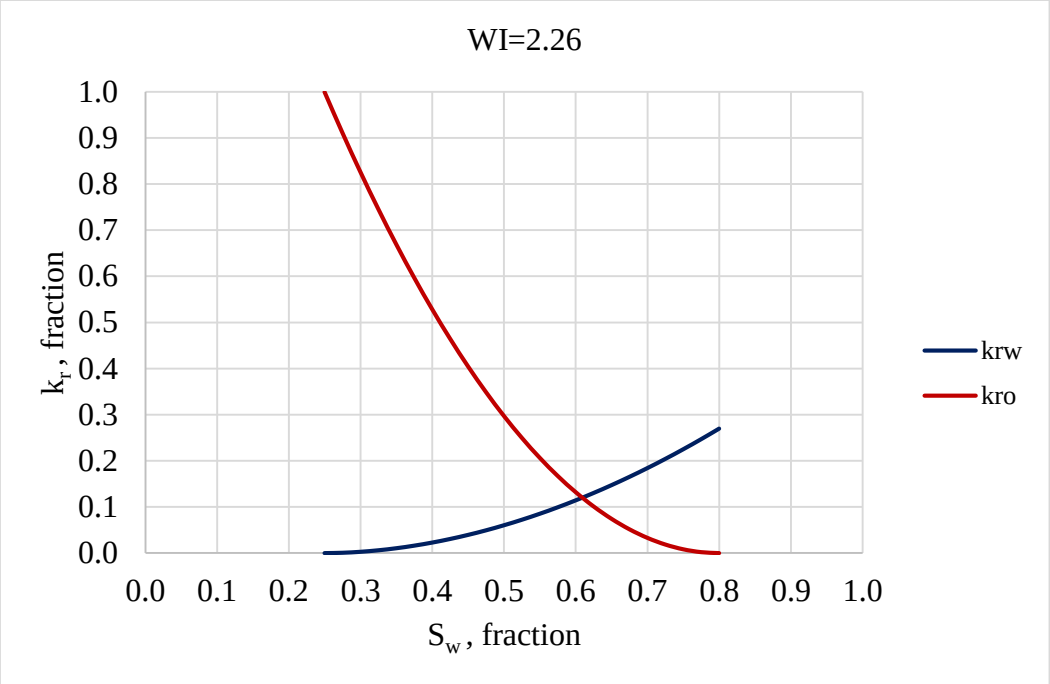

Figure 137 Relative permeability curves for WI=2.26

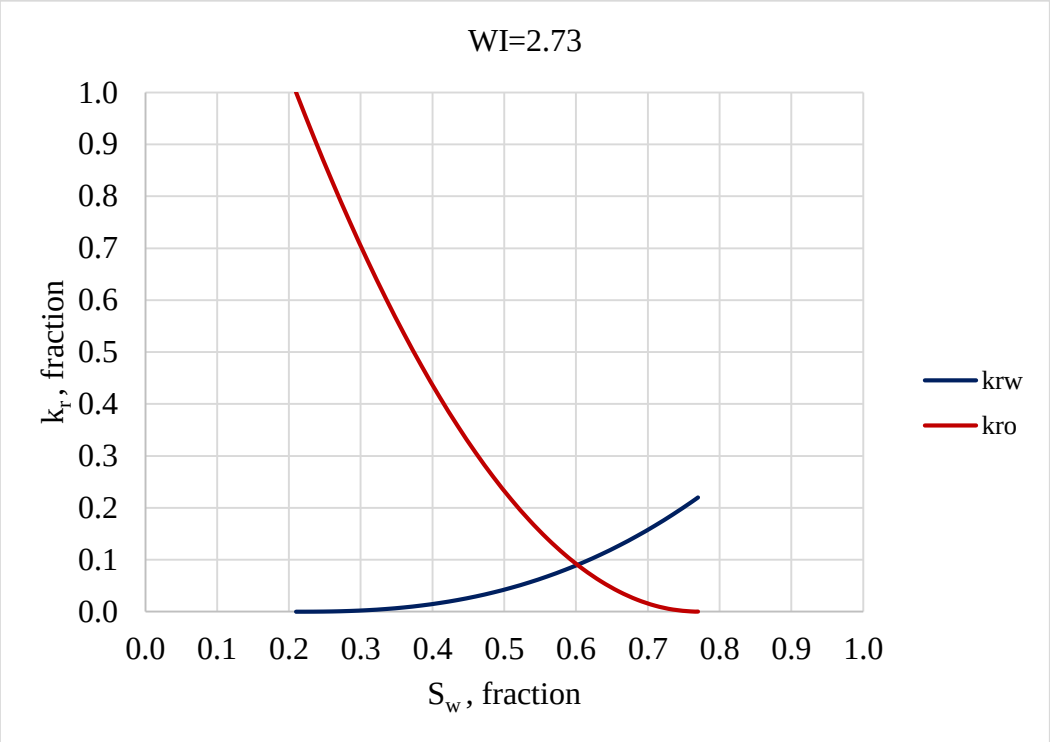

Figure 138 Relative permeability curves for WI=2.73

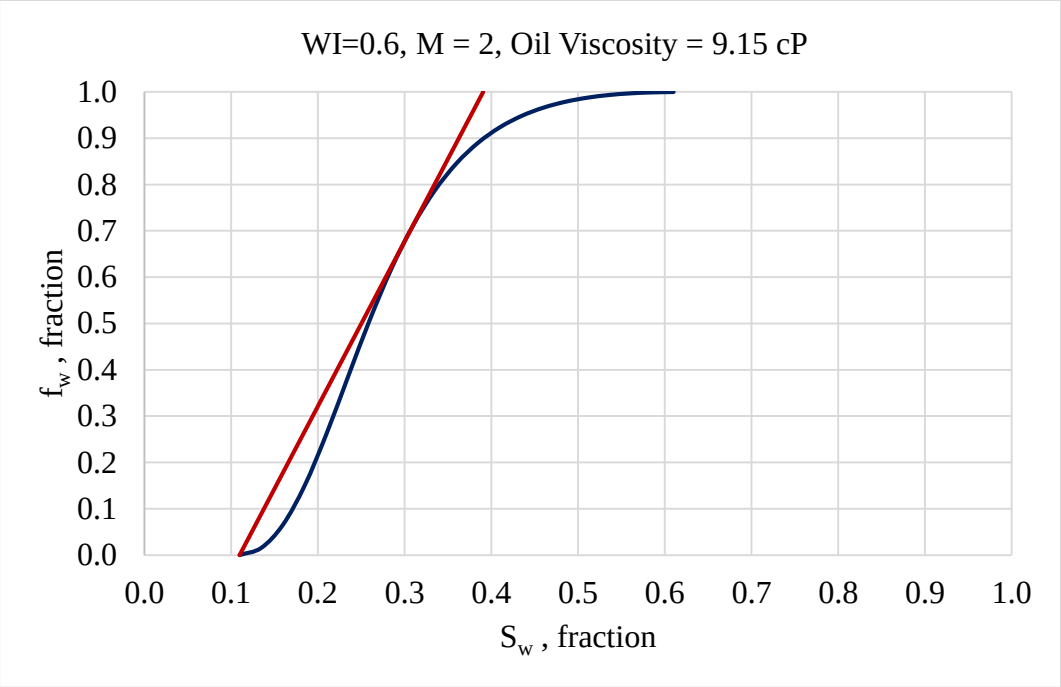

Figure 139 Fractional flow curves for WI=0.6

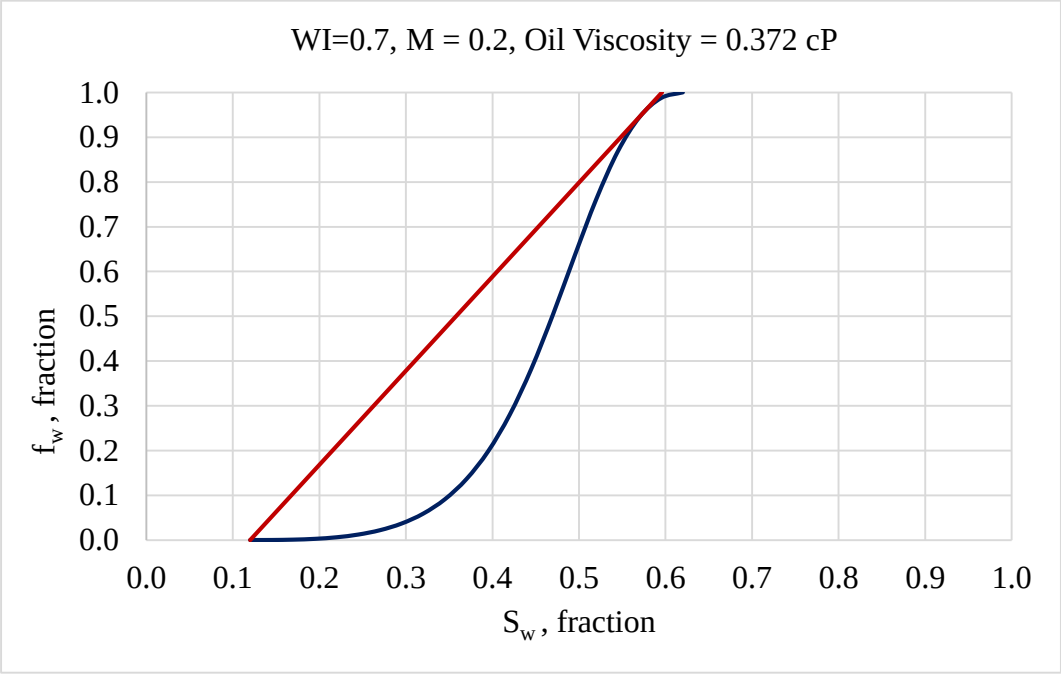

Figure 140 Fractional flow curves for WI=0.7

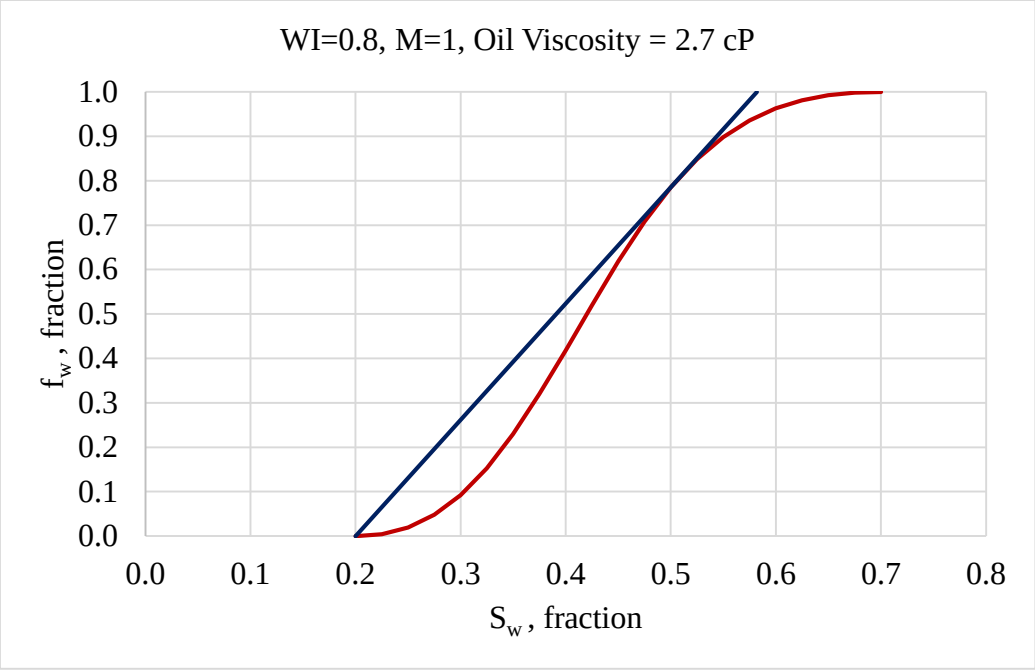

Figure 141 Fractional flow curves for WI=0.8

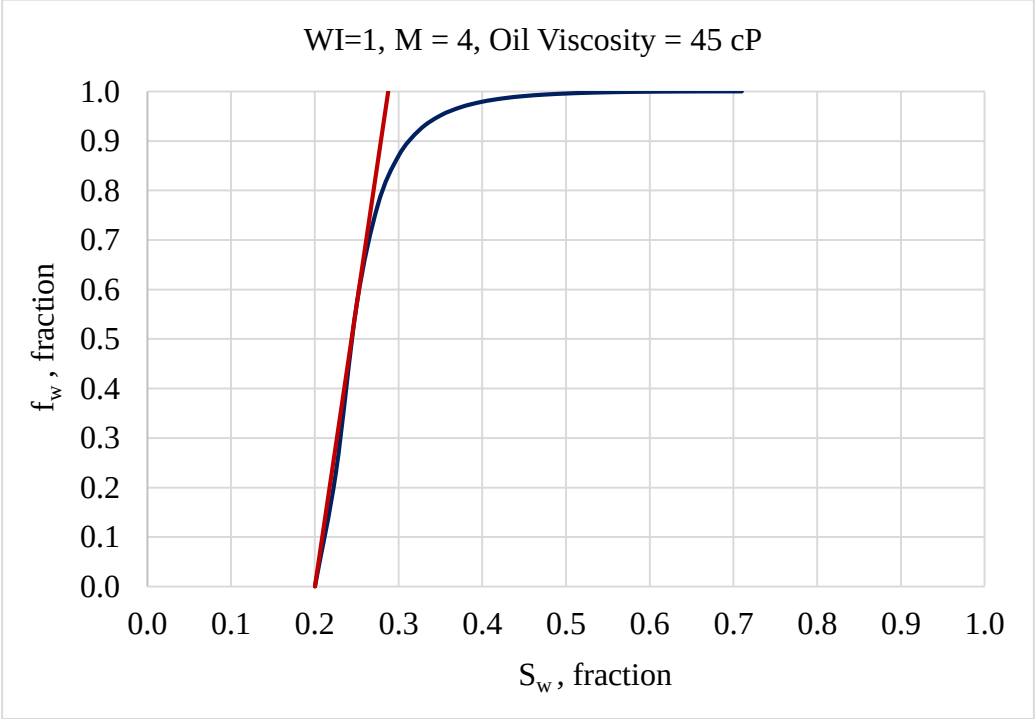

Figure 142 Fractional flow curves for WI=1

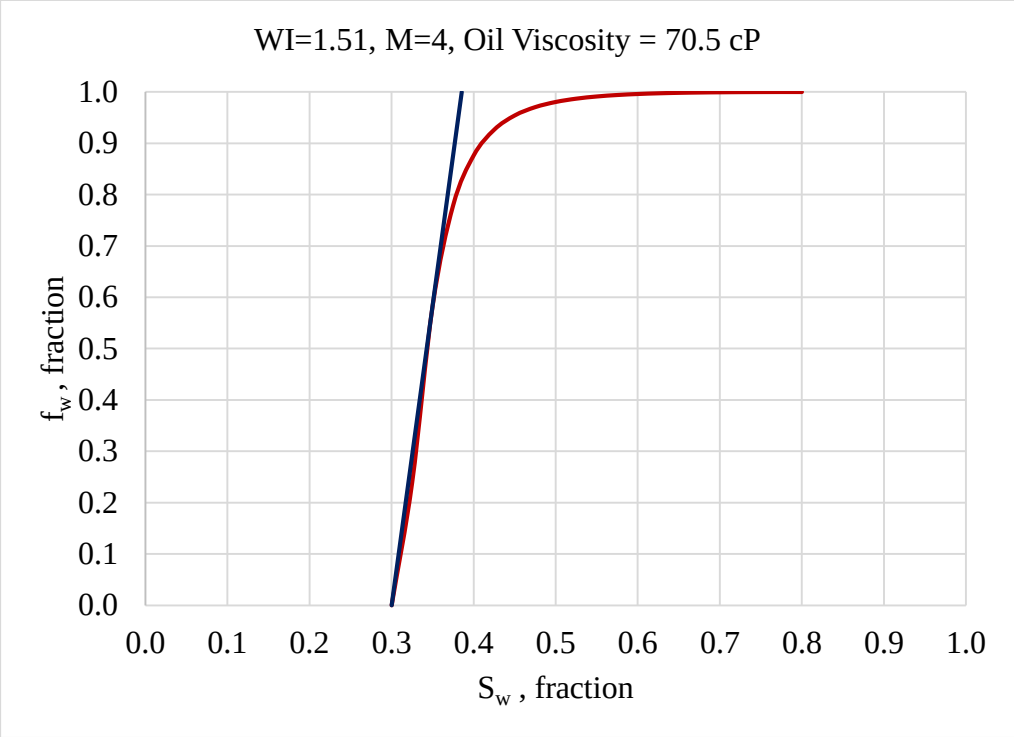

Figure 143 Fractional flow curves for WI=1.51

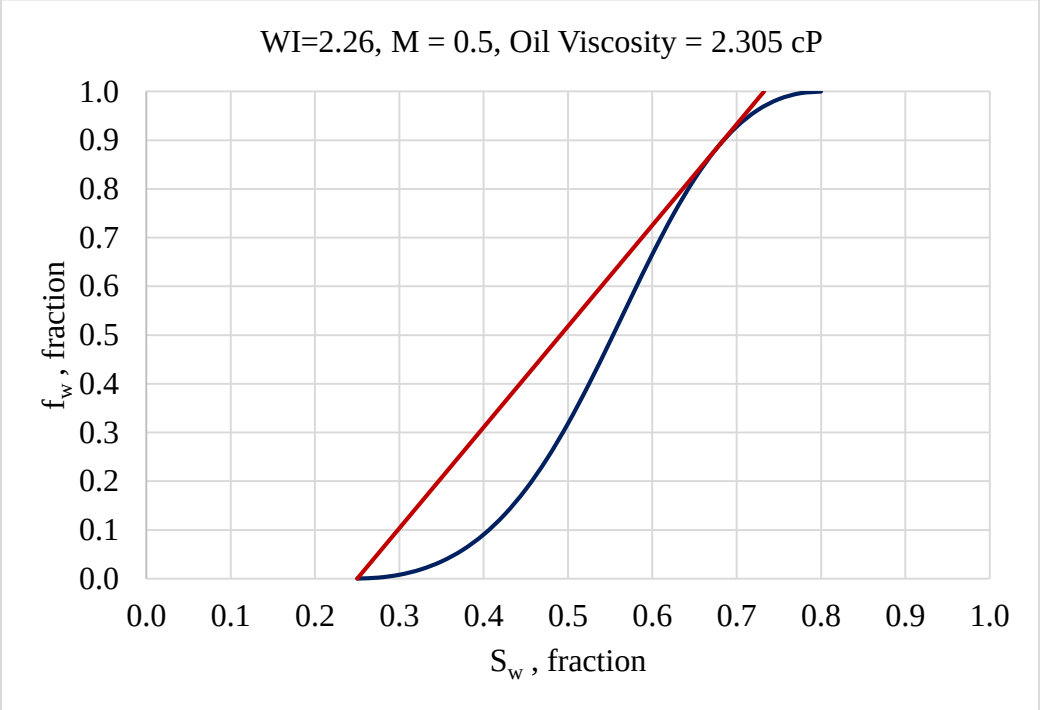

Figure 144 Fractional flow curves for WI=2.26

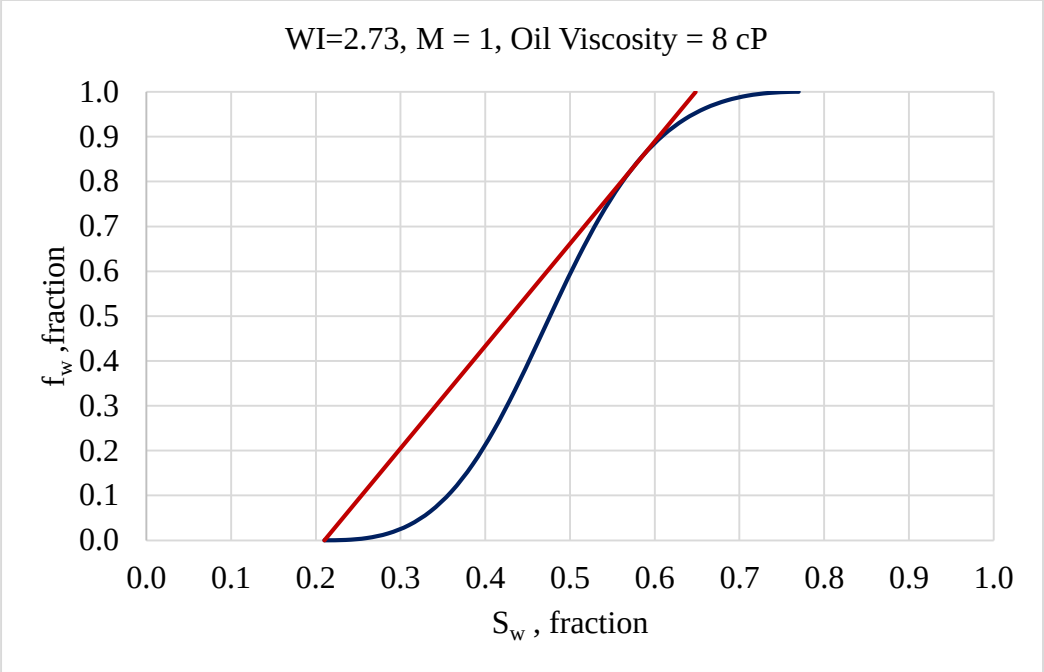

Figure 145 Fractional flow curves for WI=2.7

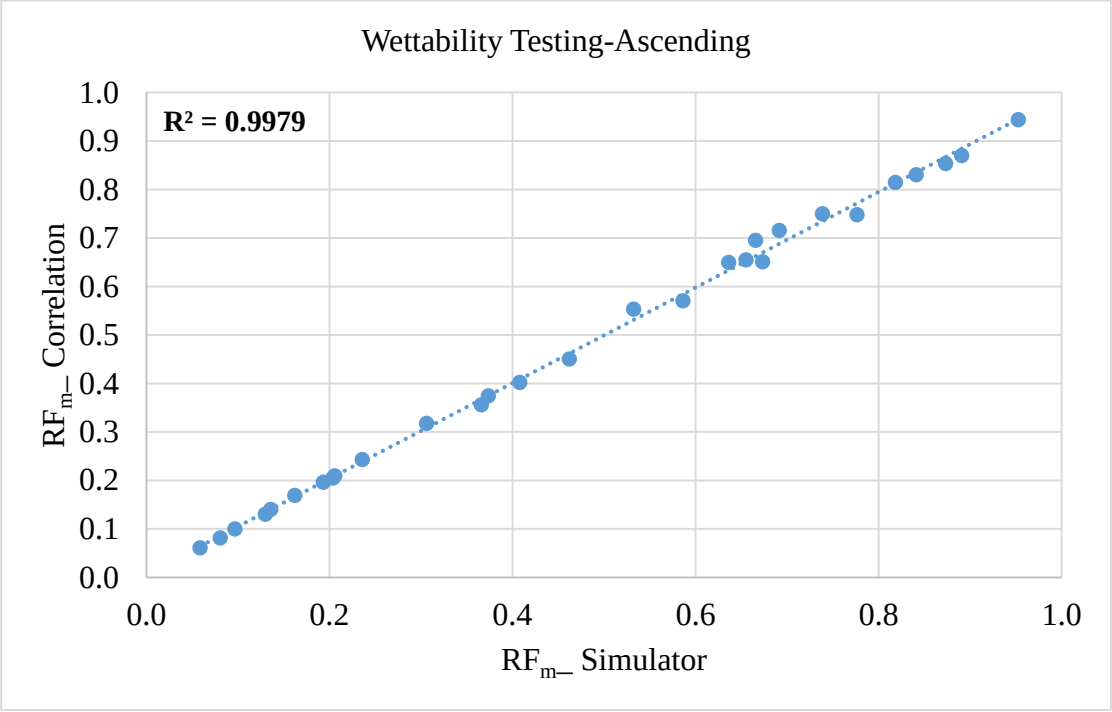

Figure 146 Scatter plot for WI testing between simulator Vs. ANN correlation for ascending

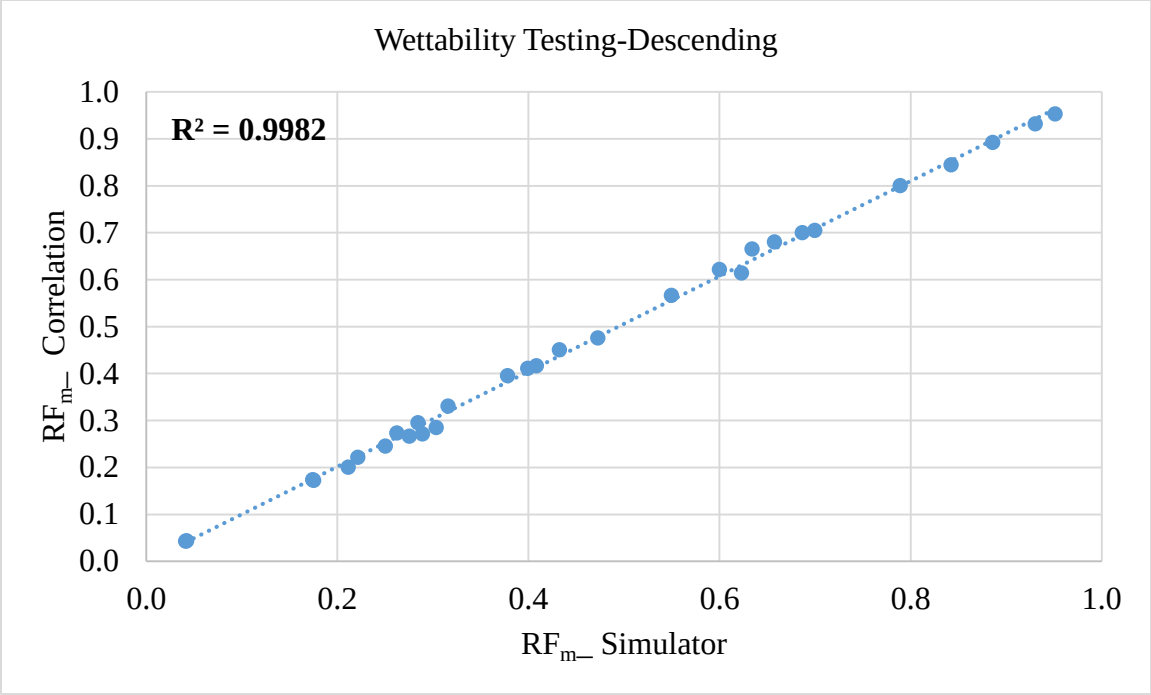

Figure 147 Scatter plot for WI testing between simulator Vs. ANN correlation for descending

6.4 Comparison with Field Data

Two different field cases were tested with the developed correlations. This field data belongs to infill wells with no primary production and was taken from the PhD dissertation by Espinel. [2]

6.4.1 Case 1: Field A

Field A is a highly heterogeneous reservoir that is flooded at a mobility ratio 0.439. Reservoir properties are presented in Table 18. Relative permeability and fractional flow curves for the reservoir are shown in Figures 148 and 149, respectively.

Table 18 Data for Field A

Data for Field A	
Parameter	**Value**
Initial water saturation, S_{wi}	0.38
Residual oil saturation, S_{or}	0.23
Initial gas saturation, S_{gi}	0.01
Water viscosity, μ_w, cP	0.9
Oil viscosity, $\mu_{o,}$ cP	1.2
Oil formation volume factor, B_o, RB/STB	1.15
Water formation volume factor, B_w, RB/STB	1
End-point oil relative perm, $(k_{ro})_{Swi}$	0.96865
End-point water relative perm, $(k_{rw})_{Sor}$	0.551
Corey's oil exponent, n_o	3.017
Corey's water exponent, n_w	1.8045
Permeability variation coefficient, V	0.8
Anisotropy ratio, k_z/k_x	0.1
Oil density, lb/ft^3	49.1
Water density, lb/ft^3	62.42

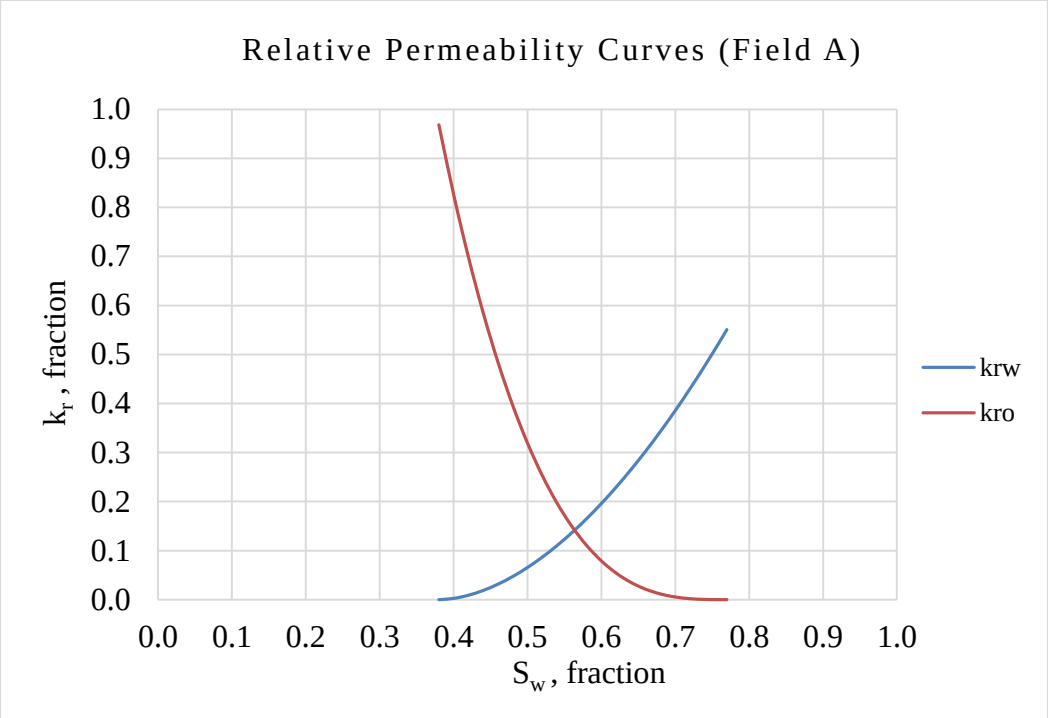

Figure 148 Relative permeability curves for field A

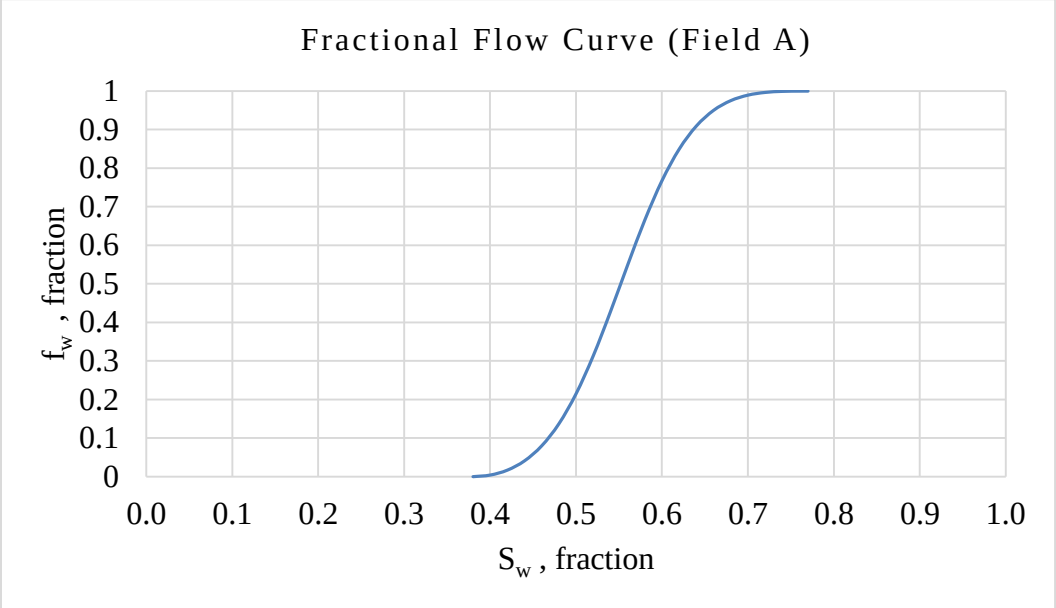

Figure 149 Factional flow curve for field A

Since the permeability arrangement for the reservoir was not mentioned in the reference, and since most reservoirs show decreasing permeability with depth, the correlation for descending case was

used for comparison purposes. As shown in Figure 150, the match is excellent between Well 2 data and the developed correlation. The new correlation matched the data very well up to RF_m = 80%. At that point, the well was apparently worked over to reduce water production (notice sudden drop in WOR). The initial deviation between the new correlation and Field A data upto WOR = 0.2 is due to the fact that water production in real fields may occur before the flood water from the injector reaches the producer. The early water breakthrough may be as a result of formation water or water coming from aquifer.

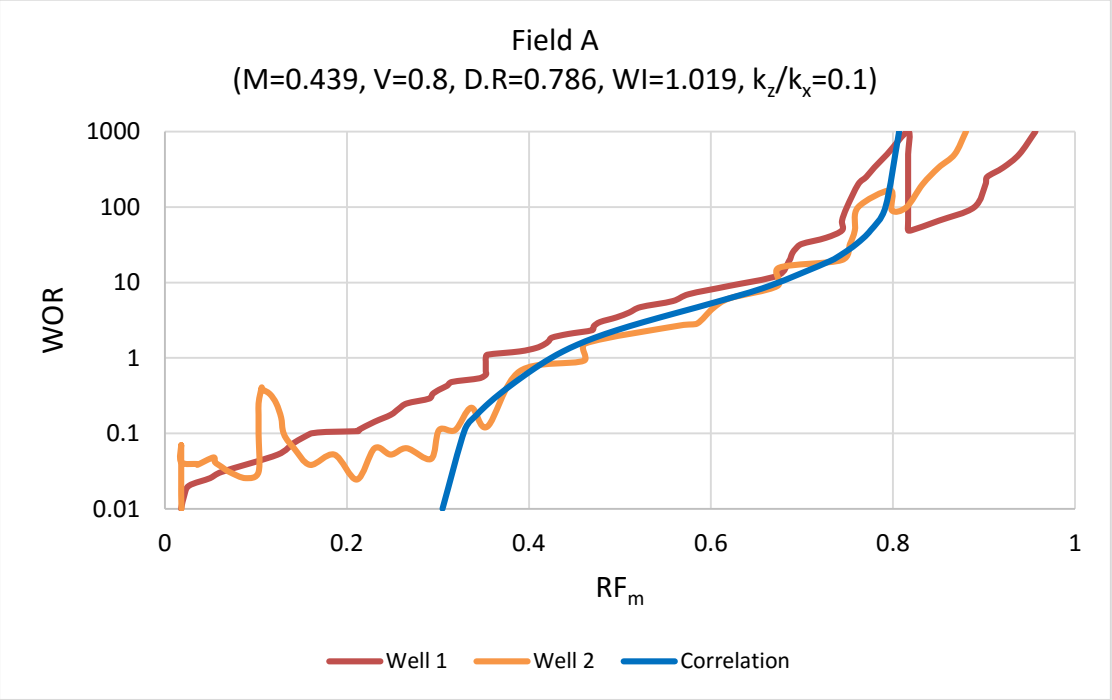

Figure 150 Comparison of water flood performance of two different wells from Field A with the developed correlation

6.4.2 Case 2: Field B

Field B is a reservoir with high heterogeneity that is flooded with a mobility ratio of 0.94. Reservoir properties for field B are presented in Table 19. Relative permeability and fractional flow curves for field B are shown in Figures 151 and 152, respectively.

Table 19 Data for Field B

Data for Field B	
Parameter	**Value**
Initial water saturation, S_{wi}	0.17
Residual oil saturation, S_{or}	0.25
Initial gas saturation, S_{gi}	0
Water viscosity, μ_w, cP	0.25
Oil viscosity, μ_o, cP	2.54
Oil formation volume factor, B_o, RB/STB	1.108
Water formation volume factor, B_w, RB/STB	1
End-point oil relative perm, $(k_{ro})_{Swi}$	1.0
End-point water relative perm, $(k_{rw})_{Sor}$	0.25
Corey's oil exponent, n_o	3.0
Corey's water exponent, n_w	2.0
Permeability variation coefficient, V	0.8
Anisotropy ratio, k_z/k_x	0.1
Oil density, lb/ft^3	49.1
Water density, lb/ft^3	62.42

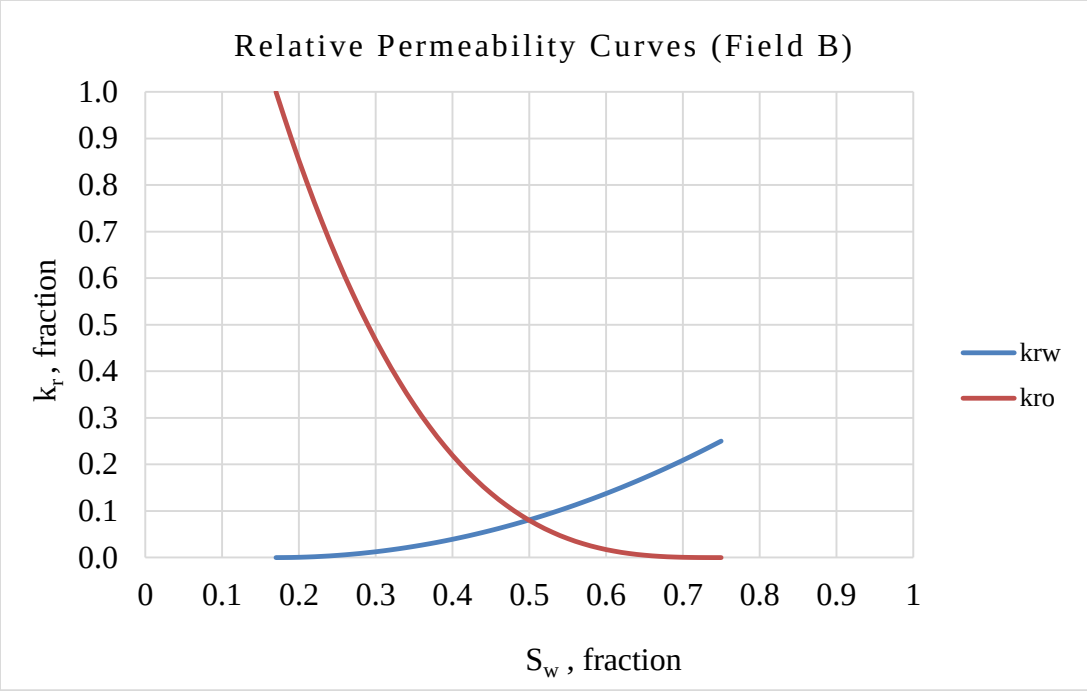

Figure 151 Relative permeability curves for field B

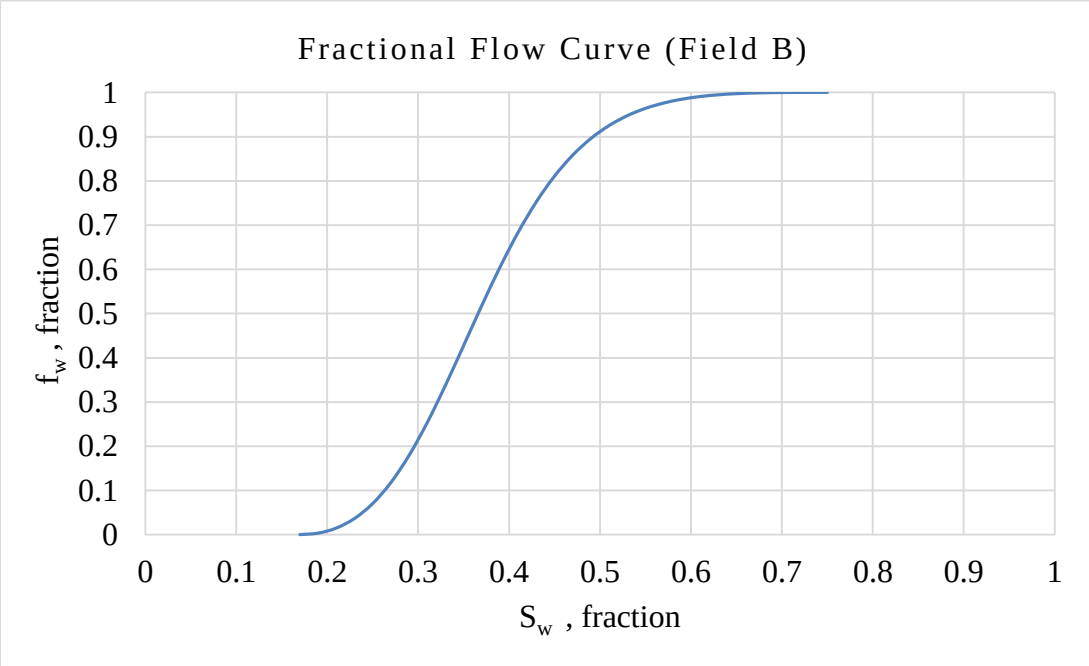

Figure 152 Factional flow curve for field B

Again, the correlation developed for the descending case was tested against field B data. Figure 153 shows excellent prediction by the correlation of Well 1 performance. The ultimate values of movable oil recovery factor are 63% and 65.6% for Well 1 and the new correlation respectively. The new correlation followed the data trend very well. The initial deviation between the new correlation and Field B data upto WOR = 0.02 is due to the fact that water production in real fields may occur before the flood water from the injector reaches the producer. The early water breakthrough may be as a result of formation water or water coming from aquifer.

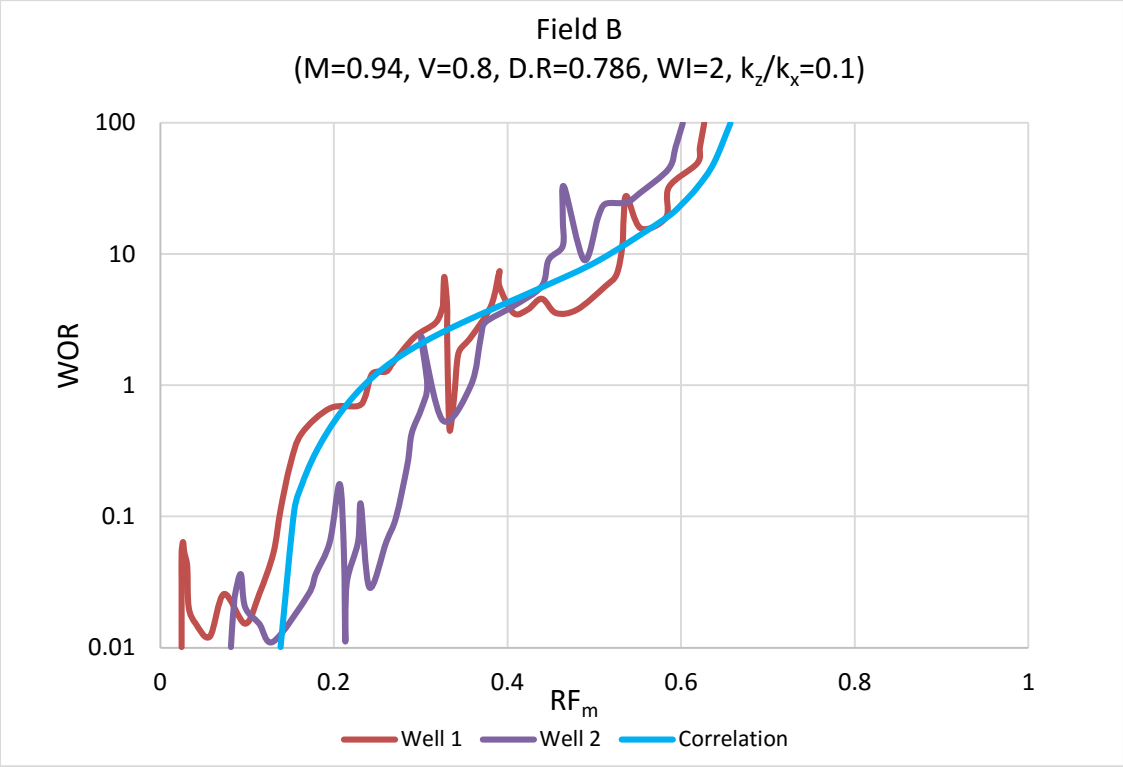

Figure 153 Comparison of water flood performance of two different wells from Field B with the developed correlation

6.5 Comparison with Craig-Geffen-Morse (CGM) Method

As mentioned in Chapter 2, the Craig-Geffen-Morse (CGM) method is used to predict 5-spot water flooding performance in homogenous reservoirs. In order to compare both of the developed correlations with the CGM method, a value of $V = 0$ was used to make the system homogeneous and the correlations were tested at several water cuts. Figure 154 shows the fractional flow curve of system B at a mobility ratio of 1.062, which corresponds to a mobility ratio of 1 according to CGM definition (M_C). The comparisons are shown in Figures 155 and 156 for ascending and descending cases, respectively. Both correlations show very good predictions at all water cuts. The maximum relative error is 10 % and 7 % for ascending and descending correlation respectively.

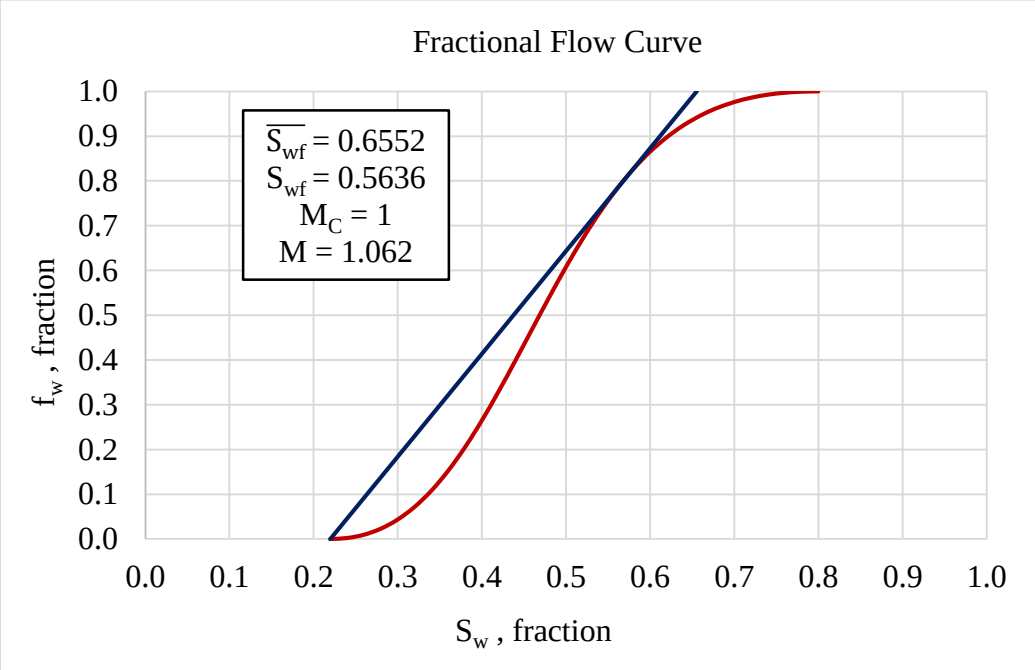

Figure 154 Fractional flow curve for System B at M=1.062

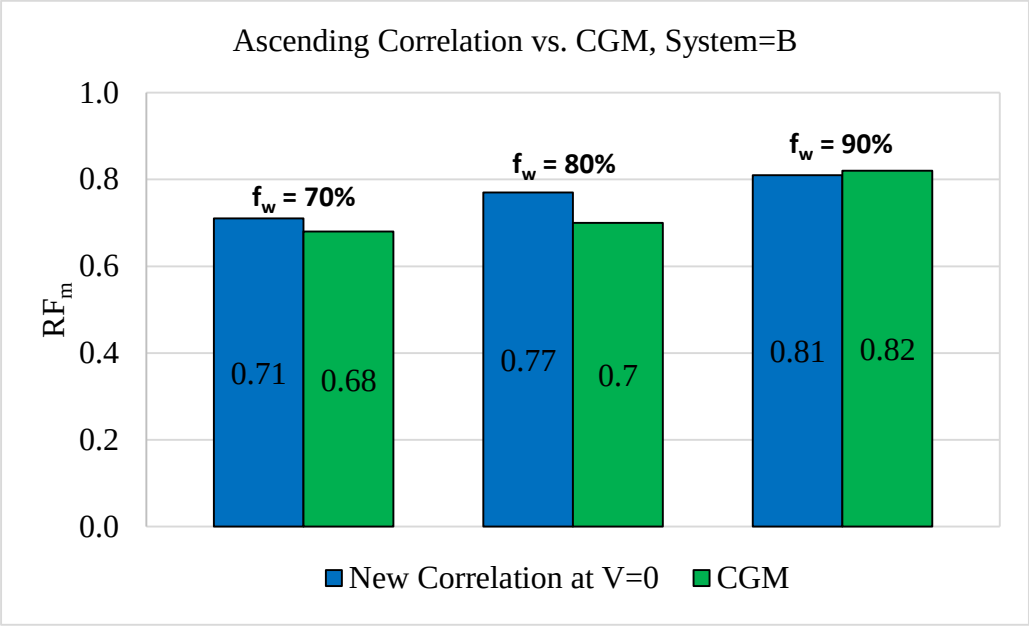

Figure 155 Comparison of Ascending Correlation with CGM Method

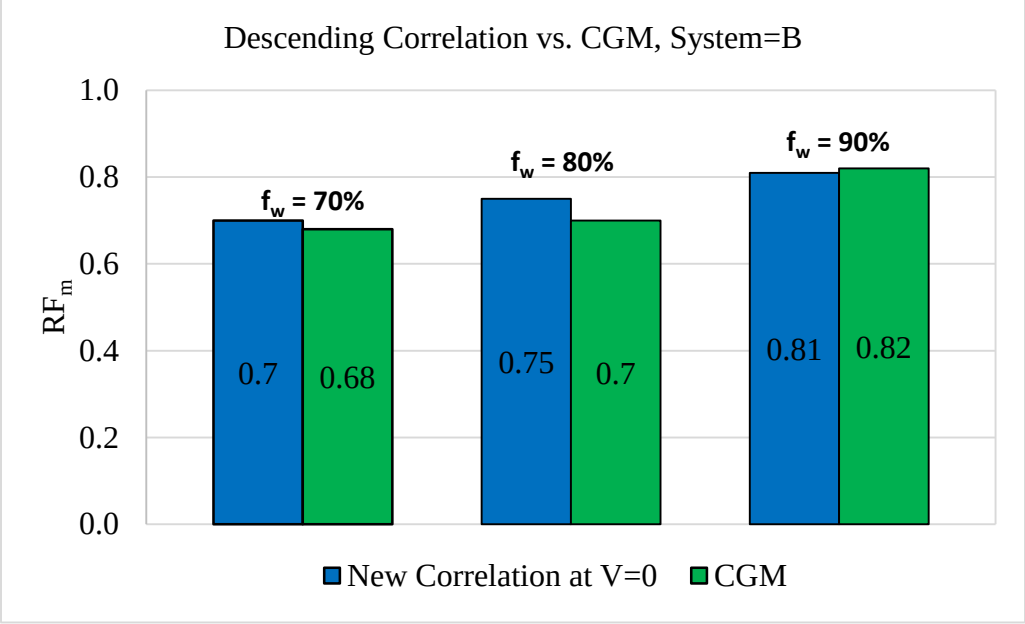

Figure 156 Comparison of Descending Correlation with CGM Method

CHAPTER 7

CONCLUSIONS AND RECOMMENDATIONS

This research work was aimed to derive empirical correlations to predict the performance of five-spot, water-flooding in communicating stratified reservoirs by considering both ascending and descending permeability arrangements. A large number of simulation runs were conducted to generate the required data by varying a number of parameters. Based on the results of this study, the following conclusions and recommendations can be deduced.

7.1 Conclusions

1. Reservoir area and thickness do not affect the oil recovery factor in water-flooding process.
2. Random sorting results are close to those obtained for descending arrangement of permeability, which shows that this permeability arrangement is valid for prediction purposes.
3. Among all the parameters considered, mobility ratio is the most influential factor for oil recovery in water-flooding.
4. The effect of vertical gravitational crossflow caused by the density ratio of oil and water is more evident as the reservoir becomes more heterogeneous and at unfavorable mobility ratios.
5. In water-flooding, the layer permeability arrangement in communicating stratified reservoirs with gravity effects has an effect on oil recovery factors, which is shown by comparing ascending and descending arrangements. The recovery factors are higher for

descending arrangement and the effect of permeability arrangement is more evident at higher density difference between oil and water.

6. Two empirical correlations have been developed in dimensionless form to predict the performance of a 5-spot water flood in a stratified reservoir for both ascending and descending permeability arrangements.
7. The correlations were developed using artificial neural networks with optimum number of weights and biases.
8. The correlations predict the movable oil recovery factor for communicating stratified reservoirs in terms of the flood's mobility ratio, the reservoir's permeability variation, density ratio between oil and water, rock wettability and production water cut.
9. A new parameter called the 'wettability indicator' has been introduced to quantify rock wettability from the relative permeability curves.
10. The descending correlation was able to match actual field data with good accuracy.
11. Both correlations were able to match CGM predictions with good accuracy.

7.2 Recommendations for Future Work

1. Capillary pressure effects were neglected in this research. Future work can be extended by considering capillary pressure effects for extreme wettability systems at higher anisotropic ratios.
2. Lorenz coefficient *(L)* should be considered for reservoir heterogeneity quantification for the future work instead of Dykstra-Parsons permeability variation coefficient because *L* also considers variation of porosity.
3. The correlations should be tested with more field data.

4. A higher values of anisotropic ratios can be considered.
5. The effect of mean permeability on oil recovery factor can be investigated.
6. The effect of injection rate at low density ratios and significant anisotropic ratios can be investigated.
7. Although five spot is the most common flooding pattern, this work can be extended by considering other flood patterns such line drive, seven spot etc.

References

[1] A. B. Dyes, B. H. Caudle, R. A. Erickson, “Oil Production After Breakthrough-as Influenced By Mobility Ratio”, October 1997, SPE-309-G

[2] Arnaldo Leopoldo Espinel Diaz, “Generalized Correlations to Estimate Oil Recovery and Pore Volumes Injectedin Water flooding Projects”, December 2010, a PhD dissertation submitted to the Office of Graduate Studies of Texas A and M University

[3] A.O. DeSouza, W.E. Brigham, “A Study of Dykstra-Parsons Curves”, Prepared By Stanford University Petroleum Research Institute, February 1995, Supri TR-29

[4] Buckley, S.E. and Leverett, M. C., “Mechanism of Fluid Displacement in Sands” May 1941, SPE-942107-G (Petroleum Technology)

[5] C. E. Johnson: “Prediction of Oil Recovery by Water Flood - A Simplified Graphical Treatment of the Dykstra-Parsons Method” pp. 2–3, SPE-373-G,1956

[6] C S. Goddln, JR, F. F. Craig, JR., J. O.Wilkes, M. R. Tek, “A Numerical Study of Water flood Performance In a Stratified System With Crossflow”, June 1966, SPE-1223-PA

[7] D. Tiab, M.E, Osman, “Extension of the Dykstra-Parsons Method to Layered-Composite Reservoirs” ,March 1986, SPE 15020-MS

[8] Dykstra, H. and Parsons, R.L., “The Prediction of Oil Recovery by Water flood” Secondary Recovery of Oil in the United States, API, (1950)

[9] E. T. Guerrero and R. C. Earlougher, “Analysis and Comparison of Five Methods Used to Predict Water-flood Reserves and Performance.”, April 1961, API-61-078

[10] F. F. Craig, “Effect of Reservoir Description on Performance Predictions,” pp. 1239–1245, October 1970, SPE-2652-PA

[11] Forrest F.Craig Jr. ,“The Rservoir Engineering Aspects of Water flooding ”,Second Edition, 1971

[12] F.F Craig Jr, T.M Geffen and R.A Morse, “Oil Recovery Performance of Pattern Gas or Water Injection Operations From Model Tests”, August 1954, SPE-413-G

[13] G.Paul Willhite, “Water flooding ”, SPE Textbook Series, Volume 3,1986

[14] J. E, Warren and J. J. Cosgrove, “Prediction of Water flood Behavior in a Stratified System”, June 1964, SPE-581-PA

[15] K.K. Pande, H.J. Ramey Jr., W.E. Brigham, and F.M. Orr J, “Frontal Advance Theory for Flow in Heterogeneous Porous Media”, April 1987, SPE-16344-MS

[16] M. Felsenthal, T. R. Cobb, and H. G.J., “A Comparison of Water flood Evaluation Methods” Proc. SPE Second. Recover. Symp., May 1962, SPE-332

[17] M.J. McGuire ,“The inclusion of viscous cross flow in a simple Dykstra Parson model”, 1968, SPE-2382

[18] Mobarak, "Water flooding Performance Using Dykstra-Parsons as Compared With Numerical Model Performance" (JPT Forum), January 1975, SPE-5186

[19] Mohammed E. Osman and Djebbar Tiab, “Water flooding Performance And Pressure Analysis Of Heterogeneous Reservoirs”, March 1981, SPE-9656-MS

[20] Noaman EI-Khatib, “Effect of Gravity on Water flooding Performance of Stratified Reservoirs” , April 2003, SPE-81465-MS

[21] Noaman EI-Khatib, “The Effect of Crossflow on Water flooding of Stratified Reservoirs”, April 1985, SPE-11495-PA

[22] Noaman EI-Khatib, “The Modification of the Dykstra-Parsons Method for Inclined Stratified Reservoirs” , December 2012, SPE-140960

[23] Noaman EI-Khatib, “Water flooding Performance of Communicating Stratified Reservoirs with Log-Normal Permeability Distribution”, March 1997, SPE-37696-MS

[24] Rustam Rauf Gasimov, “Modification of The Dykstra-Parsons Method To Incorporate Buckley-Leverett Displacement Theory For Water floods”, August 2005, a thesis submitted to the Office of Graduate Studies of Texas A and M University

[25] Schlumberger Eclipse Technical Description Manual, 2009.1

[26] Stiles, W.E., “Use of Permeability Distribution in Water flood Calculations”, January 1949, SPE-949009

[27] Tarek Ahmed, “Reservoir Engineering Handbook” , Third edition, 2006, Page No. 76

[28] Welge, H. J., “A Simplified Method for Computing Oil Recovery by Gas or Water Drive”, October 1951,SPE-124-G

[29] W. M. Cobb and F. J. Marek, “Determination of Volumetric Sweep Efficiency in Mature Water floods Using Production Data”, October 1997, SPE-38902

Vitae

Name	:	Usama Yousuf
Nationality	:	Pakistani
Date of Birth	:	09/05/1987
Email	:	osamayousaf@hotmail.com
Address	:	Bahadurabad, Karachi, Pakistan.
Academic Background	:	**Masters in Petroleum Engineering**
		King Fahd University of Petroleum & Minerals
		Dhahran, Saudi Arabia
		BE in Petroleum Engineering
		December, 2009
		NED University of Engineering & Technology, Karachi
		Pakistan